An Integrated Approach to Studying the Regulation of Erythromycin Biosynthesis in *Saccharopolyspora erythraea*

A thesis submitted to the University College London for the degree of

Doctor of Philosophy

Vetjaera Mekupi Haakuria

April 2014

The Advanced Centre for Biochemical Engineering
Department of Biochemical Engineering
University College London
Torrington Place
London WC1E 7JE
United Kingdom

Abstract

S. erythraea is the main producing organism of erythromycin, an important broad spectrum antibiotic. Its yield is low because the carbon source utilisation, product kinetics and the regulatory pathways are not yet fully understood. This work provides a detailed characterisation of the carbon source metabolism of *S. erythraea*. The organism was cultured under various conditions and the growth and product kinetics investigated.

In batch bioreactor fermentations, *S. erythraea* was cultured on both glucose and gluconate as sole carbon and energy sources. The culture was subsequently evaluated in bolus feed addition fermentations using phosphoenolpyruvate, oxaloacetate, propionate and methyl oleate with glucose as main carbon source. On both glucose and gluconate, erythromycin production depended on the nature of the carbon source and the growth rate. On glucose, growth was fast with erythromycin production commencing after the growth phase. On gluconate, growth was subdued and erythromycin production was growth-related. Two phases were distinguished for both carbon sources: 1) erythromycin synthesis and 2) precursor accumulation phase. Erythromycin production was enhanced by increased activity of the pentose phosphate and the anaplerotic pathway. Growth rate and the carbon source uptake rate were found to have a major effect on erythromycin production. The split in pathway activities at key branch points was found to be dependent on the growth rate and the rate of carbon source uptake. During bolus feed addition fermentation in shake flasks, erythromycin levels were increased by the addition of oxaloacetate, propionate and methyl oleate respectively. The effect of metabolite supplementation on erythromycin levels depended on the phase during which feeding is done. In bioreactor culture, levels of erythromycin were enhanced following addition of OAA or methyl oleate. The pyruvate metabolite node was found to be flexible responding to supplementation and the nature of the sole carbon and energy source. Carbon allocation to pyruvate was 1.7 % and 5.4 % for growth on glucose and gluconate respectively. This metabolite node is, therefore, critical to improving the biosynthesis of erythromycin. However, the phosphoenolpyruvate node appears rigid and addition of PEP was excreted as 7-*O*-rhamnosyl flaviolin (red pigment). The ratio of the rate of carbon source consumption and oxygen uptake was concluded to be a critical parameter in the biosynthesis of erythromycin.

In memory of my grandmother

Louise Mbapeua Haakuria

Acknowledgements

Various individuals and organisations have greatly contributed to the ultimate completion of this work. Advanced research such as this cannot be carried on and completed without the contributions from many quarters.

I am forever indebted to my grandmother, Louise Mbapeua Haakuria, for laying a solid foundation that paved the way for the development of focus, resilience and strong-willed determination, qualities that have been pillars of strength in my journey to submitting this thesis. The submission of this work for the award of a PhD degree is the culmination of the early efforts by the Roman Catholic Church through the late Father Edward Kangootui who toiled without any compensation to give rural children an education. It is equally the culmination of the work of the late Father Anton Biesel who provided material and moral support during my early years when quitting school was an easier option.

I am indebted to my supervisors Dr Frank Baganz and Prof John Ward for their guidance and insight throughout the project's life cycle. Scholarship support provided by the Government of the Republic of Namibia through the Ministry of Education is highly appreciated. Raoul and Ursula Matzopoulos deserve special mention for having been there throughout and having had a hand in shaping my eventual academic destiny. I am grateful to Andy Tait for advice on the more complex parts of enzymology and enzyme kinetics, Brian O'Sullivan who was always available when I needed a quick answer to a chemistry related problem and Jean Aucamp for help with the Covaris sonicator and the Dionex HPLC. The help of Deji Akinrinsola during the early stages of my research is greatly apprecioated.

Dannii Ripuree Haakuria and Ketu Karukongo have been the constant in maintaining a presence when I needed support. A word of thanks also goes to the Cloister 2.1 crew, namely Shaukat Ali, Omar Ramadani, Naqash, Miguel Angel Pardo, Nick Silk and Tom Paoli for camaraderie in an all-male office.

Without the support of my wife, Emeltha and daughters, Vesora and Kasuko, I would have found it difficult to push through to the end.

Table of Contents

1.0 INTRODUCTION
1.1. Background to the study *12*
1.2. Overview of the study *13*
1.3. SYSTEM UNDER INVESTIGATION *15*
1.3.1. Saccharopolyspora erythraea as a production organism *15*
1.3.2. The order Actinomycetales *15*
1.3.3. Secondary metabolite production *16*
1.3.4. Erythromycin *17*
1.3.5. *Biosynthesis of erythromycin* *18*
1.4. REVIEW OF APPROACHES TO ERYTHROMYCIN PRODUCTION
1.4.1. Genetic engineering *20*
1.4.2. Engineering of morphological; and physiological differentiation *21*
1.4.3. Engineering of primary metabolism *22*
1.4.4. Engineering methyl-malonyl-CoA mutase *25*
1.4.5. Manipulation of culture conditions to improve yield *26*
1.4.6. Utilising oils to enhance antibiotic production. *27*
1.4.7. Physiological characterisation of metabolism. *29*
1.4.8. Induction of erythromycin production *30*
1.4.9. Bioreactor operational mode *31*
1.4.10 A model for the production of erythromycin in batch and cyclic batch fermentation *32*
1.5. CARBON FLUX DISTRIBUTION APPROACHES *33*
1.5.1.1. Constraint-based flux analysis *34*
1.5.2. ^{13}*C-based fluxanalysis* *36*
1.5.2.1. Radio respirometry *37*
1.5.2.2. Combined isotope labelling and GC-MS analysis *37*
1.5.3. Metabolic physiology investigations based on biochemical Studies *38*
1.5.4. Current research approach *39*
1.6 **AIMS** *40*
1.7 **OBJECTIVES** *40*
1.8 **HYPOTHESIS** *40*
2.0 RESEARCHMETHODS
2*.1 Bacterial strains and culture conditions* *41*
2.2 Reagents and chemicals *43*
2.3 Fermentation conditions *43*
2.3.1 Shake flask culture conditions *43*
2.3.2 Bioreactor culture conditions *44*
2.4 Sampling and quenching *45*
2.4.1 Samples for biomass, glucose, nitrate, extracellular metabolites, enzymes and pyridine cofactors *45*
2.4.2 Samples for ATP, ADP and AMP *45*

2.5 ANALYTICAL DETERMINATIONS 47
2.5.1 *Biomass determination* 47
2.5.2 Erythromycin 47
2.5.3 Organic acids, glucose, nitrate and red pigment 48
2.5.4 Enzyme sample preparation and determoination of enzyme Activity 48
2.6 Determination of pyridine cofactors 50
2.7 Determination of adenylate nucleotides 50
2.8 Calculation of yield coefficients and rates 52
2.9 Carbon balance determination 52
3.0 ANALYTICAL METHOD DEVELOPMENT
3.1 Rationale for method development 53
3.2 Evaluation of the analytical method for enzyme activity Determination 53
3.2.1 Sonication trial 53
3.2.2 Results 54
3.2.3 Assay development and evaluation 55
3.2.4 Evaluation of the optimised assay protocol 56
3.2.5 Review of the method for metabolite extraction 58
3.3 Evaluation of the pyridine cofactor method 60
3.3.1 Optimisation of protocol and analytical parameters 61
3.3.2 Evaluation of the accuracy and robustness of the assay 62
3.4 Development of the assay for adenylate nucleotides 64
3.4.1 Evaluation of the effect of the extraction procedure on the Recovery of AMP 66
3.4.2 Optimisation of the buffer conditions for myokinase reactions 67
3.4.3 Investigation of storage conditions on the stability of ATP 68
3.4.4 Evaluation of the accuracy and robustness of the assay protocol for the adenylate nucleotides 69
3.4.5 Evaluation of the reproducibility of the analytical procedure on samples 73
3.5 Summary 74
4.0 PHYSIOLOGY OF METABOLITE PRODUCTION AND ERYTHROMYCIN BIOSYNTHESIS
4.1 Carbon screening studies in shake flask fermentations 75
4.2 Introduction 76
4.3 Research design 78
4.4 Results and discussion 79
4.5 Summary 84
4.6 BIOREACTOR BATCH FERMENTATIONS 84
4.6.1 Research design 86
***4.6.2* GLUCOSE AS A SOLE CARBON AND ENERGY SOURCE**
4.6.2.1 Growth charactersistics 87
4.6.2.2 Effect of glucose uptake rate on erythromycin production 89
4.6.2.3 Correlation between specific uptake rate, erythromycin production and cofactor generation 90
4.6.2.4 Correlation between cell energetics, specific glucose uptake rate product formation 91

4.6.2.5 Effect of glucose uptake rate on the activities at PPP/EMP, AP/TCA, cycle and EMP/TCA cycle branch points 93
4.6.2.6 Effect of glucose consumption rate on the excretion of organic acids 95
4.2.6.7 Carbon balance determination for glucose fermentation 97
4.6.3 DISCUSSION 98
4.6.3.1 Growth phase 99
4.6.3.2 Metabolite accumulation phase 100
4.6.2.3 Erythromycin production phase 101
4.6.3.4 Correlation between the specific glucose uptake rate and the growth rate 103
4.6.3.5 Glucose and oxygen consumption rate as a regulator of Metabolite overflow 104
4.6.4 Carbon utilization 105
4.6.5 A model for the production of erythromycin on glucose as a sole carbon as a sole carbon and energy source 106
4.6.6 Model explanation 108
5.0 GLUCONATE AS A SOLE CARBON AND EENERGY SOURCE
5.1 Growth characteristics 109
5.2 Correlation between gluconate uptake rate, branch point enzymes, product formation and cofactor generation 113
5.3 Correlation between cell energetics, gluconate uptake rate and product biosynthesis 116
5.4 Excretion of organic acids and the activities of enzymes 118
5.5 Relationship between the rate of oxygen consumption and the biosynthesis of erythromycin 119
5.6 Carbon balance 121
5.7 DISCUSSION 122
5.7.1 Growthcharacterstics 122
5.7.2 Metabolic pathway activity and antibiotic production 123
5.7.3 Relationship between the specific gluconate uptake rate, growth rate and secondary metabolite production 125
5.7.4 Relationship between the rate of gluocnate consumption and the the respiratory activity 126
5.7.5 Model explanation 131
5.7.6 Summary of findings for both growth conditions 131
5.7.7 Conclusions 133
6.0 THE EFFECT OF METABOLITE SUPPLEMENTATION UNDER SHAKE FLASK CONDITIONS
6.1 Introduction 127
6.2 Bolus feed additions shake flask studies 128
6.3 Results 138
6.3.1 Control fermentation 138
6.3.2 Phosphoenolpyruvate supplementation 139
6.3.3 Oxaloacetate supplementation 142
6.3.4 Propionate supplementation 143
6.35 Methyl oleate supplementation 144

7.0 THE EFFECT OF METABOLITE SUPPLEMENTATION UNDER BIOREACTOR CONDITIONS
***7.1* OXALOACETATE BOLUS FEED ADDITION FERMENTATIONS** *147*
7.1.1 Supplementation at 45h and 71h *147*
7.1.2 Effect of oxaloacetate supplementation on the activities of key enzymes *149*
7.1.3 Excretion of organic acids *151*
7.1.4 Effect of oxaloacetate supplementation on the generation of pyridine cofactors and adenylate nucleotides *153*
7.1.5 Effect of oxaloacetate supplementation on the respiratory energy generation *156*
7.2 DISCUSSION *157*
7.2.1 Growth characteristics *157*
7.2.2 Effect of oxaloacetate addition on flux partitioning at the AP/TCA cycle branch point *159*
7.2.3 Flux dynamics at the pyruvate metabolite node *161*
7.2.4 The role of gluconeogenesis *165*
7.2.5 Regulation of oxidative phosphorylation *167*
7.2.6 Conclusions *171*
7.3 METHYL OLEATE BOLUS FEED ADDITION FERMENTATIONS
7.3.1 Experimental design *173*
7.3.2 Effect of methyl oleate supplementation on biomass synthesis and and respiration *174*
7.3.3 Distribution of carbon fluxes through PEPC, ICD and ICL *175*
7.3.4 Effect of feeding on the energy status of the cell *176*
7.3.5 Effect of methyl oleate addition on the excretion of organic acids *177*
7.3.6 Effect of methyl oleate addition the generation of NADH and NADPH *179*
7.3.7 Comparison of the two bolus feed addition bioreactor fermentations: Oxaloacetate and Methyl oleate fermentations *181*
7. 4 Discussion *184*
7.5 Conclusion *186*
7.6 General observations and conclusions
7.6.1 General discussion and conclusions *188*
7.6.2 Process-scale implications for industrial biopharmaceutical Production *189*
8.0 FUTURE WORK ***191***
9.0 REFERENCES ***193***

List of figures

Figure 1: Some colourful antibiotics produced by Actinomyces……..16
Figure 2: Profile of the red pigment, 7-Orhamnosyl flaviolin……...16
Figure 3: An illustration of the structure of erythromycin……18
Figure 4: The major steps involved in the biosynthesis of erythromycin…….....19
Figure 5: A simplified layout of sample handling and processing……46
Figure 6: Calibration curve for the determination of NADH…….....63
Figure 7: Calibration curve for the determination of NADPH……..64
Figure 8: Calibration curve for ATP determination……...72
Figure 9: Calibration curve for the determination of ADP……72
Figure 10: Calibration curve for the determination of AMP……73
Figure 11: Pathways of carbon degradation for different carbon sources……..76
Figure 12: Time courses of biomass and red pigment formation during growth on glucose in shake flask fermentation……79
Figure 13: Profiles of biomass and red pigment formation during growth on gluconate in shake flask fermentation……..81
Figure 14: Profiles of biomass and red pigment concentration during growth on xylose in shake flask fermentation……82
Figure 15: Profiles of biomass formation of *S. erythraea* during growth on methyl oleate in shake flask fermentation……..82
Figure 16: Profiles of the red pigment for growth of *S. erythraea* on various carbon sources……83
Figure 17: Time courses of the concentratiom of biomass, glucose and and nitrate for growth on glucose as a sole carbon source……..84
Figure 18: Profiles of the OUR and CER for growth on glucose as a sole carbon and energy source……..……88
Figure 19: Relationship between glucose uptake rate and erythromycin production….90
Figure 20: Profiles of NADH, NADPH and erythromycin concentrations for growth on glucose as a sole carbon and energy source……91
Figure 21: Profiles of the respiratory quotient and glucose uptake rate during growth on glucose as a sole carbon and energy source……92
Figure 22: Profiles of the energy charge erythromycin production for growth on glucose as a sole carbon and energy source……..93
Figure 23: Corellation between the glucose uptake rate and the ratio between key branchpoint and pathway enzymes during growth on glucose……..95
Figure 24: Time courses of organic acids concentrations during growth on glucose as a sole carbon and energy source……....96
Figure 25: Pathway activity during the metabolite production and erythromycin biosynthesis phases for growth on glucose as a sole carbon and energy source……..……...107
Figure 26: Growth profiles of *S. erythraea* during growth on gluconate as as a sole carbon and energy source……111
Figure 27: Profiles of OUR and CER during growth on gluconate……112
Figure 28: Relationship between RQ and gluconate uptake rate during growth on gluconate……112

Figure 29: Correlation between the specific gluconate uptake rate and the production of erythromycin……114
Figure 30: Correlation between the specific gluconate uptake rate and the split in pathway activity during growth on gluconate……115
Figure 31: Correlation between the specific gluconate uptake rate, erythromycin production and the pyridine cofactors during growth on gluconate…..116
Figure 32: Profile of the relationship between erythromycin production and the energy charge…..……....117
Figure 33 Profiles of the organic acids and the red pigment excretion during growth on gluconate as a sole carbon and energy source……..…….119
Figure 34: Metabolic pathway activity in *S. erythraea* during the metabolite accumulation and erythromycin biosynthesis phase for growth on gluconate as a sole carbon and energy source……130
Figure 35: Growth profiles of *S. erythraea* for the control batch fermentation.....139
Figure 36: Profiles of erythromycin production at 48 hours after bolus feed additions in shake flask culture……...……...…140
Figure 37: Profiles of erythromycin production at 72 hours after bolus feed additions in shake flask culture……...……...…141
Figure 38: Profiles of erythromycin production at 96 hours after bolus feed additions in shake flask culture……...……...…141
Figure 39: Growth profiles of *S. erythraea* after supplementation with oxaloacetate in bioreactor culture……...148
Figure 40: Profiles of OUR and CER for *S. erythraea* bioreactor culture supplemented with oxaloacetate……....149
Figure 41: Profiles of the enzyme activities activity for *S. erythraea* bioreactor culture supplemented with oxaloacetate……151
Figure 42: Profiles of organic acid secretion for *S. erythraea* bioreactor culture supplemented with oxaloacetate……152
Figure 43: Profiles of NADH and NADPH for *S. erythraea* bioreactor culture supplemented with oxaloacetate ……...…….154
Figure 44: Profiles of the energy cofactors for *S. erythraea* bioreactor culture supplemented with oxaloacetate…….……..….155
Figure 45: Relationship between OUR/GUR ratio and RQ for *S. erythraea* bioreactor culture supplemented with oxaloacetate ……...156
Figure 46: Growth profiles of *S. erythraea* after supplementation with methyl oleate in bioreactor culture ……...174
Figure 47: Profiles of the activities of enzymes of *S. erythraea* after supplementation with methyl oleate in bioreactor culture …..….....176
Figure 48: Profiles of the cell energetics for after supplementation with methyl oleate in bioreactor culture fermentation……...……....177
Figure 49: Organic acid and red pigment secretion for during growth on glucose supplemented with methyl oleate…….…..178
Figure 50: Pyridine co-factor generation during growth on glucose supplemented with methyl oleate……..180
Figure 51: Comparison of the energy charge and the production of erythromycin during growth on glucose supplemented with methyl oleate…….181

List of Tables

Table 1: Composition of the basic growth media……42
Table 2: Composition of the trace element solution……42
Table 3: Effect of sonication duration on the absorbance of enzymes in the lysate……55
Table 4: Comparison of the effect of sonication duration on the activities of G6PDH……..55
Table 5: Protocol and analytical parameters for enzyme assays……57
Table 6: Evaluation of the activities of central metabolism enzymes in *S. erythraea* based on the optimise reagent combinations and analytical parameters ……58
Table 7: Effect of the extraction procedure on the concentrations of NADH and NADPH…….....61
Table 8: Protocol for the determination of pyridine cofactors……...62
Table 9: Reproducibility of cofactor assay…….....64
Table 10: Percentage recovery of AMP concentrations after treatment…….....67
Table 11: Effect of buffers on the activity of myokinase…….....67
Table 12: Effect of storage on the concentration of ATP …….....69
Table 13: Optimised protocol for determination of adenylate nucleotides……71
Table 14: Reproducibility of the ATP and ADP assays…….....74
Table 15: Specific growth rate, yield and yield coefficient for growth on glucose…….....87
Table 16: Carbon balance for growth on glucose as a sole carbon and energy source...98
Table 17: Specific growth rate, yield and yield coefficient during growth on gluconate……...109
Table 18: Carbon balance for growth on gluconate as a sole carbon and energy source……...121
Table 19: Kinetic parameters of *S. erythraea* culture on glucose supplemented with oxaloacetate……..149
Table 20: Specific production and consumption rates of *S. erythraea* culture on glucose supplemented with oxaloacetate…….....153
Table 21: Specific production rates of adenine and pyridine cofactors of *S. erythraea* culture on glucose supplemented with oxaloacetate……...155
Table 22: Specific growth rate, yield and yield coefficient for fed batch and the methyl oleate supplemented batch fermentation……..175
Table 23: Specific substrate consumption rate, biomass concentration product formation during the methyl oleate supplemented fermentation…….183
Table 24: Specific rate of adenylate and pyridine cofactor production for the methyl oleate fed batch culture of *S. erythraea*……..... 184

Table of Abbreviations

ACT	Actinorhodin
ADP	Adenosine diphosphate
AMP	Adenosine monophosphate
AP	Anaplerotic Pathway (from phosphoenolpyruvate to oxaloacetate)
ATP	Adenosine triphosphate
CER	Carbon Dioxide Evolution Rate
CoA	Coenzyme A
DEBS	6-Deoxyerythronolide B
EC	Energy Charge
ED	Entner-Doudoroff Pathway
EMP	Embden-Meyerhof-Parnas Pathway
ETC	Electron Transport Chain
F6P	Fructose-6-phosphate
G6P	Glucose-6-Phosphate
G6PDH	Glucose-6-Phosphate Dehydrogenase
GALD	Glyceraldehyde-6-phosphate
GC	Gas Chromatography
GLUR	Specific Gluconate Uptake Rate (gluconate consumption rate)
GUR	Specific Glucose Uptake Rate (glucose consumption rate)
HPLC	High Performance Liquid Chromatography
ICD	$NADP^+$-dependend Isocitrate Dehydrogenase
ICL	Isocitrate Lyase
MS	Mass Spectrometry
NADH	Nicotinamide adenine dinucleotide (reduced form)
NADPH	Nicotinamide adenine dinucleotide phosphate (reduced form)
NRRL	Northern Region Research Laboratory
OUR^1	Oxygen Uptake Rate
PEPC	PhosphoEnolPyruvate Carboxylase
PEPCK	Phosphoenolpyruvate carboxykinase
PGI	PhosphoGlucose Isomerase (Glucose-6-phosphate isomerase)
PKS	Polyketide Synthase
PPP	Pentose Phosphate Pathway
RED	Undecyl-prodigiosin
RPM	Revolutions per Minute
RQ	Respiratory Quotient
TCA	Tricarboxylic Acid
TE	Tris-EDTA
VVM	Volume per Volume per Minute

1.0 Introduction

1.1 Background to the study

Antibiotics are a major part in human efforts to control prevent, treat or eradicate many diseases that afflict mankind today. Lives have been extended owing to the treatment of diseases using antibiotics. Infant mortality has dropped significantly in many parts of the world though in the tropics, diseases caused by tropical organisms are still a major concern for health authorities. The problems in this regard have to do with access to antibiotics owing to their high cost, logistics in health care extension, social upheavals and poor infrastructure, among other things. For many diseases, effective treatment in the form of antibiotics does exist. However, any antibiotic resistance is a major concern in relation to diseases that had been thought to have been successfully contained as conventional treatments are no longer effective. *Plasmodium falciparum*, the protozoon which causes malaria, has developed resistance to chloroquine. Various strains of *Mycobaterium tuberculosis* are resistant to current treatment regimes. Penicillin-resistant *Streptococcus pneumonia* has developed resistance to almost all antibiotics except imipenem (Staunton, 1997). In addition, the methicillin-resistant *Staphylococcus aureus* and *Clostridium deficille* have emerged in hospitals in developed countries proving that the problem is not only confined to developing countries.

There is, therefore, a need to develop and produce new drugs and/or increase the production of existing effective antibiotics. Producing antibiotics at affordable prices requires that production volumes be significantly increased. One parameter that is critical in process economics of bulk products is product yield. A high yield reduces production cost through the reduction of batch numbers or volumes. Overall higher yields enable the production of antibiotics in bulk at reduced cost which make medicines accessible to many more countries around the world.

To improve yield, research has focussed on understanding the physiology and biochemistry of the production organism. It is often an arduous and lengthy process before production can be improved to bulk scales. For penicillin, it has taken 50 years of extensive physiological and other studies before production levels reached bulk levels (Jaques, 2004).

For erythromycin, production levels at an industrial scale are far lower when compared to those of penicillin or other antibiotics. Industrial yields are in general proprietary information, but yields of up to 60 g/L have been reported for many antibiotics (Smolke., 2010). In contrast, the highest yield reported for erythromycin is about 4 g/L (Smolke., 2010).

The physiological basis for the production of erythromycin has not been extensively studied. As such, it is not known why the production of erythromycin remains low given its potential (Gonzalez-Lergier *et al*., 2006). Much of the work conducted has focussed on the manipulation of genes in the product pathway without regard for the role of central metabolism. Central metabolism is important for supplying the building blocks of erythromycin and its regulatory mechanisms will affect the supply of precursors to the product pathway. Information obtained from the study of central metabolic flux distribution and regulation will form the basis for genetic interventions to optimise product biosynthesis.

Therefore, the aim of this study is to elucidate the regulatory mechanism of erythromycin production in *S. erythraea* in order to improve its production. The scope of the project will be limited to the physiological characterisation of the metabolism of *S. erythraea*. Growth and product kinetics will be investigated under different growth conditions. The interplay between primary and secondary metabolism during growth will be investigated with regard to product formation, carbon consumption, generation of pyridine cofactors and energy usage. Integrating the generation of cofactors and energy with enzyme selected activities, growth rate, carbon uptake rate and product formation rate could give the information required to better understand the overall regulatory mechanisms in *S. erythraea*. Such information would be useful in subsequent studies to improve the production of erythromycin in *S. erythraea.*

1.2 Overview of the study

To achieve the above aim within the stated scope, Chapter 1 provides the background and context within which the research is conducted. The chapter provides a detailed review of the literature relevant to the study. It critically reviews the methods and approaches taken by others to improve antibiotic production in various Actinomycetes.

It points out limitations and strengths of each approach and, where possible, suggests alternatives.

Chapter 2 details all the analytical and assay methods used throughout the study. A rationale for the selection of each method is provided.

Chapter 3 focuses on the development and validation of the analytical methods and assays. The approach taken in studying the physiology of metabolism in *S. erythraea* has not been done before, therefore, all methods and assays have to be developed, evaluated or adapted to the system under investigation. Limitations and problems are outlined and improvements steps are suggested. Optimal quenching and extraction techniques are developed for adenylate nucleotides. Adenylate assay protocols for luminescence are optimised. The extraction of enzymes and pyridine cofactors are investigated and the analysis on the spectrophotometer optimised. Method validation provides confidence in the results so generated.

In Chapter 4, carbon sources are screened in shake flask fermentations for their ability to support growth of *S. erythraea*. Good growth is used as a basis for selection of a carbon source for use in subsequent experiments. A physiological investigation of metabolism focussing on flux distribution as a function of the carbon source (glucose and gluconate) is conducted in Chapter 5. The results are integrated to reveal regulatory mechanisms. Chapter 6 deals with fed-batch fermentations to investigate the physiological basis of increases in the production of erythromycin. Investigations focusing on carbon flux dynamics around the TCA cycle to determine optimum feeding conditions. Carbon sources used for supplementation are evaluated in shake flask studies. The selection of supplemented carbon sources was based on their ability to increase erythromycin concentration. Based on the findings in Chapter 5, potential constraints of erythromycin biosynthesis by metabolite pools are investigated in fed-batch bioreactor fermentations. Results from these experiments are integrated to reveal constraints in antibiotic production.

Finally, Chapter 7 provides an overall conclusion and a basis for future work.

1.3 System under investigation

1.3.1 *Saccharopolyspora erythraea* as a production organism

Saccharopolyspora erythraea is the major producer of erythromycin, a broad-spectrum antibiotic that is effective against many infections. It is a soil organism that belongs to the same order of Actinomycetales as *Streptomyces* sp. *S. erythraea* was originally classified under Streptomyces as *Streptomyces erythreus*. However, this has since been revised and it now resorts under the genus *Saccharopolyspora* which shares the same order of Actinomycetales as *Streptomyces*. Two variants are known to exist depending on the pigment formed. The red variant produces the red pigment and is the one commonly used in research work. Industrial fermentations are based on the white variant, though many of these are probably mutants with unknown classically-derived mutations.

1.3.2 The order Actinomycetales

The group of actinomyces is a diverse group of microorganisms that are well known for producing a wide variety of medically important secondary metabolites. Actinomycetaceae are filamentous gram-positive bacteria with high GC content. In this family, *Saccharopolyspora erythraea* belongs to the order Actinomyctales with characteristic formation of filaments, spores and aerial hyphae. This particular order is well known for producing a vast array of colourful clinically important antibiotics. Common examples of this are *Streptomyces coelicolor* (actinorhodin and undecylprodigiosin), *Streptomyces lividans* (actinorhodin and undecylprodigiosin), *Streptomyces griseus* (streptomycin), *Streptomyces cinnamonensis* (monensin), *Streptomyces ambofaciens* (spiramycin) and various others. Some of the antibiotics and secondary metabolites produced by this group are shown in Figure 1 and Figure 2 below.

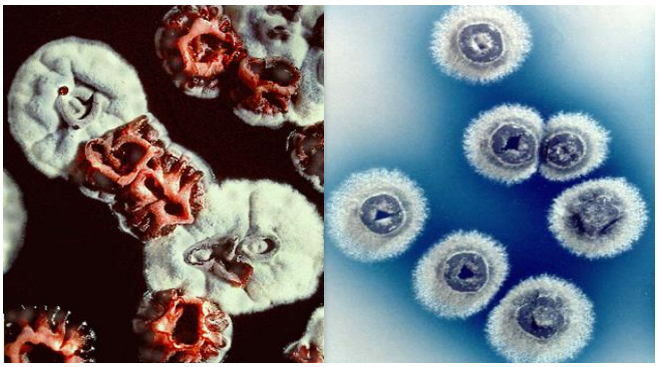

Fig. 1 Some antibiotics actinorhodin (blue) and undecylprodigiosin (red) both produced by *Streptomyces coelicolor* and *Streptomyces lividans* (Images courtesy of John Innes Centre, Norwich).

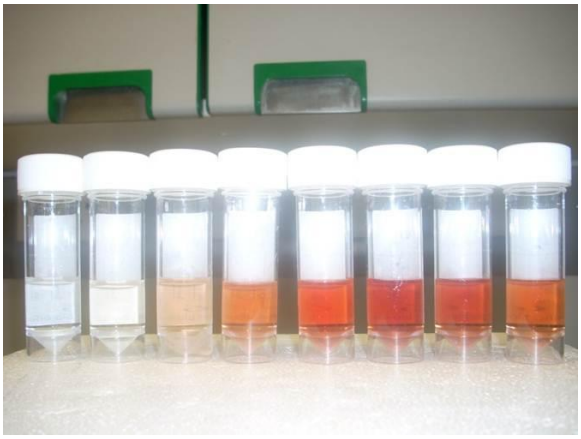

Fig. 2 Profile of the red pigment, 7-O-rhamnosyl flaviolin produced by *S. erythraea*. The pigment is thought to be a mixture of compounds (taken from Jaques., 2004).

1.3.3 Secondary metabolite production

Secondary metabolites are generally described as those metabolites produced after growth have ceased. This is not strictly true as these metabolites can be produced during the growth phase depending on the growth conditions. A more accurate definition describes secondary metabolites as those metabolites not required for growth irrespective of when they are produced. Secondary metabolites are generally produced during a period of imbalance in the enzymatic reactions. During primary metabolism when enzymatic reactions are balanced, metabolites are produced to meet cell

requirements. Disturbing the balance results in overproduction of metabolites not required for growth. This has led to the question as to why these metabolites are produced if they are not actually required for growth. Many of these metabolites have antimicrobial properties and are probably used in conferring a competitive advantage during competition for nutrients (Firn & Jones., 2003). However, not all are antimicrobials, some have unknown functions. Recently, the conventional view that secondary metabolites are not needed for growth has come under scrutiny. Work by Price-Whelan *et al* (2006), Banin *et al* (2005) and Hernandez *et al* (2004) have suggested that secondary metabolites could function in helping organisms persist in the environment, supporting growth or to acquire iron during quorum sensing. However, because of their clinical importance, their production has been the focal point of investigations, notably in the order Actinomycetales.

1.3.4 Erythromycin

Erythromycin is a macrolide antibiotic that was isolated from *S. erythraea* in 1952 (Staunton & Wilkinson, 1997). It is a very important antibiotic with sales worth billions of pounds annually (Rawlings., 2001). The annual production volume of erythromycin was 2 tonnes and demand increases every year (Brunker *et al*., 1998). The antibiotic is a polyketide with a 14-member macrolactone ring and two sugars attached to the ring (Fig. 3). Clinically, erythromycin is used in treating infections caused by gram-positive bacteria and is used as an alternative in patients who are allergic to penicillin (Staunton., 1997). Various types of the antibiotics are produced, mainly Erythromycin A, B, C, D and K depending on the position of the mycarose sugar. Of these, erythromycin A is by far the major component of the total erythromycin produced. Erythromycin binds to the 50S subunit protein and inhibits the formation of peptide bond by binding to the L15 and 23S rRNA at the peptidyltransferase active site (Slonczewzki & Foster, 2009).

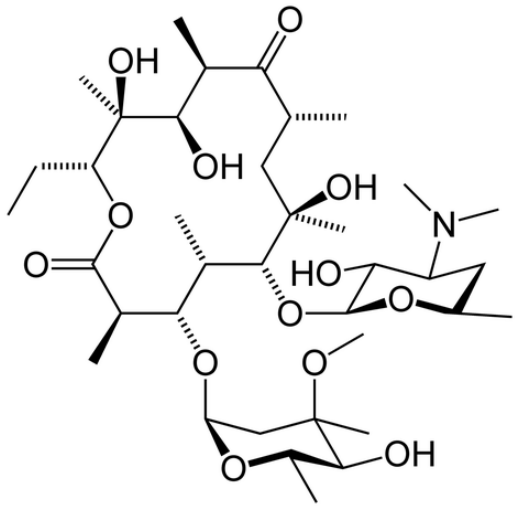

Fig. 3 An illustration of the chemical structure of erythromycin A.

1.3.5 Biosynthesis of erythromycin

Erythromycin is produced through successive condensation of one propionyl-CoA and six methylmalonyl-CoA esters by polyketide synthase (PKS) modular system. The PKS system consists of modular enzymes with active sites able to catalyse the addition of extender units. The PKS modular system consists of a complex of several protein subunits which serve as an assembly line for polyketide synthesis (Fig. 4). With each condensation, a β-keto group is added to the growing carbon chain until it reaches 13 carbons to form the macrolide ring, 6-Deoxyerythronolide (6-DEBS). The two sugars, mycarose and desosamine are subsequently added at the C-3 and C-5 respectively.

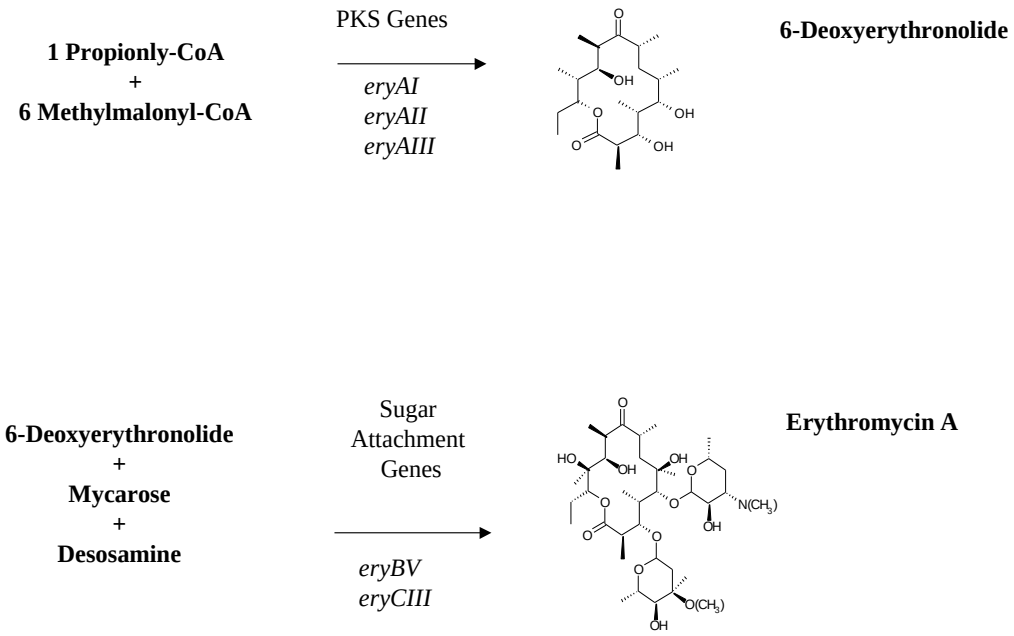

Fig. 4 The major steps in the biosynthesis of erythromycin (adapted from Ushio, 2003).

1.4 Review of approaches to improve erythromycin production

The aim of any industrial production process is to achieve a high product titre, which is the concentration of product in the broth. Since productivity is defined as the amount of product per unit time, it is influenced by titre and yield. Since yield is the amount of product formed per unit carbon source consumed, it is clear that titre is influenced by yield. Both these parameters affect production cost. A high product titre reduces cost and the need for increasing volumes. It is common knowledge that improvement in upstream processing raises production titres which subsequently drives down production cost and creates excess capacity. In industry upstream titre has a major influence the cost of goods (Kelly, 2009). In contrast low titres often necessitate higher volumes which increase downstream processing efforts.

For these reasons, improvement in industrial fermentations has focused on strain improvement and optimisation of upstream process parameters.

The pathways of secondary metabolism are not fully understood, even though formation of these metabolites are reported to be regulated by nutrients, growth rate, feedback control and the inactivation and induction of enzymes (Demain, 1998). Primary metabolism in general is well understood and many pathways are adequately characterised. Various approaches to improving yield have been adopted ranging from optimising growth media, manipulating fluxes through product pathways, metabolic engineering of the product pathway, heterologous expression of pathway-specific genes and studying the physiology. A review of the major approaches is provided in the next section.

1.4.1 Genetic engineering

Much research on improving the production titres for antibiotic fermentations has focused on genetic engineering probably because more information is available on the genomes of organisms. For related organisms, genes from strains not fully characterised yet can be compared to databases of those whose genomes have been fully sequenced by performing BLAST searches. The presence or absence of genes of interest in a target organism can be confirmed.

One approach taken by Brunker *et al* (1998) was to express the *Vitreoscilla* haemoglobin gene (*vhb*) in *S. erythraea*. The aim was to increase the productivity of erythromycin by improving oxygen metabolism in *S. erythraea*. Oxygen metabolism was thought to be a possible limiting factor. Shake flask cultures of *S.erythraea* with chromosomally integrated *vhb* gene expressed the gene and produced 60% higher erythromycin titre relative to the control strain. The researchers found that the increase was due to a higher rate of erythromycin production in the first three days combined with an additional increase after day 7. Interestingly, biomass for the recombinant strain was not higher than that for the control strain. The conclusion was that biomass did not play a part in increasing erythromycin but that an increase in the activity of an oxygen dependent step was the likely cause of the improved production titre. It was also argued that improving oxygen metabolism increased the flux of erythromycin biosynthesis. The transformed strains were tested by the same researchers for genetic stability and performance in bioreactor fermentations. The findings at shake flask scale were confirmed with the mutants producing 70% higher titre relative to the control strains

(Minas *et al*., 1998). Notably, in bioreactor fermentations the mutants produced between 25 - 40% less biomass than the controls. However, the rate of erythromycin production was higher for the mutant strains. The yield of erythromycin per biomass (g erythromycin/g DCW) was higher compared to that for the control strain. Thus it appears that improving oxygen metabolism depressed growth and therefore biomass formation but enabled the cells to produce more of the antibiotic. The cultures diverted more carbons towards erythromycin production than to biomass formation. It appears unusual that improvement in the utilisation of oxygen depressed growth rate.
Respiration is generally expected to increase in response to an enhanced oxygen level in the system and growth rate can be limited by the rate of respiration (Andersen & Meyenberg, 1980). However, since the researchers did not actually determine the growth rate, it is not known if this was lower relative to the control strain although reduction in biomass formation is associated with reduced growth rate.

Despite its potential, genetic engineering has limitations. Metabolic networks are highly interconnected. Thus, perturbations such as a mutations or gene deletion can set in motion a cascade of events that affect other reactions in the system. In general, small disturbances are unlikely to bring about large cascades if the system is highly robust. It has been found that the likelihood of failure cascades in a metabolic network is very small (Ottino *et al*., 2008). To protect against potential harmful effects of mutation or gene deletions, metabolic networks have evolved to be very robust (Ottino *et al*., 2008). Relatively large disturbances are required to overcome the robustness to bring about the desired effect. However, large deletions could compromise the fitness of mutants relative to the wild type strains.

1.4.2 Engineering morphological and physiological differentiation

S-adenosyl methionine (SAM) is a molecule produced by SAM synthetase from L-methionine and ATP (Shin *et al* (2006). It is known to influence morphological differentiation and to regulate secondary metabolism in Actinomycetes (Huh *et al*., 2004; Kim *et al*., 2003). Morphological differentiation, especially the formation of aerial hyphaea has been strongly associated with the onset of secondary metabolite production (Akinrinsola, 2008). Okamoto *et al* (2003), overexpressed SAM synthetase in *S. coelicolor* to investigate its effect on the production of actinorhodin (ACT). This

enzyme was subsequently found to be 5 - 10-fold higher in the mutant relative to the control. The level of intracellular SAM was increased resulting in the overproduction of ACT. To confirm the link between ACT overproduction and SAM, Okamoto and colleagues added SAM to the culture medium of the wild type *S. coelicolor* strain. The production of ACT was induced upon the addition of SAM. In *S. lividans*, the overexpressed SAM synthetase inhibited sporulation and formation of aerial mycelia but improved the biosynthesis of ACT in liquid media as well as on agar plates (Kim *et al*., 2003). SAM seems to function as a signal molecule that induces transcription of the pathway-specific regulator actORF4 (Okamoto *et al*., 2003). Work by Huh *et al* (2004), Shin *et al* (2006) and Wang *et al* (2007) suggested that SAM has a widespread role in the activation of antibiotic production in Actinomycetes.

Following the positive effect of SAM synthetase in other Actinomycetes, Wang *et al* (2007) overexpressed this enzyme from *S. spectabilis* in *S. erythraea* E2. The production of erythromycin was significantly enhanced (by 54%). Intracellular SAM was implicated in the initiation of secondary metabolite production in *Streptomyces*. As in the findings with other strains, SAM retarded sporulation as well.

Chng *et al* (2008) discovered a developmental transcriptional factor *BldD* that activates the expression antibiotic biosynthetic pathway enzymes. It was concluded that *BldD* regulates both the biosynthesis of erythromycin and morphological differentiation.

Thus it appears that morphological differentiation can be manipulated to improve the biosynthesis of erythromycin in *S. erythraea*. However, production titres are still lower than those for penicillin by a factor of up to 10 (Wang *et al*., 2007).

1.4.3 Engineering primary metabolism

Primary metabolism generates precursor metabolites and cofactors that connect pathways and generates energy required for fueling anabolic reactions. The 12 precursor metabolites from which all cellular constituents are formed, are produced during primary metabolism (Rokem *et al*., 2007). Large numbers of carbon sources are degraded to only the 12 metabolites namely glucose-6-phosphate, fructose-6-phosphate, erythrose-4-phosphate, ribose-5-phosphate, glyceraldehyde-3-phosphate, 3-

phosphoglycerate, phosphoenolpyruvate, pyruvate, acetyl-coenzyme A, oxaloacetate, α-ketoglutarate and succinyl-coenzyme A (Rokem *et al*., 2007). As polyketides have a carbon backbone, limitations in these metabolites and/or the cofactors that knit reactions together could constrain the production of the antibiotics. For example, penicillin is thought to be constrained by limitations in the supply of NADPH rather than in the supply of carbon precursor metabolites (van Gulik *et al*., 2000). Much work has been done with regard to increasing the supply of precursor metabolites to improve the antibiotic production.

NADPH is the cofactor associated with reductive biosynthesis of polyketides. This cofactor is typically generated through the Pentose Phosphate pathway (PPP). If limitations in this cofactor constrain the production of the antibiotic, then enhancing its generation could improve productivity. This approach was taken by Butler *et al* (2002) who deleted *zwf1* and *zwf2* both of which encode isozymes of glucose-6-phosphate dehydrogenase. The levels of Zwf activity was reduced by half relative to the control. Higher antibiotic titres were observed for the mutants compared to the wild type. Lower carbon flux through the PPP correlated with increase in the production of actinorhodin. The conclusion was that lower PPP flux enabled a more efficient utilisation of glucose which resulted in improvement of antibiotic production. Thus for *S. lividans*, increased PPP flux decreased actinorhodin production. NADPH is the major product of the oxidative PPP activity and reducing carbon fluxes through this pathway could limit the supply of this cofactor. The increase in antibiotic production at reduced PPP flux suggests that NADPH was in excess or adequately supplied. In addition, NADPH may have been generated through other pathways. For example, isocitrate dehydrogenase is $NADP^+$-dependent and could supply NADPH in the absence of glucose-6-phosphate dehydrogenase activity. However, Butler and co-workers did not investigate the activities of isocitrate dehydrogenase and it is therefore not possible to draw a conclusion on the how NADPH was supplied. Nevertheless, their work demonstrated that primary metabolism can be genetically manipulated to improve antibiotic production.

As the biosynthesis of secondary metabolites is dependent on the provision of precursors from primary metabolism, the availability of these metabolites is critical for

improved production of antibiotics (Ryu *et al*., 2006). These researchers created *S. coelicolor* mutants in the isozymes *zwf1* and *zwf2* and *pgm* (phosphoglucosemutase gene) to investigate conversion of G6P as the first intermediate of glucose catabolism. Flux to actinorhodin production was found to be more dependent on *zwf2* than on *zwf1*. In *zwf2* mutants, the specific glucose uptake rate and the specific actinorhodin production rate were decreased. However, the yield ($Y_{Act/gluc}$) was increased. In general these findings are in agreement with those of Butler *et al* (2002) in which decreased PPP flux enhanced the production of actinorhodin. In *pgm*-mutants, glycogen formation was increased while actinorhodin production decreased. It was concluded that carbon storage has a major influence on actinorhodin biosynthesis. Stored glycogen during growth on glucose is a possible drain on carbon resources that could go towards the production of the antibiotic. Of the 12 precursor metabolites needed for cellular constituents, acetyl-coenzyme A (acetyl-CoA) is one of the most important precursors for polyketide production (Rokem *et al*., 2006). For *S. coelicolor*, Ryu and colleagues argued that directing carbon flux from acetyl-CoA towards malonyl-CoA could increase the production of the antibiotic. The argument was based on the fact that malonyl-CoA and methylmalonyl-CoA are the most common chain extender units for the reductive biosynthesis of polyketide antibiotics (Ryu *et al*., 2006; Hopwood & Sherman., 1990). Both ACT production and the glucose rate were increased though little change was observed in the growth rate. Also the yields ($Y_{Act/gluc}$ and $Y_{Act/x}$) increased significantly suggesting that overexpression of acetyl-CoA carboxylase (ACCase) caused more carbon fluxes to be diverted to antibiotic production rather than to biomass formation. However, since fructose-6-phosphate is the main control point of the rate of and flux through the Embden-Meyerhof-Parnas pathway (EMP pathway), it would have been a good target for manipulation to investigate the effect. Other researchers have attempted to increase acetyl-CoA levels to enhance the production of other useful metabolites. By overexpressing pantothenate kinase, an upstream rate controlling enzyme, Vadali *et al* (2004) were able to increase the intracellular acetyl-CoA levels in *E. coli*. This illustrates the importance of acetyl-CoA in the biosynthesis of many metabolites of industrial importance. However, there is no literature on the manipulation of this important precursor for *S. erythraea*.

1.4.4 Engineering methylmalonyl-CoA mutase

Erythromycin biosynthesis proceeds via succinyl-CoA, methylmalonyl-CoA, propionyl-CoA and eventually to propionate which is the priming unit for chain elongation along the polyketide synthase assembly line (Reeves *et al., 2007*). Methylmalonyl-CoA mutase (MCM) isomerises methylmalonyl-CoA to succinyl-CoA and its inactivation could increase erythromycin production. In *Acremonium erythreum*, knocking out *mutB*, the gene that encodes MCM, resulted in 75% increase in erythromycin production on starch-carbohydrate medium (Reeves *et al.,* 2004). *S. erythraea mutB* knockouts produced 125% improvement in yield. On soybean oil-based medium, *mutB* knockout resulted in 65% drop in the production of erythromycin. Following up on these findings, Reeves *et al* (2007) predicted that if MCM inactivation decreases erythromycin production then overexpressing MCM genes should result in increased antibiotic biosynthesis in the same medium. This was indeed what was found when MCM operon was duplicated via chromosomal integration. When the entire operon was duplicated, erythromycin production was increased by 50%.

Many of these investigations have focused on engineering enzymes or other metabolites in the product pathway. As precursor metabolites required for antibiotic production are generated during primary metabolism, the product pathway would be subject to the overall control of central metabolism (Martin & Demain., 1980). Optimised enzyme activities and carbon fluxes in the product pathway will probably shift control to central metabolism as precursor metabolites become depleted. Given this situation, genetic engineering is likely to have limited success. A full physiological characterisation comprising primary and secondary metabolism is required to generate primary metabolic leads for subsequent genetic manipulation. Genetically engineered organisms often suffer from instability that results from unstable integration of plasmids and other effects. As such, they tend to be less fit in competition with wild type strains.

1.4.5 Manipulation of culture conditions

The biosynthesis of secondary metabolites is a complex process that is highly dependent on the medium composition and cultivation conditions (El-Enshasy *et al*., 2008). The type and concentration of the carbon source regulate the production of erythromycin (El-Enshasy *et al*., 2008). The growth medium constitutes a large portion of the cost in a bioprocess and impacts on process economics. In erythromycin production, as in many other antibiotics produced by Actinomycetes, the carbon source is often in excess in the medium. Polyketide antibiotics have a carbon backbone and excess carbon ensures adequate supply for the production of the antibiotic. The choice of the carbon source therefore has important cost implications for process economics in industrial fermentations. In an attempt to lower the cost of the growth medium, El-Enshasy *et al* (2008) investigated the suitability of different carbon sources for erythromycin production in shake flask fermentations. The highest volumetric erythromycin production was obtained with a combination of 60 g/L sugar cane molasses as a sole carbon source and a combination of corn steep liquor and ammonium sulphate as nitrogen source. On this medium, erythromycin production was 33% higher than on glucose-based medium. Interestingly, the production of erythromycin was very low on galactose, fucose and arabinose despite good growth on these carbon sources. This probably suggests that when growing on these carbon sources, precursors were mainly diverted to biomass formation relative to erythromycin biosynthesis. The fact that a higher biomass formation resulted in lower antibiotic may have to do with inactivation of erythromycin biosynthetic enzymes or lack of precursors. It is also consistent with faster growth which normally results in high biomass formation and little antibiotic production. Other carbon sources such as sucrose, trehalose, maltose, β-lactose also and α-lactose resulted in low antibiotic production. However, growth on both propionate and 1% (v/v) *n*-propanol significantly increased erythromycin production. It was found that yield ($Y_{p/x}$) was higher relative to the medium without *n*-propanol supplementation. It was suggested that this was partly due to better mass transfer due to increased membrane permeability (Moragues *et al*., 1994). These researchers subsequently developed an industrial growth medium by combining sugar cane molasses, corn steep liquor and ammonium sulphate with *n*-propanol supplementation which resulted in

erythromycin production 80% higher than the initial industrial growth media under the same conditions.

Because sugar cane molasses is a by-product of the sugar industry and therefore a cheap alternative to glucose, this represents an improvement in the process economics of erythromycin fermentations. However, the levels of erythromycin produced are far below the levels obtained for penicillin.

1.4.6 Utilising oils to enhance antibiotic production

Oils are commonly used in industrial fermentation media to enhance the production of secondary metabolites. Among the advantages are their high energy content compared to carbohydrates on a weight by weight basis in addition to the fact that they are sources of precursors for the biosynthesis of many secondary metabolites (Cavanagh *et al*., 1994; Large *et al*., 1998). As such, the use of oils either as supplements to other carbon sources or as sole carbon source have been investigated in various fermentations with different organisms. The production of clavulanic acid in *Streptomyces clavuligerus* on olive oil as a sole carbon source has been studied by Efthiomiou *et al* (2008) in bioreactor fermentations. The rationale for this study was the fact that *S. clavuligerus* utilises glycerol which is a product of oil degradation by lipases. Higher biomass and clavulanic acid yields ($Y_{p/x}$) were obtained on olive oil as compared to glycerol as sole carbon source. The increases in biomass and the antibiotic were 2.5-fold and 2.6-fold higher relative to growth on glycerol. Under the conditions tested, olive oil enhanced both biomass formation and the rate of antibiotic production. The cells were able to take up the fatty acids and utilise them for energy generation and/or precursor synthesis (Efthiomiou *et al*., 2008). Fatty acids are known to be metabolised via the β-oxidation pathway resulting in increased propionate levels. An interesting observation was the fact that protein concentrations increased even when growth had stopped. Biomass formation is dependent on proteins and its decline should be reflected in the rate of protein synthesis. The increase in protein synthesis in the absence of growth may reflect increased biosynthetic enzyme activity. Increased production of lipases to facilitate oil degradation in the medium and the synthesis of biosynthetic enzymes in the clavulanic pathway may account for the observed steady increase in protein concentration.

The use of oils as carbon source to enhance erythromycin production in *S. erythraea* was evaluated by Hamedi *et al* (2004). Though a large variety of seed and nut oils as well as shark oil were evaluated, none were suitable as a sole carbon and energy source. However, when used as supplements to the medium containing dextrin and soya bean flour as main substrates, black cherry kernel oil (55 g/L) yielded the highest titre of erythromycin (4.5 g/L). On shark oil, cotton seed oil and coconut oil, the culture produced a higher biomass, produced the red pigment and yielded the lowest amounts of erythromycin titres. As reported earlier, erythromycin production appears to be enhanced by lower biomass formation. In the competition for precursors, biomass formation seems to be favoured over secondary metabolite production. This is not surprising since metabolic pathways are optimised for growth. Thus, the red pigment may be produced to maintain equilibrium at high growth rates. It may be produced as an energy-spilling reaction, which is also called overflow metabolism. Limiting biomass synthesis through oxygen limitations appears to reduce the excretion of the red pigment and enhance the production of erythromycin. The oils that yielded the highest titres, black cherry oil, water melon seed oil and melon seed oil, produced low biomass and did not lead to the excretion of the red pigment. It has been shown previously that improved growth rate on oil-based medium resulted from improved oxygen uptake (Mirjalili *et al*., 1999).Also, the production of erythromycin and the red pigment under oxygen limitations has been reported in Clark *et al* (1995). The results from the studies of Hamedi *et al* (2004) indicate that the oils were co-metabolised with dextrin as carbon sources to produce precursor metabolites. The oils were found to cause the formation of longer hyphaea and lengthen the vegetative phase of the culture. Similar observations were made for *Streptomyces hygroscopicus* cultured on glucose-based supplemented with 0.5% methyl oleate (Gojgic-Cvijovic *et al*., 2000). They were able to increase the titre of erythromycin by 2.5 times and the mycelium yield by 27% relative to the medium without methyl oleate addition. Less proteolytic activity was measured for the fermentations supplemented with 0.5% methyl oleate and 0.5% Tween 80 respectively. It seems oil enhances mycelium formation and prolongs the vegetative production phase. The positive effect of methyl oleate on antibiotic production may partly be due to their ability to enhance valine uptake. In the same study, valine dehydrogenase activity increased significantly in the fermentation supplemented methyl oleate. Greater amino

acid uptake did improve the productivity of antibiotics in some strains (Mouslin & El-Haloui., 1997; David *et al*., 1992).Though oils can improve the production of erythromycin, there are oxygen uptake limitations associated with oil-based growth media. The positive effect of oil supplementation on *S. erythraea* fermentations is dependent on the scale. At 7L scale, addition of rapeseed oil to dextrin-based medium increased erythromycin production at 700 RPM. However, at 2L scale oxygen limitations at 500 RPM resulted in lower erythromycin titres relative to the 7L fermentation. Another finding was that growth rate was less dependent on the initial oil concentration, though increasing the agitation rate increased growth rate (Mouslin & El-Haloui., 1997).

Using oils as carbon sources has distinct disadvantages particularly with regard to limitations in oxygen uptake. Such fermentations typically have higher oxygen requirements compared to carbohydrate-based fermentations (Stowell., 1987). In addition, residual oil makes purification and subsequent analysis more difficult necessitating the use of more elaborate downstream processing techniques. More elaborate downstream operations may result in product loss and increases process cost.

1.4.7 Physiological characterisation of metabolism

Primary and secondary metabolisms interact to produce secondary metabolites. The primary aim of carbon source degradation is to generate carbon skeletons and energy required for cell synthesis and maintenance. During this process, degradation proceeds via a variety of pathways depending on the nature and concentration of the carbon source, cell requirements and other culture conditions. The growth process draws off precursor metabolites generated by central metabolic pathways mainly for biomass formation. In general, glycolysis is associated with generation of energy and NADH as a cofactor. The Pentose Phosphate pathway generally generates the biosynthetic cofactor NADPH. There is, therefore, a link between primary and secondary metabolism in the production of secondary metabolites as both compete for precursors.

Though central metabolism provides the precursors for secondary metabolite formation, many of these precursors are themselves required for primary biosynthesis. Therefore,

regulatory control is integrated and exerts overall influence on flux distribution and other processes. This type of regulatory control affects different biosynthetic processes and operates as a function of the growth rate (Demain & Martin, 1980). Individual pathways, on the other hand, are regulated by inducers, precursors, catabolites and end products. For example, fluxes through central metabolism are known to be directed by energy and electron donors in *Saccharomyces cerevisiaea* (Ayar-Kayali, 2011; Horne *et al*, 1970; Vaseghi *et al*, 1999) which are themselves essentially products of primary metabolism. To successfully increase the yield of target antibiotics, strain improvement strategies should therefore involve both the specific product pathway and central metabolism. Given the nature of the two types of metabolism, the supply of precursor metabolites generated during primary growth could constrain the biosynthesis of secondary metabolites. Much research has focussed on the link between primary and secondary metabolism in various organisms. Since organisms are optimised for growth, primary metabolism takes preference in the allocation of carbons.

1.4.8 Induction of erythromycin production

To investigate the onset of erythromycin production, Giles *et al* (1995) manipulated the relationship between the production of the antibiotic and the culture growth rate. By changing the nature of the growth-limiting substrate, they were able to monitor the changes in the concentrations of uncharged amino acyl $tRNA^{LEU}$ and charged $tRNA^{LEU}$. The rationale for their approach is the fact that the rate of protein synthesis and tRNA charging are dependent on the amount and rate of change of nutrient availability in the medium (Koch, 1980). mRNA was undetectable during the accelerated growth phase and was only detected after the growth rate had decreased which suggests that regulation is at transcription level. Though erythromycin was growth-related in the nitrogen-limited medium, its production in carbon-limited medium was non-growth related. However, under both growth conditions, the onset of antibiotic production coincided with the drop and increase in the concentration uncharged tRNA and charged tRNA respectively. Notably, in the nitrogen-limited medium, the rate of protein synthesis was significantly decreased throughout the fermentation time. Erythromycin was produced during this period of elevated charged tRNA concentrations. It appears

there is a correlation between the rate of protein synthesis and the onset of erythromycin production.

Their findings confirmed those of Reeves and Baumberg (1998) who concluded that part of the control of erythromycin production is exerted at transcriptional level. The conclusion of Reeves and Baumberg (1998) was based on the finding that erythromycin production was repressed when ammonium was used as a nitrogen source. Using Northern Blot, they detected no *ery* mRNA in the RNA from the culture grown on ammonium. However, the actual control of the onset of the antibiotic production is probably a much more complex process that involves genetic control of signalling and cascade reactions.

1.4.9 Bioreactor operational mode

In batch culture, secondary metabolites are produced upon depletion of the limiting nutrient as stated earlier. Whether the production follows a classical pattern or is growth-related depends on the nature and identity of the growth limiting substrate (Giles *et al*., 1995). If the production of the secondary metabolite follows a classical pattern, the titre is improved by prolonging the stationary phase. However, operating in batch mode poses a process design conflict in that good growth is required while the depletion of the growth-limiting nutrient is essential for product biosynthesis (Lynch *et al*., 1995). Increasing the growth-limiting substrate results in better growth but simultaneously increases the time required for the onset of the product formation. The result is a much longer production process and higher production cost.

Some of the drawbacks of batch culture can be overcome by operating in fed batch mode. The exponential growth rate is often controlled by controlling the feed rate. This strategy has been used to avoid oxygen limitations in yeast fermentations (Reed & Peppler., 1973). If the growth rate is carefully controlled by controlling the supply of crucial nutrients, the stationary phase and, therefore, the production phase can be prolonged. This is well-established strategy in biopharmaceutical production processes (Bushell., 1988; Bushell *et al*., 1994). Gray and Vu-Trong (1987) increased tylosin production by feeding the growth-limiting nutrient at intermittent intervals in *Streptomyces fradiae*. However, fed batch culture has the disadvantage of straining

cultures due to the build-up of metabolic waste. This also often results in low antibiotic production due to high toxins levels that accumulate in the culture.

A much more novel strategy was employed by Lynch *et al* (1995) to describe the physiology of erythromycin production in cyclic fed batch culture. The approach was based on the work of Giles *et al* (1995) and Clark *et al* (1995) which linked the onset of erythromycin production to the decrease in protein synthesis and hence the growth rate. The decrease in growth rate was assumed to trigger the production of the antibiotic. The quasi-steady state concept of Pirt (1975) was assumed. By feeding immediately after the increase in biomass formation, a quasi-steady state was achieved during which specific growth rate was equal to the dilution rate. Having established the quasi-steady state conditions, the growth phase was down-regulated without having to reduce the concentration or feed rate of the limiting nutrient. The strategy allowed the manipulation of growth rate independent of the nutrient concentration which allowed for simultaneous increase in productivity and product titre. Increasing the concentration of the growth-limiting nutrient resulted in increases in the antibiotic titre. Increases of up to 180% in erythromycin production were obtained at low dilution rates relative to the batch culture.

1.4.10 A model for the control of erythromycin in batch and cyclic fed batch fermentation

Bushell *et al* (1997) proposed a model for the control of erythromycin in batch and cyclic fed batch culture. This was based on the findings of Giles *et al* (1995), Lynch *et al* (1995) and their own work. In essence, the model suggest an explanation for the growth rate kinetics observed for glucose-limited and nitrate-limited cultures in Giles *et al* (1995). By measuring the substrate affinities, it was found that lower affinity for nitrate leads to early down-regulation of growth rate resulting in apparent early onset of erythromycin. This explained why the production of the antibiotic was growth-related in nitrogen-limited media. The much higher affinity for glucose meant that growth continued for much longer and the charged tRNAs were not produced until after growth had stopped. As a result, the antibiotic was only produced after the growth phase. The conclusion that down-regulation in protein synthesis results in antibiotic production was made in earlier work by Wilson and Bushell (1995). The model places the highly

phosphorylated guanidine nucleotide ppGpp, at the centre of control of antibiotic production. Many bacteria use this nucleotide, which is also called the stringent factor, for sensing nutrient starvation and triggering adaptive responses (Hesketh *et al*., 2007). In *E. coli*, ppGpp down-regulates tRNA biosynthesis and the production of ribosomes when the culture is starved of aminoacids (Hesketh *et al*., 2007). The role of ppGpp in regulating antibiotic production in *Streptomyces* is discussed extensively in Hesketh *et al* (2007).

In other work, ppGpp is reported to be initiated by the accumulation of tRNA (Lamond & Travers, 1985). However, other groups have reported production of antibiotics in the absence of this nucleotide (Takano *et al*., 1992; Bascaran *et al*., 1991). Clearly, this model requires further refinement, given the conflicting findings regarding the role of ppGpp from the different groups.

This work has established the important role of growth rate in the production of erythromycin production. Understanding the physiology of growth kinetics is a critical aspect of studies. However, since the regulation of antibiotics is complex involving overall integration of various central metabolic and product-specific pathways and associated metabolites, a more comprehensive investigation is required. Focusing on the growth rate, growth conditions or genetically manipulating product pathways without thorough characterisation of the physiology is likely to have limited success. Such an investigation will need to include key branch point enzymes, energy nucleotides and cofactors and other intracellular and extracellular metabolites in an integrated form.

1.5 Carbon flux distributions approach

The study of carbon flux distribution in microorganisms is used as part of rational strain improvement. The classical approach to strain improvement was based on random

mutagenesis and repeated selection of strains with desirable traits. Studying the distribution of carbon fluxes identifies potential targets for genetic manipulation. The strategy can generate useful information on the split of fluxes at branch points and identify points of constraint in pathways. To be useful, an evaluation of the distribution of fluxes through the pathways requires a good understanding of cellular physiology

and biochemistry of the producing organism. A useful tool here is Metabolic Flux Analysis (MFA) in which intracellular metabolic fluxes are quantified based on mass balances around intracellular metabolites under pseudo-steady state conditions (Kim *et al*., 2007).

1.5.1 Constraint-based flux analysis

Determination of flux distributions using stoichiometric equations is used widely as part of metabolic flux analysis. Often only stoichiometric knowledge is required to compute stationary fluxes and optimise constraints. The simplicity and ease of use are perhaps its advantages over other methods. The strategy was successfully used by Vallino and Stephanopoulos (1994) to identify constraints in the production of lysine in *Corynebacterium glutamicum.* Knowing that the Pentose phosphate pathway in this organism generates NADPH, they investigated the flexibility of the G6P branch point. Responses of flux distribution to alterations in the glucose-6-phosphate dehydrogenase were investigated for their possible constraints on lysine production. It is known that improved lysine production results from significant changes in the flux partitioning at G6P, PEP and pyruvate branch points (Broer *et al*., 1993). An additional perturbation was created by growing the culture on gluconate supplemented with glucose to avoid linear growth. Gluconate is metabolised via the PPP thereby creating different carbon flux split dynamics at the key branch point under investigation. Constraints in the production of lysine were found to be suboptimal partitioning of fluxes at the three branch points (G6P, PEP, pyruvate). Suboptimal generation of precursors required for lysine production constrained product formation. G6P was found to be of average rigidity suggesting the yield was constrained at either PEP or pyruvate branch point.

A further example of the use of carbon flux analysis in fed batch fermentation was provided by Li *et al* (2007). They calculated carbon fluxes in propionate fed batch fermentation in shake flasks. The experiment was aimed at evaluating the changes in carbon fluxes through the PPP and the anaplerotic reaction and the flux from pyruvate to acetyl-CoA through metabolic flux analysis. The changes in the pathways were then correlated with the production of streptoglydigin. G6P and the pyruvate nodes were found to be potential bottlenecks for the improvement of the antibiotic.

Metabolic flux analysis based on stoichiometric knowledge was successfully employed by van Gulik *et al* (2000) to develop a stoichiometric metabolic model for the growth and penicillin G production in *P. chrysogenum*. Flux distribution through the network was calculated as a function of biomass synthesis rate and the rate of penicillin production. Calculation of the metabolic flux based on the model revealed that penicillin production correlated with significant flux alterations in primary metabolic pathways. Such changes would occur at principal metabolite nodes which are potential bottlenecks. These predicted changes were confirmed in carbon-limited chemostat cultures on glucose, ethanol and acetate as carbon sources. Based on measured fluxes, metabolic flux analysis showed significant differences in flux partitioning around the predicted principal metabolite nodes when the culture was grown on the different carbon sources without affecting the production of the antibiotic. The conclusion was made that primary carbon metabolic flux did not constrain penicillin production. Metabolic flux analysis predicted flexibility of the glucose-6-phosphate node raising the possibility that it could be manipulated to enhance antibiotic production. *P. chrysogenum* was grown on different combinations of carbon and nitrogen sources namely glucose and NH_3, Xylose and NH_3, glucose and NO_3 and Xylose and NO_3. The total cytosolic NADPH demand was manipulated and correlated with penicillin G production. The model revealed that penicillin G is constrained by the supply in cytosolic NADPH. However, NADPH is generated by other dehydrogenases including isocitrate dehydrogenase, mannitol dehydrogenase and acetaldehyde dehydrogenase, so it could not be concluded where the actual constraint lies (Loftus *et al*. 1994; Hult *et al*., 1980; Postma *et al*., 1989). There are other sources of NADPH depletion such as the presence of NADPH oxidase (Djavadi *et al*., 1980). It requires detailed knowledge of the physiology of the production organism to gain useful information from metabolic flux information. For example, it is not known if NADPH oxidase is present in *P. chrysogenum* and therefore its potential contribution to NADPH depletion should not be overlooked. Determining activities of glucose-6-phosphate dehydrogenase and isocitrate dehydrogenase would reveal the contribution of each to NADPH depletion.

In *S. lividans* metabolic flux analysis was used to reveal the dependence of carbon flux distribution through pathways on growth rate and the carbon and energy source

(Avignone -Rossa *et al*., 2002) and the pathway and fluxes that affect the production rate of the calcium-dependent antibiotic in *S. coelicolor* (Kim *et al*., 2004). Using metabolic flux analysis, Daae and Ison (1999) discovered that the pathway fluxes in *S. lividans* were mainly influenced by the rate of oxygen utilisation. Oxygen utilisation could be used as a regulatory parameter in *S. lividans* fermentations.

Though metabolic flux analysis can generate important information, it relies heavily on intuitive assumptions. There are many more reactions in the network than there are available quantitative metabolic data. The calculations for such an underdetermined system depend on assuming that metabolic goals such as biomass production are optimum even though the growth of biological systems is often suboptimal (Feng *et al*., 2010). In addition, there are some native processes that cannot be described by FBA (Feng *et al*., 2010).

The method assumes that all reactions do take place even though they may be thermodynamically unfavourable. Constraints are needed to assume flux directions that correlate with corresponding changes in Gibbs free energy (Kim *et al*., 2007). Many other assumptions are often made with regard to product concentrations and energy generation. Another drawback is that the method does not account for any changes in metabolite concentrations such as product accumulation or substrate depletion and enzyme inhibition. Results of metabolic flux analysis are hypothetical and therefore this type of flux analysis cannot accurately describe the cellular metabolism. In addition, actual cellular metabolism can operate in suboptimal modes rendering the optimisation-based results less accurate (Palsso *et al*., 2003; Fischer & Sauer., 2005).

1.5.2 ^{13}C-based flux analysis

In ^{13}C-based flux analysis *in vivo* fluxes are calculated based on labelled substrates for example glucose. This is a more accurate representation of fluxes since the actual carbon flow through a particular branch is measured (Nielsen, 2003; Sauer, 2006). In tracer studies both the extracellular fluxes and biosynthetic requirements are indirectly inferred from ^{13}C data obtained through Nuclear Magnetic Resonance (NMR) or Mass Spectrometry (Sauer, 2006). The distribution of fluxes is identified by fitting the

unknown fluxes to the measured data. Mathematical models describe the relation between the unknown flux and the measured data. This method has a weakness in that it is restricted to only 10 - 15 preselected fluxes that are directly accessible from the measured data (Sauer, 2006). Since flux distribution is identified by iterative fitting of fluxes to the measured data, obtaining accurate flux values throughout the network based on such a low number of fluxes is likely to yield inaccurate results. The flux ratio method quantifies the relative contribution of converging pathways to the formation of a particular product. As such, this method provides direct evidence for the relative in vivo activities of a particular reaction (Sauer, 2006).

1.5.2.1 Radio-respirometry

Obanye *et al* (1996) evaluated carbon flux distribution in *Streptomyces coelicolor* to study the physiology of methylomycin production. The metabolism of glucose was monitored by means of a radio-respirometry technique. Using the degree to which labelled carbon atoms of glucose were released from the respective metabolic pathways as CO_2, they were able to determine the flux ratios between different pathways. Methylenomycin production was associated with increased PP pathway flux relative to flux to the EMP pathway. Because the PP pathway generates NADPH and this metabolite is required for reductive biosynthesis of polyketides, its supply was suggested as a potential constrain to antibiotic production.

1.5.2.2 Isotope labelling combined with GC-MS analysis (tracer studies)

A similar approach was used by Jonsbu *et al* (2001) to study in vivo central metabolic fluxes during nystatin production in *Sreptomyces noursei* in batch culture. The ^{13}C-labelling patterns of amino acids in biomass were measured using GC-MS together with calculated fluxes. Their findings indicate that most of the NADPH required for growth went towards the synthesis of amino acids. Though this was based on the assumption of NADPH requirement for growth for *P. chrysogenum* and *S. noursei* on defined medium, the findings probably give a fairly good indication of the high growth demands for NADPH in general. Together with the calculated carbon fluxes, such information is

useful in determining the constraints in the production of the antibiotic. Subsequent mutagenesis then becomes more targeted and not random as in classical techniques.

While intracellular fluxes can be estimated relatively accurately using ^{13}C-based analysis, its complexity when dealing with large metabolic network is a drawback (Kim *et al*., 2007).

1.5.3 Metabolic physiology investigations based on biochemical studies

Though carbon flux analysis is useful, it generates no information on the metabolite concentrations such as the pyridine cofactors NADH and NADPH or the energy nucleotides ATP, ADP and AMP. As such, it is not possible to account for the energetics in a fermentation based on carbon flux analysis alone. To get a clearer picture of the overall metabolism, biochemical studies that involve enzyme kinetics and the energetics in addition to flux distribution are necessary. Fluxes can be inferred from enzyme activities and pathway products. Such a physiological study will account for metabolism that operate in suboptimal conditions and probably yield results that more accurately describe *in vivo* metabolism. This approach was used by Ayar-Kayali (2011) to analyse the PPP flux in *Amycolatopsis orientalis* and characterise the physiology of vancomycin production.

It is clear from the literature survey that the physiology of erythromycin production in *S. erythraea* has not been adequately investigated. Much of the physiological characterisation has focused on engineering the product pathway without regard for the overall central metabolism. As such, the role of primary metabolism in supplying precursor metabolites for erythromycin production has not been thoroughly investigated in *S. erythraea*. As a result, the physiology and the metabolic basis for the production of erythromycin are poorly understood. In contrast, the increase in penicillin productivity achieved, is a result of extensive physiological characterisation of central metabolism in *C. chrysogenum*. After extensively characterising the physiology, metabolic flux analysis was employed to yield meaningful information regarding bottlenecks and constraints in the production of penicillin (van Gulik *et al*., 2000).

1.5.4 Current research approach

To understand the regulation of erythromycin production in *S. erythraea* requires comprehensive characterisation of its metabolic physiology. We have seen that other antibiotic producing organisms such as *S. coelicolor* and *P. chrysogenum* have been extensively studied in terms of their physiology. In contrast, very little information is available on the physiology of erythromycin production in *S. erythraea*. There is, therefore, a gap in the knowledge of the overall regulatory control in *S. erythraea* needed to increase the production of erythromycin. There is little information available regarding the distribution and control of fluxes in *S. erythraea*. Equally, little information exists on flux partitioning at metabolite nodes and how such partitioning affects erythromycin productivity.

The current research, therefore, focuses on characterising growth and product kinetics and attempts to provide a physiological basis for product formation. This involves investigating the link between primary and secondary metabolism. The change in flux from primary to secondary metabolism is correlated with changes in enzyme activities at key branch points. An analysis of the behaviour of key enzymes is conducted to investigate changes in pathway flux. Since pathways are connected by common use of pyridine cofactors and adenylate nucleotides, assaying these metabolites could provide important information on the changes in flux between pathways. Results from these studies will provide a body of information upon which subsequent rational genetic manipulations can be based. Such information is also important for metabolic flux analysis as it provides detailed physiological and kinetic information required for meaningful estimation of optima. The design of the research methods to carry out these investigations is provided in Chapter 2.

1.6 Aims

- To investigate the carbon metabolite distribution in *Saccharopolyspora erythraea* during the growth phase and the erythromycin synthesis phase
- To investigate how *Saccharopolyspora erythraea* controls the production of erythromycin

1.7 Objectives

- Determine growth and product kinetics during growth on glucose and gluconate
- Measure the activity of branch point enzymes to determine pathway activity
- Data will be integrated to construct a metabolite flow model for the growth and erythromycin production phases respectively
- Determine the effect of feeding precursor metabolites on the production of erythromycin

1.8 Hypothesis

Erythromycin production in *Saccharopolyspora erythraea* is constrained by limitations in the supply of precursor metabolites.

2.0 Research Methods

The need to characterise the physiology of *S. erythraea* in terms of growth and product kinetics was discussed in Chapter 1. As a brief summary, it was pointed out that to characterise the metabolism in an organism, detailed knowledge of the physiology and biochemistry is required. With the sequencing of the complete genome of *S. erythraea*, many more targets are available for genetic manipulation as part of strain improvement. However, genetic interventions are only successful if based on sound physiological information. This project focuses on metabolite profiling combined with growth and product formation kinetics under different growth conditions to reveal the regulation of erythromycin production.

2.1 Bacterial strain and culture conditions

Saccharopolyspora erythraea NRRL2338, wild type, red variant strain was used for the current work. The strain was maintained in 20% glycerol in 1 ml working cell banks stored at -80 °C. All fermentations were performed in defined media that were prepared in ultrapure water. Nitrogen-limited media were used for all experiments throughout the project. Glucose was autoclaved separately from the salt solution containing the phosphate buffer and nitrate to prevent it from caramelising. The growth media were prepared in the quantities listed in Table 1. The trace elements were prepared by first dissolving $MgSO_4.7H_2O$ in ultrapure water and then adjusting the pH to 2 with 0.2 M H_2SO_4. The rest of the trace elements were added in the order listed in Table 2. The trace elements were sterilised by filtering through a 0.22µm filter (Sartorius, UK). All prepared media components were stored at 4°C when not in use. Glucose and the trace elements were added to the media in a ratio of 10:1. A C/N ratio of 36:1 was used for all experimental work performed based on the work of Ushio (2003).

Table 1 Composition of the basic medium.

Component	**Concentration (g/L)**
Glucose	30
$NaNO_3$	2.38
K_2HPO_4	7.87
KH_2PO_4	3.37
Trace element solution (volume)	10% of glucose volume

Table 2 Composition of trace element stock solution.

Component	**Concentration (g/L)**
$MgSO_4.7H_2O$	25
$FeSO_4.7H_2O$	1.38
$CuCl_2.2H_2O$	0.067
$CoCl_2.6H_2O$	0.101
$CaCl_2.2H_2O$	1.38
$ZnCl_2$	1.04
$MnCl_2.4H_2O$	0.97
$Na_2MoO_4.2H_2O$	0.035

2.2 Reagents and chemicals

All reagents were sourced from Sigma-Aldrich (Gillingham, UK) unless otherwise stated in the text.

2.3 Fermentation conditions

2.3.1 Shake flask culture conditions

Results presented in Chapter 3 and 4 were from fermentations performed in 2 L shake flasks. The cultures were grown at 28°C and an agitation rate of 200 RPM. To prevent clumping and enhance mixing, spherical springs were inserted into the flasks. A two stage inoculum development was maintained for all fermentations. One 1 L shake flask with a working volume of 100 mL was inoculated with content from one cryovial (1 mL) and grown for a period ranging between 28 and 32 hours before being used to inoculate 3 shake flasks of 2 L volume containing 150 mL growth medium. Each of the 2 L shake flask was inoculated with 45 mL of the first stage culture. Glucose and the trace element solution were first added to the basic medium before the inoculum was transferred. The trace element solution was sterilised by filtration trough a 0.22 µM filter (Sartorius, UK) under sterile conditions.

For the bolus-feed addition fermentations, oxaloacetate was sterilised through a 0.22µm filter (Sartorius) to avoid degradation if autoclaved. Methyl oleate was autoclaved at 121°C for 15 minutes. Feeding was done by adding 2% (v/v) of the precursor metabolite carbon source to the shake flask culture. The cultures were grown on glucose as a sole carbon source and both biomass and erythromycin determined. Concentrations of 2 mM, 3 mM and 4 mM were used for each of the following: phosphoenolpyruvate (PEP), oxaloacetate (OAA) and propionate. For methyl oleate the following concentrations were used: 5 $g.L^{-1}$, 7.5 $g.L^{-1}$ and 10 $g.L^{-1}$. Feeding was done at 30, 45 and 60 hours.

For bolus feed addition fermentations in bioreactors, the same procedure was followed as was used for the shake flask cultures. However, 3 mM oxaloacetate was fed at 45 and 71 hours while 10 $g.L^{-1}$ methyl oleate was added at 60 and 86 hours. In shake flask

culture, addition of PEP did not increase the level of erythromycin significantly and was therefore not used in bioreactor fermentations. Propionate was not used in bioreactor culture due to technical reasons.

Bolus-feed additions shake flask fermentations

Three concentrations each of phosphoenolpyruvate, oxaloacetate, methyl oleate and propionate were prepared representing a high (4 mM), low (2 mM) and midpoint (3 mM) concentration. In the case of methyl oleate, these cocentrations were 10, 7.5 and 5 $g.L^{-1}$. Using a design of experiments approach, each metabolite concentration was matched to a 30, 45 and 60 hours fermentation point. Samples were collected at 48, 72 and 96 hours. For the culture fed at 60 hours, samples were collected at 72 and 96 hours only.

2.3.2 Bioreactor culture conditions

For the bioreactor fermentations, stage one inoculum was prepared the same way as in the case of shake flask cultures. A volume of 45 mL was transferred from the 1L shake flask to a 2 L shake flask containing 400 mL 455 mL growth medium (400 mL basic medium, 50 mL glucose and 5 mL trace element solution). After growth for 27 hours, 500 mL from each 2 L flask was used to inoculate each of three New Brunswick bioreactors containing 4 L growth medium.

Fermentations were performed in 7 L bioreactors (New Brunswick Scientific Co. Inc.) with Bioflow 110 control units and Biocommand Plus version 3.28 software controls. The working volume was 5 L and agitation was controlled at 700 RPM with Rushton turbine impellers. pH 7 was maintained by automatic addition of 2M H_2SO_4 and 4M NaOH via peristaltic pumps. Foaming was controlled manually by sterile injection of Dow Corning DB-110 A silicone based antifoam (Barry, UK). The VG Gas Analyzer Prima 600 mass spectrophotometer was used for off gas data analysis. The flow rate of air into the bioreactors was set at 2.5 VVM. The minimum dissolved oxygen concentration in the reactors was set at 30%.

2.4 Sampling and Quenching

A brief outline of the sampling process and sample processing is given in Fig. 5.

2.4.1 Samples for biomass, glucose, nitrate, extracellular metabolites, enzymes and pyridine cofactors

A volume of 20 mL of broth was collected rapidly in plastic sample bottles and frozen immediately by placing into a dry ice/methanol bath. The samples were stored at -80 °C for further analysis. Samples for pyridine cofactors were not quenched but were flash frozen in a dry ice/methanol.

2.4.2 Samples for ATP, ADP an AMP

The samples for adenylate nucleotides were quenched in a 10 mL quenching solution consisting of 60% (v/v) methanol/70 mM HEPES pH8 (Faijes *et al*., 2007). The quenching solution was prepared beforehand and stored at -80°C. The solution was kept in a methanol/dry ice bath during and immediately after sampling to maintain the -80°C temperature. Sampling was done by adding 10 mL of the sample to 10 mL quenching solution precooled to -80°C. The sample was directly placed in the methanol/dry ice bath and stored at -80°C for further analysis. The whole process of sampling took a maximum of 10 seconds per sample to complete. The samples were quenched within 5 seconds as they were collected directly into the precooled solution.

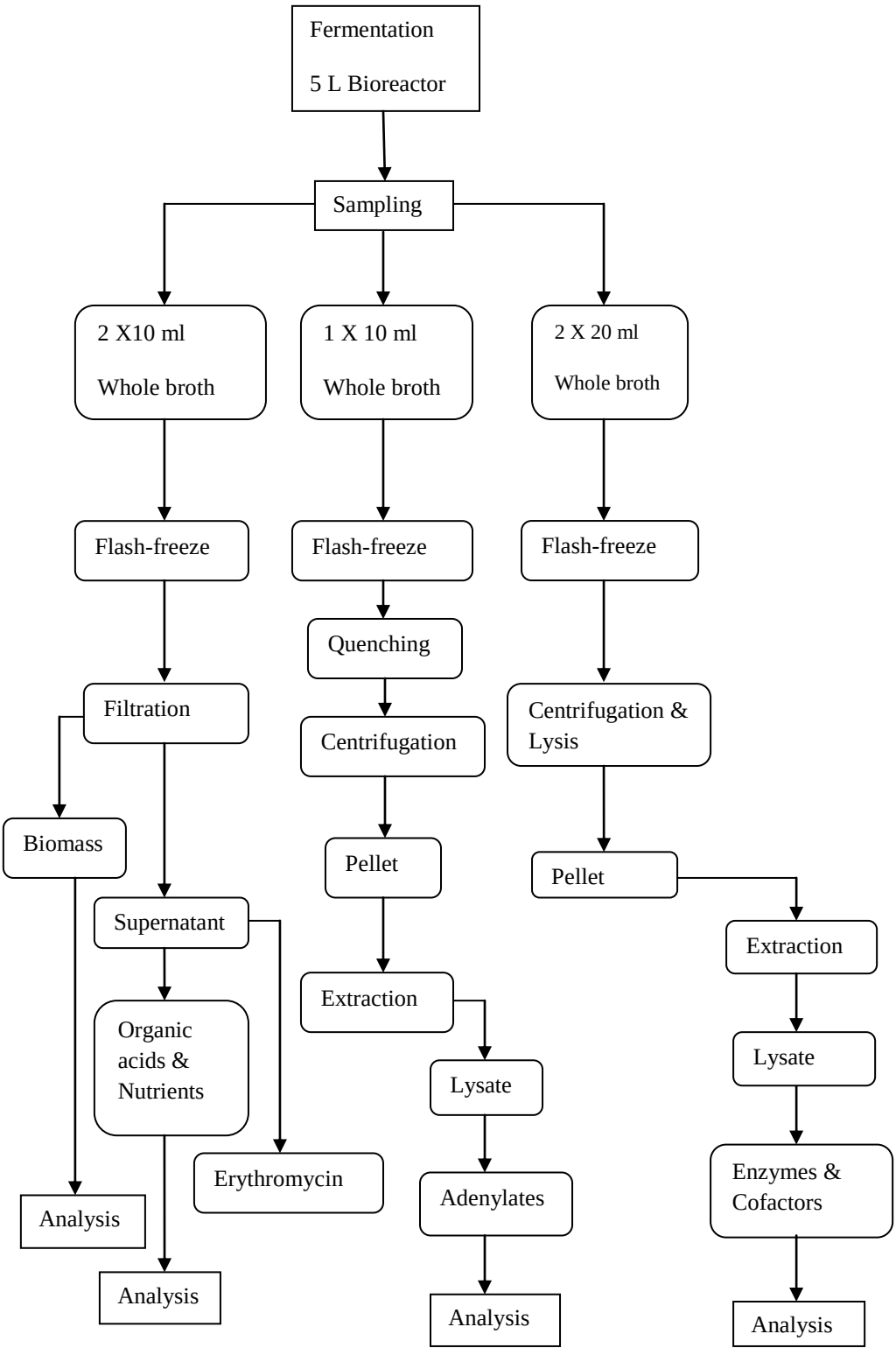

Fig. 5 Layout of the sampling procedure before analysis. Duplicate samples were taken for biological replication. Sample grouping was done based on sample treatment after flash freezing. All sampling was done manually.

2.5 Analytical Determinations

2.5.1 Biomass determination

Samples were thawed on ice after which 10 ml was filtered through pre-weighed glass fibre prefilters (Millipore, Watford, UK). No cell breakage, clumps or pellets were observed. It is not clear if any metabolite leakage occurred as this was not assessed. However, it was assumed that cooling on ice would reduce potential shock and subsequent metabolite leakage. The filtrate was retained for the analysis of extracellular metabolites. The filters containing the biomass were then dried at 90 °C for 18 hours. After reweighing the filters, the dry cell weight of the biomass was determined from the difference in the weights.

2.5.2 Erythromycin

Erythromycin was captured on C18 Bond Elut solid phase extraction column (Varian Inc., Oxford, UK) as described in Heydarian *et al* (1998). The column was equilibrated with a volume of 5 mL each of 1% diethylamine (DEA)/methanol (v/v) and potassium phosphate buffer (10 mM, pH7.2).The pressure was maintained below 6 mm Hg throughout. After rinsing with potassium phosphate buffer, 5 mL of sample was applied after which the column was washed with 1 mL of 45% methanol to remove red pigment that could interfere with analysis. Erythromycin was eluted with 1 mL of 100% methanol. The final product was filtered through 0.22 μm filter (Sartorius) and stored at -20 °C for further analysis.

Erythromycin was quantified according to the method of Heydarian *et al* (1998) using a Dionex Summit HPLC System with UV (UVD) and refractive index detection. The column used was a reversed phase PLRP-S 8μm, C18 with dimensions 150 X 4.6 mm and guard column with dimensions 5 x 30 mm (Varian Inc., Oxford, UK). The mobile phase was 55% (v/v) 10 mM potassium phosphate (pH7.2)/45% (v/v) acetonitrile. The flow rate and temperature were maintained at 1 mL/minute and 60 °C respectively. The injection volume was 50 μL and the antibiotic was detected at 215 nm. For Chapter 5 results, erythromycin was detected at 200 nm. For all other chapters, erythromycin was

detected at 215 nm due to technical reasons. A comparison of the results at both wavelengths indicates that they were comparable. Quantification was done by integrating the peak areas and comparing the values with those obtained using solutions containing known amounts of erythromycin derived from a standard curve.

2.5.3 Organic acids, glucose, nitrate and the red pigment

The supernatant was filtered through 0.22 μm filter (Sartorius, Loughborough, UK) and frozen at -20 °C. An Aminex HPX-87H (30 x 2.5 cm) column was operated at 60 °C using the Dionex HPLC summit system (Surrey, UK) with a 5 mM H_2SO_4 mobile phase at a flowrate of 0.6 mL/min. The injection volume was 50 μL and analytes were detected by UV absorbance at 215 nm except for glucose which was detected on the refractive index detector (Shodex). Quantification was done by integrating the peak areas and comparing them with calibrated standard solutions of the metabolites.

The red pigment was measured at A_{485} using the Ultraspec 500 pro spectrophotometer (Amersham Biosciences, UK). The concentration was calculated using the equation

$C = A_{485}/1.086$ according to method by Ushio (2003), where C is the pigment concentration (g/L).

2.5.4 Enzyme sample preparation and determination of activity

Broth was thawed on ice and 2 mL was centrifuged at 16100 *g* for 15 minutes on the Eppendorf centrifuge 5415 precooled to 2 °C. The pellet was resuspended in a buffer containing 800 μL of 0.2M Tris-HCl, pH 7.6, 100 μL of 4 mM $MgCl_2$ and 100 μL of 2 mM DTE (Hua *et al*., 2003). Enzyme release was achieved by using the Covaris® AFA E210 Adaptive Focused Acoustics Ultra Sonication sonicator. Sonication was performed at acoustic power of 76 W for 120 seconds at 8 °C. The lysate was then centrifuged at 14000 *g* for 10 minutes at 2 °C. Samples were kept on ice at all times between steps. The samples were then frozen at -20 °C until required for analysis.

Glucose-6-phosphate isomerase (EC number = 5.3.1.9) was determined based on the method of Fraenkel and Levison (1967). The total assay volume of 300 μL consisted of

195 µL of 0.1 M Tris-HCl, pH7.5, 15 µL of 10 mM MgCl, 20 µL of 1µg/µL glucose-6-phosphate dehydrogenase, 20 µL of 0.2 mM $NADP^+$ and 10 µL lysate. The reaction was started with the addition of 40 µL of 0.4 mM fructose-6-phosphate (Sigma-Aldrich, Gillingham, UK). The rate of change in absorbance was monitored at 340 nm and correlated with the activity of the enzyme.

The activity of glucose-6-phosphate dehydrogenase (EC number = 1.1.1.49) was determined according to the method of Ryu *et al* (2006). The assay volume consisted of 205 µL of 0.1 M Tris-HCl pH 7.5, 15 µL of 1M $MgCl_2$, 10 µL lysate and 30 µL of 0.2 mM $NADP^+$. The assay was started by adding 40 µL of 1 mM glucose-6-phosphate. The absorbance was measured at 340 nm.

Phosphoenolpyruvate carboxylase (EC number = 4.1.1.32) activity was determined according to the method of De Nisi and Zocchi (2000). The reagents were mixed in a total volume of 300 µL in the following proportions: 200 µL of 0.1M Tris-HCl pH8.0, 10 µL of 5 mM $MgCl_2$, 10 µL of 10 mM $NaHCO_3$, 20 µL of 0.2 mM $NADP^+$, 10 µL lysate and 20 µL of 15µg mL^{-1} malate dehydrogenase. The reaction was started by adding 30 µL of 2.5 mM PEP and the change in the rate of absorbance measured at 340 nm.

Isocitrate dehydrogenase (ICD, EC number =1.1.1.42) was determined according to the method of Tian *et al* (2005). Reaction mixtures contained 205 µL of 0.05 M HEPES pH8.0, 15 µL of 10mM $MgCl_2$, 10 µL lysate and 30 µL of 0.25 mM $NADP^+$. The reaction was started with 40 µL of 1mM isocitrate (Acros Organics, Oxford, UK) and the change in absorbance over time measured. Reactions were performed on the FLUOstar Optima spectrophotometer with injection mode.

These enzymes were chosen because they are at branch points of pathways. To determine the split in carbon flow between glycolysis and the pentose phosphate pathway, G6P branch point enzymes are important. It was also important to determine the role of the TCA cycle and the anaplerotic pathway from PEP to oxaloacetate in the production of erythromycin. To do this, PEPC and ICD were included in the analyses.

Pyruvate is a strategic metabolite in antibiotic synthesis and its enzymes pyruvate carboxylase and pyruvate kinase, would have been interesting to assay. Equally, it would have been interesting to assay methylmalonyl-CoA mutase as it is on the product pathway. However, for operational reasons, the number of enzymes to be assayed had to be limited.

2.6 Determination of NADH and NADPH

Two millilitres of broth thawed on ice were centrifuged at 16100 *g* for 20 minutes. The Eppendorf centrifuge 5415 chamber was precooled and maintained at 0 °C throughout. The pellet was resuspended in 300 µL NaOH (0.2 mM). The samples were incubated in a water bath at 50 °C for 10 minutes. A volume of 300 µL of 0.1 M HCl was added drop wise to each sample while vortexing. After this, samples were centrifuged at 16100 *g* for 25 minutes at 0 °C. The supernatant was stored at -80 °C. Analysis was done within 24 hours of extraction as there was evidence of degradation when analysed after this period.

Analysis was performed as described by Matsumura and Miyachi (1980) and San *et al* (2002). The composition of the assay mix for the respective cofactors was taken directly from Matsumura and Miyachi (1980). The concentrations of enzymes used for NADH and NADPH analysis were 100 U/mL alcoholdehydrogenase (ADH) and 35U/mL glucose-6-phosphate dehydrogenase (G6PDH). ADH and G6PDH were reconstituted in 0.1M Bicine buffer pH8.0 and 0.1M Tris-HCl pH7.5 respectively. Fifty mM glucose-6-phosphate was used as substrate for glucose-6-phosphate dehydrogenase. The assay was calibrated with standard solutions prepared from NADH and NADPH. The absorbance versus time graph was plotted and slope of this (reflecting the change in absorbance/minute) used to determine the concentrations. The assays were performed using 90 µL ultrapure water, 15 µL lysate and 15 µL of enzyme. The reactions were started by injecting 180 µL assay mix (San *et al*., 2002; Matsumura and Miyachi., 1980). The absorbance was monitored at 544 nm for 30 minutes to allow for the colour development to stabilise. All reactions were performed at room temperature and measurements were made using the FLUOstar Optima spectrophotometer (BMG

Labtech, UK). The assay mix was protected from light to prevent degradation of the colour. A fresh assay mix solution was prepared and a new calibration curve was determined each time analyses were performed. This was done to reduce potential inaccuracies due to variation in colour development of the assay mix solution.

2.7 Determination of ATP, ADP and AMP

Analysis was conducted using a modified method adapted from Ball and Atkinson (1975) using the ATP Determination Kit (Invitrogen, UK). The assay mix was prepared according to the manufacturer's instruction. Residual assay mix could be stored at 4°C for up to two weeks without losing viability provided it was well protected from light. When diluted, luciferase was sensitive to storage at -80°C. A new nucleotide calibration curve was made for analyses done on different days. Variations in colour were observed when the assay mix was stored for longer than 24 hours. Analysis was performed on the FLUOstar Optima (BMG Labtech, UK) spectrophotometer with injection mode. Luminescence was correlated to the concentration of ATP in the sample. No wavelength was required as the intensity of luminescent light was measured. Samples were kept on ice at all times. Analysis was performed at room temperature. The 300 µL reaction volumes consisted of 200 µL lysate, 35 µL 75 mM potassium phosphate buffer pH 7.3, 5 µL 15 mM $MgCl_2$ and 10 µL 0.5 mM phosphoenolpyruvate . The reactions for ADP contained 20 µg pyruvate kinase as an additional reagent. Pyruvate kinase (20 µg) and 25 µg myokinase were added to the reactions for AMP determination. Pyruvate kinase and myokinase were reconstituted in 0.1M TE buffer pH7.7 and 0.05M KH_2PO_4/K_2HPO_4 pH7.3 respectively. After incubation at 30 °C for 40 minutes, 30 µL of each sample was transferred to a new reaction plate. All reactions were performed in 96 well Krystal^{TM} 2000 microplates, white with clear bottom (Porvair Sciences Leatherhead, UK). Reactions were started by adding 270 µL of the assay mix.

Dilutions in volumes were accounted for in the calculation of concentrations of ADP and AMP. Net ADP concentrations were obtained from the difference between ATP and raw ADP values. AMP was obtained from the difference between the raw AMP and the net ADP concentrations.

2.8 Calculation of yield coefficients and rates

All the data was normalised to the maximum biomass. Rates have been normalised to the maximum biomass. Specific uptake rates were calculated as the rate of carbon source uptake per mean biomass generated.

2.9 Carbon balance determinations

For the determination of carbon balance, all calculations were based on the biomass molecular formula, $CH_{1.8}O_{0.5}N_{0.2,}$ as detailed in Doran (1995) and performed according to the method of Atkinson and Mavituna (1983).

The molecular weight of the biomass for *S. erythraea* was based on the general molecular formula of biomass, $CH_{1.8}O_{0.5}N_{0.2}$ (Doran, 1995). Using this formula, the average molecular weight of biomass is about 24.6 g, which is equivalent to one mole. As verification, the total biomass weight obtained for *S. erythraea* was 23.7 g for growth on glucose. Therefore, the weight of one mole of biomass for *S. erythraea* was within 3.6% of the general tabulated weight of 24.6 g for bacteria. A biomass value for a related species was provided by Bushell and Fryday (1982). Based on the elemental composition, Bushell and Fryday determined the biomass formula for *Streptomyces cattley* to be $CH_{1.6}O_{0.58}N_{0.17}$. This formula translates into a biomass weight of 25.26 g for *Streptomyces cattley* as calculated by the authors.

Metabolites were calculated as moles of carbons for each metabolite and then converted to mass. The mass of carbons in each metabolite was calculated as a percentage of the total carbon mass in either glucose or gluconate.

The molecular weight of *7*-O-rhamnosyl flaviolin (red pigment) of 352 $g.mol^{-1}$ was used as determined by Cortes *et al* (2002).

Chapter 3

3.0 Analytical Method Development

3.1 Rationale for development of method

Saccharopolyspora erythraea is a gram positive filamentous organism with a high GC content. It is a spore-forming organism belonging to the *Actinomycetales* family known for growing slowly and for its ability to produce a variety of colourful secondary metabolites. Often, processing and analysis of samples is largely dependent on the cell characteristics including its morphology, anatomy and physiology. Methods which have been developed and used for some organisms may be less suitable when used for others. For example, optical density (OD) produces reproducible results for *E. coli* for biomass determination but is a lot less reliable for *S. erythraea*. This is because the characteristic filaments formed by *S. erythraea* often interfere with the methods of biomass determination and can compromise reproducibility of results. Methods for the processing of samples for the analysis of enzymes, pyridine cofactors and adenylates were adapted from published work, evaluated, developed and validated for *S. erythraea*.

3.2 Evaluation of the analytical methods for the determination of enzyme activities

A small scale study was conducted to determine the effect of storage at -80° C on the activity of enzymes. Results from samples stored at -80°C for a month were comparable to those analysed one day after sampling. This suggested that samples for enzyme analyses could be stored at -80° C as whole broth without significantly compromising their integrity. However, lysates were stored at -20°C as storage at -80°C resulted in loss of activity.

3.2.1 Sonication trial

For the results to be an accurate reflection of the metabolic status of the cell at a particular point in time, complete release of all enzymes is critical. To achieve this, sonication should ensure maximum release while maintaining the integrity of the

enzymes. Enzymes are often susceptible to degradation and care must be taken during the sonication process. Important optimisation parameters in sonication are the duration

(seconds), acoustic power (Watts) and duty cycle (%). Three volumes of 2 mL each from the same broth were centrifuged at 16100 x g and the pellet retained and reconstituted in buffer containing 800 µL of 0.2 M Tris-HCl pH7.6, 100 µL 4 mM $MgCl_2$ and 100 µL 2 mM Dithiothreitol (DTE). Thereafter, the samples were sonicated in the Covaris® AFA™ Sonicator (K Biosciences, Hertfordshire, UK). The operation was carried out at 76 W acoustic power, and 20% duty cycle. Sonication was carried out for 30, 60 and 120 seconds respectively. Results of this are presented below.

3.2.2 Results

The absorbance at 340 nm measures the total protein released from the sample. Higher absorbance values were obtained when the samples were sonicated for 120 seconds compared to sonication for 30 and 60 seconds (Table 3). The AFA technique sends acoustic energy wave packets in the form of mechanical energy. The energy is intense because it is focused on a focal zone and creates a shock which disrupts the cells. The intensity also requires that the sonication time be as short as possible to avoid the risk of possible damage to enzymes due to excessive heat. The highest absrbance values were obtained by sonicating for 2 minutes at the set parameters (Table 3). Sonicating for 2 minutes was also found to be optimum for the activities of the G6PDH (Table 4). A detailed investigation of the effect of different parameters on the activity of various enzymes is outside the scope of this work. Of critical importance was that the conditions developed for the enzyme assays be kept the same throughout the duration of the investigations. This would ensure that any changes in the activity of the enzymes would be a reflection of the *in vivo* situation in the cell. It is, therefore, reasonable to assume that for all the enzymes tested, sonicating for 2 minutes produces optimal results under the conditions tested. The conditions for sonication were maintained throughout to reduce variation due to different sensitivities of the enzymes to heat and mechanical damage.

Table 3 Effect of sonication duration on the absorbance (A_{340}) of enzymes in the lysate.

Duration (s)	G6PDH	PGI	ICD
30	0.1258 ± 0.02	0.0433 ± 0.02	0.0561 ± 0.003
60	0.1171 ± 0.02	0.0346 ± 0.02	0.0549 ± 0.020
120	0.1315 ± 0.01	0.0490 ± 0.01	0.07225 ± 0.005

Table 4 Comparison of the effect of sonication duration on the activities of G6PD

Sonication duration (s)	Rate $\Delta A_{340}.min^{-1}$	Activity $mMole.min^{-1}.ml^{-1}$
30	0.048	154
60	0.038	122.1
120	0.064	205.7

It is not clear why sonication at for 60 seconds yielded lower absorbance values for all three enzymes. However, the difference between sonication for 30 and 60 seconds was relatively small. Sonication for 2 minutes produced the highest absorbance values and this was therefore used in all enzyme release operations in this research. Keeping the duration of sonication constant ensured that it did not contribute to any variation observed in the activities of enzymes under the various conditions.

3.2.3 Assay development and optimisation

The assay was developed, evaluated and optimised for the FluoStar Optima plate reader (BMG Labtech, Buckinghamshire, UK). Each assay has a dynamic range for the signals in the different plate wells based on the position. To obtain the optimum results, a gain adjustment is recommended. Finding the widest signal range for the brightest well gives the gain value at which the assay has maximum sensitivity. This gain value was determined to be 1250 for the enzyme assays carried out at an absorbance of 340 nm. The combination of the widest signal range for the brightest well gives the optimal

sensitivity for the assay. Gain adjustment is necessary since all wells on the plate do not exhibit the same the same brightness. This could compromise results as the well position becomes an extra parameter that influences the output. Gain adjustment ensures the contribution of the well position is reduced to a minimum. Three biological replicates were analysed for each of the enzymes. Various combinations of reagents were investigated. Presented here are the reagent combinations for which maximum absorbance values were obtained.

The plate reader was operated in injection mode to ensure standardisation of reaction times and to reduce potential errors caused by manual handling. An initial reading was taken before injection to account for the contribution of the assay mix. This was followed by another reading during injection. These two readings were discarded since all samples included a control containing all reagents except the sample. Absorbance due to reagents was deducted from all other sample values.

3.2.4 Evaluation of the optimised assay protocol

An protocol developed for the enzyme assays is provided in Table 5. A set of shake flask fermentations were conducted to evaluate the developed assays using fresh samples. Samples were collected from the exponential growth phase, processed and analysed using the protocol shown in Table 5. The results show good consistency and reproducibility based on the small standard deviations obtained (Fig. 6). Protocols for PEPC and ICL were later developed based on the results of the three enzymes shown in Table 6.

Table 5 Protocols and analytical parameters for the different enzyme assays.

Enzyme	Reagent volumes	Reaction starting reagent	Gain	Absorbance λ (nm)
G6PDH	205 µL 0.1M Tris-HCl pH7.5 15 µL 1M $MgCl_2$ 30 µL 0.2 mM $NADP^+$ 10 µL lysate	40 µL 1 mM G6P	1250	340
PGI	195 µL 0.05M Tris-HCl pH7.5 15 µL 10 mM $MgCl_2$ 20 µL G6PDH 20 µL 0.2 mM $NADP^+$ 10 µL lysate	40 µL 0.4 mM F6P	1250	340
ICD	205 µL 0.05M HEPES pH8.0 15 µL 10 mM $MgCl_2$ 10 µL lysate 30 µL $NADP^+$	40 µL Isocitrate trihydrate (1 M)	1250	340
PEPC	200 µL 0.1 M Tris-HCl pH8.0 10 µL 5 mM $MgCl_2$ 10 µL $NaHCO_3$ 20 µL 0.2 mM NADH 20 µL 15µg/mL MDH 10 µL lysate	30 µL 2.5 mM PEP	1568	340
ICL	180 µL 0.1 M K_2HPO_3/KH_2PO_3 pH7.6 10 µL 5mM $MgCl_2$ 5 µL 4 mM Phenylhydrazine-HCl 5 µL 2.4 mM Cysteine-HCl 70 µL lysate	30 µL Isocitrate trihydrate (1 M)	1250	340

Table 6 Evaluation of the activities of central metabolism enzymes in *S. erythraea* based on the optimised reagent combinations and analytical parameters.

Enzyme	Activity $mMole.min^{-1}.mL^{-1}$
Glucose-6-phosphate dehydrogenase	28.9 ± 4.5
Phosphoglucose isomerase	43.4 ± 0
Isocitrate dehydrogenase	94.0 ± 37.5

This could be expressed as specific activity (per gram biomass) as is normally the convention. However, the developmental work was for demonstrative purposes. It, therefore, suffices to show that the assays do work reliably and robustly. All subsequent enzyme activities throughout this research were expressed as specific activities (per gram biomass).

3.2.5 Review of the methods for the extraction of metabolites

A good extraction procedure should be able to inactivate and precipitate proteins, RNA and DNA while extracting all intracellular metabolites. However, metabolites of interest must be able to dissolve in the extraction solvent as well. A mild polarity is often required as energy nucleotides have some polarity. Often organic solvents are mixed with water to confer polarity and improve metabolite solubility.

Shryock *et al* (1986) reported good results with 80% hot methanol (70°C) at pH7.0 for endothelial cells. However, there are concerns about the effect of this high temperature on heat labile metabolites. Most of these intracellular metabolites are prone to degradation at elevated temperatures. This study did not investigate the effect of the procedure on the recovery of the metabolites. However, 80% methanol may have insufficient polarity leading to inefficient solubilisation of metabolites. Working at high methanol percentages may increase protein precipitation, but high evaporation rates could introduce errors in the concentrations of metabolites. Perchloric acid (PCA) and trichloroacetic acid (TCA) were also investigated by Shryock *et al* (1986). Unsatisfactory results were obtained due to the effect of high acid concentrations on metabolites. In a study by de Koning and van Damm (1992), chloroform was found to

cause sufficient solubilisation at -40°C. In the presence of chloroform, enzymatic conversions were found to drop below 10% suggesting that the solvent does inactivate ATP degrading enzymes. A disadvantage of this method is the large amounts of cells required for extraction (de Koning and van Damm., 1992). Chloroform is carcinogenic and working with it in a standard extraction procedure requires that all processing be carried out in a fume hood which is not practical for sampling from bioreactors. Other researchers including Gonzalez *et al* (1997) have used ethanol to extract metabolites from *S. cerevisiaea* cells. Low acidity reduces metabolite concentrations (Shryock *et al*., 1986; Gonzalez *et al*., 1997). To get around this problem, Gonzalez *et al* (1997) used 75% methanol/70 mM HEPES (pH7.5), buffered to reduce metabolite degradation. The mixture was boiled at 80°C before being used for extraction. Compared to the procedure used by de Koning and van Damm (1992), this procedure also has the disadvantage of metabolite degradation caused by elevated temperatures. These findings also confirmed those of de Koning and van Damm (1992) who concluded that keeping the temperature below -20°C improved metabolite concentrations.

In another work, Faijes *et al* (2007) presented comparison of different extraction methods for ATP and NAD^+ in terms of their efficiencies. The procedures investigated and compared were extraction with cold methanol at -80°C, 35% perchloric acid at -20°C, chloroform/methanol at -80°C, chloroform/water at -80°C and hot ethanol (90°C) respectively. Optimal extraction efficiency for *Lactobacillus plantarum* was obtained when the pellet was directly resuspended in cold methanol at -80°C. The efficiency of this method was ascribed to the low temperature, moderate pH values and the absence of salts. High temperatures, extreme pH values and the presence of salts are known to reduce extraction efficiency. However, these researchers noted that degrading enzymes may not have been completely inactivated and stressed the need to carefully control the temperature throughout as suggested by Mashego *et al* (2007).

Following the recommendations of Mashego *et al* (2007) and Faijes *et al* (2007), the temperature was carefully controlled throughout. In the current work, samples were kept in the dry ice/methanol bath before being transferred to storage at -80°C. Samples were thawed on ice and centrifuged at 0°C. Direct extraction from broth produces unfavourable results (Faijes *et al*., 2007) possibly due to errors produced by the dilution

effect. The sample was therefore centrifuged, the pellet resuspended in cold methanol and the extraction carried out at -80°C overnight. A drawback of this procedure is that undiluted methanol has a high evaporation rate which could introduce errors in metabolite concentrations. To reduce evaporation, samples were stored at -20°C between analyses. It was also found that residual water in the pellet caused it to freeze solid thus compromising the extraction process. It is therefore recommended that as much water as possible be removed from the pellet before adding methanol for extraction. First, water was removed using a first 500 µL pipette. Then a 10 µL pipette was used to remove residual water around the pellet. Additional amounts of water could be removed but this would have required increasing either the centrifugation time or rate.. However, this would have generated a more compact pellet that could not be easily resuspended in a buffer.

3.3 Evaluation of the method for the determination of the pyridine Cofactors

Pyridine cofactors have a a high turnover rate and are sensitive to oxidative degradation. To get around the problem of oxidation of NADH to its oxidised form, a rapid sampling and freezing technique was developed. The sample bottle was attached to the sampling port. After opening the sampling valve, the sample was drawn into the bottle using a 50 mL syringe. The sample bottle was removed from the port, capped and rapidly dipped into the dry ice/methanol bath to arrest the interconversion between the cofactors. Since NADH and NADPH are sensitive metabolites, the very extraction procedure could compromise the integrity of the samples. Two milliliters of the thawed broth was centrifuged as described in Section 2.6. Extraction involved the addition of 300 µL of 0.2 M NaOH and 0.1M HCl respectively to the pellet followed by heating at 50°C (San *et al*., 2002). The extraction process is described in Section 2.6. To evaluate the effect of the extraction procedure on the concentrations of the cofactors, known concentrations of the cofactors were prepared and treated as samples. Results of this investigation are presented below. In work by Shryock *et al* (1987), extreme pH values were found to potentially reduce cofactor concentrations. The extraction method evaluated here showed a very high percentage recovery suggesting that the pH values involved did not

contribute to the degradation of NADH and NADPH (Table 7). Though the extraction was performed in 0.2 M NaOH at 50°C for 10 minutes, neutralising the solution with 0.1 M HCl meant that overall pH was marginally basic rather than acidic. Many of these cofactors have greater stability in basic conditions (Shryock *et al*., 1987).

Table 7 Effect of the extraction procedure on the concentrations of NADPH and NADH.

Cofactor	Standard (µM)	Recovery (µM)	% Recovery
NADPH	0.05	0.0515 ± 0.01	103 ± 20
NADH	0.05	0.0498 ± 0.005	99.5 ± 12.5

3.3.1 Optimisation protocol and analytical parameters

The protocol was based on San *et al* (2002) and Matsumura and Miyachi (1980). However, all measurements were performed at 544 nm based on the available filter. All reagents with the exception of the enzyme and lysate, were added together in an assay mix which was used to start the reactions. The colour of the assay mix was sensitive to prolonged storage and exposure to light. The assay mix was stored in a sample bottle around which aluminium foil was wrapped to protect it from light. When protected from light and stored at 4°C for 24 hours, the sensitivity was not significantly reduced. Nevertheless, a new calibration curve was prepared every time sample analyses were performed since reduction in sensitivity was observed when reagents that have been stored for over a week have been used. A time period of thirty minutes was allowed for the reaction to go to completion and for the colour of the assay to develop and stabilise. The background absorbance was accounted for by running a control with reagents for the reaction except the lysate which was substituted with ultrapure water.

To allow for the colour of the assay to fully develop, the assay was run for 20 cycles. Preliminary studies indicated that 10 cycles did not allow time for full colour development. Each cycle was of 60 seconds duration. This means that after injection, readings were taken in cycles of one minute each. Taking readings in cycles ensured

that the development of the colour could be expressed as a rate. The one minute cycle time. Since the intensity of the colour is correlated with the concentration of the cofactors, full colour development equates to maximum cofactor concentration. When the absorbance values became constant, it indicated full colour development and the end of the assay reaction. To calibrate the assays, the rates (A340/min) are plotted against time. Reagents were added in the quantities stated in Table 8. The assay was calibrated by plotting the rates (A_{544}/min) against known standards to generate a calibration curve and using the linear fit to calculate the unknowns.

Table 8 Developed protocol for the determination of pyridine cofactors.

Cofactor	**Reagent composition**	**Reaction starting reagent**	**Gain**	**Wavelength (nm)**
NADH	90 µL Water 15 µL lysate 15 µL ADH (100 U/mL)	180 µL Assay mix	700	544
NADPH	90 µL Water 15 µL lysate 15 µL G6PDH (35 U/mL)	180 µL Assay mix	700	544

3.3.3 Evaluation of the accuracy and robustness of the assay

The accuracy of the assay was evaluated with a calibration curve using known concentrations of the cofactors. Known concentrations of both NADH and NADPH were prepared and added to the assay mix as samples in separate experiments. The NADH assay consisted of 90µL RO water, 15 µL alcohol dehydrogenase reconstituted in 0.1M Bicine buffer pH 8.0 and 15 µL extract. The reaction was started by adding the assay mix which was prepared as described in section 2.6 of Chapter 2. Reagents were kept on ice during the assay preparation. The exponential portion of the curve was observed during the first 20 minutes for all samples. A reaction time of 30 minutes was allowed for the colour development to stabilise. The linear portions were plotted as the change of absorbance against time in minutes (ΔA544/min) to obtain the calibration

curves. Matsumura and Miyachi (1980) detected cofactors at 570 nm. Due to operational limitations, the change in colour was detected at 544 nm.

After the test for accuracy, the robustness and reproducibility of the assays were tested

on actual fermentation samples. Single point samples were collected from shake flask fermentations and analysed. The calibration curves previously plotted were used to calculate the unknowns. The assays were calibrated with 0.1 – 1.0 µM serial standards for NADH and NADPH.

Both assays were found to be very accurate with a regression of R^2 = 0.998 for NADH (Fig. 6) and R^2 = 0.992 for NADPH (Fig. 7). All cofactor determinations were performed at the wavelength of 544 nm to ensure accuracy and reproducibility. The assay for NADH had a reproducibility of above 70 % as indicated by the results presented in Table 9.

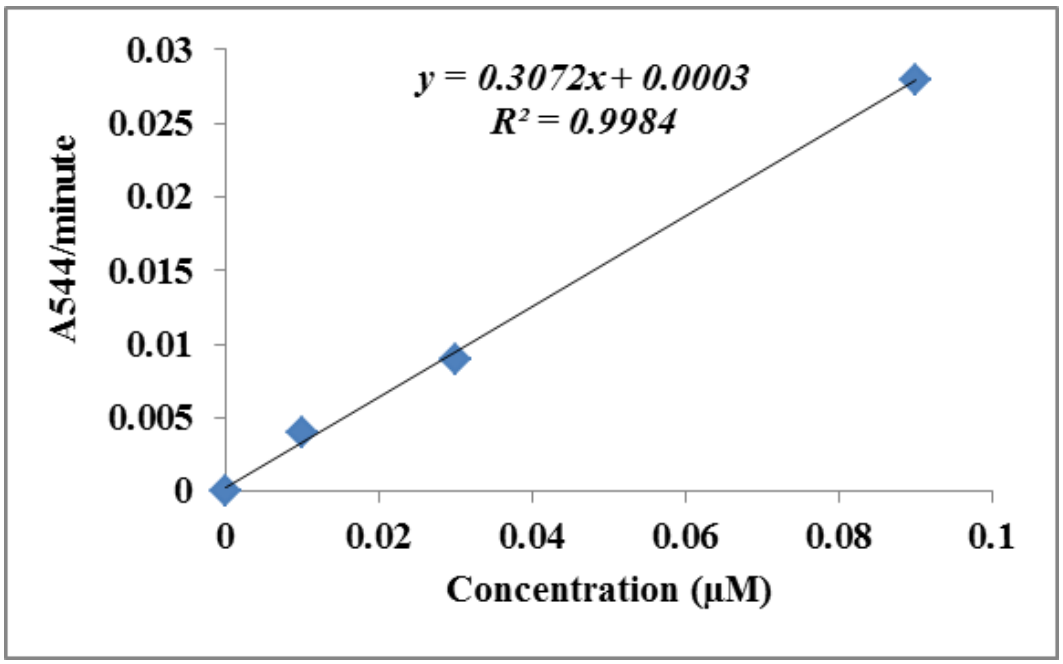

Fig. 6 The calibration curve for the determination of NADH.

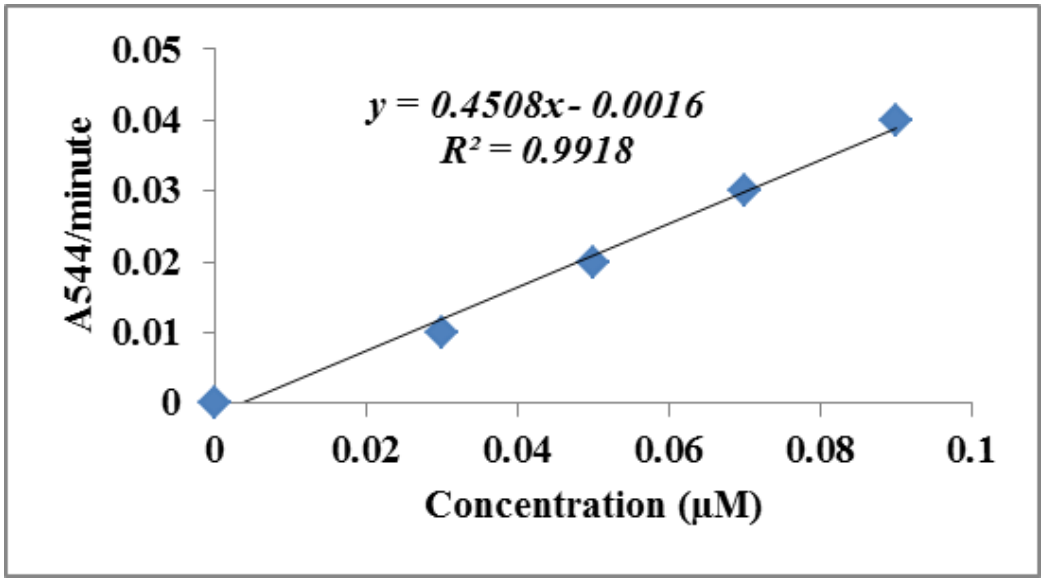

Fig. 7 The calibration for the determination of NADPH.

Table 9 Test of reproducibility of cofactor assay on samples from *S. erythraea* broths. Values reflect means of three biological replicates.

Cofactor	Sample (µM)
NADPH	0.112 ± 0.08
NADH	0.042 ± 0.01

The samples were obtained from shake flask fermentations where pyridine cofactor values are likely to be low due to suboptimum growth at this scale. Reproducibility at such low concentrations is difficult to obtain at best. Perhaps the 29% reproducibility of the NADPH assay is a reflection of this. However, this was an established assay which was being evaluated under these conditions. Therefore this was thought not to be a reflection of the sensitivity of the assay but rather of the handling of the sample prior to analysis.

3.4 Development of the assay for adenylate nucleotides

The critical aspect for *in vitro* analyses of adenylate cofactors is to ensure that the sample is a true reflection of the *in vivo* status of the cells. If the method compromises

the integrity of samples, results from such analysis will produce flawed results and conclusions. To achieve this, all major steps involved from sampling, quenching, storage and analysis should preserve the integrity of the cells and ensure the accurate reflection of the *in vivo* conditions. This is a challenge because metabolic rates for growing cells are much faster than for resting cells. Cytosolic ATP and ADP have turnover rates ranging from 1.5 mM s^{-1} to 2 mM s^{-1} (Theobald *et al.*, 1997). The sampling method should therefore be able to instantaneously arrest metabolism to ensure accurate representation of the *in vivo* conditions. There are various procedures for the extraction of intracellular metabolites reported in the literature. Procedures are often specific to a particular group of organisms and need to be validated and adapted before they can be used for a different organism. The basic aim of quenching is to inactivate the enzymes that catalyse the conversions of metabolites of interest. In the context of energy nucleotides, quenching should instantaneously inactivate ATP degrading enzymes. Organic solvents are the commonly used solvents for arresting metabolism mainly because of their ability to denature and precipitate proteins. A further advantage is their ease of removal because of their general low boiling points. The standard approach used for quenching is reported in de Koning and van Damm (1992) who used 60% methanol (pH7.0) at -40°C to instantaneously stop metabolism in *Saccharomyces cerevisiaea* cell. These researchers reported that reliable results would be obtained as long as the temperature was maintained at or below -20°C. Working at the lowest possible temperature appears to be essential to stopping metabolism instantly.

A comprehensive investigation was conducted by Faijes *et al* (2007) who evaluated various quenching procedures for different cultures to establish the optimum conditions. Their findings indicate that for different samples from the same culture and for samples from a different batch, 60% methanol/70 mM HEPES (pH5.5) at -40°C and 60% methanol/0.85% ammonium carbonate (pH5.5) at -80°C were the most efficient in preventing ATP leakage. High ATP leakage during quenching would lead to underestimation of energy charge and its constituent nucleotides. These findings suggest that the two methods are the most suitable for instant quenching of metabolism under the conditions tested. However, Faijes *et al* (2007) based their quenching procedures on

Lactobacillus and not on Actinomycetes. Therefore, the method had to be evaluated and adapted for use in Actinomycetes.

The quenching procedure used in this work was adapted from these findings. It was earlier indicated that metabolite concentrations were improved by keeping the temperature of the quenching solution below -20°C and the alkalinity above pH7. To avoid introducing salts that could interfere with downstream processes of extraction and analysis, the methanol/HEPES combination was selected as the preferred method for use in this work. However, methanol was buffered to pH8.0 with 70 mM HEPES and the quenching was done at -80°C. The quenching solution was kept at -80°C in a dry ice/methanol bath before and immediately after sampling. Samples bottles were prefilled with the quenching solution and the sample was poured immediately into solution for instant inactivation of metabolism.

3.4.2 Evaluation of the effect of the extraction procedure on the recovery of AMP

The effect of extracting solvents has been discussed in earlier sections of this chapter. These range from harsh conditions caused by extreme pH values and high temperatures to error caused by evaporation of solvents. There may be other unknown effects of solvents on metabolite stability including the potential extraction of lipids from membranes which could interfere with downstream analytical processes. Often extraction methods are developed for specific organisms making such methods less effective when used for a different organism without validation and possible optimisation. This is often the case because organisms differ in terms of cell membrane composition and other cellular features. Therefore, it is necessary for an assay to be evaluated before it can be used for an organism in which it was not used before. Equally, it important to ensure the analytical method does not interfere with the integrity of the sample.

Therefore, the possible effect of the extraction procedure on the concentrations of AMP was investigated. A known concentration of AMP was prepared in triplicate and treated like a sample by subjecting it to the extraction process and determining the percentage recovery. Three samples of 80 nM were subjected to the extraction procedure. A mean

recovery of 99.5 ±5 % was obtained which suggests that the extraction procedure is suitable for AMP.

The extraction procedure does not appear to reduce the concentration of AMP as indicated by the almost 100% recovery and a very small standard deviation.

The recovery of ATP and ADP has been assessed in a separate experiment (not presented).

Table 10 Percentage recovery of known AMP concentration after treatment as a sample.

Concentration (nM)	% Recovery	Mean (%)
80	94.54	
80	104.81	99.46 ± 5.14
80	99.04	

3.4.3 Optimisation of the buffer conditions for the myokinase reaction

The activity of myokinase was crucial to obtaining reliable results for the AMP determination. To optimise the activity of this enzyme, it was reconstituted using different buffers and its activity evaluated. In addition, the enzyme was also evaluated in various reaction buffers to determine the optimal catalytic activity. Results of these studies are presented in Table 10 below.

Table 11. The effect of reaction and reconstitution buffers on the activity of myokinase. The analysis represents three replicates for each condition presented.

Cofactor	Reconstitution buffer	Reaction buffer	RLU
ADP	TE	K_2HPO_4/KH_2PO_4	924.7 ± 150.05
ADP	TE	TEA	1245.3 ± 29.32
AMP	K_2HPO_4/KH_2PO_4	TEA	1207.2 ± 64.08
AMP	Water	TEA	1190.9 ± 0.45
AMP	K_2HPO_4/KH_2PO_4	K_2HPO_4/KH_2PO_4	1084.5 ± 55.64
AMP	Water	K_2HPO_4/KH_2PO_4	1088.6 ± 47.33
AMP	TEA	TEA	1133 ± 62.25

The optimum conditions for both ADP and AMP was obtained with 50 mM TEA pH7.7 as reaction buffer. Optimum relative luminescence unit (RLU) values were obtained with the reconstitution of myokinase in ultrapure water as well as in as in potasium phosphate buffer at pH7.5. Though higher luminescence values were obtained with the combination of phosphate and TEA buffers, results obtained with the combination of water and TEA were more reproducible. These results also show that the method has the highest reproducibility (1190.0 ± 0.45) for the combination of water-reconstituted myokinase in 50 mM TEA (pH7.7) as reaction buffer (Table 10).

3.4.4 Investigation of the effect of storage conditions on the stability of ATP

The condition in which samples are stored can have a profound effect on the stability of metabolites. Three different samples were taken each from a different time point in the shake flask fermentation. Each sample was split into two, one of which was stored as broth while the other was centrifuged and the pellet extracted overnight at -80°C.

Three different samples were taken at different time points from a shake flask culture grown on glucose as sole carbon source. One set of samples was stored at - 80°C, the other was processed and stored as extract at the same temperature. All samples were stored for two weeks before analysis. The results of these analyses are presented in Table 11.

Storing the samples at -80°C as broth prevented degradation and resulted in higher concentrations for ATP (Table 13). When the samples were first processed and stored as extracts at -80°C for two weeks, the decrease in the concentrations was significantly higher relative to those stored as broths (Table 12). The improved metabolite stability in the broth was probably due to the buffering effect of the broth environment. When extracted, the pH changes and the environment could become less buffering for the nucleotides. However, some reduction in the concentrations could have been caused by the processing environment including higher temperatures during centrifugation and loss during the extraction process. Extracting with cold methanol did not cause significant reduction in the concentration of both ATP and ADP (data not shown).

Table 12 The effect of storage at - 80 ºC on the concentration of ATP (nM) in whole broth, processed and fresh samples. Samples were collected at different timepoints of the fermentation.

Concentration in broth (nM)	Concentration in extract (nM)	Concentration in fresh sample (nM)
33.84	11.21	-
105.35	14.00	125±7
26.95	18.00	-

3.4.5 Evaluation of the accuracy and robustness of the assayprotocol for ATP, ADP and AMP

The protocol for the assays was optimised as illustrated in Table 10 below. The assay is based on the luciferase requirements of ATP to produce light and the linear relationship between the amount of light produced and the ATP required. This relationship is illustrated in reaction scheme 1 below

$$\text{Luciferin} + \text{ATP} + O_2 \xrightarrow[MgCl_2]{luciferase} \text{oxyluciferin} + \text{AMP} + \text{pyrophosphate} + CO_2 + \text{Light} \ldots (1)$$

While ATP is detected directly, both ADP and AMP are detected through coupling reactions that convert both to ATP. The coupling of these reactions is based on the equations below

$$2\ \text{ADP} + 2\ \text{Pi} \xleftrightarrow{Pyruvate\ kinase} 2\ \text{ATP} + 2\ H_2O \ldots\ldots\ldots\ldots\ldots\ldots (2)$$

$$\text{ATP} + \text{AMP} \xleftrightarrow{Myokinase} 2\ \text{ADP} \ldots\ldots\ldots\ldots\ldots\ldots\ldots\ldots (3)$$

ADP was converted to ATP by the action of pyruvate kinase before it could be detected. The final ADP concentration was, obtained from the difference between the ATP itself and that resulting form the conversion of ADP by puruvate kinase. An important point here was to ensure that all the ADP is converted to ATP by adding suffcient enzyme (20

U/mL). Pyruvate kinase was reconstituted in 0.1M TE buffer (pH7.7). It was critical to saturate pyruvate kinase by adding enough phosphoenolpyruvate (10 µL) to avoid any substrate limitations to the activity of the enzyme. This volume was concluded to be optimal since increasing it to 15 µL did not improve the output (relative luminescence units).

AMP is first converted to ADP by myokinase (scheme 3) which itself is subsequently converted to ATP via the action of pyruvate kinase (scheme 2). The reaction was optimised to contain sufficient myokinase (26.5 U/mL) for total conversion of all AMP to ADP. A large lysate volume (200 µL) was added to limit the chances of myokinase limitation by depletion of its substrate, AMP. It was assumed that 200 µL contained sufficient AMP to saturate myokinase. To standardise all reactions, the same amount of lysate was added for all reactions. The full optimised reagent constitution is presented in Table 13 below.

To test the accuracy of the assay protocol, calibration curves for all three nucleotides were prepared by plotting known serial concentrations against the relative lumenescence units (RLU) obtained from analysing the prepared standards treated as samples. For all three nucleotides, regression of at least 0.99 was obtained suggesting that the assays are indeed accurate and reliable under the conditions tested (Fig. 8, Fig. 9, Fig. 10). In general, the accuracy of the assays increased in the order from AMP, ADP and ATP (Fig.8 Fig. 9, Fig. 10, Fig. 11). It may not be that surprising considering that detection of ATP was direct and ADP and AMP involved one and two additional reaction steps respectively. The complexity of the conversions would have introduced error due to possible suboptimal enzyme activities and human error during addition of reagents. The RLU values for ADP and AMP reflect the raw output values obtained directly from analyses.

Table 13 Optimised protocol for the determination of adenylate nucleotides. Concentrations of reagent components and the identity of the buffer are specified in Chapter 2.

Nucleotide	Assay composition	Starting reagent	Gain	Wavelength (λ)
ATP	200 µL lysate 35 µL Buffer 15 µL $MgCl_2$ 10 µL PEP	Assay Mix	1495	N/A
ADP	200 µL lysate 35 µL Buffer 15 µL $MgCl_2$ 10 µL PEP 10 µL Pyruvate kinase	Assay Mix	1495	N/A
AMP	200 µL lysate 35 µL Buffer 15 µL $MgCl_2$ 10 µL PEP 10 µL Pyruvate kinase 12.5 µL Myokinase	Assay Mix	1495	N/A

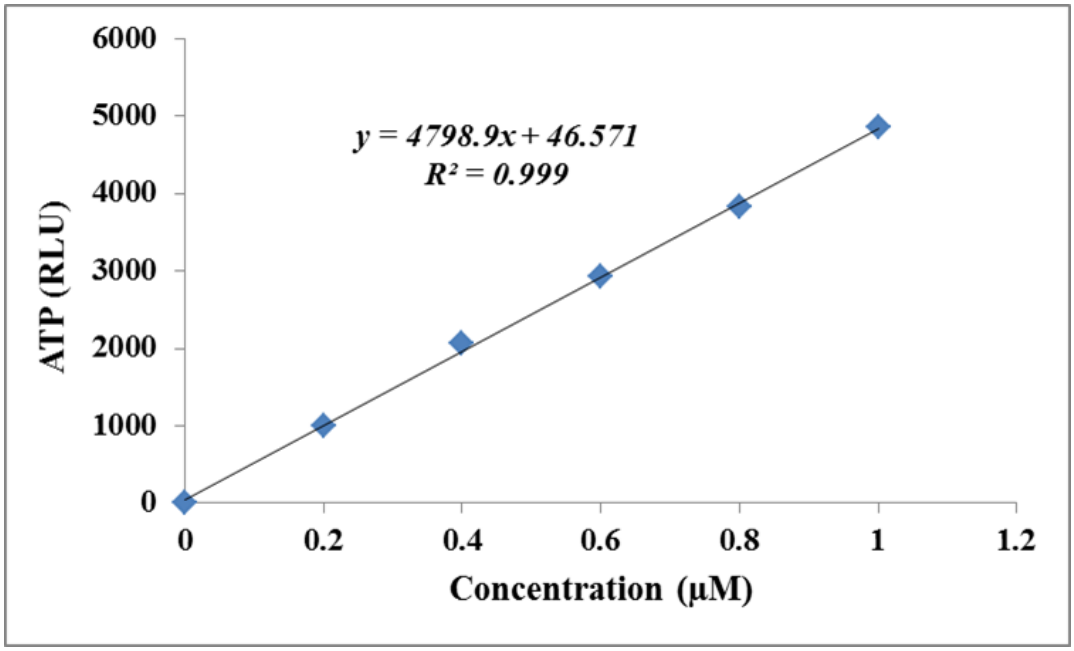

Fig. 8 The calibration curve for the determination of ATP.

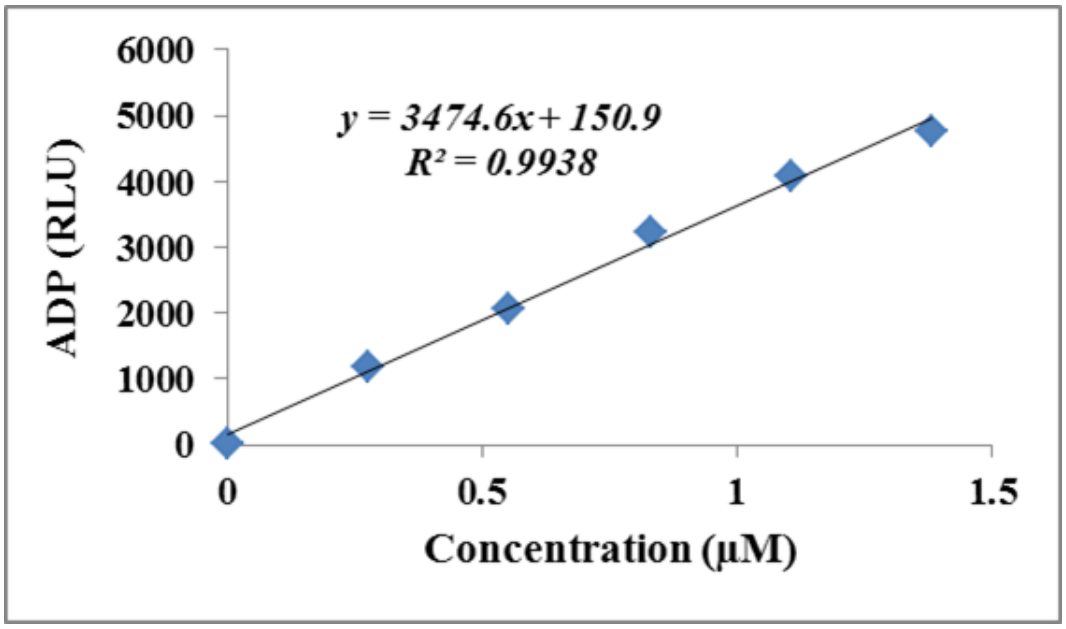

Fig. 9 The calibration curve for the determination of ADP.

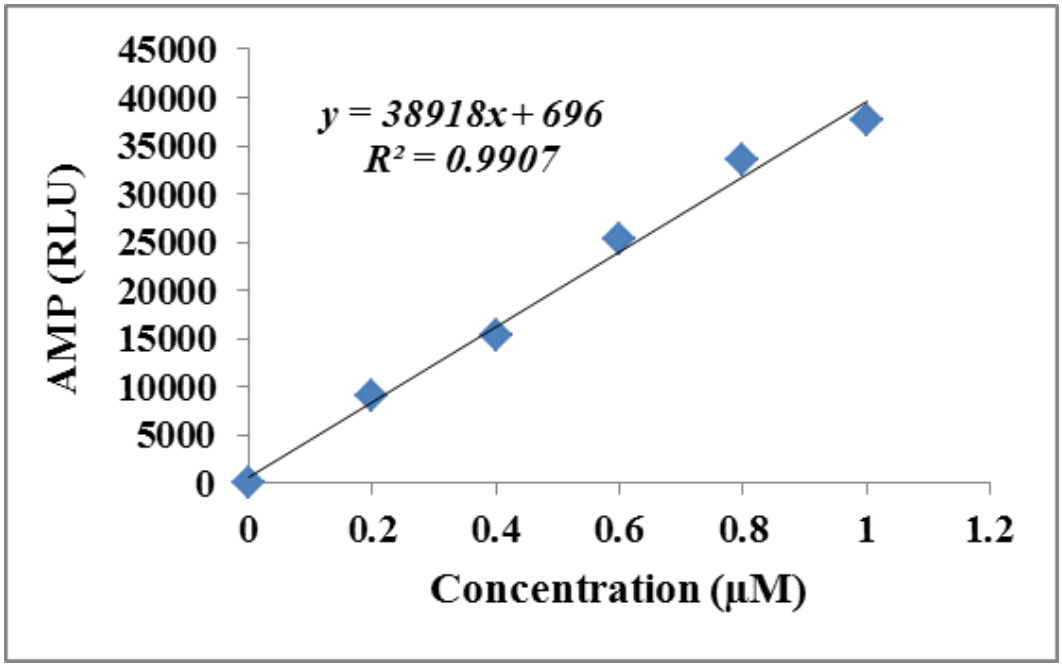

Fig 10. The calibration curve for the determination of AMP.

3.4.6 Evaluation of the reproducibility of the analytical procedure on samples obtained from shake flask fermentations.

The analytical procedure was tested for its robustness in terms of reproducibility on actual fermentation samples. Samples from a shake flask fermentation representing three biological replicates from one time point were analysed for ATP and ADP. The results showed good reproducibility particularly for ATP (Table 14). There was significant variation in the results for ADP relative to ATP. However, after verification with additional analyses, acceptable reproducibility was obtained for ADP as well. In general, reproducibility was better as it is directly correlated to the luminescent light intensity. Both ADP and AMP have to be converted to ATP via coupling enzyme reactions. Though the assay conditions were optimised, there is greater chance for error because of the successive reaction steps involved.

Table 14. Reproducibility of ATP and ADP in actual fermentation samples.

Cofactor	Concentration (nmole)
ATP	125 ± 7
ADP	60 ± 28

A particular challenge of this assay is the very low concentrations involved which make errors easily significant. The overall conclusion is that the assays can be used but great care should be taken to during the extraction and analysis to ensure sample integrity and to minimise error. The assays have been used before for other organisms. Though the regression may not be a reliable way of assessing good fit, it gives a good indication of the reliability of the assay. The aim of the experiment was to assess the reliability of the assay method by using known concentrations of the adenylate cofactors.

3.5 Summary

The optimised conditions for the determination of enzyme activity, pyridine cofactor and adenylate nucleeotide concentrations were suitable for use in the analyses for this research work. Given the reproducibility of the results, the sampling, extraction and analytical procedures evaluated and optimised are reliable for use in actual experimental work. Pyridine cofactor detection can be improved by monitoring NADH at 570 nm where its detection is optimal compared to 544 nm. However, all determinations of pyridine cofactors were conducted at the same wavelength to avoid any variability in the method. The wavelength though not optimal, was not a factor in the determinations of the cofactors. Based on the good linearity, reproducibility and the regression of 0.99, it can be concluded that the analytical methods were reliable.

Chapter 4

4.0 Physiological basis for metabolite distribution and erythromycin production

This chapter is aimed at characterising growth and product formation kinetics. Possible correlation between the rate of carbon uptake and respiration and its effect on the distribution of fluxes at key branch points are investigated. The overall growth characteristics of an organism depend on the growth conditions. In the context of flux distribution, this link is even more pronounced since different carbon sources have different entry points into the metabolic network. This chapter will investigate the link between growth conditions and the partitioning of fluxes between key branch points in the context of product formation.

First an initial evaluation of potential carbon and energy sources is conducted in shake flask experiments.

4.1 Carbon source screening studies in shake flasks

Secondary metabolites are produced by microorganisms from a combination of the carbon, energy and nitrogen source and various other media constituents and externally supplied compounds. The carbon source provides carbons that form the backbone of the various precursor metabolites for the biosynthesis of secondary metabolites with antimicrobial properties. The distribution of carbon fluxes among the central metabolic pathways depends on the nature of the carbon source. Entry points into the metabolic network vary with the nature of the carbo source. This chapter aims to evaluate the growth of *S. erythraea* on selected carbon sources as basis for selection for use in subsequent investigations.

4.2 Introduction

Glucose, a 6-carbon sugar, is metabolised through glucose-6-phosphate by many microorganisms including *S. erythraea*. For many cells, glucose transport into cells is an active process catalysed by glucokinase at the expense of ATP through the phosphotransferase system (PTS). However, there are various modes of glucose uptake into cells depending on the organism involved. When glucose is actively transported against its concentration gradient, it accumulates in the cells as it is.

Some carbon sources are transported across the membrane through passive diffusion and are unable to accumulate inside the cell. The mode of transport of a carbon source into the cell will have an effect on the growth rate and subsequently the distribution of fluxes through the pathways. Gluconate, on the other hand, is a 6-carbon organic acid generally known to enter the metabolic network directly at 6-phosphogluconate (Fig. 11). Degradation proceeds via the Entner-Doudoroff pathway (White, 2007). Its uptake is also coupled to energy expenditure and is catalysed by gluconokinase. In general the Entner-Doudoroff pathway (ED pathway) produces less energy compared to glycolysis and this is likely to affect the growth rate on gluconate as a sole carbon sources. *Streptomyces lividans*, a related organism, does grow on gluconate as sole carbon and energy source (Avignone -Rossa *et al*., 2002). Xylose is a 5-carbon aldose that is abundant in soil. Given its relative abundance, soil organisms may be able to metabolise it easily. Its point of entry into the metabolic network is illustrated in Figure 11. The common path of xylose conversion to xylulose-5-phosphate is through consecutive isomerisation reactions catalysed by xylose isomerase. Some organisms are unable to grow on xylose despite it being a common carbon source. *Bacillus subtilis* is unable to utilise xylose despite the fact that the organism synthesises isomerase (Krispin & Allmansberger., 1998). The reason for this is that *B. subtilis* lacks transporters and, therefore, is not able to transport the sugar across the membrane into the cell. The complex reasons for the potential of organisms to utilise a carbon source are illustrated by the above example. However, yeasts including *Saccharomyces cerevisiaea* reduce xylose to xylitol through xylose reductase and can utilise it to produce ethanol. Clearly, though xylose is the most abundant pentose in nature, not all organisms have the ability to utilise it.

Methyl oleate is another common carbon source often used to enhance the production of antibiotics in industrial fermentations (Efthimiou *et al*., 2008; Hamedi *et al*., 2004; Mirjalili *et al*., 1999; Large *et al*., 1998; Cavanagh *et al*., 1994). While the addition of oils to antibiotic fermentations to improve productivity is a common practice, its use as a sole carbon and energy source has not been fully investigated. Oils are viscous and their use by micoorganisms is very much

dependent on the physical parameters such as the agitation rate and possibly the rate of supply to the culture. Through β-oxidation, fatty acids are sequentially oxidised to eventually yield Acetyl-Coenzyme A which enters the TCA cycle to produce ATP Bacterial lipases are responsible for the degradation of triacylglycerates (TAGs) by secreting these enzymes into the environment (Peacock *et al*., 2002). However, there are a variety of mechanisms involved in the uptake of oils by cells ranging from simple diffusion in the case of *S. coelicolor* (Banchio *et al*., 1997) to the possible involvement of lipases (Berk, 1996; Cavanagh *et al*., 1994, Large *et al*., 1998). Odd-chain triacylglcerates, degraded through the β-oxidation pathway, are the most commonly used oils in antibiotic fermentations. Such TAGs enter the metabolic network at the acetyl-Coenzyme A metabolite node and their degradation has been reported to proceed via valine pathway (Zmijewski *et al*., 1986; Boeck *et al*., 1990; Mouslin *et al*., 1997). In studies with *Streptomyces hygroscopicus,* Mouslin *et al*

(1997) found methyl oleate to stimulate the uptake of valine and influenced the long-chain fatty acid content of cells resulting in improved production of the polyether antibiotics nigericin and abierixin.

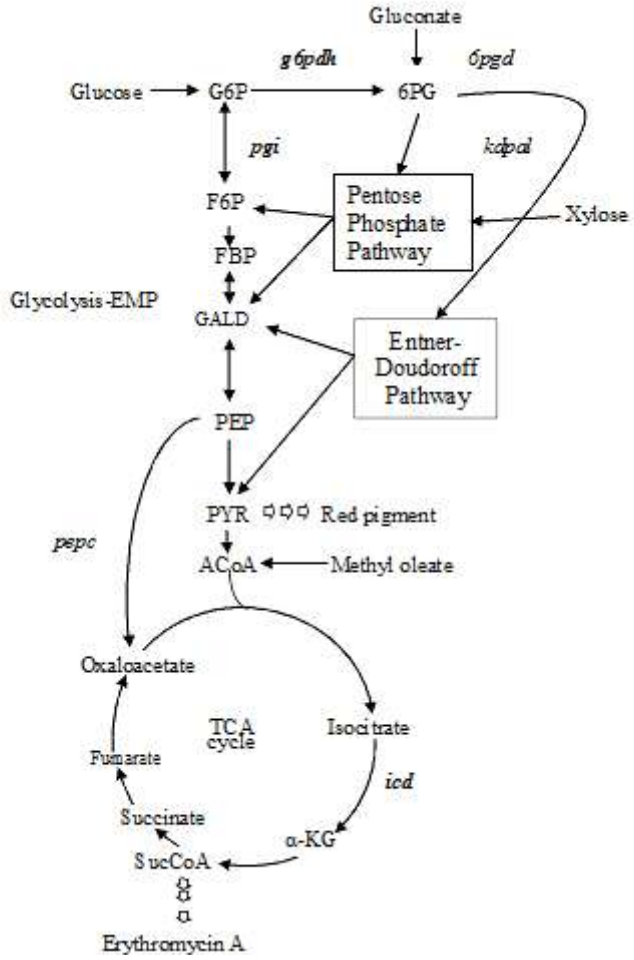

Fig. 11 The major pathways of carbon catabolism including the route to erythromycin biosynthesis in *S. erythraea*. Glucose-6-phosphate dehydrogenase - g6pdh, glucose-6-phosphate isomerase - *pgi*, phosphoenolpyruvate carboxylase - *pepc*, isocitrate dehydrogenase - *icd*, 6-phosphogluconate dehydratase - *6pgd*, 2-keto-3-deoxy-6-phosphogluconate aldolase - *kdpal*.

4.3 Research design

Four single 1L shake flask fermentations were conducted each using glucose, gluconate, xylose and methyl oleate as the sole carbon and energy source. For each of the fermentations, a C/N ratio of 36:1 was used .The cultivation, sample preparation and analyses were performed as outlined in Chapter 2.

4.4 Results and Discussion

To select carbon sources for use in the physiological characterisation, growth and the production of the red pigment in *S. erythraea* were evaluated in shake flasks. Selection of the red pigment as a parameter was based on its potential drain of carbon sources that could have gone towards product biosynthesis. The findings of Ushio (2003) and Jaques (2004) indicated that this red metabolite correlate negatively with the production of erythromycin. Measuring the concentration of the red pigment is also less complicated and therefore convenient compared to erythromycin. *S. erythraea* was cultured on a single carbon and energy source.

Growth of *S. erythraea* on glucose is well-established though product formation has not been fully characterised. Some work has been done by Jaques (2004) on modelling metabolic pathways using flux balance analysis (FBA). Biomass was highest on gluconate (5.79 $g.L^{-1}$) and glucose (5.84 $g.L^{-1}$) compared to the other carbon sources. . With the exception of glucose, the growth phase extended over 72 hours (Fig. 12 - 15). However, less red pigment was produced when the culture was grown on gluconate compared to growth on glucose. Up to 0.67 $g.L^{-1}$ of the red pigment was excreted compared to nearly 0.2 $g.L^{-1}$ for gluconate. Thus, when grown on glucose as a sole carbon source, *S. erythraea* biomass formation was accompanied by the excretion of large amounts of pigment. Pigment formation increased significantly after the growth phase (48 hours) and continued until the end of the fermentation. However, when grown on gluconate, pigment production started during the growth (24 hours) and reached maximum levels at 48 hours after which the levels dropped significantly (Fig. 13). Though growth profiles were somewhat different, both glucose and gluconate supported growth of *S. erythraea.*

S. erythraea was able to grow on xylose as a sole carbon and energy source. However, with a maximum biomass of 3.3 $g.L^{-1}$, growth xylose supported the lowest growth of all carbon sources investigated (Fig. 14). The combination of a long lag phase and low biomass formation possibly reflects the need for the synthesis of isomerase and/or transporter proteins to enable xylose metabolism. The actual mechanism of xylose import into the cell is not known for *S. erythraea*. Though much lower levels of the red pigments were excreted on xylose, the profile

resembled that observed for glucose. Significant amounts of pigment production only started after the growth phase (48 hours) and continued until the end of the fermentation (Fig. 14). However, the fact that xylose supported growth suggests that *S. erythraea* does possess xylose isomerase and a mechanism for the uptake of this pentose sugar. Compared to growth on gluconate, *S. erythraea* produced more pigment and less biomass on xylose (Fig. 13, Fig. 14). These two carbon sources are different in that gluconate is a 6-carbon organic acid while xylose is a 5-carbon sugar. Their entry point into the metabolic network is, therefore, different. It is also worth pointing out that the mechanisms of uptake into the cell may be quite different. All this could explain the variation in the rates of growth and the production of the pigment. The relationship between biomass synthesis and the formation of the pigment suggests a negative correlation between the two products. Since primary and secondary metabolism compete for precursor metabolites from central metabolism (Rokem *et al*., 2007), it can be expected that the drain of precursors for secondary metabolism will constrain primary metabolism. The observed negative correlation between biomass synthesis and pigment formation could be due to this situation.

As expected, no pigment was observed for the culture grown on methyl oleate (Fig. 15). Methyl oleate is an ester of fatty acids which is oxidised via the β-oxidation pathway to generate Acetyl-Coenzyme A. As such, it bypasses the pyruvate node from which the red pigment formation is derived. Given the physical effects of viscosity on the oxygen and carbon source uptake rate, it was not surprising that growth on methyl oleate produced a maximum biomas concentration of 1.9 $g.L^{-1}$ (Fig. 15). High viscosity due to oils reduces the rates of oxygen transfer (OTR) and uptake (OUR) causing limitations. Nevertheless, very low biomass was produced on methyl oleate in the absence of any draining of precursors for pigment formation. Of all carbon sources investigated, biomass concentration on methyl oleate was the lowest. This could be due to viscosity effects or limitations in lipases production (Mirjalili *et al*., 1999). However, it may also be due to the treatment of samples during preparation. To remove any residual oil, samples were washed with 1 mL ethanol/Tween 80 solution. This treatment could have reduced biomass by removing membrane lipids. *S. erythraea* appears to have the enzymes necessary to utilise various common and uncommon oils (Hamedi *et al*., 2004). Other actinomycetes

have also been reported to utilise oils as sole carbon sources (Efthimiou *et al*., 2008). *Streptomyces clavuligerus* was able to produce a higher biomass on olive oil than on glycerol as sole carbon and energy sources, but clavulanic acid production was lower for the oil. Based on the low biomass formed, methyl oleate is not likely to be suitable as a sole

carbon and energy source.

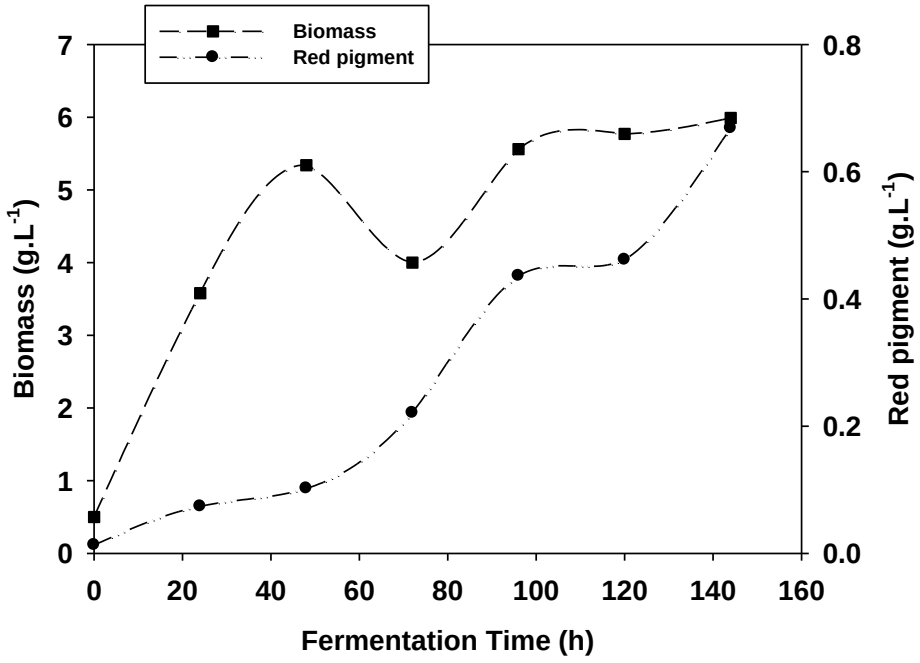

Fig. 12 Time courses of biomass (g.L-^{1}) and red pigment (g.L^{-1}) during growth of *S. erythraea* on glucose in shake flask culture.

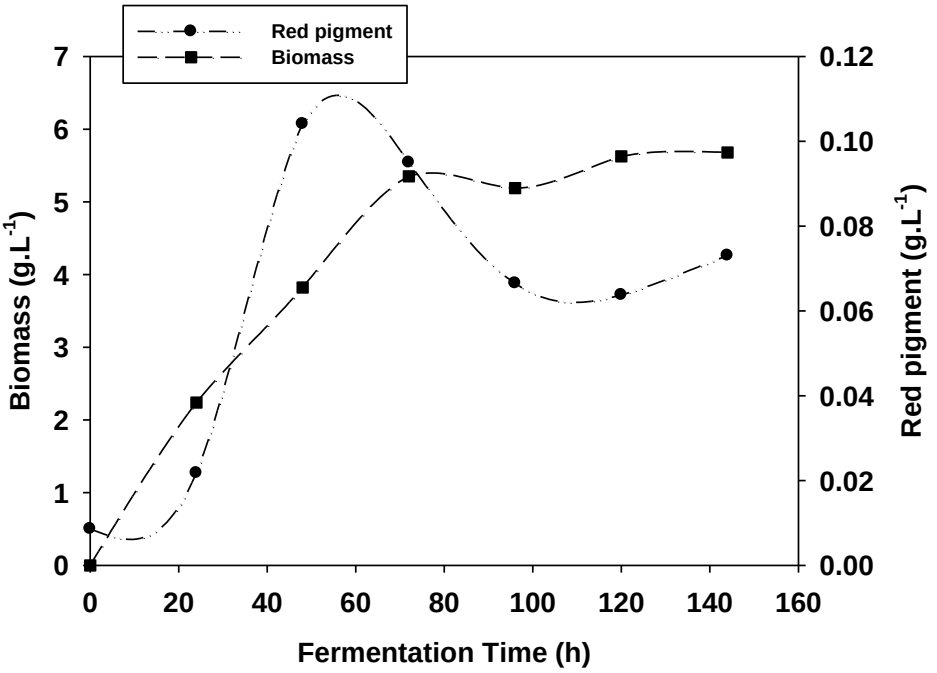

Fig. 13 Profiles of biomass ($g.L^{-1}$) and red pigment ($g.L^{-1}$) during growth on gluconate as a sole carbon source in shake flask culture.

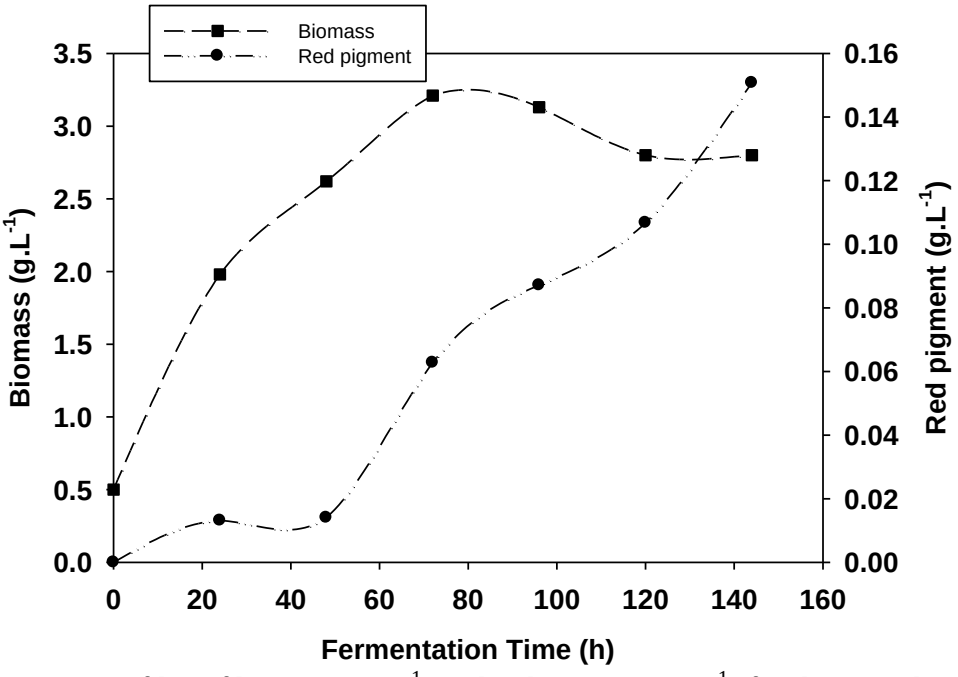

Fig. 14 Profiles of biomass ($g.L^{-1}$) and red pigment ($g.L^{-1}$) for the growth of *S. erythraea* on xylose as a sole carbon source in shake flask culture.

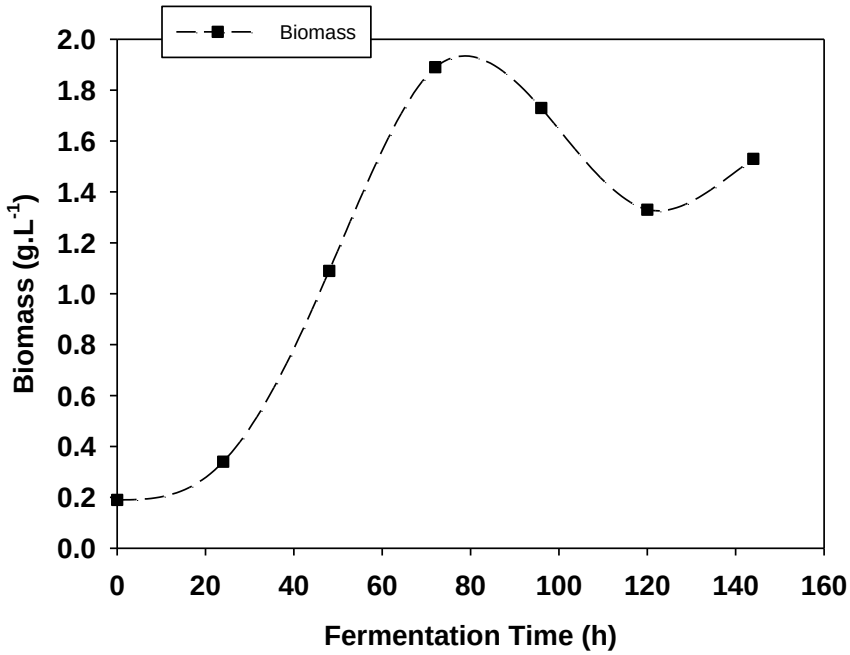

Fig. 15 Profile of biomass ($g.L^{-1}$) for shake flask growth of *S. erythraea* on methyl oleate as a sole carbon source in shake flask culture.

When *S. erythraea* was grown on methyl oleate as a sole carbon and energy source, no red pigment was observed (Fig. 16). However, methyl oleate has been reported to support microbial growth as a sole carbon source (Efthimiou *et al*., 2008). In the current work, *S. erythraea* produced a relatively low biomass. It is suggested that the inability of methyl oleate to induce the production of the red pigment may promote the production of erythromycin. However, this suggestion was not tested under the current conditions but will be investigated in bioreactor studies in subsequent studies.

Fig. 16 Profile of red pigment produced by *S. erythraea* during growth on different carbon sources.Vials represent from left to right: gluconate, methyl oleate, glycerol, xylose and glucose. Glycerol was included for comparative reasons only.

4.5 Summary

Glucose, gluconate, xylose and methyl oleate all support growth of *S. erythraea*. However, *S. erythraea* grows very slowly on methyl oleate. Production of low amounts of the red pigment is desirable as this could indicate potential to produce higher levels of erythromycin. Excretion of the red pigment could reduce the production of the antibiotic. Gluconate produced low levels of erythromycin but a higher biomass concentration was obtained. On xylose, *S. erythraea* had a long lag phase produced an average biomass concentration. All four carbon sources screened are used in subsequent studies either as sole carbon sources or in combination with other carbon sources.

4.6 Batch bioreactor fermentations

Antibiotics are produced from the precursor metabolites generated during primary metabolism. In addition to supplying carbon precursors, primary metabolism generates the energy and the reducing equivalents, NADH and NADPH associated with energy generation and reductive biosynthesis respectively.

There is an interaction between primary and secondary metabolism (Fig.1) that enables the production of antibiotics (Jonsbu *et al*., 2000). While it is not clear how the two metabolic modes interact to effect the production of secondary metabolites, changes in the specific growth rate have been observed to lead to changes in the distribution of fluxes among the central metabolic pathways. For example, the production of nystatin is correlated with decreased fluxes through the pentose phosphate pathway (PPP) and increased TCA cycle activity (Jonsbu *et al*., 2000). These researchers found significant changes in the PPP, TCA cycle and anaplerotic pathway fluxes (from pyruvate to oxaloacetate) when the specific growth rate decreased and the antibiotic production increased. This confirms the pivotal role of primary metabolism in secondary metabolite production. Earlier work by Penzikova & Levitov (1966) has hinted at the effect of flux distribution on antibiotic production. Other studies have concluded that antibiotic production is affected by carbon storage metabolites produced during primary metabolism. This suggests that precursor metabolites that accumulate during primary metabolism are required for secondary metabolite production. Clavulanic acid was observed to increase in response to the accumulation of glyceraldehyde-3-phosphate in *Streptomyces clavuligerus* (Li & Townsend, 2006). In *Streptomyces coelicolor,* fructose-6-phosphate and glucose-6-phosphate accumulation correlated positively with increased levels of undecylprodigiosin and actinorhodin (Borodina *et al*., 2008). Clearly, the pathways of carbon degradation are of vital importance since they determine metabolite pool sizes. Various studies have focussed on flux distributions through pathways to elucidate mechanisms of control of antibiotic production (Avignone-Rosa *et al*., 2002; Daae and Ison, 1999; Naeimpoor & Mavituna, 2000). Other studies have focused on the role of NADPH in the production of antibiotics (Obanye *et al*., 1996; van Gulik *et al*., 2000). In general NADH and NADPH are generated through glycolysis and the PPP respectively. However, some organisms including *S. erythraea* and *S. lividans* have a NAD^+-dependent 6-phosphogluconate dehydrogenase and therefore generate both NADPH and NADH through the PP pathway (Jaques, 2004; Butler *et al*., 2002). This has implications for flux distribution. The supply of reducing equivalents can be manipulated to enhance product yield either through genetic engineering (Butler *et*

al., 2002) or changing the culture conditions (Avignone-Rosa *et al*., 2002). Though the interaction between primary and secondary metabolism has been studied extensively in many genera, such investigations remain largely unexplored for *S. erythraea*.

In this chapter the partitioning of carbon fluxes at key branch points as a function of the carbon source will be characterised and their possible correlation with intracellular metabolites and erythromycin biosynthesis investigated.

4.6.1 Research design

Glucose was used as a sole carbon source in the first set of experiments to study the flux distribution at the pentose phosphate pathway/Embden-Meyerhoff-Parnas pathway (PPP/EMP) and between the anaplerotic reaction from phosphoenolpyruvate (PEP) to oxaloacetate (Hodgson, 2000) and the TCA cycle (PEP/TCA). The rationale for this selection is that glucose is a common carbon source on which many actinomycetes can easily grow. In the second set of experiments gluconate was used as a sole carbon source. Gluconate is a 6-carbon organic acid and is known to be degraded through glucose-6-phosphate dehydrogenase, the first enzyme of the pentose phosphate pathway and then through the Entner-Doudoroff pathway (White, 2007).

Fermentations were performed in triplicate in 7.5 L New Brunswick fermenters under the conditions described in Chapter 2. Sampling, sample handling and analysis was done as described in Chapter 2.

In bioreactor fermentations, xylose had a very long lag phase and no measurable growth was observed for seven days. It is not clear why *S. erythraea* was able to grow on xylose in shake flasks but failed to grow significantly at 7.5 L scale. On methyl oleate *S. erythraea* produced measurable growth only after 6 days of culturing suggesting that the organism needed to synthesise the required lipases to metabolise the oil. This finding is agreement with those Mirjalili *et al* (1999). In that study, after addition of 10 gL^{-1} oil, significant specific lipase activity was only observed after 130 hours of *S. erythraea* growth.
Consequently, both xylose and methyl oleate were not used as sole carbon and energy sources.

4.6.2 Glucose as a sole carbon and energy source

4.6.2.1 Growth characteristics

The exponential growth phase lasted 48 hours and had two distinct phases. The first 24 hours were characterised by high rates of glucose uptake (0.34 $g.g^{-1}h^{-1}$) and biomass formation. Respiration, as indicated by the OUR, was high during the accelerated exponential phase which supported a maximum biomass of 2.3 $g.L^{-1}$(Fig. 17, Fig. 17). The carbon uptake rate, OUR and CER increased during the first 24 hours of the log phase. However, biomass reached a maximum of 3.5 $g.L^{-1}$ by48 hours.(Fig. 17). The overall specific growth rate was 0.06 h^{-1} (Table 15). The culture consumed nitrate rapidly, depleting it within the first 24 hours of growth upon which growth rate subsequently decreased.

Table 15. Specific growth rate, biomass and product yields for growth on glucose.

Culture conditions	**Growth parameters**			
Carbon source	Growth rate (h^{-1})	$Y_{x/s}$ ($g.g^{-1}$)	$Y_{p/s}$ ($mg.g^{-1}$)	$Y_{p/x}$ ($mg.g^{-1}$)
Glucose	0.06	0.17	2.73	20.54

The first 24 hour growth period was followed a 15 hour phase from 24 to 39 hours during which time CER briefly dropped significantly and then continued to increase at the about the same rate as OUR (Fig. 18). The culture increased its consumption of oxygen much more than the increase in the evolution of CO_2. The balance observed between these two parameters during the exponential growth phase, was disturbed in favour of OUR^1 during the period from 24 hours to 39 hours. Glucose uptake rate was increased from 0.3 $g.g^{-1}.h^{-1}$ to 0.6 $g.g^{-1}.h^{-1}$ over the 15 hour period. The respiratory quotient (RQ) dropped by 34% despite the rapid carbon source uptake. During this time the levels of erythromycin remained negligible. It appears *S. erythraea* simultaneously increased its consumption of glucose and oxygen while reducing its growth rate. Thus, precursors generated during this phase appeared not to have been diverted towards growth.

The balance observed between the rates of carbon and O_2 uptake and CO_2 evolution in the previous phase was disrupted. The rate of glucose consumption dropped from 0.6 $g.g^{-1}.h^{-1}$ to 0.01 $g.g^{-1}.h^{-1}$ from 39 to 48 hours (Fig. 17). This slow uptake rate coincided with decreased respiration as indicated by the decrease in the OUR levels (Fig. 18). The production of erythromycin was triggered during this phase of growth (Fig.18). However, this also coincided with depletion of nitrate which could have caused a reduction in the demand for both glucose and oxygen. Glucose was consumed rapidly 15 hours after the depletion of nitrate, with the levels dropping from 19 to 10 $g.L^{-1}$ between 24 and 39 hours.

Between 48 and 72 hours glucose consumption was increased from 0.01 to 0.3 $g.g^{-1}.h^{-1}$. Respiration continued to decrease while coinciding with a drop in the level of erythromycin from 18 to 14 $mg.L^{-1}.g^{-1}$ (Fig. 17, Fig. 18).

By 96 hours almost all glucose was depleted and its rate of consumption fallen to 0.01 $g.g^{-1}.h^{-1}$. The RQ reached a maximum of 1. Erythromycin production reached a maximum of 21 $mg.L^{-1}.g^{-1}$ from 18 $mg.L^{-1}.g^{-1}$ in the previous phase.

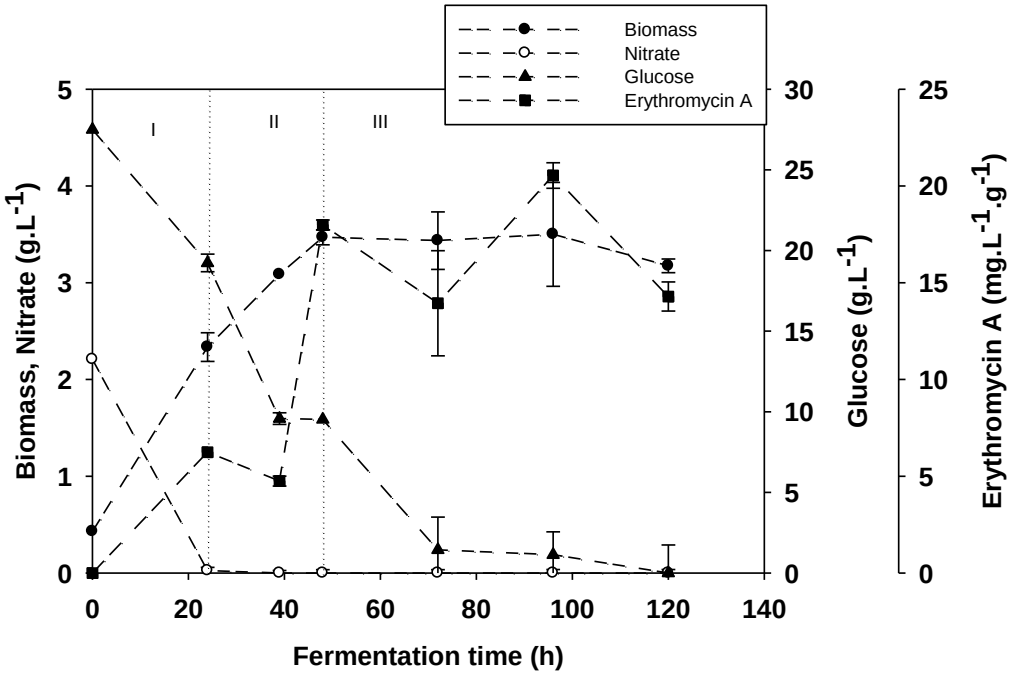

Fig. 17 Time courses of biomass, glucose and nitrate and erythromycin A for the culture grown on glucose. Data represent means of three separate fermentations of which three samples were analysed. This represents three biological and technical replicates.

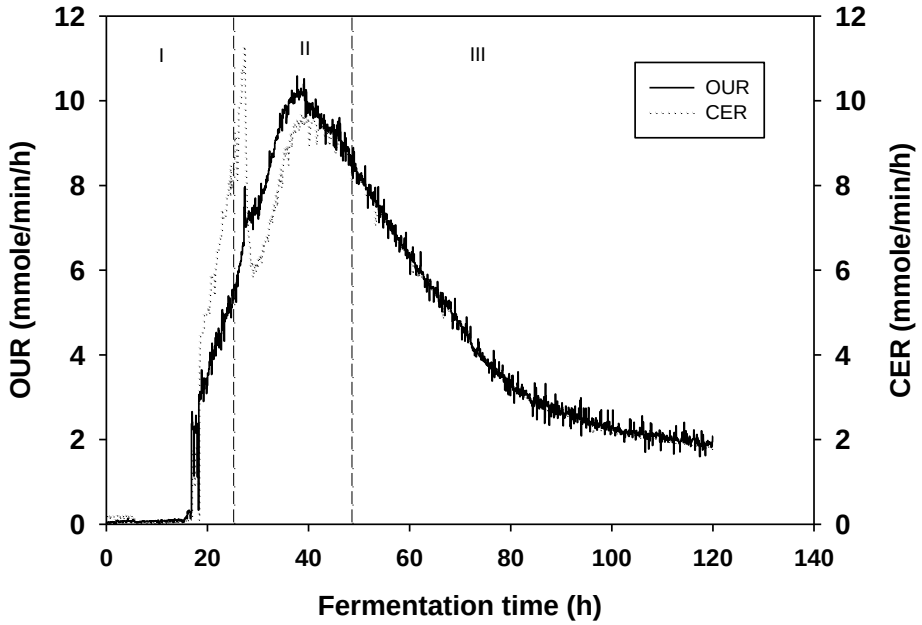

Fig. 18 Profiles of OUR and CER for the culture grown on glucose as a sole carbon and energy source.

4.6.2.2 Effect of glucose uptake rate on erythromycin prodcuction

The increase in the production of erythromycin was preceded by a period of rapid glucose uptake rate and reduced respiration. The rate of glucose consumption subsequently dropped during the antibiotic production phase (Fig. 19). Before the onset of erythromycin production, glucose uptake rate did increase from 0.3 to 0.6 $g.g^{-1}h^{-1}$between 24h and 39h. When the uptake rate dropped from 0.6 to 0.01 6 $g.g^{-1}$ between 39 and 48 hours, the production of erythromycin increased from 4.7 to 18 $mg.L^{-1}.g^{-1}$, a trend that was repeated between 48 and 96 hours. Glucose concentration increased from 0.01 to 0.3 $g.g^{-1}$ between 48 to 72 hours after which it dropped to0.01 $g.g^{-1}$ from 72 to 96 hours. These two phases (48 - 72 hours and 72 - 96 hours) coincided with a decrease and an increase in the production of the antibiotic respectively. The increase in the production was preceded by a phase of imbalance between the specific glucose uptake rate and the rate of respiration. In general, a

negative correlation was observed between the rate of glucose consumption and the increase in the levels of erythromycin (Fig. 19).

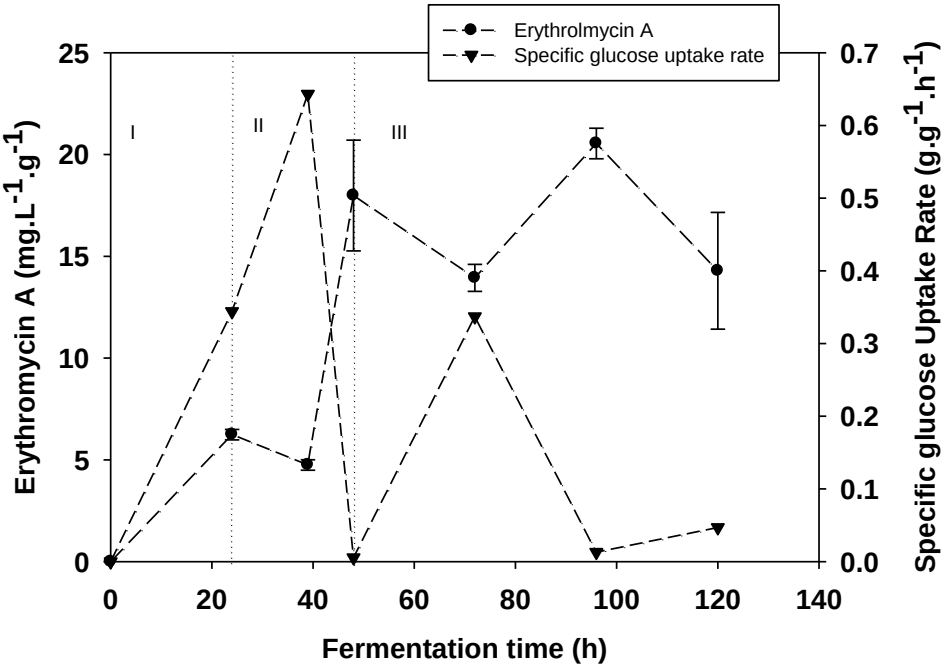

Fig. 19 Relationship between the specific glucose uptake rate and erythromycin A. Data represent means of three biological and technical replicates.

4.6.2.3 Correlation between the production of erythromycin and the generation of pyridine cofactors

For the accelerated log phase, the concentrations of both NADH and NADPH were below detectable levels (Fig. 20). However, NADH levels increased marginally from 0 to 0.03 µM.g^{-1} between 24 to 48 hours (Fig. 20). The increase was higher by 57% between 39 and 48 hours when the uptake of glucose dropped by 99%. The concentrations of NAD appeared to increase with decreasing specific glucose uptake rate. No apparent correlation was observed between the levels of NADH and erythromycin production after 48 hours. NADPH remained undetectable until after the growth phase at 48 hours. This cofactor was only detected between 48 and 72 hours and correlated negatively with the production of erythromycin.

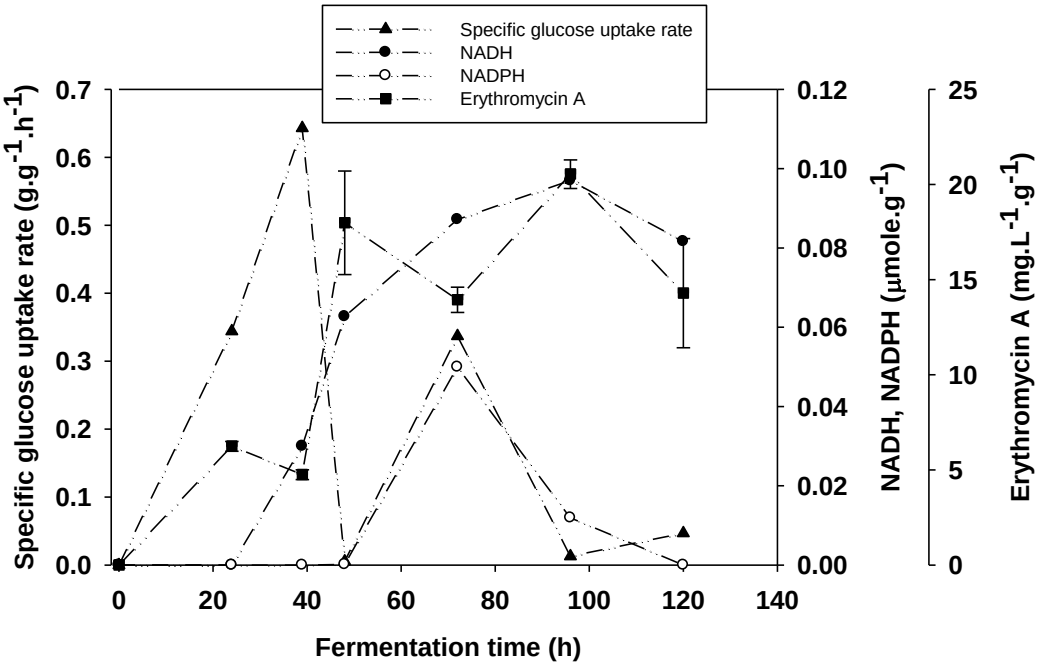

Fig. 20 Profiles of NADPH, NADH and erythromycin A during growth on glucose as sole carbon and energy source source. Data represent means of three biological and technical replicates.

4.6.2.4 Correlation between cell energetics, specific glucose uptake rate and product formation

The energy charge (EC) of the cell is defined as the energy available for metabolic processes in the cell. Much of this energy is present as ATP, though the energy charge consists of contributions from ATP and ADP in the equation

Energy charge = [(ATP) + 0.5*(ADP)]/[(ATP) + (ADP) + (AMP)]

When the energy charge is 1, ATP and the energy of the cell is at its maximum. An energy charge of zero (0) indicates energy deficiency and maximum levels of AMP.

The energy charge increased from 0 and reached a maximum of 0.9 at 39 hours (Fig. 22). This trend correlated with increasing specific glucose uptake rate over the same period (Fig. 21). After the accelerated growth phase, the energy charge remained constant for 15 hours between 24 and 39 hours and then continued to decrease until 72 hours (Fig. 22). Thus the energy charge increased steadily during the biomass synthesis phase and only started to decreased at the onset of the erythromycin production phase (Fig. 20, Fig. 22). The respiratory quotient increased during the biomass synthesis phase up to 24 hours after which it decreased and remained

relatively constant at a value of 1 (one) (Fig. 21). The very high respiratory quotient during the accelerated exponential growth phase coincided with an increase in the rate of glucose uptake. However, after the growth phase, the rate of glucose consumption and the respiratory quotient were independent of each other. While the rate of glucose consumption continued to decrease and increase, the respiratory quotient was maintained constant around the value of 1 (one).

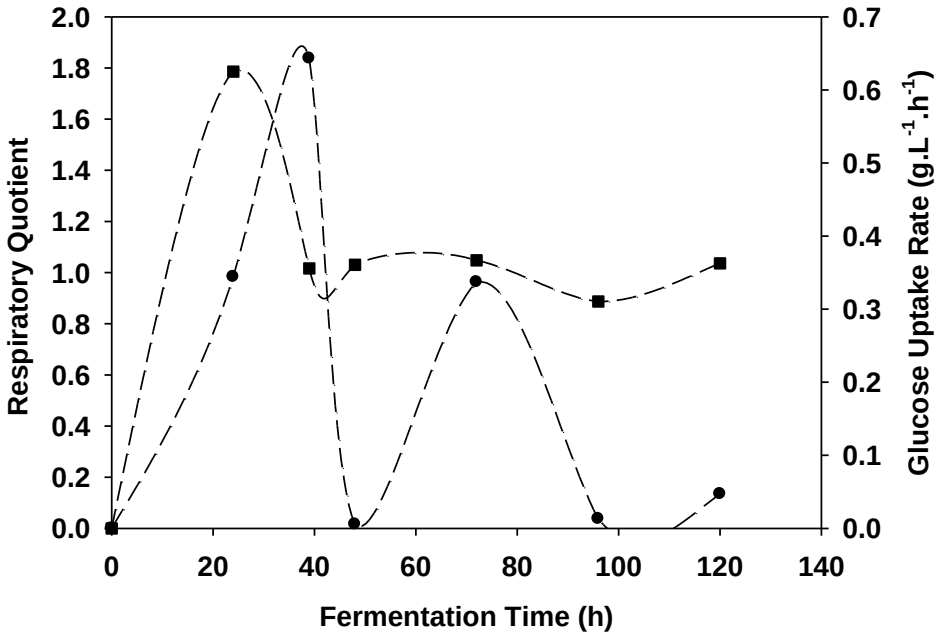

Fig. 21 Profiles of the respiratory quotient (■) and glucose uptake rate (●) for *S. erythraea* grown on glucose as a sole carbon and energy source.

Overall, there was a negative correlation between the energy charge and the production of erythromycin (Fig. 22). This trend continued throughout the duration of the fermentation. Increases in both the rate of glucose consumption and the energy charge appeared to coincide with a decrease in the production of the antibiotic (Fig. 21, Fig. 22).

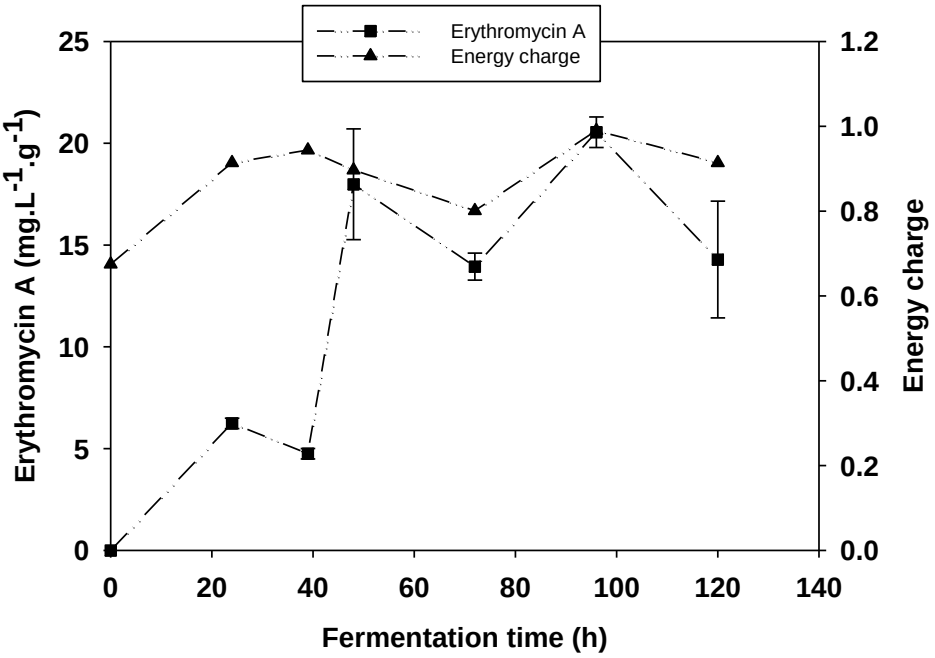

Fig. 22 Profiles of the energy charge (▲) and erythromycin A (■) for *S. erythraea* grown on glucose as a sole carbon and energy source.

4.6.2.5 Effect of glucose consumption rate on activities at PPP/EMP, anaplerotic pathway/TCA cycle and EMP/TCA branchpoints

The pathways of carbon degradation, their intersections and key branch point enzymes are given in Fig. 11. During the biomass synthesis phase, the activities of phosphoglucose isomerase were dominant up to hours after which those of glucose-6-phosphate dehydrogenase (G6PDH) significantly increased to reach a maximum at 48 hours (Fig. 23). The ratio of G6PDH/PGI remained low during the fast growth phase from 0 to 24 hours (Fig. 23) suggesting that phosphoglucose isomerase (PGI) activities were dominant. The rate of glucose consumption and the energy charge increased to a maximum during the growth phase up to 39 hours. However, from 24 to 39 hours, the activities of G6PDH increased significantly. The increase in the ratio suggests a switch to the pentose phosphate pathway as the main route of glucose degradation. Since G6PDH is the branch point enzyme between glycolysis and the pentose phosphate pathway (PPP), the increase in G6PDH activities may indicate an increase in flux through the PPP. If this is the case, such an increase in PPP flux could be due to the high rate of glucose consumption observed during the same period. However, no actual fluxes were measured and therefore this is only a

suggestion.

During the accelerated growth phase, the low ratio suggests that the activities of isocitrate dehydrogenase (ICD) were dominant relative to the anaplerotic reaction (Fig. 23). Since ICD activities are a reflection of the TCA cycle activity, it appears that the TCA cycle played a major role during the exponential growth phase up to 24 hours. The activity of the TCA cycle appeared to increase significantly between 24 and 39 hours as indicated by a decrease in the ratio of the enzymes. No erythromycin production was observed during this period. The rate of glucose consumption and the energy charge were observed to reach a maximum during this period. However, there appeared to have been a switch between 39 and 48 hours when the ratio increased significantly indicating an upregulation in the activities of PEPC. In the previous section, this period was associated with a drop in both the levels of glucose consumption and energy charge and the onset of erythromycin production. The anaplerotic activity remained relatively constant during the erythromycin synthesis phase from 48 to 96 hours. The ratio of PGI/PEPC indicates that glycolytic activity increased during the growth phase up to the early stage of erythromycin synthesis production phase at 48 hours. It can be observed that, at the onset of erythromycin production between 39 and 48 hours, the pentose phosphate pathway, glycolysis and the anaplerotic reaction play a major role. Therefore, there appears to be a link between the production of the antibiotic and the activities of G6PDH, PGI and PEPC. After the growth phase, PEPC activity was observed to be important during both the precursor accumulation phase (48 to 72 hours) and production (72 to 96 hours). However, what is consistent is PGI and PEPC activity during the production of erythromycin. This suggests that the glycolysis and anaplerotic reaction is essential for the production of the antibiotic. The pentose phosphate pathway appears to be necessary for the onset of erythromycin production. However, after the production of the antibiotic was triggered, G6PDH activity does not appear to play an important role. G6PDH activity dropped during the accumulation phase from 48 to 72 hours, However, NADPH levels were observed to have increased during the same period. NADPH is known to be generated by the activities of G6PDH and ICD. It appears therefore, that ICD provided NADPH during this period. It is noteworthy

that the ratio of PEPC/ICD did not increase between 48 and 72 hours which could suggest that the TCA cycle activity was probably enhanced.

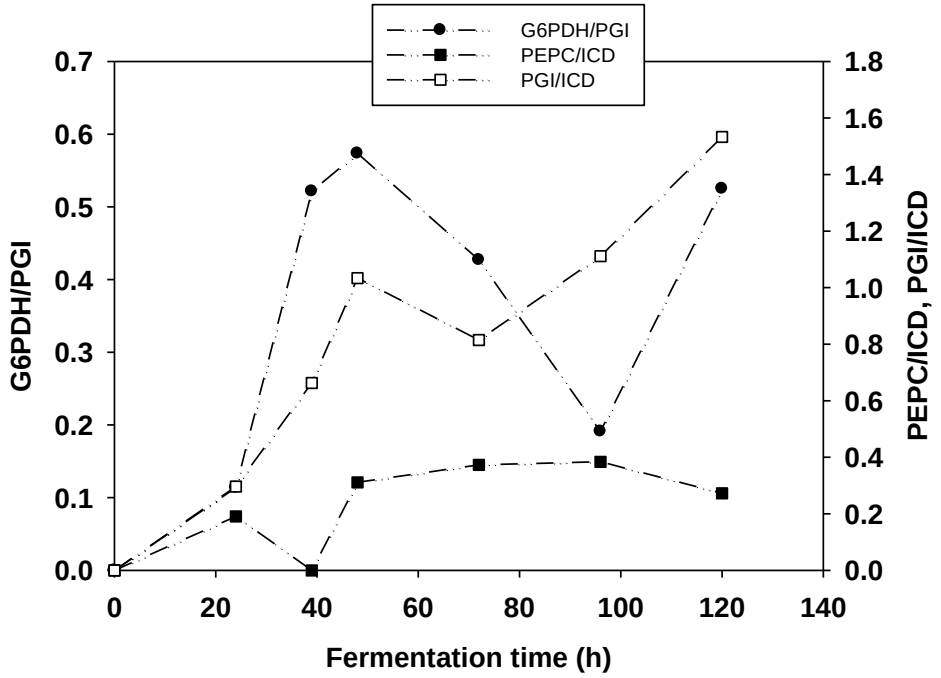

Fig. 23 Correlation between the ratios of activities of branchpoint enzymes and key pathway enzymes for the culture grown on glucose as a sole carbon and energy source Phosphoglucose isomerase - *pgi*, phosphoenolpyruvate carboxylase - *pepc*, isocitrate dehydrogenase - *icd*, G6PDH, PGI, PEPC and ICD represent fluxes to the PPP and ED, EMP, the anaplerotic pathway from PEP to oxaloacetate and the TCA cycle respectively. Enzymes activities were expressed as activity specific to biomass and the ratios calculated to yield a unitless value. Branch point enzymes give a better picture if expressed as ratios rather than single entities.

4.6.2.6 Effect of glucose consumption rate on the excretion of organic acids

No organic acids were excreted during the fast growth phase. However, the excretion of α-ketoglutarate started from 24 hours of growth (Fig. 23). Excretion of pyruvate and propionate commenced at 24 hours and reached maximum at 48 hours. Fumarate was only observed between 24 and 39 hours. When the growth rate decreased at 24 hours, the red pigment was excreted until the end of the fermentation. However, significant increase in the excretion of the red pigment was only observed after the growth phase at 48 hours. The excretion of propionate started at 24 hours, reached a maximum at 48 hours and dropped to zero between 48 to 72 hours. Pyruvate

excretion reached a peak at 39 hours and declined gradually thereafter until it reached zero at 72 hours. It is interesting to note that the excretion of the red pigment occurred when the glucose uptake rate was significantly increased. The increase in the specific uptake rate also resulted in the excretion of organic acids. However, this happened only after growth had slowed significantly. There was a decrease in the level of the red pigment possibly due to degradation or production at constant rate during the period from 72 to 96 hours. Nevertheless, the production of the red pigment appears to increase with increased rate of glucose consumption between 48 and 72 hours and again between 96 and 120 hours (Fig. 23). This appears to have been occurring simultaneously with the significant decrease in glucose levels (Fig. 17, Fig. 23). It could be that a high rate of glucose consumption results in the excretion of large amounts of the red pigment.

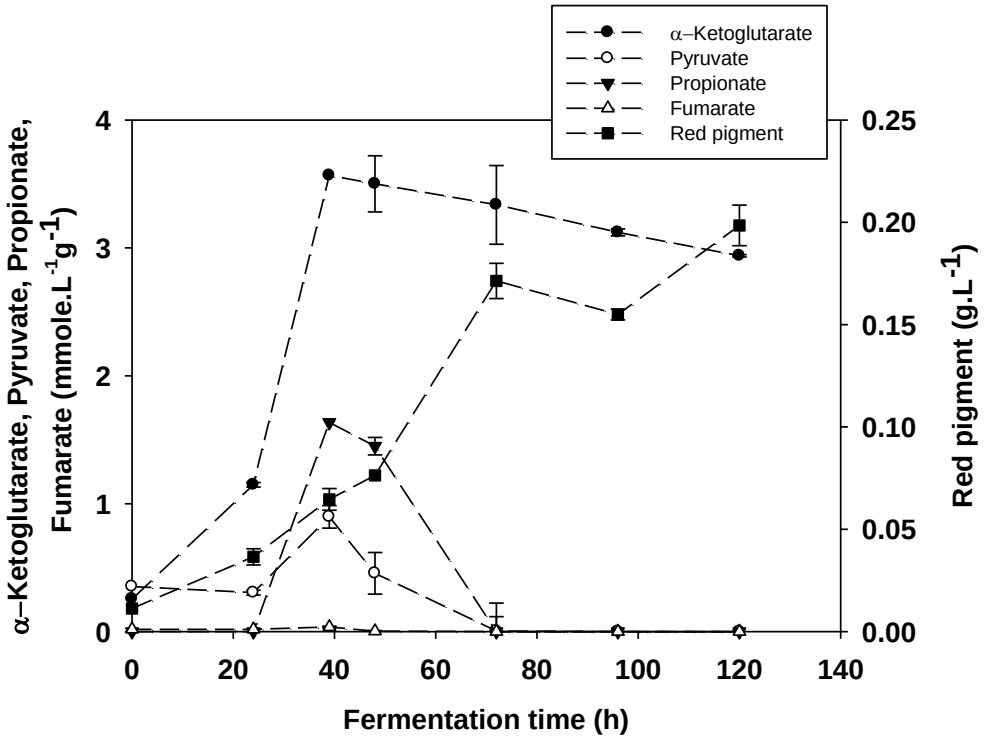

Fig. 24 Time courses of specific values of α-ketoglutarate, pyruvate, red pigment, propionate and fumarate during growth on glucose as a sole carbon and energy source.

A general observation is that significant amounts of organic acids were observed between 24 and 39 hours. The maximum amounts of all measured organic acids were

reached at 39 hours. The exception to this is the red metabolite whose excretion increased after 48 hours. The time of organic acid excretion correspond to the phase during which glucose consumption and and energy charge were at maximum levels.

4.6.2.7 Carbon balance determination

The molecular weight of the biomass for *S. erythraea* was based on the general molecular formula of biomass, $CH_{1.8}O_{0.5}N_{0.2}$ (Doran, 1995). Using this formula, the average molecular weight of biomass is about 24.6 g which is equivalent to one C-mole of biomass. The total biomass weight obtained for *S. erythraea* was 23.7 g for growth on glucose. This value is within 3.6% of the general tabulated weight of 24.6 g for bacteria. A biomass value for a related species was provided by Bushell and Fryday (1982). Based on the elemental composition, the Bushell and Fryday determined the biomass formula for *Streptomyces cattleya* to be $CH_{1.6}O_{0.58}N_{0.17}$. This formula translates into a biomass weight of 25.26 g for *Streptomyces cattleya* as calculated by the authors. It was, therefore, reasonable to use the general formula, $CH_{1.8}O_{0.5}N_{0.2}$ as proposed by Doran 1995) as a basis for calculating carbon utilisation in *S. erythraea*.

The carbon portion in the biomass amounted to 47.5%. In the absence of elemental determination, the percentage carbon for this work was calculated to be 48.8% based on the general biomass formula, $CH_{1.8}O_{0.5}N_{0.2}$ (Doran, 1995).

Biomass accounted for almost 50% of the carbons derived from the carbon source (Table 16). Of the organic acids, about 36% of the carbons were excreted as α-ketoglutarate. Since all organic acids were excreted during the growth phase, carbon wastage therfore occurred during growth. After the growth phase, the red pigment accounted for most of the carbons wasted (Table 16). *S. erythraea* allocated equal percentage of carbons from glucose to erythromycin and pyruvate. Perhaps the low percentage alloacated to pyruvate reflects the 4.5% carbons that went into red pigment formation. Overall, 97% of the carbons derived from glucose could be accounted for. The balance may have gone into other unmeasured compounds. It is important to note that most the carbons from glucose were utilised during the growth

phase either in biomass synthesis or excreted as organic acids. This suggests that growth rate may be a critical parameter in carbon utilisation.

Table 16. *Carbon balance for S. erythraea growth on glucose.*

C Recovery	Glucose	Biomass	Pyr	Red	α-KG	Suc	Fum	Prop	Ery	$^{b}CO_2$
Initial mmole C	915.7	-	-	-	-	-	-	-	-	-
[a]Millimole C	-	447	15.7	41.3	328.3	-	0.7	30.2	15.6	12.7
Percentage C	-	48.8	1.7	4.5	35.9	-	0.1	3.3	1.7	1.4
Total millimole C recovered		891.5								
Total % C recovered		97.4								

[a]*Millimole C calculated as follows: mmole x number of C in metabolite*
[b]*Millimole C in CO_2 calculated as per 5L working volume of bioreactor*
Percentages were calculated as millimole carbon in each metabolite as a percentage of the total initial millilmole carbon in glucose.
Pyr - pyruvate, α-KG - α-Ketoglutarate, Suc - Succinate, Prop - propionate ,
Fum - Fumarate, Ery - Erythromycin A, Red - Red pigment

4.6.3 Discussion

The production of secondary metabolites requires precursor metabolites and the reducing equivalent associated with reductive biosynthesis, NADPH. Distribution of carbon fluxes through the various pathways can be expected to affect the levels of carbon precursor and pyridine cofactor pools. Therefore the flux split ratio between glycolysis-EMP and the pentose phosphate pathway will have a bearing on the production of antibiotics (Penzikova & Levitov, 1966). The split in fluxes at PPP/EMP, anaplerotic pathway/TCA cycle and the EMP/TCA cycle branch points, are probably dependent on the physiological state of the cell. Therefore, the rate of carbon source consumption could affect the distribution of fluxes through the system since it is dependent on cell requirements.

The following three general phases where observed during the fermentation and will be discussed in detail.

1. Growth phase (0 - 24 h)
2. Metabolite accumulation phase (24 - 39 h, 48 - 72 h and 96 - 120 h)
3. Erythromycin production phase (39 - 48 h and 72 - 96 h)

4.6.3.1 Growth phase

It was observed that during the exponential phase, the rate of glucose uptake was high compared to that during the decelerated growth phase. Biomass synthesis increased by 81%. The high glucose uptake rate (GUR) was probably due to the high growth demands. Glucose degradation proceeded mainly via glycolysis during the first 24 hours. Since glycolysis produces ATP and to some extent NADH, this was probably to meet high demands for these metabolites during the growth phase. It is perhaps reasonable to assume that a large proportion of glucose was completely oxidised to CO_2 to meet the high demand for energy and carbon precursors caused by the accelerated growth rate. Confirming this assumption, OUR and GUR were high during the early log phase. Elevated rates of O_2 uptake and CO_2 evolution were observed indicating the high rate of respiration. Considering that glucose uptake rate was high, the high O_2 uptake rate appears to be in excess of the oxidative requirements to ensure complete oxidation of all glucose taken up. This is plausible considering the high demand for precursors and, therefore, the need for increased oxidation of glucose due to high growth. Glycolysis was the major route of glucose degradation (catabolism) to generate the required carbon precursors and to meet energy demands. The TCA cycle has the dual role of generating NADH which is consumed in the respiratory chain (electron transport chain) and NADPH for reductive biosynthesis through the activity of $NADP^+$-dependent isocitrate dehydrogenase. It was notable that ICD activities were the highest of all the measured enzymes during the log phase corroborating the findings of Roszkowski *et al* (1971) with *Streptomyces* sp. In the absence of high G6PDH activities, ICD probably supplied the NADPH required for growth. The TCA cycle generates NADH, an essential respiratory cofactor. Given that the accelerated growth phase has high respiratory requirements, the increase in the activity of the TCA cycle is expected. ICD activity was observed to be relatively high during the growth phase up to 39 hours, where after PEPC became dominant. Equally, when G6PDH activities decreased between 48 and 72 hours, the ratio of PEPC/ICD ceased to increase. This possibly indicates increase in ICD and therefore, TCA cycle activity. It is not known

if *S. erythraea* posseses $NADP^+$-dependent ICD. If it does, the combination of increased ICD and reduced G6PDH activities could have adequately met NADPH demands. The fact that no NADH and NADPH were observed during the growth phase was perhaps due to the high demands of growth. A carbon balance determination revealed that most of the carbons derived from glucose were utilised during the growth phase, which confirms that demand is highest during this phase.

4.6.3.2 Metabolite accumulation phase

When biomass synthesis declined between 24 and 39 hours, the rate of glucose uptake dropped by 5% while the uptake of O_2 was up-regulated by 51%. This increase in OUR could represent an increase in respiration. Increases in the respiratory quotient (RQ) coincided with increases in the rate of glucose consumption during the accelerated growth phase. However, from 24 to 39 hours, RQ decreased while the rate of glucose consumption continued to increase. Such a situation is likely to lead to incomplete oxidation as there may be inadequate oxidising power to meet the increased demands of glucose. There was a positive correlation between the carbon uptake rate and respiration. α-Ketoglutarate, pyruvate and propionate accumulated and reached maximum levels during this phase. A combination of decreases in the rate of respiration with an increase in the supply of carbon skeletons suggests that incomplete oxidation led to the observed increase in organic acids excretion. This would be consistent with accumulation of precursor metabolites which are themselves products of incomplete oxidation. Thus, during this phase glucose was degraded and stored as carbon storage compounds some of which serve as precursors to the biosynthesis of antibiotics. At the onset of the accumulation phase, both G6PDH and ICD activities increased. This coincided with an increase in the levels of the energy charge during the same period. A high energy charge coincided with a reduction in erythromycin production. On the other hand, high ATP levels inhibit ICD to slow down the TCA cycle and reduce the production of excess amounts of the nucleotide in the absence of demand (Alvarado & Flores, 2003; Dawes, 1986). Glycolysis is also controlled by elevated ATP levels through the inhibition of phosphofructokinase (Alvarado & Flores, 2003; Voet & Voet, 2004; Dawes, 1986). If that is the case, then it can be expected that glucose would not be

completely oxidised to CO_2 in the respiratory chain precisely because O_2 supply was limited. In addition, ICD activity decreased by 19% confirming that the TCA cycle slowed down. No PEPC activities were observed indicating that the anaplerotic pathway from phosphoenolpyruvate to oxaloacetate was not active. However, in this case the constraint was not O_2 limitation but inhibition of key enzymes by elevated ATP levels. It appears *S. erythraea* regulates its respiratory capacity according to the demands for carbon precursor metabolites. The increase in the G6PDH activities points to a switch in flux from the EMP to the PPP. The absence of NADPH during the growth phase indicates a high demand for this cofactor and the need to replenish its pools. NADPH is not likely to accumulate when its demand is high. It could be speculated that during this phase (Fig. 25) increased PPP activity enables the accumulation of NADPH, whereas slow glycolytic activity enhances carbon precursor metabolites. Flux through glycolysis during the accumulation phase correlated positively with TCA cycle activity suggesting that both glycolytic and TCA cycle precursors needed to be replenished. The excretion of pyruvate, α-ketoglutarate, propionate and fumarate correlated with increased ICD activity. This also confirms the glycolytic role of metabolite accumulation during this phase. An illustration of the model for the accumulation of precursors and NADPH is provided in Fig. 25 and Fig. 26.

4.6.3.3 Erythromycin synthesis phase

The production of erythromycin was triggered between 39 and 48 hours and coincided with a significant drop in the specific uptake rate of glucose and down-regulation in OUR. This phase was the reverse of the metabolite accumulation phase discussed in the previous section in terms of the specific uptake rate of glucose and respiration. The activities of ICD decreased which suggests a decrease in flux through the TCA cycle (Fig. 21, Fig 22). With the TCA cycle activity decreased, respiration is likely to decrease due to limitations in the supply of NADH. The anaplerotic pathway was significantly up-regulated and coincided with increased flux through the PPP. Flux through glycolysis increased slightly over the same period. We can conclude here that the increase in the production of erythromycin coincided with increased flux through both the PPP and the anaplerotic pathway

from PEP to oxaloacetate and reduced flux through the TCA cycle. Reduced ICD activity, which represents a reduction in the TCA cycle flux, is associated with increases in erythromycin level (Alvarado & Flores, 2003). As expected, the levels of NADH increased reflecting the reduction in the respiratory demand for this nucleotide. This is consistent with a switch in flux to the energy consuming anaplerotic pathway. High [NADH/NAD^+] ratio inhibits citrate synthase, pyruvate dehydrogenase, isocitrate dehydrogenase and α-ketoglutarate dehydrogenase (Alvarado & Flores, 2003; Voet & Voet, 2004; Weitzman, 1972). Thus, the inhibition of any of these enzymes is likely to enhance the anaplerotic pathway. This may explain why the increase in the production of the antibiotic coincided with increased flux through the anaplerotic flux.

Switching carbon catabolism to the PPP would enhance the supply of NADPH through the actions of the oxidative branch of the pathway. Interestingly, the rate of glucose consumption dropped to practically zero during this phase. It is reasonable to argue that very little if any precursors would accumulate during this phase given that glucose uptake had stopped. This perhaps explains the need for increased glucose uptake combined with reduced respiration to accumulate precursors and NADPH before erythromycin production can increase again. Depletion of NADPH and carbon precursors is likely to constrain the production of the antibiotic since both metabolites are essential for its biosynthesis (van Gulik *et al*., 2000). This was indeed what was observed when the production of the antibiotic decreased between 48 and 72 hours. The production of the antibiotic correlated negatively with the levels of NADPH. However, in this case erythromycin decreased even though both G6PDH and ICD activities were high. In fact, 0.05 μmole.$(g\ Biomass)^{-1}$ NADPH was produced between 48 and 72 hours. This is a deviation from the trend observed earlier. Therefore, it is unlikely that NADPH supply limited the production of erythromycin. In addition, the requirements of NADPH for the synthesis of erythromycin are not known. Therefore, it is difficult to determine if NADPH was limiting. The likely cause of this decrease in erythromycin levels is the availability of precursor metabolites. As was discussed in earlier, all organic acids decreased after 48 hours. Accompanied by this decrease was significant increase in the levels of the red pigment after 48 hours. The red pigment appears to drain pyruvate pools. The

carbon balance analysis revealed that *S. erythraea* allocated 4.5% carbons to the red pigment and 1.7% to pyruvate. As the red pigment is derived from pyruvate, it is reasonable to conclude that this metabolite competes with pyruvate for carbons. Draining pyruvate pools will affect the concentrations of precursors going into the TCA cycle and those derived from them.

4.6.3.4 Correlation between the specific glucose consumption rate and growth rate

Increased growth rate promoted glucose degradation through EMP. Increased fluxes through PPP were only observed during the decelerated growth phase. This may suggest that biomass synthesis has high demands for precursor metabolites and energy since both of these are supplied through glycolytic flux. As expected, a strong correlation was observed between the specific glucose uptake rate and biomass synthesis. In the competition for central metabolic precursors, high specific glucose uptake rate promoted diversion of carbons to biomass synthesis resulting in fast growth rate. It can be concluded that much less of the precursors were allocated to secondary metabolite production. As a result, less erythromycin was produced at rapid growth rates. Erythromycin production coincided with significant down-regulation in the specific uptake rate. Given the high carbon demands of biomass synthesis, it is likely that precursor limitations constrained the biosynthesis of erythromycin. This may explain why the antibiotic was produced after biomass synthesis had decreased. The biosynthesis of erythromycin was dependent on both the specific uptake rate and growth rate. Both primary and secondary metabolism draw carbon precursor metabolites from central metabolism. Consequently, at high growth rate, growth demand for precursors will be likely to cause up-regulation in the consumption rate of glucose.

In the absence of PPP flux, NADPH was provided by the TCA cycle through the activity of $NADP^+$-dependent ICD as indicated by the high activity of this enzyme during the accelerated growth phase. Demand for NADPH was not likely to be high because the majority of the NADPH is generated through the PPP (Bruheim *et al.*, 2002) which had little flux through it. ICD activity would, therefore, have been unlikely to meet the high NADPH demands of the polyketide biosynthesis (Rowe *et*

al., 1998; Hutchinson *et al*., 1993) simultaneously with those of biomass synthesis. This partly explains why erythromycin was not produced during the accelerated growth phase. The production of the antibiotic was possibly constrained by limitations in the supply of both carbon precursor metabolites and NADPH. Decreased demand for precursor metabolites when growth decreased resulted in more precursor metabolites being diverted to erythromycin biosynthesis as indicated by the yield coefficients (Table. 15).

4.6.3.5 Glucose and oxygen consumption rate as regulators of metabolite overflow

There is a close relationship between the glucose consumption rate and the rate of respiration. Respiration is dependent on the rate of glucose consumption and both these parameters increase when the culture is growing exponentially. As the exponential growth has high carbon precursor demands, it can be expected that the rate of glucose consumption will be increased to meet demand. The rate of respiration would be expected to increase to generate sufficient energy for the growth phase. Oxygen consumption increased after about 18 hours of growth. During this period, glucose was consumed while little oxygen was taken up. As discussed earlier, this situation favours the accumulation of carbon storage compounds. However, growth demands for precursors would have drained these pools preventing accumulation. On the other hand, there was little biomass at this stage to produce meaningful precursor amounts. The absence of overflow in the form of organic acids spillage confirms this situation. The consumption of glucose remained low during the accelerated exponential phase and increased only after about 18 hours of growth. This lag phase was most likely due to low biomass concentration at that stage. Respiratory metabolism plays a major role in energy metabolism since oxidative phosphorylation is linked to respiration. Respiration and energy generation are influenced by the rate of glucose consumption. The rate of glucose consumption is dependent on the growth rate of the culture. After the growth phase, the consumption of glucose dropped drastically perhaps due to the reduced growth. The rate of oxygen consumption appeared to decrease gradually. This was particularly observed between 39 and 48 hours where the uptake of glucose

decreased to practically zero while the decrease in the consumption of oxygen decreased gradually. Therefore, based on the general trends observed, there seems to be a delicate negative relationship between the uptake rate of glucose and the rate of respiration (OUR). However, it is important to point out that these two parameters where expressed in different units making direct comparison difficult. It was not possible to express the off-gas data in the same units as the other parameters. Nevertheless, since glucose requires oxygen for degradation, the ratio of both rates is likely to influence precursor production, erythromycin biosynthesis and energy generation. The ratio of glucose consumption to oxygen consumption appears to be regulated on demand. *S. erythraea* continues to consume glucose in the absence of significant growth. This has been observed and described as inefficient use of glucose by Jaques (2004). Nevertheless, it appears the apparent imbalance between the glucose consumption rate and the growth rate gives rise to overflow metabolism. The ratio of GUR/OUR is likely to be regulated based on cell requirements. Both GUR and OUR are themselves regulated based on cell requirements. If glucose is consumed while the uptake of oxygen is reduced, substrate oxidation may not be efficient leading to the accumulation of precursors. This is further compounded by the decreased growth demands of the stationary phase. Therefore, generation of carbon precursor metabolites in excess of the capacity to oxidise them to CO_2 results in the spillage which is observed as excretion. Increased levels of the red pigment and α-ketoglutarate were excreted. The TCA cycle flux remained high generating NADH in excess of oxidative capacity. Thus it appears that the excretion of metabolites is a result of continued glucose consumption during the stationary phase. Continued glucose consumption also generates excess energy (ATP) in the absence of growth and respiratory demands. This scenario is undesirable for the organism as it wastes carbons, cofactors and energy. To restore redox balance and reduce generation of excess energy, the TCA cycle is slowed down probably through the inhibition of citrate synthase by high [$NADH/NAD^+$] ratio and pyruvate dehydrogenase by increased NADH concentrations. As to how all these enzyme and cofactor dynamics are involved in the regulation of erythromycin production must be investigate in future studies. This is beyond the scope of the current work.

4.6.4 Carbon utilisation

Up to 97.4% of the initial carbon could be accounted for at the end of the fermentation (Table 16). Therefore, *S. erythraea* utilised most of its carbon substrate for biomass synthesis (Table. 16). Interestingly a large portion (35.9%) of the carbon was excreted as α-ketoglutaric acid. About 4.5% was excreted as the red pigment, 7-*0*-rhamnosyl flaviolin and only 1.7% made its way into the antibiotic. This constitutes a loss of carbons that potentially could be diverted to the production of the antibiotic. Given the large amount of carbons allocated to α-ketoglutaric acid, the TCA cycle activity, indicated by ICD activities, appears to be a major drain on carbons. Slowing down the TCA cycle can potentially reduce carbon wastage and enhance the production of erythromycin. This could be achieved by culturing *S. erythraea* on a substrate that promotes slow growth.

4.6.5 A model for the production of erythromycin on glucose as a sole carbon source

High glucose uptake routes fluxes through glycolysis and the TCA cycle and results in the accumulation of precursor metabolites. Reduced glucose uptake rate enhances flux through the PP and the anaplerotic pathway and generates NADPH needed for the biosynthesis of the antibiotic. Erythromycin production commences during the phase of low uptake rate and continues until the precursor metabolites are depleted. Since high levels of NADPH inhibit G6PDH through feed-back mechanism, a low uptake rate of glucose will keep this cofactor below levels that could inhibit the enzyme. This could explain why fluxes through the PPP are enhanced when the specific glucose uptake rate decreases. When G6PDH is inhibited, fluxes are directed primarily through glycolysis and the TCA cycle. The high levels of NADH observed probably have to do with the route of degradation of glucose. The PPP in *S. erythraea* produces one NADPH and one NADH per glucose molecule degraded (Jaques, 2004). This fact, in addition to the high fluxes through glycolysis and the PPP, could explain the elevated levels of NADH. In general, there appears not to be a clear correlation between the levels of NADH and erythromycin production. The levels of NADH increased continuously from 24 hours of growth and only decreased

after 96 hours.

The decrease in pyruvate concentration when the EMP/TCA cycle flux ratio increased suggests that flux through pyruvate dehydrogenase was up-regulated during a time of increased erythromycin production. However, since NADH was adequately supplied, increasing flux to the TCA cycle would have been in excess of requirements. The high concentrations of NADH diverted flux away from the TCA cycle through inhibition of pyruvate dehydrogenase (Shen & Atkinson, 1970) leading to increased EMP flux. This flux was subsequently routed through the anaplerotic pathway. The anaplerotic flux was enhanced when the concentration of erythromycin was increased. This suggests that during the production of erythromycin, flux split between glycolysis and the TCA cycle was disproportionate. Based on the activity of branch point enzymes, much higher fluxes were observed through glycolysis relative to those through the TCA cycle. This is consistent with the increased anaplerotic flux observed.

Based on the findings, a diagrammatic model for the distribution of flux during metabolite accumulation and production of the antibiotic is presented in Fig. 25.

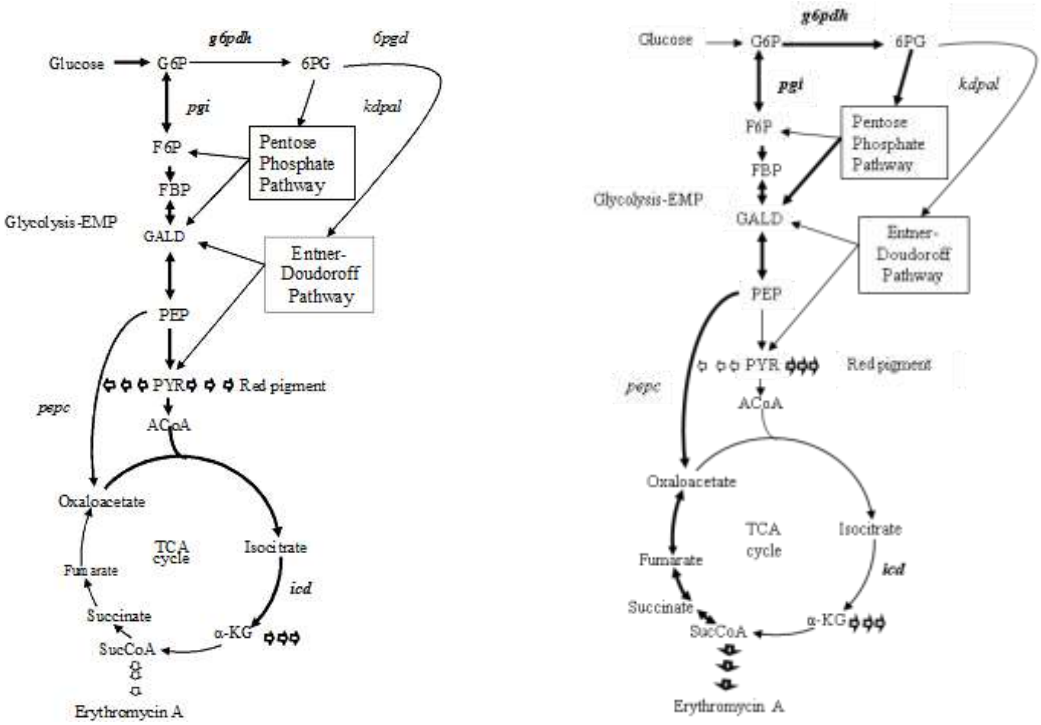

Fig. 25 Carbon flux distribution in *S. erythraea* during growth on glucose as a sole carbon and energy source. Glucose-6-phosphate dehydrogenase - *g6pdh*, glucose-6-phosphate isomerase - *pgi*, phosphoenolpyruvate carboxylase - *pepc* and isocitrate dehydrogenase - *icd*. Left figure - Precursor accumulation phase, Right - Erythromycin biosynthesis phase

Model Explanation

Growth phase/Precursor accumulation phase

Glucose degradation proceeds mainly via glycolysis, the anaplerotic pathway and the TCA cycle until nitrate is depleted. Upon nitrate depletion, respiration drops but the rate of glucose consumption increases. Large amounts of organic acids, particularly α-ketoglutaric acid, accumulate and are excreted via the via the TCA cycle. Carbons are also lost in the form of CO_2 and organic acids. The excretion of the red pigment, 7-*O*-rhamnosyl-flaviolin, increases which further contributes to the loss of carbons. Little erythromycin is produced. During the growth phase, biomass production is greatly increased.

Erythromycin production phase

The activities of G6PDH increase significantly and the TCA cycle slows down considerably. The rate of glucose consumption decreases and ATP levels drop. At the G6P node, fluxes are mainly routed through the PPP while the anaplerotic reaction (PEPC) dominates at the expense of the TCA cycle (ICD). Carbon fluxes switch to proceed through oxaloacetate, malate, fumarate and succinyl-CoA. ICD activities remain low. Erythromycin production is greatly enhanced.

Chapter 5

5.0 Physiology of metabolite production and erythromycin biosynthesis during growth on gluconate substrate

In preliminary carbon screening experiments discussed in Chapter 4, *S. erythraea* was found to utilise gluconate both for energy generation and to meet its carbon requirements. As discussed in Chapter 4, gluconate is metabolised through the Entner-Doudoroff pathway. Given the difference in the metabolism between glucose and gluconate, very different patterns of pathway activities, erythromycin production and cofactor generation can be expected when *S. erythraea* is cultured these substrates as sole carbon and energy sources.

All sampling, sample processing and analyses were performed as specified in Chapter 2.

5.1 Growth characteristics

Growth on gluconate was slower than that obtained for glucose (Table 15, Table 17). Nitrate was depleted 15 hours later than on glucose of growth in line with slower growth rate. As a result, metabolite accumulation and erythromycin production phases observed in the glucose fermentation were all delayed relative to those obtained for glucose. Three distinct phases were observed during exponential growth. Gluconate was consumed at a slow specific growth rate of 0.03 $g.g^{-1}h^{-1}$ during the first 24 hours (Table 17). In contrast to growth on glucose, erythromycin production was growth-related and reached a maximum of 69.7 $mg.L^{-1}.g^{-1}$ after 24 hours of growth. Biomass synthesis increased by 83% within 24 hours (Fig. 26).

Table 17. Specific growth rate, biomass and product yields during growth on gluconate as a sole carbon and energy source.

Culture condition	Growth parameters			
Carbon source	Growth rate (h^{-1})	Yx/s ($g.g^{-1}$)	Yp/s ($mg.g^{-1}$)	Yp/x ($mg.g^{-1}$)
Gluconate	0.032	0.14	1.84	20.15

Between 24 and 39 hours, the rate of biomass synthesis decreased by 49%. When the consumption rate of gluconate was up-regulated by 93% to 0.51 $g.g^{-1}h^{-1}$ (Fig. 29), the concentration of erythromycin subsequently dropped by 46% (Fig. 26). This was accompanied by increased O_2 uptake rate of 42% and a significant decrease in the rate of CO_2 evolution and the respiratory quotient (Fig. 27). Respiration increased significantly at the same time that the uptake of gluconate was increased significantly. This phase corresponds to the metabolite accumulation phase observed in the culture grown on glucose as a sole carbon source.

Another phase of rapid gluconate consumption rate was observed after 39 hours. Between 39 and 48 hours the specific consumption rate was increased by 66% to 1.5 $g.g^{-1}.h^{-1}$ while respiration was down-regulated (Fig. 27, Fig. 28). The rate of biomass synthesis increased by 37% from 39 h to 48 h. Very little antibiotic was observed during this phase (Fig. 26).

The production phase resumed from 48 to 72 hours with erythromycin concentration increasing by 40% (Fig. 28) while gluconate consumption rate decreased by 64% to 0.537 $g.g^{-1}.h^{-1}$ (Fig. 29). However, when gluconate was depleted between 72 and 96 hours, the uptake rate dropped by 99% and coincided with a 32% decrease in the production of erythromycin over the same period. It can be concluded that the drop in the production of the antibiotic was due to the depletion of carbon precursor metabolites.

The rate of gluconate consumption was low for the first 24 hours of growth but increased significantly thereafter to reach a maximum at 48 hours. The production of erythromycin started during this period. At this early stage, biomass was low and, therefore, gluconate was consumed at slow specific growth rate. As biomass increased, consumption of the carbon source increased significantly. A low specific gluconate uptake rate was observed to enhance biomass synthesis and erythromycin production (Table 17). Pico *et al* (2004) have reported a similar relationship between the glucose consumption rate and the specific growth rate for *E. coli*. More gluconate was diverted to biomass formation than to erythromycin production when the culture was grown on gluconate. Growth on glucose produced 18% higher yield of erythromycin per biomass ($Y_{p/x}$) than the culture grown on gluconate (Table 15, Table 17). Furthermore, on glucose $Y_{p/s}$ was 33% higher than that for the gluconate fermentation. However, chemostat culture would be a better method to determine

and compare yields between two carbon sources. This is partly because in chemostat culture, one has better control over the growth rate.

Two phases of imbalance between OUR and CER were observed, suggesting that *S. erythraea* regulated its consumption of gluconate based on the cell metabolic status. This was observed between 24 and 39 hours and again from 72 hours to 96 hours (Fig. 27). Notable changes in the balance between OUR and CER occurred mainly between 24 and 48 hours. The observed dynamics in the respiratory activity coincided with notable changes in the rate of glucose consumption, production of erythromycin and the energy charge. This suggest the observed changes in OUR and CER over this period are real and not an artefact.

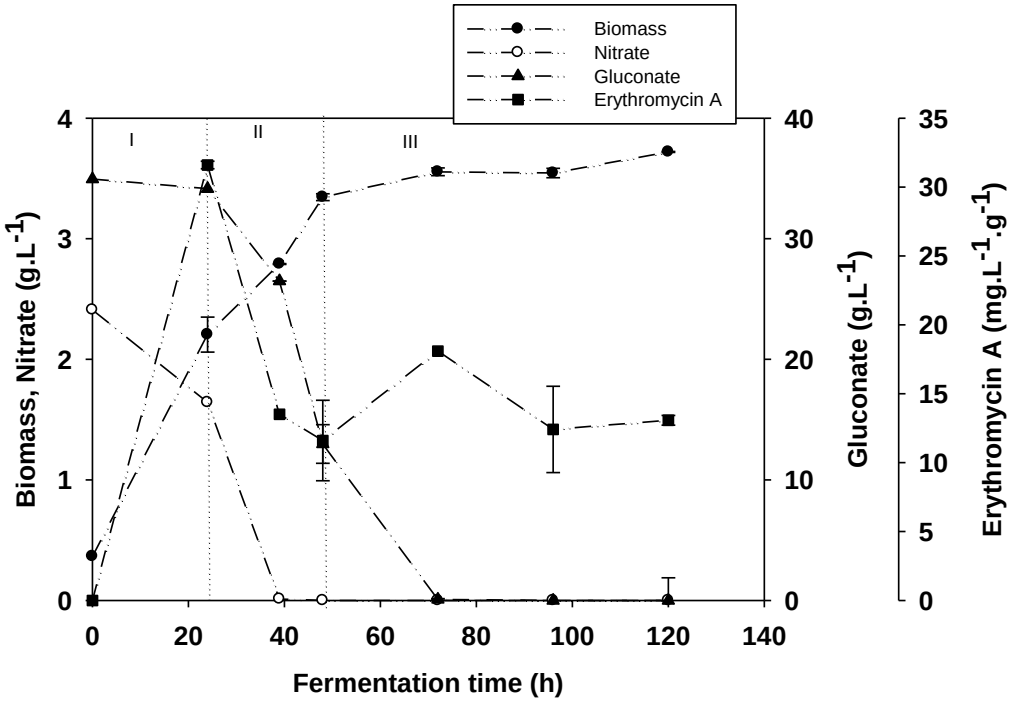

Fig. 26 Time courses of biomass (●), gluconate (▲), nitrate (○) and erythromycin (■) when *S. erythraea* was cultured on gluconate as a sole carbon and energy source. All Data represent means of three biological and technical replicates.

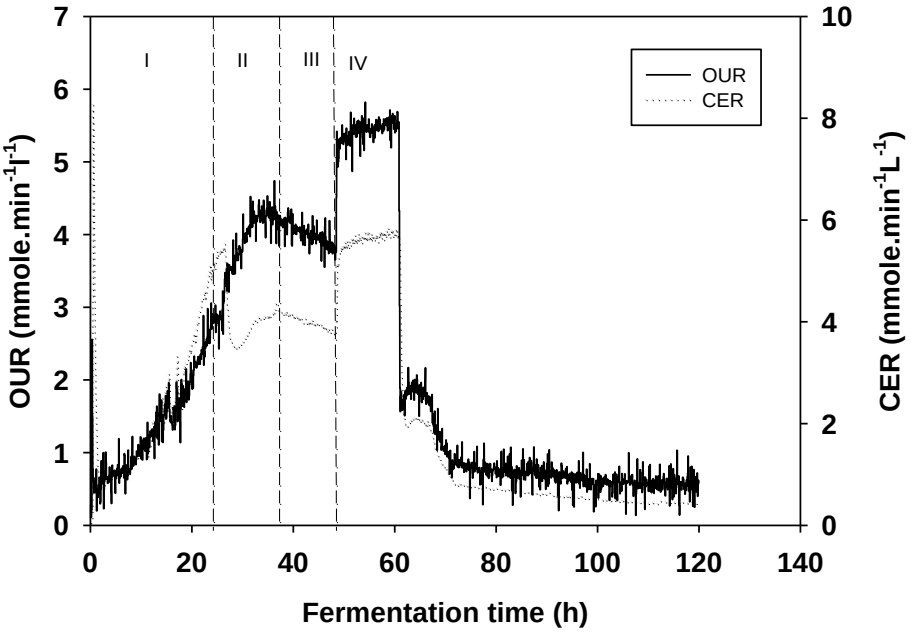

Fig. 27 Time courses of OUR and CER during growth on gluconate as a sole carbon and energy source. Notable changes in OUR and CER between 24 and 39 hours and between 50 and 60 hours.

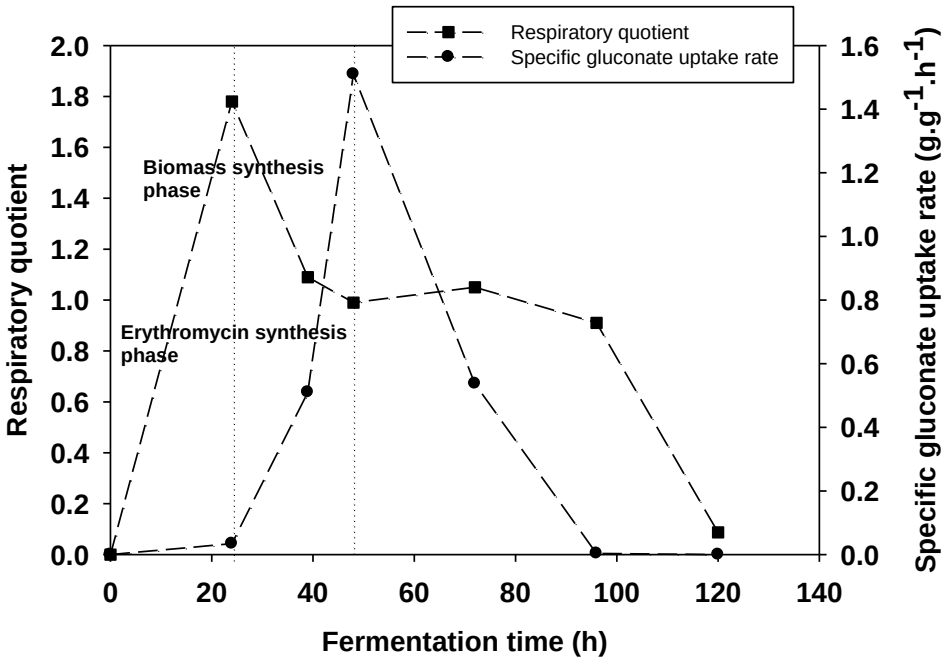

Fig. 28 Relationship between the Respiratory Quotient (■) and the specific gluconate uptake rate (●).

Comparison of the two growth conditions reveals that the consumption rate of the carbon source is determined by the growth rate and the nature of the carbon source. As argued earlier, the lower consumption rate of gluconate could be a reflection of the lower rates of both growth and respiration.

Thus growth demands due to the lower specific growth rate determine the fate of carbon precursors in *S. erythraea*. They may either be diverted to biomass synthesis or the biosynthesis of secondary metabolites or excreted as in overflow metabolites.

5.2 Correlation between gluconate uptake rate, branch point enzymes, product formation and cofactor generation

At the PPP/EMP branch point, G6PDH was the most active enzyme during the 24 hour period of slow gluconate uptake (Fig. 29, Fig. 30). No NADPH and NADH were observed during this phase (Fig. 31). The elevated G6PDH activity and depleted NADPH levels coincided with maximum antibiotic production at 24 hours. At this point, the TCA played a lesser role than the anaplerotic reaction which showed high PEPC activity (Fig. 30). In agreement with the findings on glucose, when gluconate uptake rate increased between 24 and 39 hours, PPP/EMP ratio dropped by 60% indicating an increase in phosphoglucose isomerase activity and by implication increase in glycolysis. . It coincided with increased ICD activity and elevated levels of NADPH and NADH concentrations (Fig. 31). The concentration of NADH increased by 96% when the ratio of G6PDH/PGI decreased between 24 and 39 hours (Fig. 30, Fig. 31). NADPH correlated negatively with the levels of erythromycin suggesting it was consumed during the production of the antibiotic. The specific production of NADPH increased from 0 to 0.03 $\mu M.g^{-1}$ biomass when that of erythromycin production declined from 14 to 12 $mg.L^{-1}.g^{-1}$ biomass over the same period. Similar trends were observed between 39 and 72 hours where NADH correlated positively with increased PGI activities. Through-out the fermentation, the ratio of PPP/EMP correlated negatively with a high rate of gluconate consumption. The drop in the enzyme ratio was observed up to 48 hours during which time the consumption rate of the carbon source was increased. The ratio only increased again between 48 and 72 hours when the carbon consumption rate had dropped from 1.5 to 0.5 $g.g.h^{-1}$. This increase in the enzyme ratio coincided with an increase in the specific concentration of erythromycin from 11.6 to 18 $mg.L^{-1}.g^{-1}$ (Fig. 29, Fig. 30).
As in the case of glucose, high carbon source consumption rate appears to reduce the

level of erythromycin (Fig. 31).

Equally, increases in the respiratory quotient appear to correlate with decreases in the production of the antibiotic (Fig. 28, Fig. 31). This expected as increased respiration would have high carbon source demands.

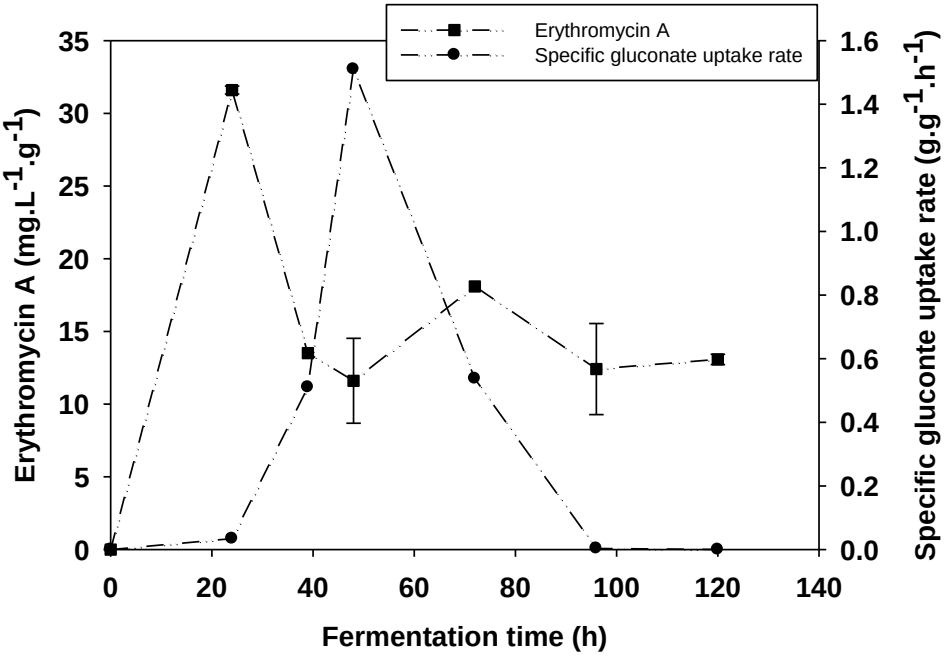

Fig. 29 Relationship between the specific gluconate uptake rate and erythromycin A. Data represent means of three biological and technical replicates.

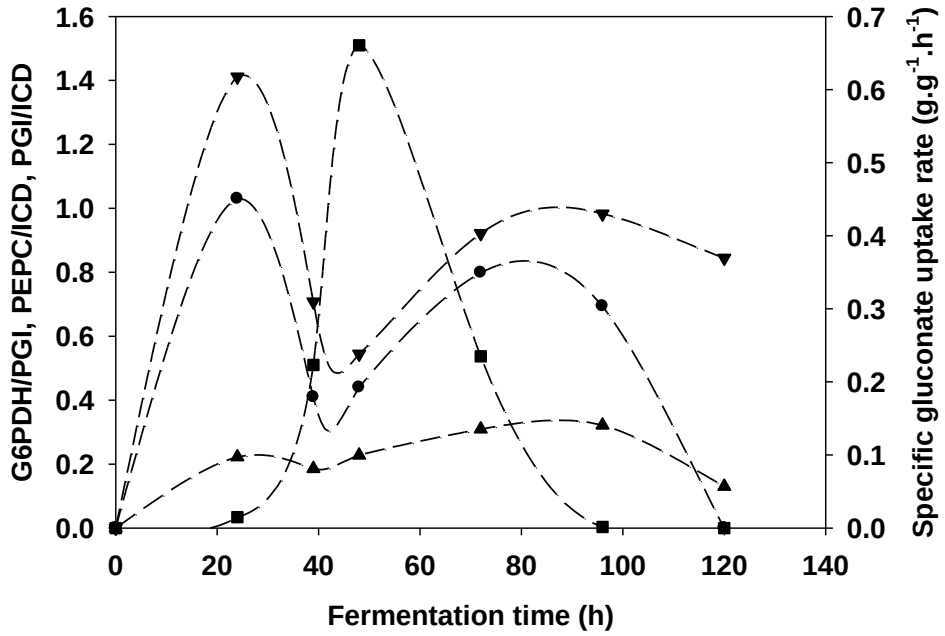

Fig. 30 Correlation between specific gluconate uptake rate and pathway split ratios: specific gluconate uptake rate (■), G6PD/PGI (▼), PEPC/ICD (▲) and PGI/ICD (●). Split ratios at PPP/EMP, EMP/TCA cycle and the anaplerotic pathway/TCA cycle are represented by G6PDH/PPP, PGI/ICD and PEPC/ICD respectively. Data represent means of three biological and technical replicates.

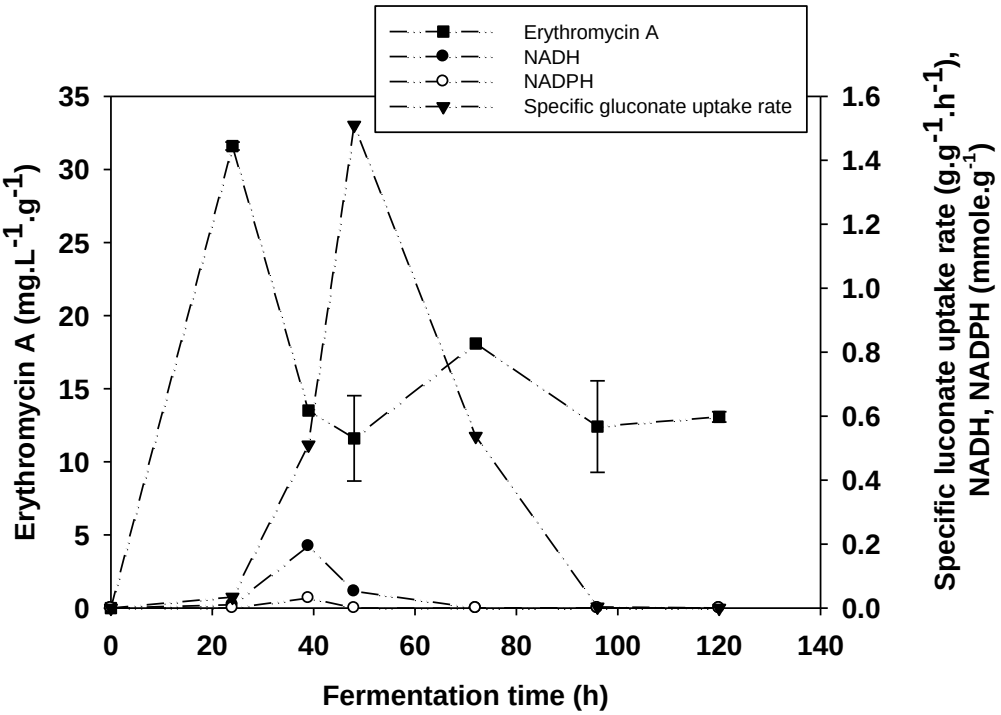

Fig. 31 Relationship between the specific gluconate uptake rate (▼), erythromycin A (■), NADH (●) and NADPH (○). Data represent means of three biological and technical replicates.

5.3 Correlation between cell energetics, glucose uptake rate and erythromycin biosynthesis

For growth on gluconate, *S. erythraea* has to carefully balance the allocation of carbon and energy resources for biomass synthesis and secondary metabolite production. Antibiotic production has high energy requirements while biomass synthesis places high demands on the supply of carbon precursor metabolites and energy for macromolecule synthesis and assembly. However, it must be pointed out that the energy requirements for erythromycin biosynthesis are not known. In the light of this fact, high rates of gluconate uptake can be expected to supply both precursors and the energy required for biomass synthesis and erythromycin production. However, the rate of gluconate consumption was low during the growth phase suggesting that precursor requirements were low as well (Fig. 27, Fig. 29). As stated before, this expected as biomass was low in the first 24 hours. When biomass reached a concentration of 2.2 $g.L^{-1}$ after 24 hours of growth, the rate of gluconate consumption increased significantly. Demand for energy must have been high during the accelerated growth phase as suggested by the energy charge value of 0.94 (Fig. 32).. The energy charge decrease to 0.83 between 24 and

39 hours which suggest a drop in energy demand. There was a simultaneous drop in the rate of respiration and the production of erythromycin (Fig. 26, Fig. 28, Fig. 32). The decrease in the specific concentration of the antibiotic from 31.6 to 13.5 $mg.L^{-1}g^{-1}$ biomass over this period was significant. CER also dropped during this period which confirms the decrease in the rate of respiration (Fig. 27). The observed increase in the specific gluconate consumption rate (GLUR) after 24 hours was probably to replenish precursor pools which must have been depleted by the combined demands of growth and erythromycin production (Fig. 26, Fig. 29).
After this 15 hour period, biomass concentration increased from 2.8 to 3.3 $g.L^{-1}$ between 39 and 48 hours (Fig. 26). Though production of erythromycin decreased over the same period, the energy charge increased to 0.94. This suggests that biomass synthesis has high energy demands relative to the production of the antibiotic. In fact, increases in the production of erythromycin coincided with reduction in the energy charge during the accelerated growth phase and between the periods from 48 to 72 and 96 to 120 hours. This appears to suggest that erythromycin does not have energy requirements overall.

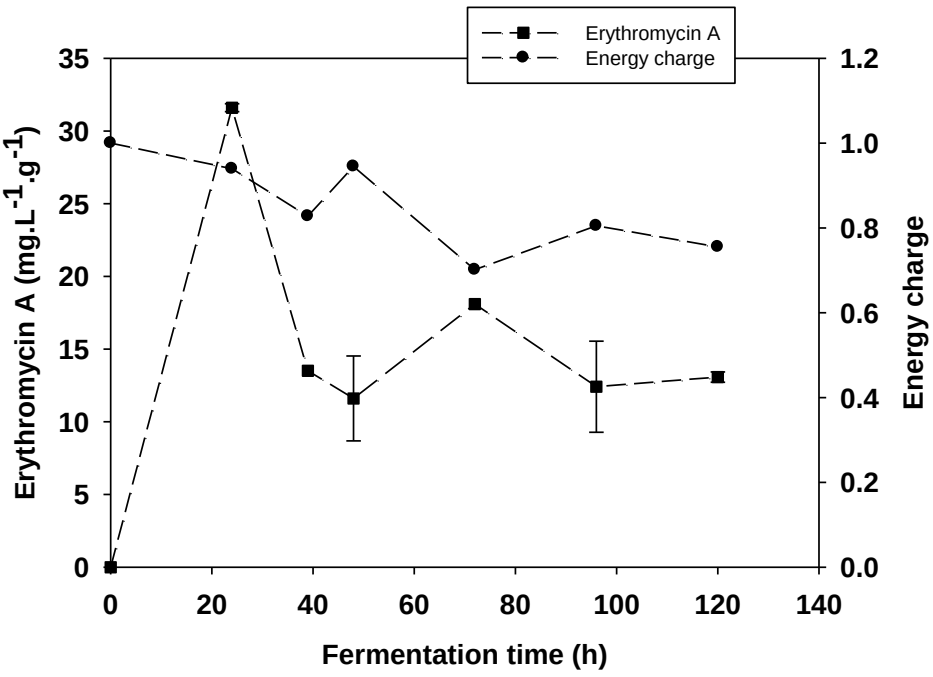

Fig. 32 Relationship between erythromycin A (■) and the energy charge (●).
Data represent means of three biological and technical replicates.

5.4 Excretion of organic acids and enzyme activities

The excretion of organic acids correlated positively with gluconate consumption rate. No organic acids were excreted during the period of slow gluconate consumption (Fig. 27, Fig. 32). However, when the specific growth rate decreased after 24 hours, the rates of respiration and gluconate consumption were increased while CER was reduced considerably (Fig. 27). This caused the carbon storage compounds to accumulate leading to the overflow of organic acids. The excretion of organic acids also correlated with the increased activities of isocitrate dehydrogenase. Organic acids were not excreted during the accelerated growth phase when the specific gluconate uptake rate was low. However, when the uptake rate was upregulated between 24 and 48 hours, significant increases were observed for pyruvate, red pigment and α-ketoglutarate (Fig. 32, Fig. 31). Only trace amounts of succinate were observed during this time while fumarate was undetectable. Increased consumption rate appeared to have promoted flux through the TCA cycle. However, the red pigment continued to be produced despite the decrease in the rate of gluconate consumption. No increases in the rate of organic acids production were observed after hours though amounts of succinate were detected. It appears the excretion of organic acids is a response to increases in the rate of respiration and carbon source consumption.

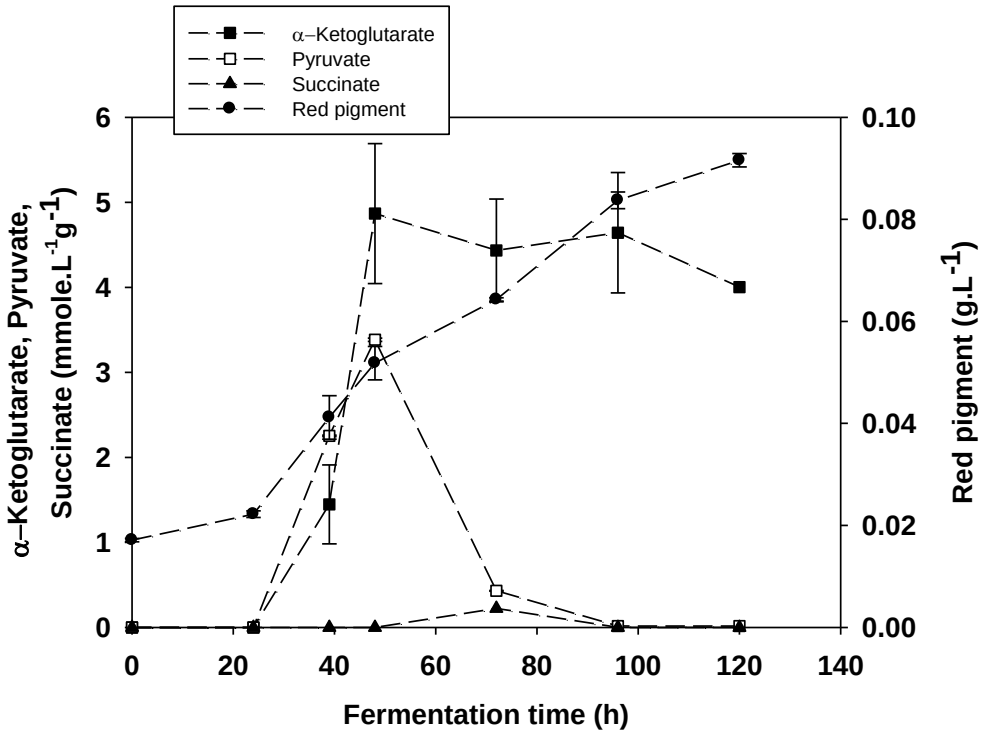

Fig. 33 Profiles of organic acid and red pigment during growth on gluconate as a sole carbon and energy source: α-ketoglutarate (α-KG) (■), pyruvate (□), succinate (▲), red pigment (●). Fumarate was undetectable. Data represent means of three biological and technical replicates.

5.5 Relationship between the oxygen uptake rate and the production of erythromycin

Oxygen is a critical parameter in antibiotic producing fermentations. Often, maintaining dissolved oxygen above a certain minimum level can increase productivity in antibiotic fermentations (Vadar, & Lilly, 1982). In some cases, antibiotic production can be improved at low DO levels while in others the percentage of dissolved oxygen determines the pattern of the antibiotic production (Varna *et al*., 1993; Van Damme *et al*, 1981; Agathos & Demain, 1986; Rollins *et al.*,1988). It is not known how the concentration of oxygen affects the biosynthesis of erythromycin in *S. erythraea*. However, it is reported that oxygen limitations in fermentations can be caused by limited external supplies or the respiratory capacity (Vadar, & Lilly, 1982). Some of this capacity is in the terminal oxidases. For example, Brunker *et al* (1998) observed a significant increase in erythromycin production with mutants containing overexpressed haemoglobin genes from *Vitreoscilla*. They ascribed the improvement to improved O_2 metabolism which suggests that limitations may exist in the respiratory capacity of *S. erythraea*. It

appears the carbon uptake rate affects the growth rate and the biosynthesis of erythromycin. While on glucose as a carbon and energy source, erythromycin was produced after the main growth phase, its biosynthesis was growth-related when gluconate was used as carbon and energy source (Fig. 17, Fig 26). When grown on glucose, erythromycin production only started when the GUR decreased significantly. On both glucose and gluconate as a sole carbon sources, the production rate of erythromycin was associated with high respiratory quotient (RQ) and a decrease in the consumption rate of the carbon source. On the other hand, reduced oxygen levels improve antibiotic levels (Martin & Demain, 1980). Given, that decreased rates of carbon source consumption and elevated RQ coincided with increases in erythromycin levels, there could be an optimum GUR/OUR ratio for antibiotic synthesis. Such a ratio would vary with the metabolic status of the cell. Thus, an imbalance in the rate of oxygen uptake with respect to the rate of carbon source uptake could have created a suboptimal flux distribution which enhanced the biosynthesis of the antibiotic. Chen and Wilde (1990) suggested that the reduced O_2 uptake rate observed at high rates of glucose uptake is caused by limitations in the enzymes. This is consistent with the inhibitory effects of high concentrations of adenylate nucleotides and possibly redox carriers observed at high carbon source uptake rates. Examples of this are the regulation of the activities of the TCA cycle and the anaplerotic pathway by NADH and the inhibition of G6PDH by elevated ATP levels. Changes in the rates of carbon source uptake bring about changes in the concentrations of redox carriers and/or ATP resulting in altered flux splits at crucial branch points. For example, oxidative phosphorylation appeared to be inhibited at high glucose uptake rate. This could be due to the inhibitory effects of elevated levels of ATP on the NADH dehydrogenase and terminal oxidases (Tanman *et al*. 1994). Working with *Streptomyces fradiae* Chen and Wilde (1991) suggested that flux shifts at high glucose uptake rate cause the inhibition of oxidative phosphorylation. A further suggestion posited by these authors is that the redox potential may trigger the metabolic shifts observed. Nevertheless, an important conclusion is that the carbon uptake rate is an important parameter in improving the production of erythromycin. The ratio of [ATP/ADP] probably regulates GLUR and indirectly the production of erythromycin. This ratio reflects the energetic status of the cell (Fig. 32) and the consumption of gluconate is most likely adjusted

accordingly.

5.6 Carbon balance utilisation for growth on gluconate substrate

A carbon balance was performed following the procedure described in section 4.6.2.7 of Chapter 4. Calculations were based on the biomass weight of 24.6 g using the formula $CH_{1.8}O_{0.5}N_{0.2}$ (Doran, 1995).

About 92% of the carbons could be accounted for. It is not clear where the balance of an estimated 8% was diverted to. As in the culture grown on glucose, biomass constituted most of the carbons, though somewhat lower. *S. erythraea* diverted more carbons to pyruvate than to the red pigment. On glucose, the red pigment had a higher carbon allocation compared to pyruvate. This is an important difference in carbon allocation between the two carbon sources. Interestingly, there was little difference in the amount of carbons allocated to α-ketoglutarate. This finding establishes α-ketoglutarate as a major carbon drain on *S. erythraea*.

Only 0.5% of the total carbons were released as CO_2 (Table. 18). This reflects the slower growth rate observed on gluconate as a sole carbon and energy source. Despite the high carbon allocation to pyruvate, this does not appear to have improved the production of erythromycin. The number of carbons allocated to erythromycin on both carbon sources was for practical purposes equal. While the α-ketoglutarate node appears rigid, the pyruvate node seems flexible.

Table 18 Carbon balance for *S. erythraea* growth on gluconate as a sole carbon and energy source.

C Recovery	Gluconate	Biomass	Pyr	Red	α-KG	Suc	Fum	Prop	Ery	[b]CO_2
Initial mmmole C	1069	-	-	-	-	-	-	-	-	-
[a]Millimole C	-	488	57.9	21	388.3	0	1.1	-	17.5	5.5
Percentage C		45.7	5.4	2.0	36.3	0	0.1	-	1.6	0.5

Total millimole C recovered	979.4
Total % C recovered	91.6

[a]Mmole C calculated as follows: mmole x number of C in metabolite
[b]Mmole C in CO_2 calculated as per 5L working volume of bioreactor
Pyr - pyruvate, α-KG - α-Ketoglutarate, Suc - Succinate, Prop - propionate , Fum - Fumarate, Ery - Erythromycin A, Red - Red pigment

5.7 Discussion

5.7.1 Growth characteristics

S. erythraea grew considerably slower on gluconate due to the route of degradation. Slow degradation of a carbon source yields low levels of precursor metabolites, pyridine cofactors and possibly energy nucleotides as well. Given the energetic burden due to both growth and antibiotic production, energy and precursor limitations could curtail growth rate. The energy charge decreased during the growth phase which could indicate a high energy burden. However, it is likely that growth rate was slowed down by constrains in the supply of carbon precursors given the low consumption rate of gluconate. In the allocation of carbons, growth requirements took preference. As a result, more carbons were diverted to biomass synthesis than the production of erythromycin. Unlike in the glucose fermentation, carbon fluxes were more equally split between glycolysis and the PP pathway. Thus NADPH was supplied by the PP pathway during the growth phase, thereby enabling erythromycin to be produced simultaneously with biomass synthesis.

Carbon degradation through this pathway generates less energy than glycolysis.

As was the case with the culture grown on glucose, the uptake rate of carbon was slow during the growth phase (Table 16, Fig. 29). Biomass increased by 83% between 0 and 24 hours. G6PDH activities were marginally higher than those of PGI suggesting increased activities of the PP pathway.

Why was growth on gluconate slower than on glucose? The answer to this question could lie in the fact that fluxes through the ED pathway join glycolysis at pyruvate and glyceraldehyde-3-phosphate (GALD) node. Fluxes at and below pyruvate node are not available for nucleotide biosynthesis because pyruvate kinase is not reversible. However, GALD can be converted to fructose-1,6-bisphosphate (FBP) by fructose-1,6-bisphosphate aldolase (FBP aldolase). FBP replenishes fructose-6-phosphate (F6P) pools at low AMP concentration which both inhibit pyruvate kinase and activate fructose-1,6-bisphosphatase (FBPase). Overexpression of FBPase has been reported to increase G6P pools and flux through the PPP (Becker *et al*., 2005). The reactions of both transketolase and transaldolase are reversible based on the cell requirements (Voet & Voet, 2004) and can be assumed to have replenished ribulose-5-phosphate (R5P) pools from F6P to enable nucleotide biosynthesis. However, the same F6P pool could have increased the glucose-6-phosphate (G6P) metabolite pool

through phosphoglucose isomerase (PGI) activity to supply the needed NADPH for biosynthesis. Microorganisms are optimised for growth and it can, therefore, be concluded that flux to R5P would have been higher than to G6P during the growth phase. Confirmation of this comes from the fact that during growth on gluconate, more carbons where channelled into biomass synthesis than into erythromycin production (Table 16). Biomass formation and secondary metabolite biosynthesis compete for precursors when nutrients are available. However, since organisms are optimised for growth, growth requirements take preference in the allocation of carbon precursors. The carbon balance computation revealed that most of the carbons are allocated to biomass (Table. 18). Based on this, it appears that the partitioning of carbon fluxes between growth and/or secondary metabolite production is, therefore, regulated at enzyme and gene possibly expression level (Avignone-Rossa *et al*., 2002). The findings from this work suggest that the of growth and carbon source uptake are important parameters in the production of erythromycin. The slow growth under the conditions of this investigation can be attributed to the metabolism of gluconate as discussed earlier.

5.7.2 Metabolic pathway activity and antibiotic production

The high ratio of G6PDH/PGI during the growth phase suggests that, fluxes through G6PD were higher than those through PGI. Gluconate enters directly into 6 - phosphogluconate metabolite pool and does not feed directly into G6P since G6PDH is not reversible and is the first committed step of the PPP (Morritz, 2000). As discussed in the previous section, G6P pools are replenished by high F6P levels. This means that the activity of G6PDH would also be subject to the inhibitory levels of ATP and AMP and indirectly to pyruvate kinase (PK) activity. Glycolysis is enhanced by increased AMP levels through its activation of PK (Voet & Voet, 2004). Since growth was low, energy demands due to growth were probably low. The overall energetic burden, however, could have been high since erythromycin was produced during the growth phase. This would have been mainly due to demands of biomass production for energy. High PPP flux during the growth phase was possible since ATP levels were probably below inhibitory concentrations. Elevated ATP concentrations can inhibit G6PDH (Horne *et al*., 1970), making this nucleotide a possible regulator of PPP flux. Increases in energy charge values correlated positively with the G6PDH/PGI ratio suggesting increased PPP flux

especially after the growth phase.

The energy charge decreased with increased antibiotic production. However, though the energy demands were high during the growth phase, demand was reduced when erythromycin production increased between 48 and 72 hours. This perhaps suggests that biomass formation places a large burden on energy requirements. Due to increased G6PDH activity, sufficient NADPH was produced to meet the demands of growth and reductive biosynthesis. Increasing the pool of F6P can increase PPP flux and NADPH supply (Borodina *et al*., 2008; Becker et al., 2005). However, because growth was slow, NADPH levels were probably below inhibitory levels for G6PDH. Throughout, the increase in erythromycin production correlated positively with increased flux through the G6PDH. Glycolysis produces energy and carbon precursors simultaneously. Therefore, when demand is low, continued flux through this pathway would amount to wastage of carbons and energy. The other implication of this switch between glycolysis and flux through G6PDH is the depletion of metabolites needed for the production of erythromycin. During the production of erythromycin, carbon precursors may be depleted since glycolytic flux is reduced. The same situation holds for NADPH which can be depleted as it is used in reductive biosynthesis of erythromycin. Replenishing these metabolites would, therefore, be necessary after an increase in the production of the antibiotic. Overall, the production of erythromycin was enhanced by a balanced flux partitioning at the PPP/EMP branch point and suboptimal partitioning at the anaplerotic pathway/TCA cycle interface (Fig. 29, Fig. 30). It appears that increased flux through the anaplerotic pathway enhanced erythromycin production while increasing flux through the TCA cycle seems to have promoted precursor accumulation. It appears *S. erythraea* simultaneously increases its consumption rate of the carbon source and TCA cycle activity when demand for precursor metabolites increases. This appears to serve the role of accumulating precursor metabolites but large amounts of organic acids, such as α-ketoglutarate, and other metabolites are excreted in the process.

The strong correlation between the excretion of organic acids and glycolytic activity confirms the role of the TCA cycle during the phase of replenishment of both precursor metabolites and NADPH. Interestingly, *S. erythraea* produced more red pigment on gluconate than on glucose. This may not be surprising given that the ED pathway joins glycolysis at glyceraldehyde-3-phosohate as well as at pyruvate pool.

With direct entry into pyruvate, fewer carbons would be lost along the network. Increased antibiotic production coincided with low levels of NADH and increased flux through both the PPP and the TCA cycle. This also coincided with decreased pyruvate concentration and increased EMP/TCA cycle ratio. Similar findings were obtained by Obanye *et al* (1996). It was suggested that flux through pyruvate dehydrogenase increased and enhanced the TCA activity. The reasoning was that increasing TCA cycle activity replenishes NADH which is utilised in the generation of NADPH via transhydrogenase reations. This is a plausible explanation since NADPH levels were at low levels making their depletion more likely. In addition, the decrease in NADH is consistent with the inhibition of pyruvate dehydrogenase by high concentrations of this nucleotide (Shen & Atkinson, 1970). Another observation was that the split in carbon flux between EMP and the TCA cycle was disproportionate resulting in less carbons being routed to the latter during erythromycin production. This was in in agreement with the findings for the culture grown on glucose in which increased flux through the anaplerotic pathway (AP) enhanced erythromycin production. However, in this case, fluxes from oxaloacetate were routed through isocitrate dehydrogenase (ICD) via citrate synthase (Fig. 15). The reason for this lies in the fact that the culture grown on gluconate produced much lower levels of NADH. As discussed in the previous section, high NADH levels or [NADH/NAD^+] inhibit various TCA cycle dehydrogenases as well as citrate synthase. Therefore lower flux through the TCA cycle was enhanced due to the lower levels of the nucleotide. This is illustrated in the metabolic model in Figure 34.

5.7.3. Relationship between the specific gluconate consumption rate, growth rate and secondary metabolite production

On glucose, *S. erythraea* grew at a faster rate than on gluconate. At fast growth rate, biomass was produced at the expense of the antibiotic. The production of the antibiotic was associated with reduced rate of glucose consumption. At increased glucose uptake rate, much of the carbons were excreted as pyruvate, α-ketoglutarate and red pigment (Fig. 23). These observations were made for growth on gluconate as well. As in growth on glucose, erythromycin production was aided by a reduced rate of gluconate uptake. However, on gluconate, both biomass synthesis and erythromycin biosynthesis were enhanced by the slow specific uptake rate. The explanation for this is that high growth rate has very high carbon precursor and

energy demands. Under the conditions tested, growth rate and specific gluconate uptake rate regulated the biosynthesis of erythromycin.

At the PPP/EMP branch point, flux partitioning between EMP and PPP was more or less evenly split. The fact that erythromycin was produced during the growth phase confirms the conclusion made earlier that its production was constrained by NADPH during growth on glucose as a sole carbon and energy source. Growth on gluconate diverted more carbons into biomass synthesis than to secondary metabolism (Table. 16).

Growth demands deplete carbon precursor metabolites and NADPH concentrations resulting in altered flux distribution to replenish these pools as illustrated in the models (Fig. 33, Fig. 34). It can be can concluded from this that growth rate regulates flux partitioning at PPP/EMP, PEPC/TCA and PGI/TCA branch points through its effect on the specific uptake rate. Since carbon uptake rate responds to cellular demands, it is therefore subject to the growth rate as a regulatory parameter. To accurately test the effect of growth rate on biomass production, a chemostat will have to be used. In a chemostat culture, growth can be accurately controlled and its effect on both biomass and the rate of carbon uptake determined more precisely. Though increased carbon source consumption is possibly caused by increased energy demands, this can only be accurately determined when growth is controlled, such as in chemostat culture. Nevertheless, the carbon consumption rate appears to influence the split in flux at key branch points in metabolic network.

5.7.4 Relationship between the specific rate of gluconate consumption and the rate of respiration

There appears to be a link between the consumption rates of both gluconate and oxygen. When both OUR and CER increased, GLUR was down-regulated. However, when respiration increased while CER and the respiratory quotient (RQ) decreased, GLUR was upregulated possibly to supply needed carbon precursors. Thus it appears there is a link between GLUR and respiration. It is not clear if GLUR responds to OUR or the CER/OUR ratio. However, it is more likely that GLUR or GUR responds to the respiration rate (OUR) since the consumption of a carbon source is responsive to energy demand. In short, increased carbon source consumption in the presence of reduced respiration rate, possibly leads to precursor storage since carbons in excess of requirements are likely to be stored or excreted. Reduced OUR

indicates decreased energy demands. Therefore, if consumption is increased despite reduction in energy demands, there probably is another regulatory mechanism involved. Thus, while the respiration rate and growth rate are dependent, consumption rate appears to be regulated independently.

In such an imbalance, gluconate would be consumed in excess of requirements. Balance between OUR and CER is accompanied by the production of erythromycin. This implicates RQ as an important parameter in erythromycin production. The combination of low RQ accompanied by increased consumption leads to accumulation of metabolites. Precursor metabolites appear to accumulate at reduced growth rate.

From the discussion in the previous section, it was concluded that increased flux through G6PDH supplies NADPH needed for erythromycin biosynthesis. It is known that glycolytic flux continuously produces carbon precursor metabolites and energy. We can conclude that the carbon precursors were greatly reduced during the growth phase. Such a reduction in precursor metabolites is consistent with the combined high demands of biomass synthesis and erythromycin biosynthesis. Therefore, it would have been necessary to switch dominant flux to glycolysis to replenish precursor metabolite pools generated by the EMP and TCA cycle. *S. erythraea* is able to regulate its respiratory capacity to meet metabolic demands for precursor metabolites. It does this by regulating respiration rate (OUR) independent of the growth rate (CER) to accumulate required precursor metabolites.

Precursor metabolites accumulate during incomplete oxidation eg when metabolism switches from aerobic to anaerobic respiration in facultative anaerobic organisms. However, since *S. erythraea* is strictly aerobic, the culture increased the specific uptake rate of the carbon source and oxygen but significantly reduced CO_2 evolution rate. Interestingly, biomass synthesis dropped by 49% perhaps suggesting it was constrained by the supply of precursor metabolites. From 39 to 48 hours, the rate of gluconate consumption was significantly increased. The respiration rate (OUR) remained higher than the CER, though both decreased slightly during this period. The decreased CER despite increased rates of specific gluconate uptake and high O_2 consumption could have created an imbalance which suggests that the respiratory capacity was limited. It suggests that gluconate was not completely oxidised to CO_2. Such an imbalance can be attributed to limited respiratory capacity and does lead to

incomplete oxidation in other organisms such as *E. coli* (Holms, 1996). Though incomplete oxidation under such conditions has been reported for *E. coli*, it is not impossible for *S. erythraea* to behave the same way. *S. erythraea* derives energy for biomass synthesis and macromolecule synthesis and assembly from the oxidation of carbon sources by aerobic means. It is, therefore, not far-fetched to assume that the organism will have to control the oxidation process by modulating both its oxygen and carbon source consumption. There was a corresponding increase in biomass synthesis, erythromycin production and increased activity of G6PDH. A logical conclusion here is that high demands of both biomass synthesis and erythromycin production for carbon precursors and NADPH led to depletion of these metabolites. It is likely this constrained the production of the antibiotic leading to a drop in the level. For growth on gluconate as sole carbon source, no NADH was produced through the activities of G6PDH because the ED pathway does not generate NADH. The TCA cycle supplied NADH, consequently the TCA cycle was fast and subsequently higher levels of organic acid excretion were observed. Owing to the slow growth rate on gluconate, NADPH was lower by a factor of two than on glucose as sole carbon source. The slow growth resulted in more carbons being diverted into biomass (Table 16). During the growth phase, biomass synthesis and secondary metabolite production compete for precursors metabolites. It appears that when the growth rate is low, carbon precursors are split more or less equally between biosynthesis and secondary metabolite production. Flux partitioning at PPP/EMP and AP/TCA cycle branch points is therefore dependent on the growth rate and the specific carbon uptake rate. Typically at low growth rate, metabolite levels are probably below inhibitory concentrations and permit flux through key pathway enzymes such as G6PDH. Therefore, growth rate appears to have the greatest effect on erythromycin production. Similar conclusions were made by Avignone-Rossa *et al* (2002). We have however found that regulation of flux distribution and erythromycin biosynthesis continued into the stationary phase when there was little variation in growth. It suggests that the regulation is perhaps due to the specific uptake rate and not the growth rate. Respiration and the growth rate were largely reduced after the growth phase. The dependence of erythromycin was observed during both the growth and stationary phase.

F6P is a crucial metabolite node when the culture is growing on gluconate. Fluxes to R5P (nucleotide biosynthesis), G6P (NADPH production) and glycolysis (NADH and ATP generation) all draw from the F6P metabolite pool. Therefore, it is not

surprising that the activities of both glycolysis and the PPP were lower than for the culture grown on glucose. Since gluconate is metabolised via the ED pathway, which does not produce NADH. Low NADH levels are consistent with reduced glycolytic flux. The levels of NADH were probably below inhibitory concentrations, which may explain why the increase in the production of erythromycin correlated positively with TCA flux. Increased [NADH/NAD^+] ratio depresses the TCA cycle through its inhibition of pyruvate dehydrogenase, isocitrate dehydrogenase and citrate synthase. Increasing the activity of the TCA cycle would produce the required NADH to meet demand since this cycle produces NADH. However, it is unclear as to why NADH levels dropped when erythromycin production increased. One explanation is the decreased demand for energy observed when the levels of the antibiotic increased. Another reason could be that NADH decreased due the activity of transhydrogenase which could have converted it to NADPH to meet the demands of reductive biosynthesis.

Figure 34 provides diagrams of the model for the distribution of fluxes in *S. erythraeae.*

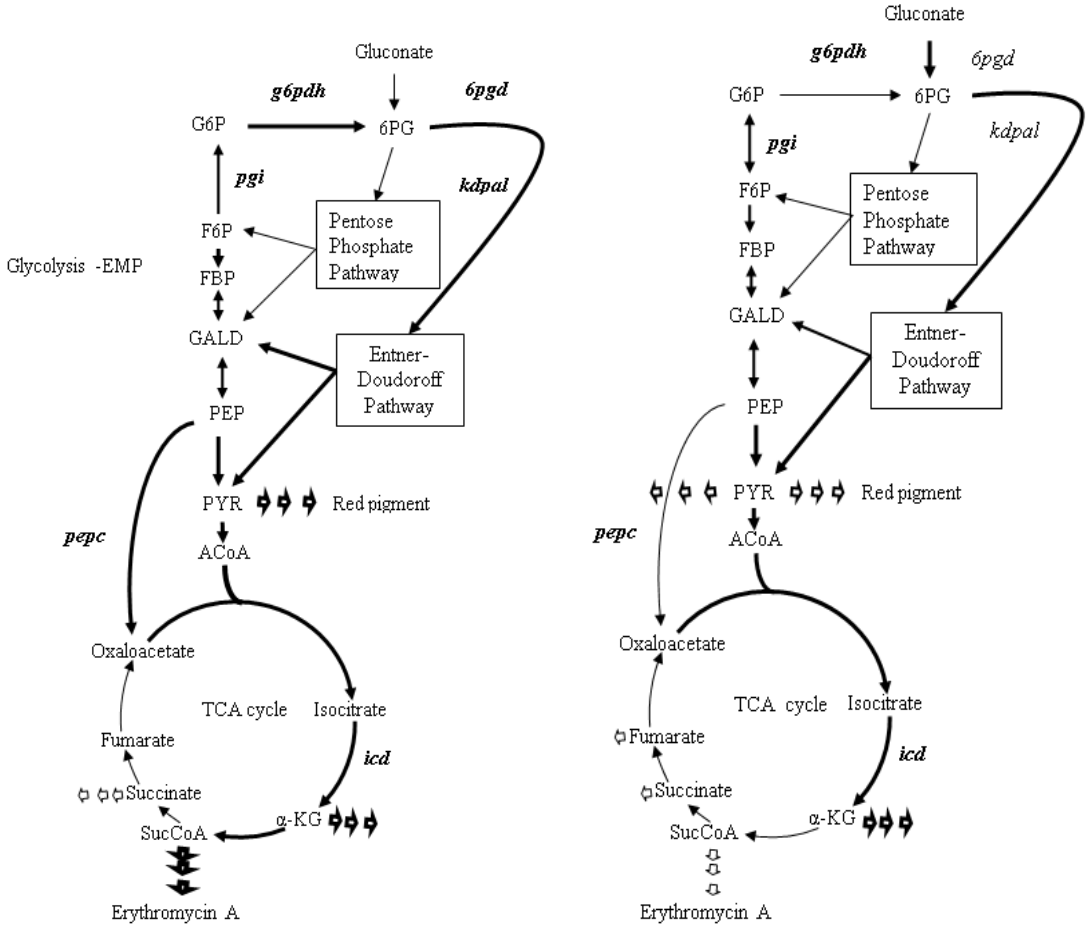

Fig. 34 Model for erythromycin biosynthesis in *S. erythraea* on glcuonate as a sole carbon and energy source. Left diagram - Erythromycin production phase, Right diagram - Precursor accumulation phase. Glucose-6-phosphate dehydrogenase - g6pdh, glucose-6-phosphate isomerase - *pgi*, phosphoenolpyruvate carboxylase - *pepc*, isocitrate dehydrogenase - *icd*, 6-phosphogluconate dehydratase - *6pgd*, 2-keto-3-deoxy-6-phosphogluconate aldolase - *kdpal*.

5.7.5 Model explanation:

Erythromycin production phase:

During the growth phase, carbons are routed simultaneously through glycolysis and the pentose phosphate pathway owing the slow growth which keeps metabolites below inhibitory concentrations. Due the low growth rate, precursor demands are low and this allows simultaneous allocation to both biomass formation and antibiotic production. At the G6P node, PP pathway flux is dominant. Carbon fluxes are routed simultaneously through both the anaplerotic pathway (AP) reaction and the TCA cycle. Simultaneous flux through AP and the TCA are possible because metabolite concentrations are below inhibitory levels due to the slow growth rate. Due to flux through both PPP and anaplerotic reaction, erythromycin is produced during the growth phase. Low ATP values due to low growth demands and high respiration rate, enabled flux through the TCA cycle. Large amounts of the red pigments are excreted. The activity of the anaplerotic reaction is necessary for the production of erythromycin. Growth rate and the nature of the carbon source determine whether erythromycin biosynthesis would be growth-related.

Precursor accumulation phase:

During this phase, carbon fluxes proceed mainly through the PP pathway and enter the bottom part of glycolysis. However, carbon fluxes are routed through to pyruvate and into the TCA cycle. The anaplerotic reaction activity is greatly reduced enabling the accumulation of precursor metabolites. In the absence of anaplerotic reaction activity, erythromycin biosynthesis is reduced resulting in decreased demand for precursor metabolites. Precursor metabolies accumulate including the excretion of large amounts of the red pigment. The anaplerotic reaction is necessary for erythromycin biosynthesis.

5.7.6 Summary of findings for growth on glucose and gluconate as sole carbon and energy sources

The biosynthesis of erythromycin is affected by suboptimal flux distribution at the PPP/EMP and AP/TCA cycle branch points. Increasing PPP flux enhanced the production of erythromycin perhaps due to its supply of NADPH. Increased erythromycin production was observed to correlate with flux through PPP and the

AP. However, routing carbon fluxes through pyruvate dehydrogenase and subsequently to the TCA cycle via isocitrate dehydrogenase depressed the production of the antibiotic when *S. erythraea* was grown on glucose. This route wastes carbons through the excretion of pyruvate and α-ketoglutarate and evolution of CO_2. However, for growth on gluconate, the production of erythromycin was enhanced by TCA cycle flux.

The partitioning of carbon fluxes at PPP/EMP, PGI/ICD and AP/TCA cycle was found to be dependent on the growth rate, specific carbon uptake rate and the nature of the carbon and energy source. At low growth rates, catabolism through the PPP and AP was enhanced, leading to increased erythromycin production. Flux through the PPP correlated positively with the production of erythromycin. Erythromycin production was enhanced by lower NADPH levels which allowed flux through G6PDH. High growth rates have high energetic and carbon precursor metabolite requirements. Therefore, the high demand for precursors and NADPH could have limited the biosynthesis of erythromycin during growth on glucose as a sole carbon and energy source.

When cultured on gluconate as a sole carbon and energy source, slow specific carbon uptake rate corresponded with almost equal partitioning of flux between the PPP and glycolysis resulting in growth-related biosynthesis of erythromycin. However, rapid specific uptake rate depressed the production of the antibiotic.

Because of the low growth rate on gluconate as carbon and energy source, NADPH concentrations were below inhibitory levels and facilitated flux through G6PDH. The oxidative branch of the PPP is known to be regulated by NADPH and G6PDH through feed-back inhibition mechanism (Ayar-Kayali, 2011, Morritz *et al*., 2000). Ayar-Kayali (2011) concluded that glucose uptake rate regulate the activities of G6PDH through the levels of NADPH. Working with *Amycolaptosis orientalis*, it was established that at high concentrations, PPP (G6PDH) activity competes with glucose kinase activities. The current study has arrived at the same conclusions regarding the role of the specific uptake rate in the regulation of the PPP flux. Though other studies have suggested that *S. erythraea* does not control its glucose uptake rate, we have found evidence to the contrary. *S. erythraea* upregulated its uptake rate when there is a high demand for the carbon precursor metabolites. When the antibiotic was being produced, the uptake rate was decreased. Fluxes through the

pathways responded to these variations in the specific uptake rate. We concluded that *S. erythraea* increases its uptake rate and down-regulates respiration when precursors were depleted and vice versa.

It was concluded that erythromycin production is constrained by limitations in the supply of precursor metabolites and NADPH.

4.7.7 Conclusions

The aim of this chapter was to characterise growth of *S. erythraea* in order to establish a physiological basis for the production of erythromycin.

During growth on either glucose or gluconate, biomass production accounts for the almost 50 percent of the carbons. Therefore, growth rate has major effect on the production of erythromycin. The distribution of fluxes and the production of erythromycin were found to depend on the specific growth rate, the nature of the carbon and energy source and the balance between the RQ and specific uptake rate of the carbon source.

At the G6P, slowing down the growth rate (using gluconate as sole carbon source) promoted balanced fluxes through the first enzyme of the pentose phosphate pathway and the EMP. The balance between the RQ and the specific uptake rate of gluconate had a similar effect at the interface between EMP and the PPP. At the anaplerotic pathway/TCA cycle interface (pyruvate node), fluxes were preferentially routed to the TCA cycle and correlated with increased production of erythromycin when the uptake rate was low. Thus a low specific uptake rate coupled with a high RQ, promoted fluxes from glycolysis to the anaplerotic pathway and the TCA cycle and enhanced the production of erythromycin.

For growth on glucose as carbon source, a slow specific uptake rate promoted the production of erythromycin. However, erythromycin production was associated with increased flux through the PPP and the anaplerotic pathway. Since for both conditions PPP and EMP fluxes were essential, it was concluded that NADPH and the carbon precursor metabolites could constrain the production of erythromycin.

Flux partitioning at key branch points is regulated by the growth rate through its effect on the carbon uptake rate. Evidence was found that *S. erythraea* is able to regulate its rate of carbon consumption based on the cells' metabolic status. Respiration was found to be regulated independently from the growth rate.

Imbalance between glucose (gluconate) uptake rate, growth rate and the rate of respiration appears to enhance the production of the antibiotic.

The anaplerotic pathway/TCA cycle branch point was found to merit further investigation since erythromycin production was produced under different split fluxes at the pyruvate node. The anaplerotic reaction was found to be necessary for erythromycin production. In terms of nodal flexibility, the pyruvate node was found to be flexible. However, the α-ketoglutarate node appears rigid. Therefore, both the pyruvate node and the anaplerotic reaction are the focus of investigations in subsequent chapters.

Chapter 6

6.0 Bolus feed additions under shake flask conditions

6.1 Introduction

The TCA cycle is important in metabolism as it generates NADH consumed during the generation of energy at the Electron Transport Chain (ETC) through oxidative phosphorylation. The importance of the TCA cycle in the production of erythromycin was discussed in detail in Chapter 4 and 5. One major conclusion of that chapter was that increased activity of the TCA cycle wastes carbons through excretion of organic acids and evolution of CO_2 and thereby reduces the production of the antibiotic. Overflow of metabolites is a form of energy spillage to reduce the production of excess energy. Excess energy generation results from the continued consumption of glucose (or gluconate) during decreased growth demands. During the growth phase, growth demands for precursor metabolites and energy ensure that the respiratory capacity of the TCA cycle is not exceeded. However, when the carbon source is consumed after growth has slowed, excess energy, respiratory cofactors and precursor metabolites are produced leading to the respiratory capacity of the TCA cycle being exceeded. Such precursors would be produced from storage compounds which, themselves, accumulate during the stationary phase.

Part of the regulation of the TCA cycle is correlated with the consumption rate of the carbon source. This is expected since the uptake of glucose is subjected to the demand for energy, respiratory cofactors (NADH, NAD^+) and carbon precursors. In fact, if precursor metabolites are depleted, the TCA would come to a standstill and respiration would be deprived of NADH. Since the TCA cycle also has an anaplerotic function, the reduced respiratory rate will depress growth rate. The activity of the TCA cycle has a direct effect on the product pathway. The production of erythromycin proceeds via succinyl-CoA to methylmalonyl-CoA and eventually propionyl-CoA. Therefore, by regulating the TCA cycle activity, the flow of carbons through the product pathway is automatically regulated.

The role of primary metabolism in supplying precursors for secondary metabolite production has been investigated in various studies (Dekleva & Strohl, 1988; Penzikova & Levitov, 1965; Penzikova & Levitov, 1966; Ikeda *et al*, 1988). Metabolites produced during primary metabolism provide the building blocks for the production of antibiotics. In addition to precursor metabolites, primary metabolism generates energy and reduces redox equivalents associated with energy generation and reductive biosynthesis. If central metabolism provides precursors, reduction in metabolite supply can constrain secondary metabolite production. Therefore, overall control can be expected to reside in primary metabolism thereby placing a limit to how much product pathways can be engineered to improve yield. Product pathways are subject to overall primary metabolic control (Kleijn *et al*, 2006).

Studying catabolic routes of carbon sources may provide information on the supply and role of energy nucleotides, carbon skeletons and cofactors in controlling antibiotic production. In *Clostridium glutamicum*, glucose catabolism through glycolysis and the pentose-phosphate pathway were found to be controlled by ATP/ADP ratio and NADPH (Moritz *et al*, 2000). In other work, antibiotic production in *Streptomyces coelicolor* was enhanced by high NADPH/$NADP^+$ ratio (Obanye *et al*., 1996). Several studies with other organisms reported the opposite effect of NADPH on antibiotic production (Jonsbu *et al*., 2001; Butler *et al*., 2002, van Gulik *et al*, 2000). The cause of this may be the difference in the rate of fluxes between glycolysis and the pentose-phosphate pathway or the rate of NADPH production. The degree to which the carbon source is reduced compared to the antibiotic and the number of NADPH-dependent reductive reactions possibly influence the amount of antibiotic produced. There is little information on any studies on the degree of reduction of Actinomycetes. Nevertheless, the improvement in penicillin production is a result of extensive physiological characterisation that involved studying the role of primary metabolism. Some work done with *S. erythraea* by Bushell *et al* (1997), Lynch and Bushell (1995) and Wilson and Bushell (1995) established a correlation between erythromycin production and a decreased rate of protein synthesis. In another work, Jaques (2004) suggested that slowing down the TCA cycle may enhance the production of erythromycin.

In this chapter, the effect of feeding precursor metabolites on the production of erythromycin will be investigated.

6.2 Bolus-feed additions in shake flask fermentations

In Chapter 4, the production of erythromycin was found to be constrained by limitations in the supply of precursor metabolites. It is, therefore, argued that supplementing the culture with appropriate precursors could enhance this supply and increase erythromycin levels. It is not entirely clear at which level in the metabolic network limitations in the precursors are. As such, precursor metabolites are selected from glycolysis (phosphoenolpyruvate), the TCA cycle (oxaloacetate and methyl oleate/acetyl-co A) and the erythromycin biosynthetic pathway (propionate) for supplementation. Oxaloacetate was selected because it replenishes the TCA cycle enabling it to continue operating to generate NADH and precursor metabolites. In Chapter 4 and 5, the activity of the anaplerotic pathway (PEPC) was observed to correlate positively with erythromycin production. Therefore, it was reasonable to postulate that feeding oxaloacetate will enhance production of the antibiotic.

Propionate is the priming/extender unit for erythromycin assembly along the polyketide synthase modular unit. It is generated by degradation of odd-chain fatty acids. Acetyl-coA is the entry point for methyl oleate into the metabolic network. Limitations in the supply of propionate and acetyl-coA are likely to constrain the biosynthesis of erythromycin. Propionate has been used to improve antibiotic biosynthesis in *Streptomyces* (Demain, 1998). The use of oils in antibiotic fermentations has been discussed in Chapter 1. To account for possible limitations in the supply of glycolytic precursors, phosphoenolpyruvate (PEP) was selected for supplementing in *S. erythraea.* PEP is issued to power the active uptake of carbon sources by certain organisms, making its role crucial in the biosynthesis of antibiotics. Oxaloacetate is commonly known to replenish the TCA cycle, thus ensuring its continued operation to generate NADH and certain precursors. The positive effect of methyl oleate on the production of erythromycin was discussed in Chapter 1.

The effect of these precursor metabolites on the biosynthesis of erythromycin was

investigated in bolus feed additions shake flask fermentations. A set of experiments where designed to investigate the effect of precursor supplementation on the levels of erythromycin. The conditions of supplementation employed are indicated on the respective figures in the results section. The rationale for conducting the experiments in shake flasks is based on the suboptimal performance of microbial cultures at this scale. The effect of feeding precursors on the levels of erythromycin would be better illustrated under suboptimal conditions. If supplementation under these conditions enhances the levels of erythromycin, performance is likely to be better in bioreactor cultures.

6.3 Results and discussion

6.3.1 Control fermentation

The control shake flask fermentation was conducted to provide a baseline erythromycin production profile for the supplemented fermentations. Erythromycin production exhibited a non-growth-related profile as was observed in the bioreactor fermentation in Chapter 4 (Fig. 17). The culture reached a maximum level of erythromycin (8.8 $mgL^{-1}.g^{-1}$ biomass) after 48 hours of growth. Relative to the 20 $mgL^{-1}.g^{-}1$ biomass obtained for bioreactor culture in Chapter 4, the shake flask culture had a 60% lower yield. This is not surprising considering that conditions in shake flask culture such as pH and oxygen supply, are less optimal compared to those in a bioreactor. Beyond 48 hours, there was a gradual decline in the levels of erythromycin (Fig. 35).

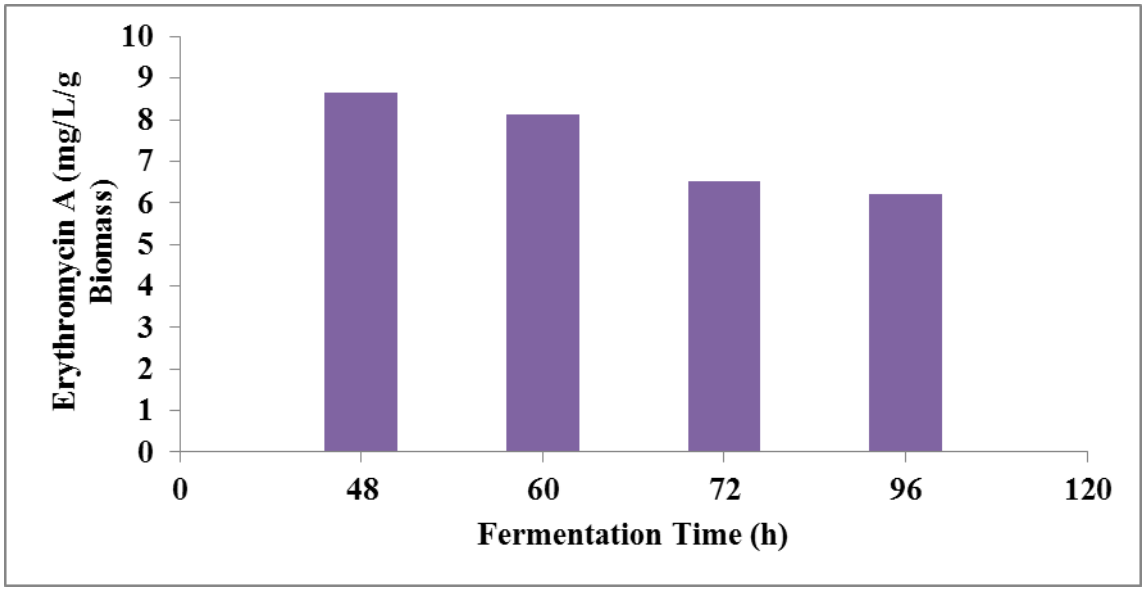

Fig. 35 Profile of erythromycin production of *S. erythraea* in shake flask on glucose as substrate.

6.3.2 Phosphoenolpyruvate supplementation

Feeding phosphoenolpyruvate (PEP) did not have any significant effect on the levels of erythromycin relative to the control culture. Samples collected at 48 and 96 hours of growth, yielded maximum erythromycin levels of 13 $mg.L^{-1}g^{-1}$ biomass irrespective of the treatment regime (Fig. 36, Fig. 38). This was not a significant improvement from the 8.8 $mgL^{-1}.g^{-1}$ produced by the control culture. However, the culture produced a large amount of the red pigment after supplementation (data not presented). Whether this reflects enhanced pyruvate pools is speculative. However, PEP is a strategic metabolite in the metabolic network since it is involved in gluconeogenesis through the actions of phosphoenolpyruvate carboxykinase (PEPCK), carbon source degradation through pyruvate kinase and glucose uptake through the phosphotransferase system (PTS). Without determining at least some of the activities of the enzymes and metabolite pools involved, any attempt at explanation would be speculative. However, the excretion of large amounts of the red pigment combined with the failure to significantly increase the levels of erythromycin suggests that this metabolite node is not very flexible. Based on the findings of Chapters 4 and 5, limitations in the supply of

precursors were postulated to constrain the production of erythromycin. It was thought that the addition of PEP would enhance its pool leading to increased TCA cycle activity. This is not what was observed experimentally. If the PTS system is present in *S. erythraea*, its operation may not drain the PEP pool significantly to limit the supply of this metabolite to TCA cycle. Apart from the red pigment, there may be unknown pathways to which PEP was diverted. It could have been useful if the oxaloacetate pool was determined after supplementation with PEP. However, the observed excretion of large amounts of the red pigment suggests that PEP enhanced the pyruvate pool. It is noteworthy that this increase was only observed at 48 hours.

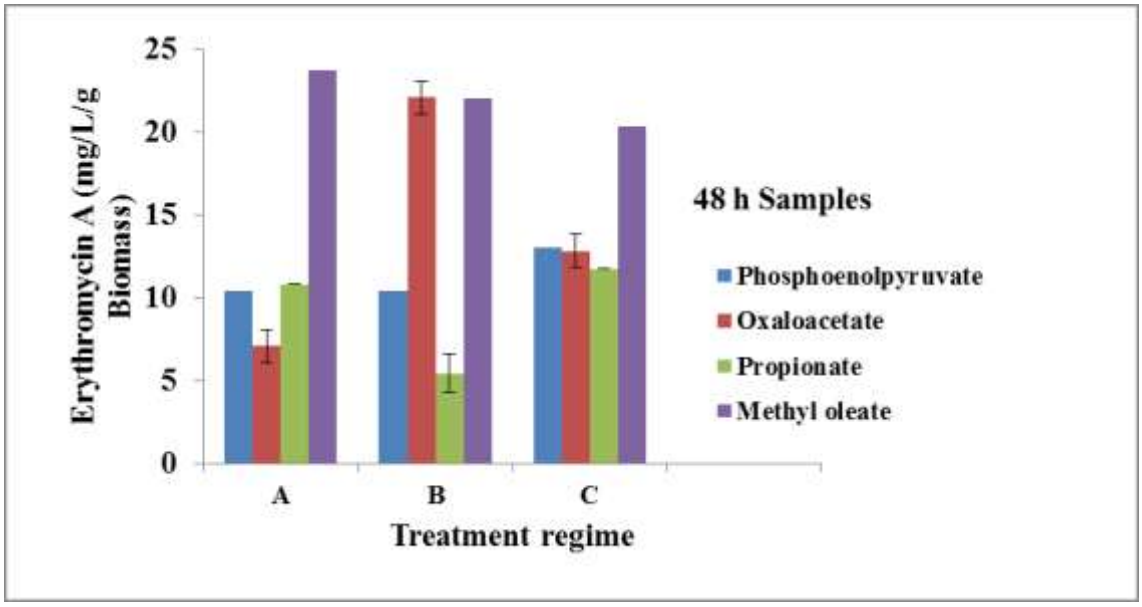

Fig. 36 Profiles of erythromycin production at 48 hours in response to precursor supplementation. Treatment regime represents a combination of concentration and time. For PEP, OAA and propionate A and B represent 2 mM and 4 mM supplemented at 30 hours respectively. At point C, 3 mM of each metabolite was supplemented at 45hours.For methyl oleate, time points A, B and C represent 5 $g.L^{-1}$, 10 $g.L^{-1}$ and 7.5 $g.L^{-1}$ supplemented at 30, 60 and 45 hours respectively. Samples represent 3 technical replicates

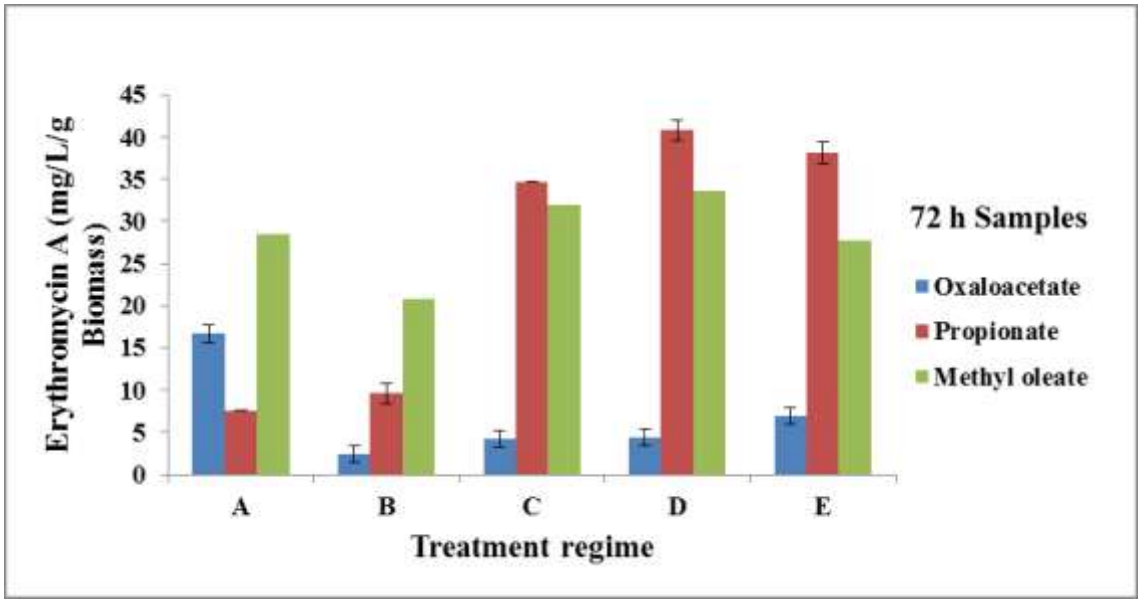

Fig. 37 Profiles of erythromycin production at 72 hours in response to precursor supplementation. Treatment regime represents a combination of concentration and time. Oxaloacetate and propionate: A - 2 mM:30 h, B - 2 mM:60 h, C - 4 mM:30 h, D - 4 mM:60 h and E - 3 mM:45 h. Methyl oleate: A - 5 $g.L^{-1}$:30 h, B - 5 $g.L^{-1}$: 60 h, C - 10 $g.L^{-1}$:30 h, D - 10 $g.L^{-1}$: 60 h and E - 7.5 $g.L^{-1}$:45 h. PEP samples were not processed due to operational difficulties. Samples represent 3 technical replicates

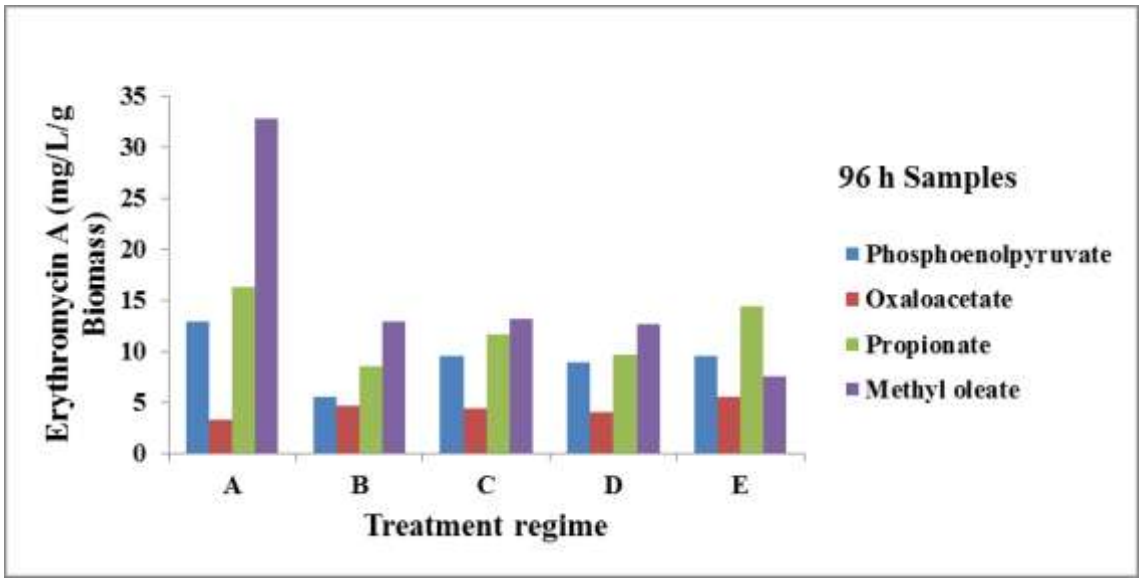

Fig. 38 Profiles of erythromycin production at 96 hours in response to precursor supplementation. Treatment regime represents a combination of concentration and time. PEP, oxaloacetate and propionate: A - 2 mM:30 h, B - 2 mM:60 h, C - 4 mM:30 h, D - 4 mM:60 h and E - 3 mM:45 h. Methyl oleate: A - 5 $g.L^{-1}$:30 h, B - 5 $g.L^{-1}$: 60 h, C - 10 $g.L^{-1}$:30 h, D - 10 $g.L^{-1}$: 60 h and E - 7.5 $g.L^{-1}$:45 h. Samples represent 3 technical replicates.

6.3.3 Oxaloacetate supplementation

The addition of oxaloacetate (OAA) produced different effects on the production of erythromycin compared to the addition of PEP. The most significant effect on the levels of erythromycin was observed at 48 hours when 4 mM oxaloacetate was added to the culture at 30 hours. The level of erythromycin increased to 23.3 $mgL^{-1}.g^{-1}$ (Fig. 36). The corresponding value for the control culture was 8.8 $mgL^{-1}.\ g^{-1}$ (Fig. 35). This represents an increase of 62% relative to the control culture. The effect on the levels of erythromycin was significant even when compared to the levels obtained with bioreactor cultures. *S. erythraea* produced a maximum of 18 $mgL^{-1}.g^{-1}$ in bioreactor culture grown on glucose as a sole carbon source (Fig. 17). The reason for this could be the time of supplementation. From the discussion in Chapter 4, it can be observed that supplementation was done midway through the precursor accumulation phase (Fig. 17). It was argued that when precursor metabolites are depleted, they need to be replenished during the accumulation phase before the antibiotic can be produced again. The results from this experiment seem to confirm this suggestion. When oxaloacetate was supplemented during the precursor metabolite phase in shake flask culture, the levels of erythromycin reached were even higher than those obtained for bioreactor cultures. The highest level obtained for the bioreactor culture was 20.5 $mgL^{-1}.\ g^{-1}$ at 96 hours (Fig. 17). Thus, productivity is enhanced when OAA was supplemented during the early precursor replenishment phase. When the concentration of OAA was reduced to 2 mM, the increase in erythromycin levels was significantly lower. Though the levels did increase, the maximum was 17.2 $mgL^{-1}.g^{-1}$ obtained after 72 hours whereupon the levels decreased significantly (Fig. 37). Thus it appears the concentration of OAA added affected both titre and productivity as a lower concentration was obtained over a longer fermentation time.

When 3 mM was supplemented at 45 hours, 13 $mgL^{-1}.g^{-1}$ was obtained at 48 hours (Fig. 36). This was an interesting finding since the culture only had 3 hours to divert the added OAA to erythromycin. However, erythromycin only increased at 48 hours and decreased significantly after this period (Fig. 37, Fig. 38). The question is: Would

additional feeding after 48 hours supply the required precursors to enhance erythromycin levels? This question is the subject of subsequent experiments.

Nevertheless, what is clear from this experiment is that oxaloacetate can enhance erythromycin production when supplemented at an appropriate concentration and time. These findings are in agreement with the conclusions drawn in Chapter 4 and Chapter 5.

6.3.4 Propionate supplementation

Propionate is on the erythromycin biosynthetic pathway forming the priming unit along the PKS module to which extender units are added for carbon chain elongation. It can, therefore, be argued that this position in the metabolic network would profoundly influence the effect of propionate supplementation.

None of the low propionate concentrations of 2 mM resulted in significant increase in the levels of erythromycin whether supplemented at 30 or 60 hours of growth. However, for the higher concentrations of 3 and 4 mM, the time point of supplementation appears to be the critical parameter. When 4 mM of propionate was supplemented at 60 hours of growth, the concentration of erythromycin reached 40 $mg.L^{-1}.g^{-1}$ at 72 hours (Fig. 37). Relative to the 6 $mgL^{-1}.g^{-1}$ obtained at 72 hours for the control culture, this increase is profound. Interestingly, the time of feeding corresponds to the second precursor accumulation phase observed in experiments as discussed in Chapter 4 and Chapter 5 (Fig. 17, Fig. 26). This means that, in an un-supplemented culture the concentration of erythromycin would have been decreasing between 48 and 72 hours. The increase would have been between 72 and 96 hours. That the culture produced this high concentration of the antibiotic after addition of propionate suggests that this metabolite was limiting in the un-supplemented cultures.

Further evidence is provided by the culture that was supplemented with 3 mM propionate at 45 hours. The culture produced 35 $mg.L^{-1}.g^{-1}$ erythromycin during the precursor accumulation phase from 48 to 72 hours (Fig. 36, Fig. 37). The levels of erythromycin produced by far exceed those obtained in bioreactor conditions.

However, when 4 mM was added at 30 hours, the effect was only observed 42 hours after supplementation. Though, the titre significantly increased, productivity was not improved. It appears the advantage lies in feeding propionate after the growth phase. It

is not clear what delayed the increase in the level of erythromycin when propionate was added during the growth phase. It may be that propionate only becomes a limiting factor after the growth phase, which is when it is required for erythromycin biosynthesis. This suggestion is supported by the fact that propionate was only excreted late in the fermentation even though it was added early on at 30 hours. In Chapter 4, propionate was observed between 24 and 48 hours and eventually dropped to undetectable levels by 72 hours (Fig. 37). Therefore, feeding at 30 hours could have been in excess of propionate requirements. It could be concluded that propionate may not be limiting during the growth phase, which explains the late effect observed on erythromycin production. The same argument may also explain the significant effect observed when propionate was fed at 45 and 60 hours (Fig. 24). Erythromycin production was significantly enhanced when propionate was fed just before (45 hours) and during (60 hours) the second accumulation phase. Some unknown metabolites appear to limit erythromycin production during the growth phase.

6.3.5 Methyl oleate supplementation

As discussed in section 1.4.6 (Chapter 1), oils are commonly used as supplements in industrial fermentations to enhance the production of antibiotics. The concentration of oil added appears to be a critical factor. When 5 $g.L^{-1}$ was added to the culture at 30 hours, erythromycin was significantly increased relative to the un-supplemented cultures in both shake flasks and bioreactors (Fig. 17, Fig. 35, Fig. 37). The highest concentration was obtained at 96 hours (Fig. 38). However, when the concentration was increased to10 mgL^{-1}, a maximum of 31 $mg.L^{-1}.g^{-1}$ was reached at 72 hours (Fig. 37). This represents a shift of 24 hours relative the culture supplemented with 5 $g.L^{-1}$ at 30 hours. It translates into improved productivity for the culture which was supplemented with 10 $g.L^{-1}$ though the titres are practically equal. This could mean that methyl oleate boosted the metabolite pools that were depleted between 48 and 72 hours as discussed in Chapter 4 and Chapter 5. It is not clear why these pools were not boosted immediately when the culture was supplemented with 5 $g.L^{-1}$ methyl oleate.

However, when the culture was supplemented with10 gL^{-1} at 60 hours, the effect was immediate. The concentration of erythromycin reached a maximum of 35 $mg.L^{-1}$ within

12 hours of supplementation. This effect was similar to the one observed for propionate supplementation.

The similarity between the findings on propionate and those on methyl oleate is consistent with the metabolism of oil. Methyl oleate enhances propionate pool since it is metabolised via the valine degradation pathway which eventually forms propionate.

The findings with methyl oleate, oxaloacetate and propionate suggest that, in shake flask culture, limitations in these precursor metabolites may play a role in constraining the production of erythromycin.

The physiological and metabolic basis for the observations under shake flask conditions will be investigated in Chapter **7.**

Chapter 7

7.0 Bolus-feed additions bioreactor fermentations

In shake flask culture oxaloacetate, propionate and methyl oleate were found to increase the level of erythromycin significantly. Addition of PEP did not increase the concentration of erythromycin significantly. However, the effect of oxaloacetate addition was significant only when this was done during the exponential growth phase between 30 and 45 hours. Any supplementation after the exponential growth phase did not increase the production of the antibiotic to any significant degree. Contrary to these findings, the levels of erythromycin were significantly increased when propionate or methyl oleate was added after the exponential growth phase. Though supplementation during the growth phase increased the concentration of the antibiotic, this effect was observed either 42 or 66 hours after supplementation. In contrast, when feeding was done after the growth phase, maximum levels of the antibiotic were observed 12 hours after supplementation. As discussed in Chapter 6, increases in the levels of erythromycin were observed when supplementation was done during the precursor accumulation phases.

This chapter aims to investigate the effect of precursor supplementation on the production of erythromycin at bioreactor scale. Scale is a critical parameter in fermentations and can affect strain performance. Also, fermentation parameters can be better controlled when operating at bioreactor scale. Therefore, it was necessary to conduct feeding experiments in bioreactors. In shake flask experiments discussed in Chapter 6, the highest increases in the level of the antibiotic were observed when feeding was done during the precursor accumulation phases. However, it is not known if supplementing during the antibiotic synthesis phase will enhance production.

The physiological and metabolic basis for improvement in the production of erythromycin was investigated in bioreactor studies. The conditions for feeding were optimised in shake flask experiments discussed in the previous section. In the batch fermentation, glucose was almost depleted after 72 hours.

All methods and procedures were carried out as described in section chapter 2.

7.1 Bioreactor culture: Oxaloacetate supplementation

All samples were treated and analysed as described in Chapter 2. In shake flask studies, feeding oxaloacetate during the late synthesis phase enhanced the levels of the antibiotic within three hours. However, increases were higher when supplementation was done at 30 hours compared to feeding at 45 hours. Nevertheless, for these observed increases in the production of erythromycin, feeding was done during the growth phase. The effect when feeding is done after the growth phase has not been investigated. The current set of experiments will investigate this. The basis for any increases in the level of erythromycin will be investigated as well. To this end, a second feeding point was introduced at 71 hours. This time point could also generate information on the effect of precursor addition during the erythromycin synthesis phase.

7.1.1 Supplementation at 45 and 71 hours

For the first 24 hours of culture, growth was similar to that in the batch culture. The rate of biomass formation was 0.07 $g.L^{-1}.h^{-1}$ compared to 0.08 $g.L^{-1}.h^{-1}$ for the batch culture (Fig. 17, Fig. 39). Nitrate consumption was equally similar with a rate of 0.1 $g.L^{-1}.h^{-1}$ compared to 0.09 $g.L^{-1}.h^{-1}$ for the batch culture (Fig. 17, Fig. 439). However, the supplemented culture consumed glucose at 59% lower rate than the batch fermentation (Table. 15, Fig. 19, Table 19, Fig. 39).

After supplementing at 45 hours, the rate of biomass production decreased and continued to decrease until the end of the fermentation (Fig. 39, Table 19). Both OUR and CER decreased from 45 hours up to 48 hours (Table 19, Fig. 40). Respiration subsequently increased up to 60 hours. However, though carbon dioxide was evolved, no growth was observed. After feeding, respiration and carbon dioxide evolution initially increased for about 15 hours, after which they then dropped. The drop in the rate of respiration was less significant relative to the decrease in growth rate. The rate of glucose consumption increased by 54% in three hours and by 83% over 26 hours. Following additional feeding at 71 hours, the rate subsequently dropped by 38%.

Though the addition of oxaloacetate triggered an increase in glucose consumption, this

was not driven by growth demands since biomass actually decreased. However, increases in the glucose consumption rate coincided with an increased rate of respiration. The production of erythromycin dropped significantly between 48 and 72 hours. The batch fermentation exhibited a slight reduction in the rate of antibiotic production over the same period (Fig. 17). Nitrate was depleted within 48 hours of growth. Though this was earlier than for the batch, nitrate consumption was similar for the accelerated growth phase (Fig. 17, Fig. 39).

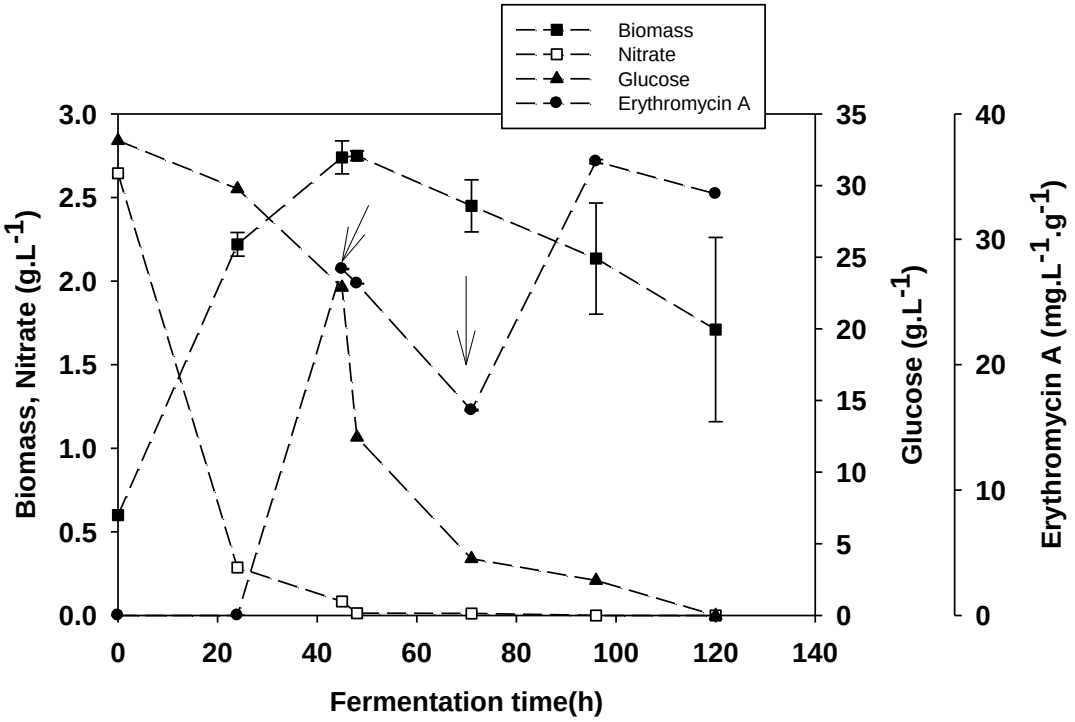

Fig. 39 Profiles of biomass (■), glucose (▲) and nitrate (□) and erythromycin (●) A during growth on glucose with 3 mM oxaloacetate supplementation. Arrows indicate the feeding points. Data represents means obtained from three biological replicates.

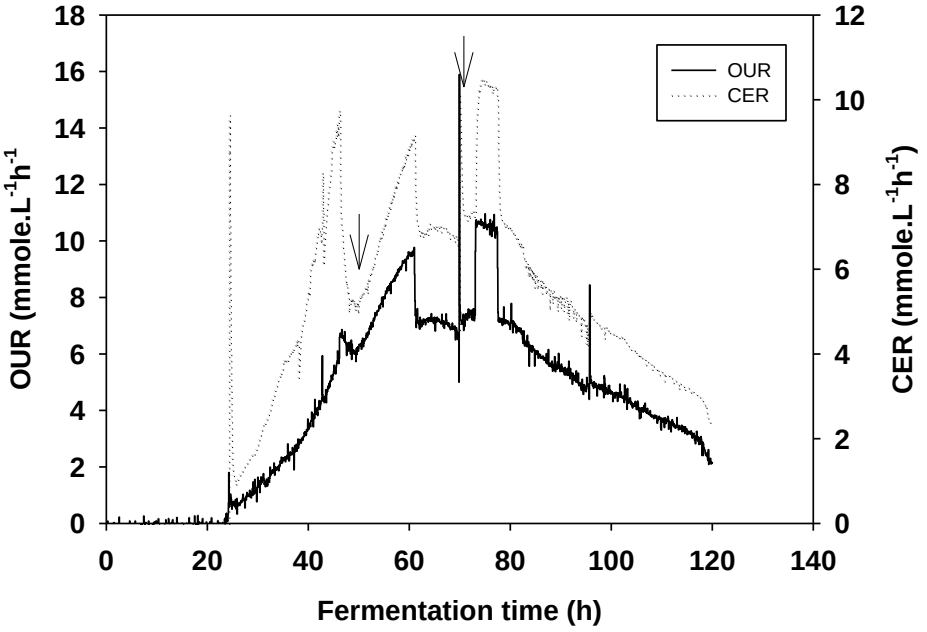

Fig. 40 Profiles of OUR and CER in *S. erythraea* fed batch fermentation. Arrows indicate the point of oxaloacetate supplementation. All data represents means obtained from triplicate fermentations.

Table 19. Specific growth rate, yields and yield coefficients for batch and supplemented batch *S. erythraea* cultivation using glucose as main carbon source. The values for the fed culture include the supplemented carbon. No distinction is made between the two carbon sources.

Fermentation condition	**Growth parameters**			
	μ (h^{-1})	**Yx/s ($g.g^{-1}$)**	**Yp/s ($mg.g^{-1}$)**	**Yp/x ($mg.g^{-1}$)**
Batch	0.059	0.17	2.73	20.54
Fed culture	0.06	0.10	2.52	50.35

7.1.2 Effect of oxaloacetate supplementation on the activities of key pathway enzymes

After feeding, the activity of glucose-6-phosphate dehydrogenase increased by 77% from 45 to 48 hours while the phosphoenolpyruvate carboxylase activity increased by 36% (Fig. 41). No further increases were observed in the activities of PGI and PEPC between 48 and 71 hours. The most significant effect was on the activity of isocitrate

dehydrogenase which decreased by 88% over the same period. No further increases were observed in the activities of PGI and PEPC between 48 and 71 hours. However, G6DH and ICD decreased over the same period. The same trend continued after a further supplementation at 71 hours. With the exception of PEPC, the remaining three enzymes were suppressed and their activities decreased after supplementation at 71 hours. At the anaplerotic reaction/TCA cycle branch point, PEPC activity increased by 68% indicating that flux switched to the anaplerotic pathway. The product yield ($Y_{p/s}$) in the fed-batch fermentation was reduced by 8 % compared to the batch fermentation (Table 15, Table 19). This may have to do with the lower rate of glucose consumption for the fed batch culture. However, biomass yield ($Y_{x/s}$) was significantly lower (by 41 %) for the fed batch culture relative to the batch fermentation as well. Thus, the added oxaloacetate appeared to have been channelled to the production of erythromycin. This also suggests that in the batch fermentation, erythromycin was constrained by the availability of oxaloacetate or other precursors derived from it. Since biomass yield was similar, precursor metabolites seems not to constrain growth. It may be that growth demands constrain precursor supply to secondary metabolism. Yield ($Y_{p/x}$) was 59 % higher for the fed batch culture suggesting that oxaloacetate enhanced yield (Table 15, Table 19). The fact that the addition of a volume of 100 mL resulted in a 59 % increase in yield suggests that oxaloacetate availability was limiting erythromycin biosynthesis. In general, the fed batch culture diverted less carbon to both biomass formation and erythromycin biosynthesis (Table 15, Table 19). However, its yield was much higher than that for the batch culture.

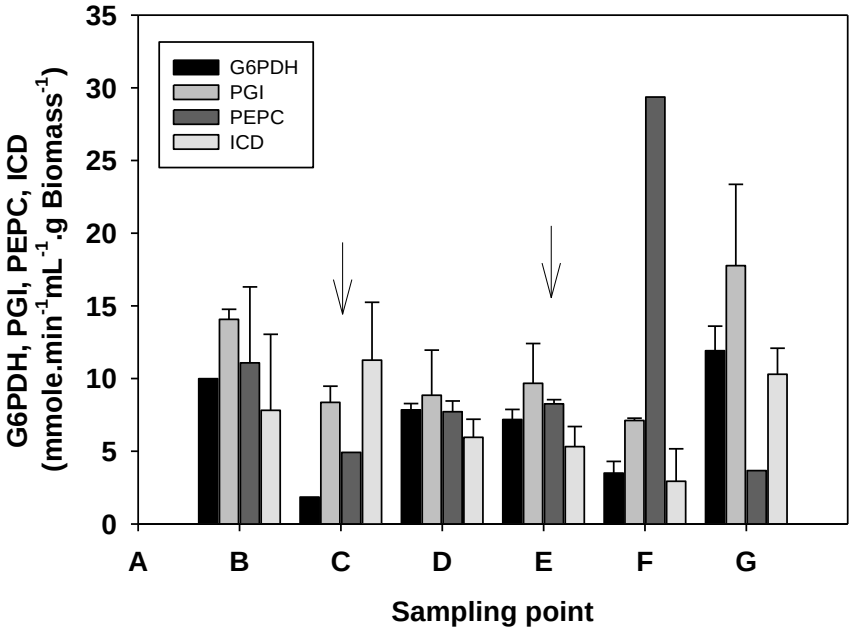

Fig. 41 Time courses of enzyme activities during the oxaloacetate bolus feed additions fermentation. PGI - phosphoglucose isomerase, G6PDH - glucose-6-phosphate dehydrogenase, ICD - isocitrate dehydrogenase and PEPC – phosphoenol pyruvate dehydrogenase during bolus-feed additions fermentation. Sampling points: A (0 h), B (24 h), C (45 h), D (48 h), E (71 h), F (96 h), G (120 h). All data represents means obtained for 3 biological replicates.

7.1.3 Excretion of organic acids

As in the previous cultures grown on glucose, the excretion of organic acids commenced after the exponential growth phase. Reduced growth rate coincided with the excretion of α-ketoglutarate, succinate and the red pigment. Pyruvate, however, was not excreted until after the end of the growth phase (Fig. 42). This suggests that demand for pyruvate was high. Upon supplementation, the concentrations of α-ketoglutarate, succinate and pyruvate increased significantly up to 71 hours (Fig. 42). For the batch fermentation pyruvate levels dropped sharply between 48 and 71 hours. Interestingly, feeding oxaloacetate did not have a significant effect on the production of the red pigment. This is, however, not surprising given that oxaloacetate enters the metabolic network below the pyruvate node. After supplementation at 71 hours, the excretion of all organic acids dropped significantly. In general, the initial supplementation at 45h appeared to have increased the excretion of organic acids resulting in decreased

biosynthesis of erythromycin. The activity of isocitrate dehydrogenase, which represents TCA cycle activity, increased significantly after feeding oxaloacetate at 45 hours. As such, oxaloacetate bolstered TCA cycle activity. Subsequent feeding at 71h increased the production of the antibiotic and depressed organic acid excretion. Dominant pathway switched from the TCA cycle to the anaplerotic pathway. The activity of PEPC increased significantly confirming the switch to the anaplerotic pathway (Fig. 41).

Lower levels of α-ketoglutarate and pyruvate were observed compared to those for the batch (control) fermentation which suggests that less carbon was wasted for the supplemented culture (Table 19). There seems to be a link between growth requirements and the wastage of precursors. At fast growth rate, biomass formation appears to correspond to the excretion of high levels of organic acids as was observed in the batch fermentations (Fig. 17). However, when less biomass was produced, lower levels of the organic acids were excreted resulting in enhanced erythromycin production (Fig. 39, Fig. 42).

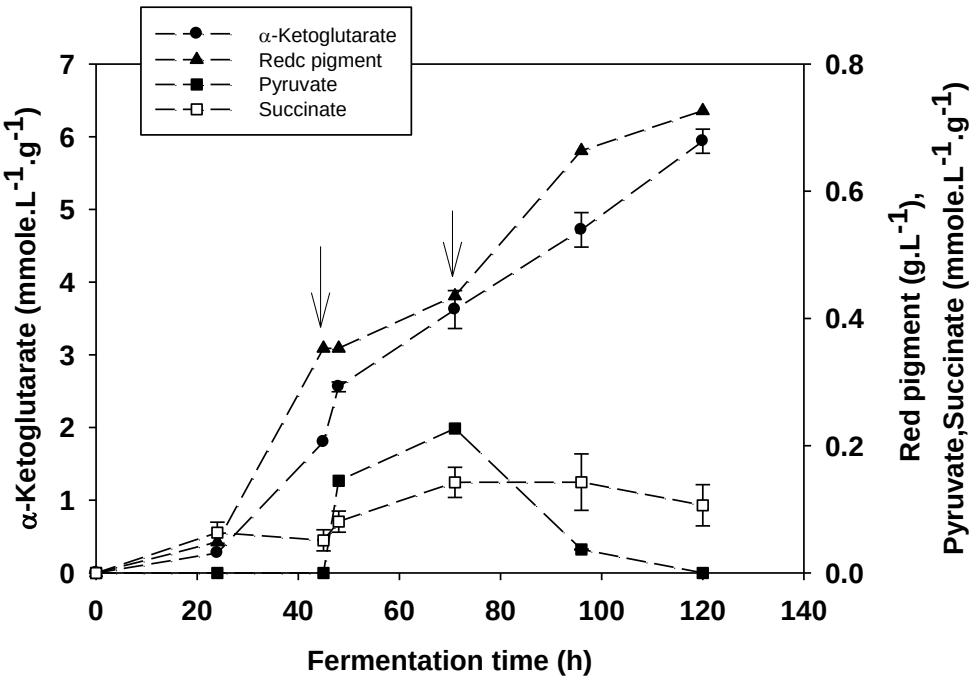

Fig. 42 Time courses of organic acids during bolus-feed additions fermentation: pyruvate (■), α-ketoglutarate (●), succinate (□), red pigment (▲) during fed batch fermentation. All data represent means from triplicate fermentations.

Table 20. Specific rates of substrate consumption, biomass production and product formation for bolus feed additions *S. erythraea* culture on glucose as main carbon source. Negative rates indicate disappearance of substrate (glucose) due to consumption, biomass decrease due to cell lysis and cessation of CO_2 evolution or pyruvate excretion.

Parameter	Phase I (0-24h)	Phase II (24-48h)	Phase III (48-96h)
qO_2 [a]	-5.6	-1.296	0.79
qCO_2 [b]	4.94	0.117	-0.759
qGlucose [c]	-0.02	-0.07	-0.021
qBIOMASS [d]	0.07	0.02	-0.01
qEry [e]	-	0.31	0.01
qα-KG [f]	7×10^{-4}	4×10^{-3}	9×10^{-4}
qPYR [g]	-	3×10^{-4}	6×10^{-5}
qSUC [h]	-	4×10^{-5}	2×10^{-5}
qRED [i]	2×10^{-3}	3×10^{-4}	6×10^{-4}

[a] Specific O_2 uptake rate (mmole.$L^{-1}h^{-1}$g DCW^{-1})
[b] Specific CO_2 evolution rate (mmole.$L^{-1}h^{-1}$g DCW^{-1})
[c] Specific glucose consumption rate (g.g $DCW^{-1}h^{-1}$)
[d] Biomass production rate (g.$L^{-1}h^{-1}$)
[e] Specific erythromycin production rate (mg.L^{-1}g $DCW^{-1}h^{-1}$)
[f] Specific α-ketoglutarate production rate (g.L^{-1}g $DCW^{-1}h^{-1}$)
[g] Specific pyruvate production rate (g.L^{-1}g $DCW^{-1}h^{-1}$)
[h] Specific succinate production rate (g.L^{-1}g $DCW^{-1}h^{-1}$)
[i] Specific red pigment production rate (g.L^{-1}g $DCW^{-1}h^{-1}$)

7.1.4 Effect of oxaloacetate supplementation on pyridine cofactors and the adenylate nucleotides

After feed addition at 45 hours, NADPH levels increased for 3 hours then gradually decreased up to 71 hours (Fig.43). This trend was in line with increased PPP activity as indicated by the increase in the activity of G6PDH (Fig. 41). The rate of NADH production also increased for the period between 45 and 71 hours (Table 19, Fig. 43) reflecting enhanced glycolytic activity. However, both cofactors remained constant for 24 hours after a further addition of oxaloacetate at 71 hours. After feeding at 45 hours, the levels of erythromycin decreased by 45% (Table 20). However, the rate of erythromycin production increased by 50% from 71h to 96h (Fig. 39). There was a corresponding increase in the anaplerotic pathway activity (Fig. 41). The levels of all three adenylate nucleotides appeared to have been supressed by the addition of

oxaloacetate at 45 hours (Fig. 44, Table 19). For ATP and AMP, the depression lasted 3 hours and followed by an incease to reach a maximum at 71 hours. Oxaloacetate suppressed ATP levels which dropped sharply by a factor of 2.5 from 71 to 96 hours (Fig. 44). A similar repressive effect was observed for AMP after oxaloacetate addition at 71 hours. Lower NADPH production rates were observed for the fed batch compared to the batch fermentation (Fig. 20, Fig. 43). Both the energy charge and ATP level showed a negative correlation with the production of erythromycin. Though the energy charge and ATP exhibited a similar pattern, changes in the former were less pronounced. A notable observation is that the NADH concentration remained unchanged each time the levels of erythromycin increased.

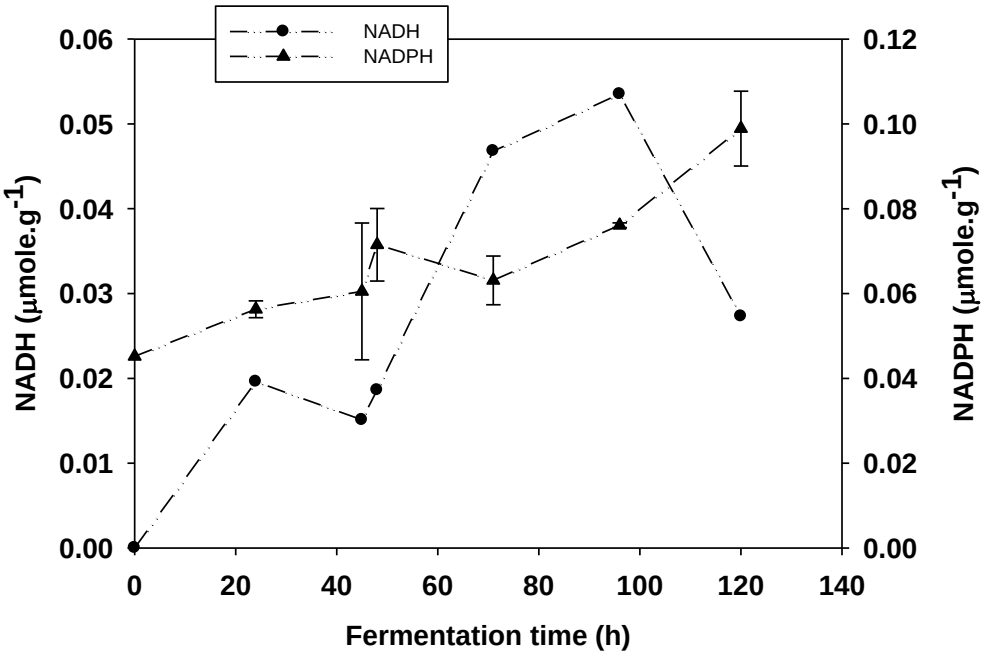

Fig. 43 Time courses of NADH (●) and NADPH (▲) during bolus feed additions *S. erythraea* fermentation cultured on glucose with oxaloacetate supplementation. Data represent means of triplicate fermentations. Arrows indicate time of supplementation with 3mM oxaloacetate.

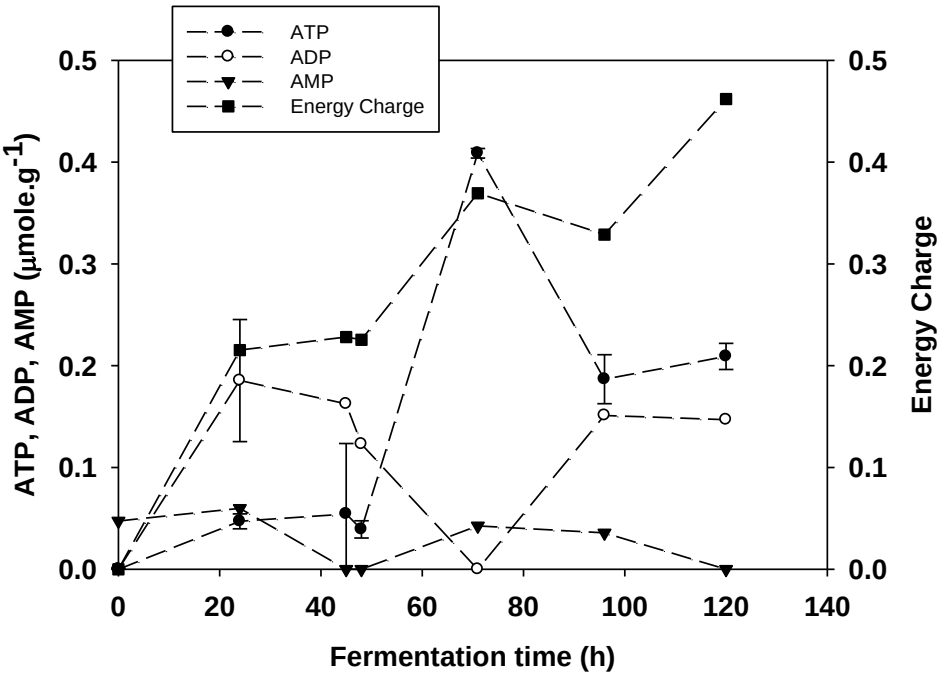

Fig. 44 Profiles of energy charge (■), ATP (●), ADP (○) and AMP (▼) during bolus feed additions *S. erythraea* fermentation cultured on glucose and fed oxaloacetate. Arrows indicate time of supplementation with 3mM oxaloacetate. All data has been normalised to biomass.

Table 21. Specific rate of adenylate and pyridine cofactor production during fed bolus-feed additions culture of *S. erythraea*. The data was normalised to the highest biomass and rates calculated as mean phase values per duration of phase.

Parameter	Phase I (0-24h)	Phase II (24-48h)	Phase III (48-96h)
qATP [a]	1.9×10^{-3}	1.9×10^{-3}	4.4×10^{-3}
qADP [b]	7.7×10^{-3}	6.5×10^{-3}	1.9×10^{-3}
qAMP [c]	2.2×10^{-3}	8.3×10^{-4}	5.4×10^{-4}
qNADH [d]	1.9×10^{-4}	7.4×10^{-4}	8.3×10^{-4}
qNADPH [e]	2.1×10^{-3}	2.6×10^{-3}	1.5×10^{-3}

[a]Specific ATP production rate (µM.g $DCW^{-1}h^{-1}$)
[b]Specific ADP production rate (µM.g $DCW^{-1}h^{-1}$)
[c]Specific AMP production rate (µM.g $DCW^{-1}h^{-1}$)
[d]Specific NADH production rate (µM.g $DCW^{-1}h^{-1}$)
[e]Specific NADPH production rate (µM.g $DCW^{-1}h^{-1}$)

7.1.5 Effect of oxaloacetate feeding on respiratory energy production

As oxidative phosphorylation is the main generator of energy for aerobic growth, its potential effect on product formation was worth investigating. Growth rate and the rate of ATP synthesis are linked to the respiration rate (Andersen & von Meyenburg, 1980). The rate of respiration and ATP synthesis through oxidative phosphorylation can limit aerobic growth (Andersen & von Meyenburg, 1980). In general, erythromycin production was enhanced by decreased respiration rate. Small changes in the rate of respiration appeared to affect the production of the antibiotic. Throughout the fermentation, NADH was observed to correlate negatively with respiration (Fig. 39, Fig. 43). Thus, while the production of the antibiotic was enhanced by increases in NADH levels, it correlated negatively with respiration and ATP concentration (Fig. 39, Fig. 43, Fig. 44). Both OUR and CER increased up to 60 h and then dropped until 71 h (Fig. 40). The respiratory quotient dropped until 71 h. At the same time, the levels of both the ATP and NADH were increased significantly (Fig. 43, Fig. 44).

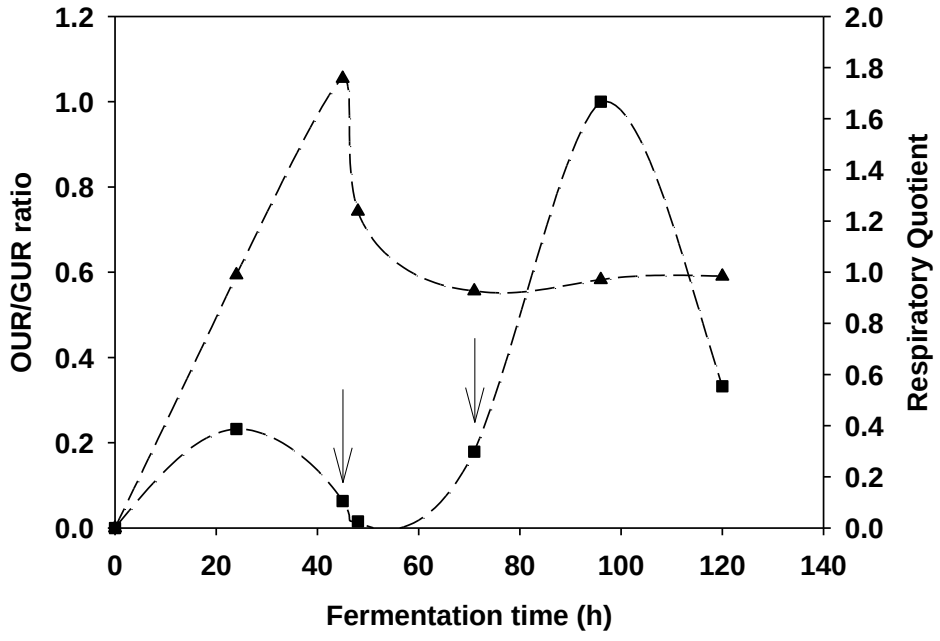

Fig. 45 Relationship between OUR/GUR (■) ratio and the Respiratory quotient (▲). Arrows indicate time point of methyl oleate feeding.

The respiratory quotient was depressed when oxaloacetate was added to the culture. In essence, this means that respiration was decreased (Fig. 45). However, the ratio of respiration to the consumption of glucose increased. It suggests that the respiration rate was increased in comparison to the rate of consumption. We have seen in Chapter 4 that this phenomenon is associated with increase in the production of erythromycin. This indeed what was observed for the supplemented culture. ATP levels decreased and erythromycin production increased from 72 to 86 hours.

7.2 Discussion

7.2.1 Growth characteristics

For growth on glucose as a sole carbon and energy source, glycolysis was the main route of catabolism at high growth rate in *S. erythraea*. Glycolysis generates energy needed for cell activities together with NADH and supplies carbons for biomass synthesis and precursor metabolites. The high growth rate accounts for the low energy charge and NADH levels observed. The corresponding elevated AMP levels are evidence of the high energy or ATP demand during the fast growth phase. When biomass synthesis decreased at 24 hours, both energy charge and ATP levels decreased. Biomass formation is energy intensive as protein synthesis has been reported to account for most of the energy demands and NADPH requirements in microorganisms (Henriksen *et al*, 1995; Jonsbu *et al*., 2001). It is probable that $NADP^+$- dependent ICD supplied most of the NADPH for growth because of its high activities during the growth phase. The high activities of ICD observed confirm the findings of Roszkowski *et al* (1971) that the TCA cycle provides NADPH through ICD in *S. erythraea*. However, growth demands for NADPH may not be high for *S. erythraea* under these conditions. The activities of $NADP^+$-dependent ICD remained unchanged during the production phase from 24 to 48 hours. The fact that both ICD and glucose-6-phosphate which produce NADPH had high activities during this phase suggests that NADPH was not limiting. Equally, the increase in NADPH levels during the fast growth phase suggests that there was excess supply. It may not be unusual for *S. erythraea* to have excess supply of NADPH as a similar observation was made by Butler *et al* (2002). They halved the activity of glucose-6-phosphate and its isoenzyme resulting in significant

improvement in yields for actinorhodin and undecylprodigiosin. Surprisingly, the concentrations of NADPH were not decreased significantly despite the fact that this nucleotide is involved in reductive biosynthesis of antibiotics. The reduction in NADPH from 24 to 48 hours was most likely due to biosynthetic demands of erythromycin as polyketide synthesis is known to have high NADPH requirements (Rowe *et al*, 1998; Jaques, 2004). $NADP^+$- dependent ICD produces only 2 NADPH molecules per glucose molecule oxidised to CO_2 compared to 6 produced by the pentose phosphate pathway (Bruheim *et al*., 2002). The high ICD activities during the fast growth phase were probably to meet the high NADPH demands. It suggests that the TCA cycle was the main supplier of NADPH. ICD possibly produced sufficient NADPH to meet growth demands.

The decrease in growth rate coincided with a reduction in nitrate. Though nitrate was not depleted, growth rate slowed down because *S. erythraea* has low affinity for nitrate in nitrogen-limited media (Bushell *et al*, 1997). This suggests that at low nitrogen levels, growth rate would slow down as protein synthesis decreases. At this point, glucose-6-phosphate activity increases possibly indicating diversion of catabolism to the pentose-phosphate pathway. Because of the high NADPH production rate of the pentose phosphate pathway, we can expect small changes in the pathway flux to have a significant effect on cofactor production. This diversion coincided with the onset of erythromycin production. The trigger for the onset of erythromycin production is probably the decreased growth rate as a result of down-regulation of protein synthesis. In work by Bushell *et al* (1997), erythromycin synthesis was found to coincide with a decrease in the rate of protein synthesis. Clark *et al* (1995) and Lynch and Bushell (1995) and Wilson and Bushell (1995) reported similar findings with *S. erythraea* and *S. hygroscopicus*. Notably, both energy charge and the rate of ATP production increased possibly in response to the down-regulation in protein synthesis. However, the demand for ATP was probably still high due to erythromycin synthesis. Though this appears like a contradiction, protein and erythromycin synthesis may not have equal ATP requirements. As stated in Chapter 1, protein synthesis has very high energy requirements, which may be higher than those of erythromycin production. If this is the case, then a decrease in protein synthesis is likely to ease the burden on ATP pools.

7.2.2 Effect of oxaloacetate supplementation on pathway activity at the Anaplerotic pathway/TCA cycle branch point

It appears that increased energy levels combined with the elevated activity of the PPP enhanced the rate of antibiotic production. The anaplerotic pathway (PEPC) also correlated with an increased rate of erythromycin production. It was observed that at slow growth rate, ATP production rate increased and the activities of glucose-6-phosphate dehydrogenase were higher than those of phosphoglucose isomerase. The activities of phosphoenolpyruvate carboxylase increased while those of $NADP^+$-dependent ICD decreased. When these conditions coincided, the rate of erythromycin production was enhanced. At cofactor level, NADPH correlated negatively with the production of the antibiotic. This was observed throughout the fermentation and was probably due to the high demands for the polyketide synthesis. From 48 to 72 hours erythromycin reached maximum production rate when ATP levels decreased and the TCA cycle activity was reduced by 44%. A 12% increase was observed in the anaplerotic activity. These trends were also observed between 71 and 96 hours. The excretion of α-ketoglutarate correlated positively with ICD activities and is evidence of the TCA cycle activity. However, the production of erythromycin continued while the TCA cycle was active from 48 to 71 hours. During this time, α-ketoglutaric acid was excreted suggesting active flux through this pathway. There appears to be a contradiction here. If elevated ATP levels inhibit PFK, how is this consistent with increased TCA cycle flux? The inhibitory effect of high ATP concentrations on G6PDH can be seen in the reduced PPP flux during this time. However, in the presence of AMP, the inhibition of PFK by ATP is reversed thus allowing flux through glycolysis (Price & Stevens, 2006; Dawes, 1986). High AMP levels stimulate glycolysis at this point by overcoming the inhibitory effects of ATP on PFK (Dawes, 1986). It is proposed here that the presence of AMP explains the glycolytic and TCA fluxes when ATP levels were high between 24h and 48 hours and between 48 and 71 hours.

In Chapter 4, a correlation was observed between increases in erythromycin production and reduced rate of glucose uptake. Both accumulation phases observed correlated with increases in the consumption of the carbon source and corresponding decreases in the

level of erythromycin. However, if catabolism proceeds through the TCA cycle and not through the anaplerotic pathway, lower levels of the antibiotic will be produced. There are several reasons for this. Routing catabolism through the TCA cycle wastes carbon skeletons through the excretion of α-ketoglutarate which could have been used for erythromycin production. Proceeding through this pathway also loses carbons as CO_2 through the actions of pyruvate dehydrogenase, isocitrate dehydrogenase and α-ketogluatarate dehydrogenase. Because *S. erythraea* continues to consume glucose in the absence of growth, excess ATP is produced. Since microbial systems are optimised for growth, catabolism will be diverted to non-ATP producing or ATP consuming pathways. Diverting metabolism to the anaplerotic pathway conserves carbon skeletons and produces no excess ATP. In addition, extra carbon is added through carboxylation of PEP while ATP is consumed in the conversion of aspartate to asparagine. It was observed that ATP levels decreased when catabolism switched to the anaplerotic pathway in both the batch and fed-batch fermentations. It appears that the routing of catabolism through PEPC enhances succinate pools which subsequently replenish succinyl-coenzyme A. Succinyl-coenzyme A is the metabolite at the entry point of the erythromycin biosynthetic pathway (Fig. 12). Succinate levels dropped between 72 and 96 hours when erythromycin reached maximum production. The yield coefficient ($Y_{p/x}$) for the fed-batch culture was higher than that for the batch fermentation by a factor of 2.9 (Table. 19) which suggests that probably most of the oxaloacetate was diverted to the production of the antibiotic. Replenishing the oxaloacetate metabolite pool possibly promoted flux to succinyl-coenzyme A and ultimately to erythromycin production. The correlation between decreased TCA activity and increased erythromycin production also supports this conclusion. A slow TCA cycle would allow for accumulation of oxaloacetate which could be diverted towards erythromycin production via succinyl-coenzyme A.

After supplementation, fluxes were diverted away from the AP to the TCA, evidence of which is provided by the activities of PEPC and ICD. The result was increased excretion of α-ketoglutarate. However, the activity of ICD dropped between 45h and 71 hours, suggesting oxaloacetate was not routed through the TCA cycle. During this time,

[NADH/NAD^+] ratio must have been high thereby inhibiting citrate synthase, an enzyme which controls the TCA cycle.

Flux through AP remained unchanged. Either flux was routed through an NADH generating pathway or perhaps NADPH was converted to NADH through transhydrogenase reactions. However, Roszowski *et al* (1971) ruled out the existence of transhydrogenases in *S. erythraea*. The reason for this increase in NADH levels remains unclear. One potential pathway is the carboxylation of pyruvate by malic enzyme to form malate which generates NADPH. Malate is subsequently converted to oxalaoacetate by the action of malate dehydrogenase. Malate dehydrogenase is NAD^+-dependent and therefore generates NADH. The NADPH generated in the carboxylation step is consistent with the observed increase in NADPH over the same period. The observed shift in the erythromycin production phase in the fed batch compared to the control was, therefore, due to routing of oxaloacetate to the TCA cycle through citrate synthase. Typically such flux would initially have gone from oxaloacetate through PEPC to PEP and then via pyruvate kinase to pyruvate. The observed activity was in the opposite direction as both PEPC and PEPCK (EC:4.1.1.32) use the same coupling enzyme and substrate. Jaques (2004) suggested that part of the flux could proceed from pyruvate to oxaloacetate. However, microorganisms have either PEPC or pyruvate carboxylase (White, 2007). The gene that encodes PEPCK is present in *S. erythraea* as SACE_7274, though it is not known if this enzyme is active. Nevertheless, Jaques (2004) suggested that this enzyme may be active in futile cycles in *S. erythraea*.

7.2.3 Flux dynamics around the pyruvate node

The bolus-feed addition fermentations confirmed the findings of the batch fermentations regarding flux distributions. While erythromycin was produced from 48 to 72 hours in the batch fermentation, this shifted to 72 to 96 hours in the bolus feed additions fermentation. Feeding oxaloacetate increased the rate of respiration resulting in increased ATP concentrations. Feeding oxaloacetate after 45 hours decreased the activities of PEPC only by 5%. However, though the rate of respiration increased considerably, TCA cycle activity decreased by 21%. This means that glucose

degradation proceeded via pathways other than mainly through the TCA cycle. Whatever the route of glucose degradation, increases in the rate of respiration resulted in an 89% increase in ATP levels. The supposed PEPC activity may actually have been PEPCK activity since high oxaloacetate levels are unlikely to activate PEPC. Both PEPC and PEPCK have common substrates and coupling enzyme. There was flux through the TCA cycle which gradually decreased as ATP levels increased to inhibit pyruvate dehydrogenase and isocitrate dehydrogenase. Evidence in support of this conclusion is provided by the decrease in the rate of pyruvate excretion and ICD activity between 45 and 71 hours.

Some of the oxaloacetate appears to have been routed through citrate synthase to replenish the TCA cycle as indicated by increases in isocitrate dehydrogenase activity. However, due to decreased growth demands, ATP levels increased causing a decrease in TCA cycle flux. Much of the flux was routed through PEPCK to PEP, eventually enhancing the pyruvate pool through pyruvate kinase activity. The inhibition of pyruvate dehydrogenase is indicated by the elevated pyruvate levels. Flux did not go through to succinyl- Coenzyme A, hence the drop in the rate of erythromycin production. Following additional feeding at 71 hours, the activities of PEPC were increased by 68% and the TCA cycle activity declined by 52%. This indicated a switch of flux from the TCA cycle to the anaplerotic pathway. The diversion of catabolism resulted in the reduction in ATP production and enhanced the rate of erythromycin production by 48%. It can also be argued that the reduction in TCA cycle activity was caused by reduced flux through citrate synthase and possibly aconitase both of which are inhibited by increased [NADH/NAD^+] ratio. NADH concentration remained high during this time. For the batch fermentation, high catabolic activity through the TCA cycle compared to the anaplerotic pathway resulted in increased ATP concentration and depressed antibiotic levels between 72 and 96 hours. It is also interesting to note that the switch in flux from the anaplerotic pathway to the TCA cycle coincided with increasing NADH levels and vice versa. Increased TCA cycle activity would increase the concentration of NADH which is what was observed. This appears to be dependent on the phase since during the stationary phase increases in the TCA cycle activity correlated with increases in NADH production. The opposite was true for the growth

phase. Nevertheless, this appears to confirm the findings of Medema *et al* (2011) that the down-regulation of citrate synthase and aconitase activity can improve antibiotic production.

While the actual control point at which the switch in fluxes is exerted is not known, the findings indicate a negative correlation between pyruvate levels and the maximum erythromycin production rates. In the batch fermentation, pyruvate levels dropped to zero between 48 and 72 hours. A similar drop was observed between 72 and 96 hours for the fed batch fermentation. In both cases, the drop in pyruvate levels coincided with increases in erythromycin production. After supplementation, the concentrations of both ATP and NADH increased significantly. Both ATP and NADH inhibit pyruvate dehydrogenase and cause pyruvate to accumulate. Increased levels of pyruvate during this time period appear to confirm this conclusion. Elevated levels of adenylate charge or ATP as well as the NADH have been reported to have the most profound effect on pyruvate dehydrogenase (Shen *et al*., 1970). Increase in pyruvate excretion after feeding at 45 hours confirms that pyruvate dehydrogenase was inhibited and not pyruvate kinase.

A correlation between increased ADP concentration and a decrease in pyruvate levels was observed for the batch and fed-batch fermentation at 72 and 96 hour respectively. One explanation for this drop in pyruvate levels is the activity of pyruvate carboxylase which produces oxaloacetate from pyruvate. However, this enzyme is not thought to be present in *S. erythraea* since microorganisms have either PEP carboxylase or pyruvate carboxylase (Roszkowski *et al*, 1971; White, 2007; Hodgson, 2000). Various fluxes proceed from oxaloacetate. The anaplerotic flux to aspartate drains the oxalaoacetate pool. However, this flux can be neglected since supplementation was done towards the end of the growth phase and no growth was observed afterwards. Increased oxaloacetate level would activate phosphoenolpyruvate carboxykinase (PEPCK) which converts oxaloacetate to PEP. It can be concluded that the observed increase in flux was actually the reverse flux to PEP catalysed by PEPCK. The assay for the two enzyme reactions uses the same coupling enzyme, malate dehydrogenase. It is unlikely that increasing the concentration of oxaloacetate would activate PEPC (phosphoenolpyruvate carboxylase).

Citrate synthase is activated by increased oxaloacetate concentration and generates isocitrate from oxaloacetate and acetyl-coenzyme A. This is the likely route through which the flux proceeded from oxaloacetate to replenish the TCA cycle. This conclusion is confirmed by the low NADH concentrations observed between 45 and 71 hour. Citrate synthase is inhibited by a high level of [$NADH/NAD^+$] ratio. NADH probably gradually increased over the 26 hour period until it reached inhibitory levels at 71 hour. The observed increase in the excretion of α-ketoglutarate appears to be in response to increased flux through citrate synthase. Elevated ATP concentration during this period meant that pyruvate dehydrogenase was inactivated making this route unlikely to have replenished the TCA cycle. The observed increase in pyruvate concentration confirms this inactivation.

But why would NADH levels decrease when the ATP increased during the same period? For NADH to decrease, flux must flow through a NADH consuming reaction. One such a reaction would be the flux from oxaloacetate through malate dehydrogenase to malate, which consumes NADH. Malate is then converted to pyruvate by malic enzyme, a reaction which produces NADPH. The results suggest that this was the likely route of flux after supplementation since NADH decreased and the levels of NADPH increased. The increase in NADPH and decrease in NADH levels are consistent with flux through these pathways. However, since ATP synthesis by oxidative phosphorylation consumes NADH, the terminal cytochrome system could be responsible for this observation. The possible role of the electron transport system in the turnover of NADH and ATP is discussed in the section under the regulation of oxidative phosphorylation.

Pyruvate concentration increased until after supplementation at 71 hours after which it started to decrease. Though pyruvate levels decreased, pyruvate dehydrogenase remained inhibited and hence no flux proceeded through this enzyme into the TCA cycle. In fact, the TCA cycle activity dropped significantly while the anaplerotic pathway exhibited a high increase. ADP increased from 71 to 96 hours, while NADH levels remained almost unchanged. In this case, flux from oxaloacetate to the TCA cycle was blocked through the inhibition of citrate synthase by increased [$NADH/NAD^+$] ratio. It is suggested that increasing concentrations of NADH and ADP

inhibited pyruvate dehydrogenase and diverted flux to the anaplerotic pathway when the demand for ATP decreased, resulting in the improvement of erythromycin production (Voet & Voet, 2004). Such a mechanism could explain the reduction in TCA cycle activity and the observed reduction in the excretion of α-ketoglutarate. Diversion of flux away from the TCA cycle is consistent with a reduction in the excretion of α-ketoglutarate.

7.2.4 The role of gluconeogenesis

Phosphoenolpyruvate carboxykinase (PEPCK) is a gluconeogenic enzyme involved in replenishing PEP pools. PEP is formed through gluconeogenesis by the actions of PEPCK from the TCA cycle. The pools of both OAA and PEP are subject to the actions of this enzyme. Thus feeding OAA can increase the activities of the TCA cycle.

However, the anaplerotic flux represents the reverse flux from oxaloacetate to PEP catalysed by PEPCK. Such fluxes would replenish the pyruvate pool. Therefore following oxaloacetate supplementation, pyruvate increased significantly. This is likely to have been the result of the activity of the anaplerotic reaction from OAA to PEP catalysed by PEPCK. This enzyme maintains a balance between PEP and OAA by draining the TCA cycle of excess carbons. However, pyruvate decreased between 71h and 96h and both citrate synthase and pyruvate dehydrogenase were probably inhibited at these NADH levels. Both pyruvate dehydrogenase and citrate synthase are inhibited at elevated NADH concentrations. In addition, as pointed out earlier, pyruvate carboxylase is not present in *S. erythraea.* This leaves $NADP^+$-dependent malic enzyme as the only reaction responsible for decreasing pyruvate by conversing it to malate. An increase in the concentration of NADPH was observed. The carboxylation of pyruvate by malic enzyme to form malate generates NADPH. It is possible that this combined with NADPH produced in the TCA cycle and the PPP is responsible for the increase in the levels of this pyridine cofactor. Some flux could also have gone from oxaloacetate through the reversible malate dehydrogenase to malate. Based on this, it can be speculated that flux to the production of erythromycin proceeded through malic enzyme and malate dehydrogenase to malate. Increase in pyruvate pool resulted in significant increase in the anaplerotic activity and erythromycin production. This suggests that the

pyruvate node is flexible and amenable to manipulation to improve the biosynthesis of the antibiotic. It could be concluded that supplementation at 45 hours enhanced the pools of precursor metabolites. The added oxaloacetate was degraded via PEPCK, pyruvate kinase and pyruvate dehydrogenase and entered the TCA cycle through acetyl-coenzyme A. The second route to precursor accumulation was through citrate synthase. After additional feeding at 71 hours, much of the oxaloacetate was channelled to the biosynthesis of erythromycin. Additional oxaloacetate fed at 71 hours significantly enhanced the PEPC and the anaplerotic flux resulting in significant increase in the production of erythromycin. Overall, supplementation lowered the activities of the key branch point enzymes perhaps decreasing fluxes. Lower NADH and NADPH concentrations were observed for the fed batch cultures compared to the control.

As to why supplementing the culture with oxaloacetate reduced energy or ATP demand, the answer is speculative. However, it probably has to do with the effect of feeding oxaloacetate on the growth rate. Biomass synthesis decreased after supplementation probably through lysis. A comparison between the batch and the fed batch fermentations reveals a marked difference in the yields. The supplemented culture diverted more carbons to the biosynthesis of erythromycin. The $Y_{p/x}$ was consequently 75% higher than for the batch culture (Table 19). Perhaps much of the added oxaloacetate went towards the antibiotic production pathway. This could mean that much of the oxaloacetate was diverted to replenishing the precursor metabolite pools. On the other hand, the bolus feed additions culture consumed only 35% more glucose for every milligram of erythromycin produced. It appears then that *S. erythraea* does not channel much of the carbon source towards the biosynthesis of erythromycin. This is consistent with the precursor metabolites limiting the production of the antibiotic. It is also consistent with the fact that biomass formation takes preference in the partitioning of precursors between growth and secondary metabolite production.

Comparison of flux distribution between the batch and bolus feed additions fermentation reveals that the availability of precursor metabolites has a central role to play in the control of erythromycin production. Secondary metabolism drains precursor metabolites gradually and eventually these metabolites reach a level that constrains the

biosynthesis of erythromycin. This can be observed in the control (batch) fermentation between 48 and 96 hours. Erythromycin biosynthesis subsequently decreased due to limitations in the precursor supply. Whereas fluxes through the anaplerotic pathway were high during the production phase, these were switched to the TCA cycle and correlated with increased glycolytic flux during the precursor accumulation phase. Precursor metabolite pools were enhanced and the biosynthesis of erythromycin commenced again between 96 and 120 hours. As expected, flux through the anaplerotic pathway was significantly increased. Since supplementation with oxaloacetate feeds directly into precursors such as pyruvate, malate and isocitrate, a shorter accumulation time is reasonable. Oxaloacetate was not converted into the required precursors immediately since erythromycin production increased only 24 hours after feeding. It is not clear if the increase in the production of the antibiotic between 71 and 96 hours was due to supplementation at 45h or 71h or perhaps both. The conclusion here is that changes in flux distribution are most likely controlled by ATP and the [NADH/NAD^+] ratio or NADH alone. Supplementation increased the production of the antibiotic probably by enhancing the precursor metabolite pools. These conclusions are consistent with those of Li *et al* (2007).

7.2.5 Regulation of oxidative phosphorylation

Erythromycin production was enhanced by decreased respiration and NADH levels. With the rate of respiration increased, more ATP is produced. NADH concentrations decrease as this cofactor is consumed during the production of energy through oxidative phosphorylation. The link between respiration and NADH points to the possible involvement of the cytochrome system of the electron transport system. The cytochrome system consists of complexes I, III and IV which represent NADH ubiquinone oxidoreductase (EC 1.6.5.3), ubiquinol cytochrome c oxidoreductase or cytochrome bc_1 complex (EC1.10.2.2.) and cytochrome aa_3 oxidase (EC1.9.3.1). Complex I is an NADH dehydrogenase and pass electrons on to coenzyme Q oxidoreductase (Co Q). The reduced Co Q is oxidised by ferricytochrome c to ferrocytochrome c (Equation 1). Cytochrome bc_1 oxidase passes the electrons generated from the oxidation of ferrocytochrome c to ferricytochrome c (Equation 2) to

cytochrome c oxidase. The electrons from ferrocytochrome are transferred by the enzyme to molecular oxygen in a reaction that translocates H^+ across the membrane creating a proton gradient that is used to drive ATP synthesis. This system is known to operate in Actinomycetes (Niederpruem & Hackett, 1960). Often microorganisms have several of these oxidases which are expressed in varying capacities to enhance oxygen uptake during oxygen limitations. These oxidases may have different affinities for oxygen. The aerobic respiratory chain of *E. coli* has two different terminal oxidases, cytochrome *d* and cytochrome *o* that are both dependent on ubiquonol-8 to reduce oxygen (Brekasis & Paget, 2003). Though both of these oxidases perform the same function of reducing oxygen, they have different affinities (Km and Vmax) for oxygen. Cytochrome *d* has a higher Km and Vmax compared to cytochrome *o*. As can be expected, cytochrome *o* functions under oxygen limitations while cytochrome d is associated with oxygen-rich conditions (Rice and Hempfling, 1978). It can be expected that both enzymes will accumulate under their respective operating conditions. The enzymes are regulated at expression level based on demand created by prevailing conditions (Cotter *et al*, 1997).

Equation 1: QH_2 + 2 ferricytochrome c ⟶ Q + 2 ferrocytochrome c + 2 H

Equation 2: 4 ferrocytochrome c + O_2 + 4 H^+ ⟶ 4 ferricytochrome c + H_2O

S. erythraea may have terminal oxidases with different kinetic parameters (Km and Vmax) since it is a soil organisms where microaerobic environments can exist. The organism needs to respond to these varying degrees of oxygen availability. Oxygen limitations can occur in these microhabitats due to waterlogging or compaction (Clark *et al*., 1995). Clark *et al* (1995) investigated the effect of oxygen limitations on the production of erythromycin and vancomycin in *S. erythraea* and *Amycolatopsis* ATCC respectively. A comparison of the findings between baffled and unbaffled shake flasks indicated that erythromycin production was improved under oxygen limitations. For an organism to grow well under oxygen-poor conditions suggests the existence of oxidases with high affinity for oxygen. In the case of *A. orientalis*, no vancomycin was produced under oxygen limitation. However, an additional secondary metabolite was only produced under oxygen limitation in *S. erythraea* (Clark *et al*., 1995) It is worth noting

that vancomycin is a glycopeptide antibiotic. Oxygen limitations are likely to cause downregulation in protein synthesis and therefore reduce biomass formation. In a study

by McIntyre *et al* (1999), vancomycin production was significantly increased when DOT was controlled between 20 and 30%. Here too, a red metabolite was only produced under oxygen limitations, which corroborates the findings of Clark *et al* (1995). It appears low oxygen tension acts as a stress factor which triggers the production of the red metabolite. Working at both pilot and industrial scales, Jung *et al* (2007) reported similar correlation between oxygen and vancomycin production. However, when DOT was increased to 40%, the level of vancomycin decreased, though biomass did increase.

We can assume that the oxidative phosphorylation generated high levels of ATP during the accelerated growth phase. This assumption is based on the high respiration rate during the first 24 hours of growth. However, much of this ATP was utilised in meeting growth requirements and its levels were subsequently low. Throughout the fermentation cultivation, the levels of ATP increased with increased respiration rates suggesting that oxidative phosphorylation was a major contributor to the overall cytosolic ATP pool. During the growth period, the growth rate had the most profound effect on ATP levels. ATP levels increased significantly when the growth rate decreased between 24 and 48 hours. Increases in ATP levels coincided with increased flux through the anaplerotic pathway while fluxes through the TCA cycle remained unaltered. This appeared to have triggered the production of erythromycin. We propose that substrate-level phosphorylation played a large role in supplying ATP during the growth phase. The basis for this assertion is the fact that both ATP and NADH levels increased during the growth phase during which time the glucose uptake rate was highest. The rate of phosphorylation would probably have been high given the high turnover rate of carbon intermediates. The electron transport chain consumes NADH in the process of synthesising ATP. It is, therefore, unlikely that ATP levels would have increased simultaneously with increases in NADH levels if much of the energy was supplied by the cytochrome system. Additional support for this conclusion comes from the fact that ATP at elevated levels has been reported to inhibit terminal cytochrome oxidases whose

function is ATP synthesis (Tanman *et al*. 1994). ATP levels remained low (between 0 and 0.05µM.g Biomass^{-1}) during the growth phase, perhaps indicating significant contribution by the respiratory chain. ATP levels increased to 0.41µM.g Biomass^{-}1 after the growth phase. The inhibitory effect of ATP on dehydrogenases has been discussed earlier. NADH dehydrogenase is the first enzyme of the cytochrome system and is itself susceptible to inhibition by ATP at elevated levels. Perhaps the increase in the NADH levels was precisely because of the reduction in the rate of respiration.

After the growth phase, the respiratory chain appeared to have continued as the major supplier of energy. Thus when respiration dropped by 3% between 72 and 96 hours, ATP levels dropped and NADH levels increased for the batch fermentation. Flux subsequently switched from the anaplerotic pathway to the TCA cycle. From previous discussion, increased flux through the TCA cycle combined with reduced respiration was associated with precursor metabolite accumulation. Throughout the stationary phase, ATP concentrations varied positively with changes in the respiration rate for both the batch and the supplemented fermentations. Owing to the inhibitory effect of ATP on pyruvate dehydrogenase, isocitrate dehydrogenase and citrate synthase, flux distribution between pathways is dependent on the concentrations of ATP. Reduced ATP concentrations that coincide with increased NADH levels confirm that the role of the cytochrome system of the electron transport system in the supply of energy. This was observed between 96 and 120 hours and correlated with balanced flux split between the anaplerotic pathway and the TCA cycle. The decrease in ATP levels coincided with improved flux through the anaplerotic pathway relative to the previous phase. A similar situation was observed between 71 and 96 hours for the fed batch fermentation. With decreased ATP levels, flux through the anaplerotic pathway was increased enhancing erythromycin production. Growth rate had a significant effect on the respiration rate and the biosynthesis of erythromycin. At high growth rate, the rate of respiration was elevated to meet the respiratory demands of growth. With high growth demands, carbon precursors were preferentially diverted to biomass synthesis. It could be argued that slowing down the respiration rate will slow down growth and improve the diversion of flux to secondary metabolism. At low respiration rate, NADH levels increased and were associated with improved flux through the anaplerotic pathway and enhanced

production of the antibiotic. The simultaneous drop in ATP was a result of both depressed oxidative phosphorylation and the energy demands of the polyketide biosynthesis.

Respiration has a significant effect on flux partitioning and the production of erythromycin. Control of flux is exerted through both ATP and NADH which are, themselves, subject to changes in the rate of respiration. By genetically manipulating terminal cytochrome oxidases, the respiration rate can be altered to create suboptimal flux distribution and improve the biosynthesis of erythromycin. Another approach would be to manipulate the supply of oxygen to enable expression of terminal oxidases. If oxygen limitation improved the production of the antibiotic, then the reduction of high affinity oxidases could create limiting conditions and potentially lead to incomplete oxidation of metabolites. Reduced respiration could compromise growth, but improve the production of the antibiotic as the findings of Clark *et al* (1995) indicate. Often reduced growth rate enhances the biosynthesis of antibiotics as discussed in section 3.4.2.

7.2.6 Conclusions

Feeding oxaloacetate enhanced the production of erythromycin by diverting carbon fluxes away from biomass synthesis. This is important since in the competition for precursors, growth demands takes preference as survival adaptation. Both primary and secondary metabolism drains precursor metabolites produced by central metabolism. Oxaloacetate was fed towards the end of the growth phase when growth demands for precursors was lower. Perhaps this is why more precursors were channelled towards the production of the antibiotic. The supply of precursors to the product pathway could, therefore, constrain the biosynthesis of erythromycin. The other constraint is the supply of NADPH which is crucial for reductive biosynthesis. The glucose-6-phosphate and pyruvate metabolite nodes are important in the production of erythromycin. Depleted G6P pool constrains flux through the PPP and subsequently the supply of NADPH needed for reductive biosynthesis. The concentration of G6P is regulated by the growth rate through the action of ATP on glucose-6-phosphate dehydrogenase. TCA cycle fluxes are necessary for carbon precursor storage and energy generation and the

production of NADH which functions in flux regulation. Pyruvate dehydrogenase is a crucial enzyme in regulating flux partitioning between the TCA cycle and the anaplerotic pathway. Routing flux through the TCA cycle wastes carbons through excretion as α-ketoglutarate and evolution as CO_2. Growth demands results in very few of the precursors trickling down for conversion into oxaloacetate and other TCA cycle compounds. Limitations in these affect the rate of respiration and subsequent generation of NADH. Flux through the TCA cycle accumulates precursor and correlates with decreased levels of NADH and ATP. Elevated levels of ATP and NADH or [NADH/NAD^+] ratio diverts flux from the TCA cycle to the anaplerotic pathway. Flux through the PPP and the AP enhances the production of erythromycin. We propose that erythromycin production could be regulated by the effect of elevated ATP levels on PFK and G6PDH. Respiration rate was observed to affect flux partitioning through its effect on ATP and possibly NADH.

Comparison with the batch fermentation reveals that adding oxaloacetate to the culture resulted in a switch in flux from the TCA cycle to the anaplerotic pathway which was possibly caused by elevated NADH levels. Whereas respiration increased during the precursor accumulation phase in the batch fermentation, it was significantly decreased after feeding oxaloacetate resulting in enhanced antibiotic production. Therefore, it is posited that limitations in the supply of precursors constrain the production of erythromycin. For the batch culture these limitations were redressed by enhancing the rate of respiration and increasing the activity of the TCA cycle. However, when oxaloacetate was externally added, the rate of respiration dropped since there was no need to accumulate precursor metabolites. Flux switched from the TCA cycle to the anaplerotic pathway resulting in enhanced production of the antibiotic. Thus, the rate of respiration is partly regulated based on the demand for precursor metabolites and the resulting increase in NADH concentrations effects the switch in flux between the TCA cycle and the anaplerotic pathway.

The pyruvate metabolite node appears to be flexible as replenishing its pools resulted in improved precursor supply to the product pathway. The conclusion is that the TCA cycle drains the pyruvate pool and thereby deprives the product biosynthetic pathway of

precursors required for the biosynthesis of erythromycin. Replenishing the TCA cycle by feeding oxaloacetate, allowed pyruvate to accumulate and enhanced the production of the antibiotic. The constraining of erythromycin production by high TCA cycle activity is consistent with the loss of carbons through CO_2 evolution and the excretion of α-ketoglutarate through this route of catabolism. The findings also suggest that the anaplerotic pathway flux is necessary for the production of erythromycin when cultured on glucose as a carbon and energy source. These findings also highlight the crucial role of NADH in regulating carbon fluxes between the anaplerotic pathway and the TCA cycle. The biosynthesis of erythromycin was affected by the rates of growth, ATP synthesis and respiration. By manipulating the rates of respiration and growth some control can be gained over the production of erythromycin.

7.3 Bioreactor culture: Methyl oleate supplementation

Oils have been known to enhance the yield of any antibiotics produced by microorganisms. Hamedi *et al* (2004) have reported improvement in erythromycin productivity using oils as carbon source. In other work, rapeseed oil was shown to enhance the efficiency of erythromycin production in *S. erythraea* (Davis *et al*., 2000; Mourjalili *et al*., 1999). Oils enter biochemical network through acetyl-coenzyme A and are then degraded via the glyoxylate pathway (Voet & Voet, 2004). Acetyl-CoA is a critical precursor metabolite drawn from central metabolism for polyketide antibiotic biosynthesis (Rokem *et al*., 2007). As such limitations in their availability are likely to affect the production of erythromycin.

7.3.1 Experimental design

The feeding strategy used in these set of experiments was derived from results obtained in chapter 6. In that chapter, the highest erythromycin concentration was obtained when 10 $mg.L^{-1}$ of methyl oleate was fed at 60 hours. Additional feeding was done at 86 hours to investigate the effect of methyl oleate addition during the antibiotic synthesis phase. All sampling, sample treatment and analysis were done as described in chapter 2.

7.3.2 Effect of methyl oleate supplementation on biomass synthesis and respiration

Methyl oleate appeared to have a pressing effect on the biomass when compared to the control culture (Fig. 46, Fig. 17). In the control culture, biomass remained constant between 48 and 96 hours. For the control culture, the decrease only set in after 96 hours. However, similar findings were obtained with other related strains (Peacock *et al*., 2003). It is worth noting that these experiments were conducted with oil (triolein) as a sole carbon and energy source. Various other studies reported that oils enhance the production of biomass (Gojgic-Cvijovic *et al*., 2000; Efthimiou *et al*., 2008). However, this comparison may not be valid as clavulanic acid is very different from erythromycin. Nevertheless, in the current work, erythromycin levels increased after methyl oleate addition at both 60 h and 86 h (Fig. 46).

Compared to the batch fermentation, the fed batch culture diverted more carbon to biomass formation and erythromycin biosynthesis though the specific growth rate was fairly similar (Table 22). The specific erythromycin concentration for the supplemented culture was 30 $mgL^{-1}.g^{-1}$ biomass compared to 21 $mgL^{-1}.g^{-1}$ biomass for the control.

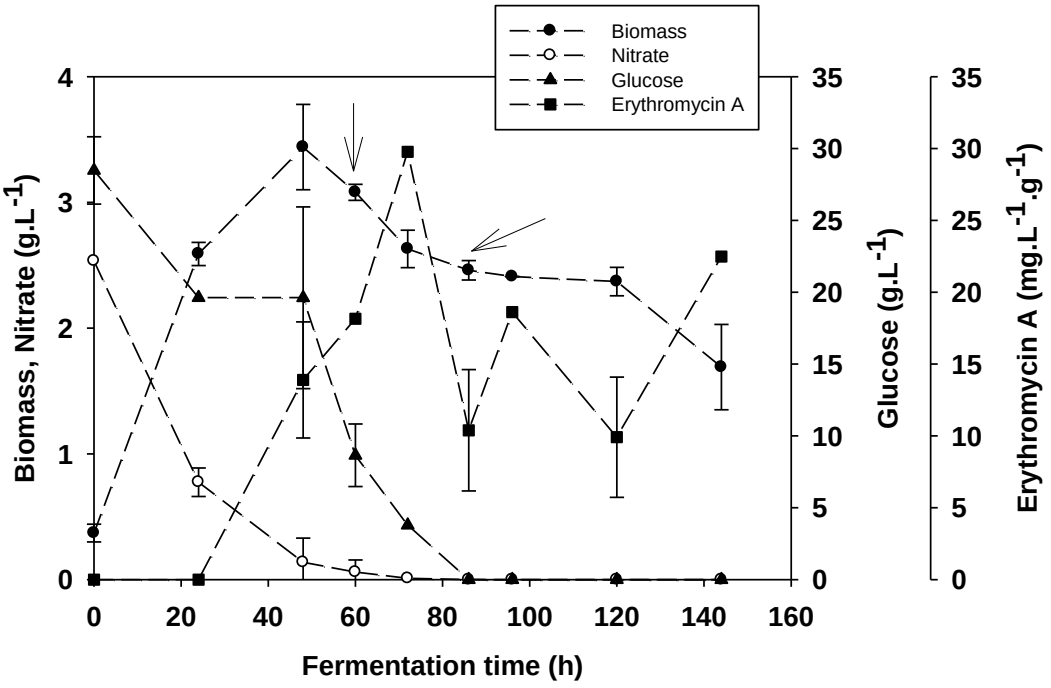

Fig. 46 Growth profile of *S. erythraea* during methyl oleate bolus feed additions fermentation. Arrows indicate points of methyl oleate feeding. Data represent 3 biological replicates.

Table 22. Specific growth rate, yields and yield coefficients for batch and methyl oleate supplemented batch *S. erythraea* cultivation using glucose as main carbon source.

Fermentation condition	**Growth Parameters**			
	μ(h^{-1})	**Yx/s (g/g)**	**Yp/s (mg.g^{-1})**	**Yp/x (mg.g^{-1})**
Batch	0.059	0.17	2.73	20.54
Bolus-fed	0.064	0.35	3.17	22.76

7.3.3 Carbon flux distribution through PEPC, ICD and ICL

There appeared not to be any obvious effect of methyl oleate supplementation on the activity of isocitrate dehydrogenase (ICD) between 60 and 72 hours. However, following feeding at 60 hours, PEPC activity dropped significantly for 12 hours. Thus the activity of the anaplerotic reaction was significantly reduced. During this time, ICD remained constant from 60 to 86 hours (Fig. 47) indicating constant TCA cycle activity. After 72 hours, the anaplerotic activities resumed and continued to increase until 120 hours. The TCA cycle increased its activities after addition of methyl oleate at 86 hours. It can be concluded that both the anaplerotic pathway and the TCA cycle were active between 86 and 120 hours.

During the time that ICD activity was constant between 72 and 96 hours, the activities of ICL were significantly increased. This indicates a switch in carbon flux from the TCA cycle to the glyoxylate pathway. This correlated with simultaneous increases in NADH, ATP and the energy charge. However, erythromycin production decreased from 30 $mg.L^{-1}.g.^{-1}$ biomass to 10 $mg.L^{-1}.g^{-1}$ biomass within 12 hours. The Glyoxylate pathway activity appears to correlate with a reduction in the production of the antibiotic. Interestingly, no ICL activity was observed for the oxaloacetate supplemented culture. Both PEPC and ICD activities increased significantly between 86 and 120 hours. Relative to the ICD activity for the batch fermentation, there was increased TCA cycle activity during the supplemented fermentation. During the growth phase, TCA cycle and the anaplerotic pathway played a major role in carbon catabolism with the former being more dominant. This trend resumed between 72 and 120 hours. However, from 96

to 120 hours, the activities of the anaplerotic reaction exceeded those of the TCA cycle indicating a a switch in dominant flux away from the TCA cycle.

It appears when the culture was supplemented with methyl oleate fluxes through ICD promoted erythromycin production. Increases in PEPC activity correlated with a decrease in erythromycin levels. In contrast, increases in ICD activity were correlated with elevated erythromycin levels. This is in contrast to the findings in the control fermentation where the antibiotic production was associated with the anaplerotic flux.

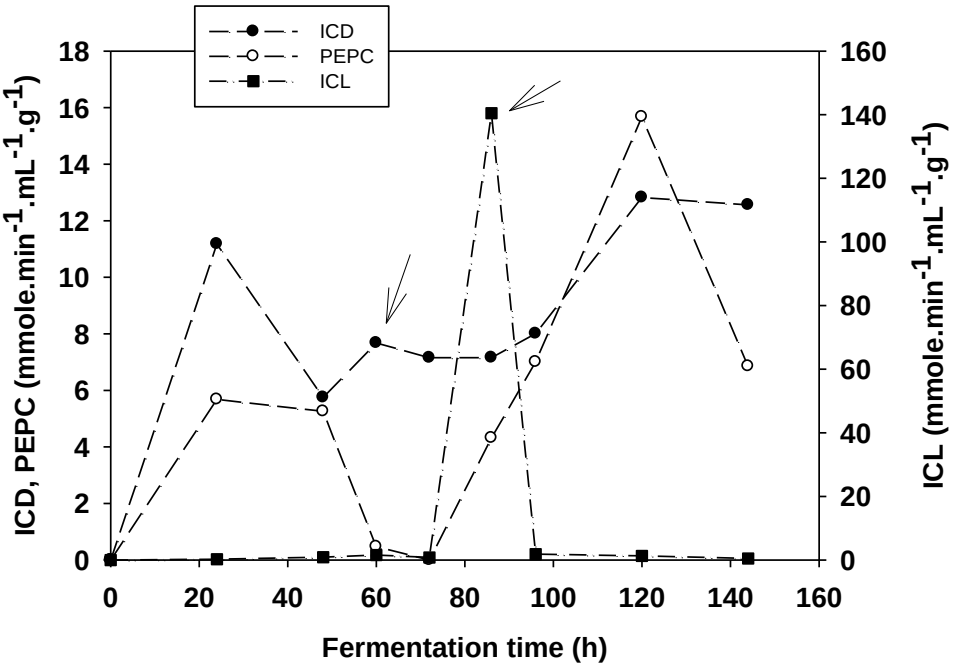

Fig. 47 Profiles of activities of phosphoenolpyruvate carboxylase (PEPC), isocitrate dehydrogenase (ICD) and isocitrate lyase (ICL). Arrows indicate points of methyl oleate additions. Data represent 3 biological replicates.

7.3.4 Effect of methyl oleate feeding on the energy status of the cell

The energy charge of a cell oscillates between 0 and 1 depending on the levels of its constituent molecules. This value is equal to 1 when all nucleotides are present as ATP and it is zero when AMP is at its maximum (Price & Stevens, 2006). Upon addition of methyl oleate, the energy charge and ATP levels first decreased for 12 hours, then increased until 86 h (Fig. 48). This trend continued after the feeding at 86 h. The effect on AMP concentration was similar to that on ATP levels. ADP levels also increased

after addition of methyl oleate, a response that is similar to that of the energy charge. The varying effects on the nucleotides are probably reflected in the response of the energy charge to oil supplementation.

The energy charge decreased after feeding, perhaps indicating reduction in oxygen consumption due to viscosity effects and the subsequent reduction in energy generation.

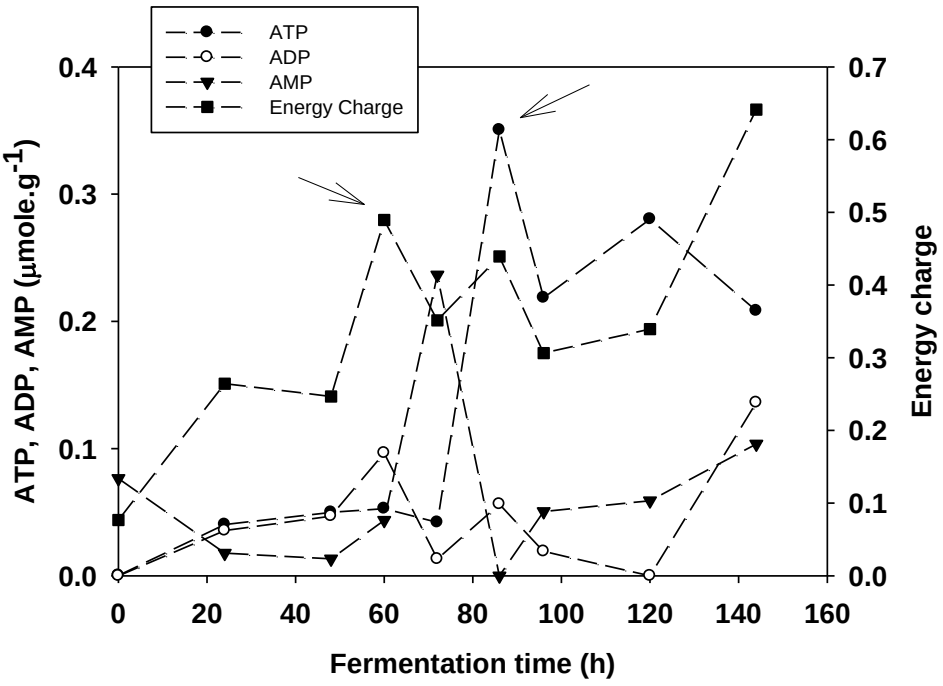

Fig. 48 Profiles of energy charge, ATP, ADP and AMP during the bolus feed additions fermentation. Methyl oleate additions were made at 6 h and 86 h. Data represent 3 biological replicates.

7.3.5 Effect of methyl oleate on the excretion of organic acids

Methyl oleate feeding appeared not to have had an obvious effect on the excretion of organic acids. However, a notable exception is the absence of any detectable levels of pyruvate throughout the fermentation time. Whereas the batch culture excreted propionate, the culture supplemented with methyl oleate excreted succinate instead. This was not due to the effects of methyl oleate as its production occurred before feeding. Both metabolites are precursors for the production of erythromycin. The levels of red pigment excreted for the supplemented culture was less than half those observed for the batch culture (Fig. 24, 49). Somehow, the oil reduced red pigment excretion. In

batch culture, *S. erythraea* produced large amounts of the red pigment after the growth phase (Fig. 24). The supplemented culture produced much less of the pigment mainly because its metabolism bypasses the pyruvate node which feeds in the pigment production. Large amounts (5.8 mmole.g^{-1} biomass) of α-ketoglutarate were produced (Fig. 56). This is consistent with elevated ICD activity observed throughout the fermentation time. Also up to 1 mmole.g^{-1} succinate was observed between 48 and 72 hours. This period correlated with increases in production of NADH and erythromycin on the one hand and decreases in ATP and PEPC activity on the other.

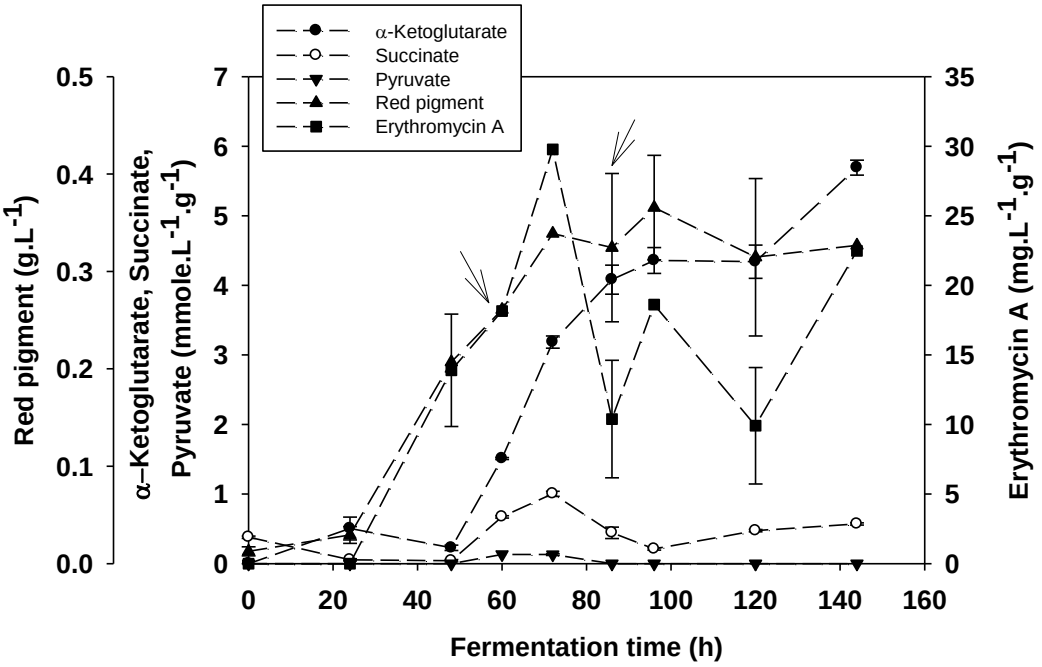

Fig. 49 Profiles of organic acid excretion during the bolus feed additions fermentation. Arrows indicate the time of methyl oleate addition (60 h and 86 h). Data represent 3 biological replicates.

The supplemented culture excreted higher amounts (5.8 mmole.g^{-1} biomass) of α-ketoglutarate compared to 3.8 mmole.g^{-1} biomass for the control. However, the amounts of the red pigment excreted were relatively similar. No detectable levels of pyruvate were observed which suggests that this metabolite was limited.

7.3.6 Effect of methyl oleate on the generation of NADH and NADPH

The levels of both NADH and NADPH were lower than those for the batch fermentation (Fig 50, Fig. 20). It is not clear why the culture produced low levels of NADH and NADPH. However, considering that methyl oleate increases the viscosity of the broth, it is possible that it reduces oxygen transfer to cells as well. If this is the case, growth will be reduced as will be the respiratory activity. This appears to be the case as the supplemented culture generated a biomass concentration of 2.6 $g.L^{-1}$ after 72 hours compared to 3.4 $g.L^{-1}$ for the control over the same period (Fig. 50, Fig. 17). However, reduction in biomass could have been due to cell lysis. Hence the lower levels of the cofactors may be a result of the reduced cell biomass.

The energy charge was equally lower for the supplemented culture rising to a maximum of 0.4 only (Fig. 51). This is in contrast to a maximum of 1 observed after 96 hours for the control culture (Fig. 20). This suggests that there was, on average, much lower energy available for the cell. The energy charge dropped after each addition of methyl oleate. The effect on erythromycin was different as levels of the antibiotic increased with each methyl oleate addition (Fig. 51). Though biomass decreased significantly after addition of methyl oleate, higher levels erythromycin were produced compared to the control. The culture produced a maximum of 30 $mgL^{-1}.g^{-1}$ biomass compared to 21 $mg.L^{-1}.g^{-1}$ biomass obtained for the control. It appears the oil directly enhanced the levels of the antibiotic. Addition at 60 hours increased the concentration from 18 to 30 $mg.L^{-1}.g^{-1}$ biomass. This increase occurred during the precursor accumulation phase observed in the control fermentation when the levels of the antibiotic actually decreased (Fig. 17, Fig. 51).

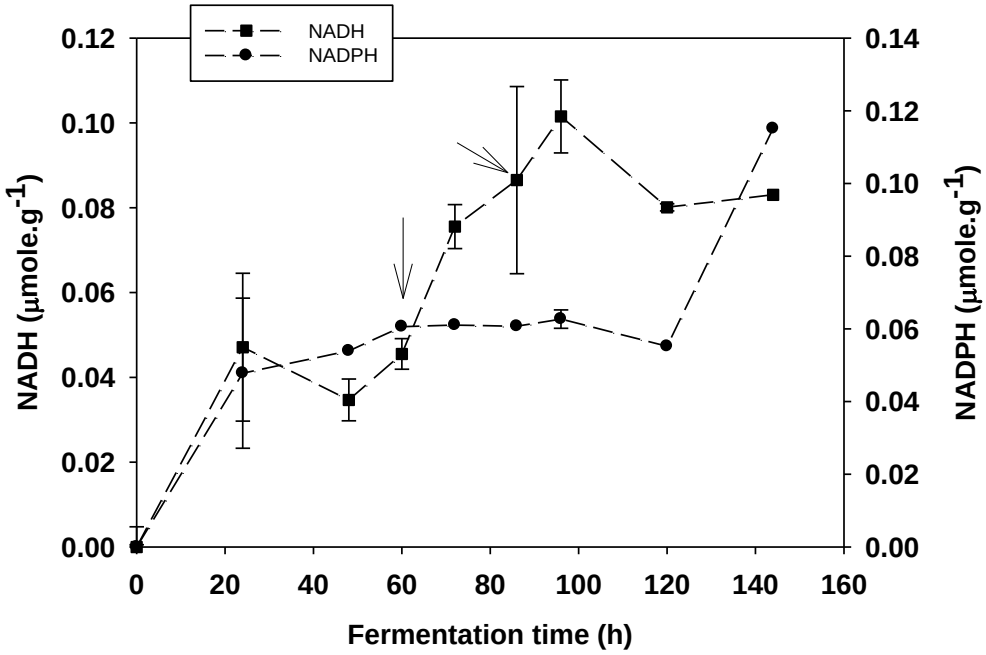

Fig. 50 Profiles of cofactor generation during the bolus feed additions fermentation. Arrows indicate the time of methyl oleate addition (60 h and 86 h). Data represent 3 biological replicates.

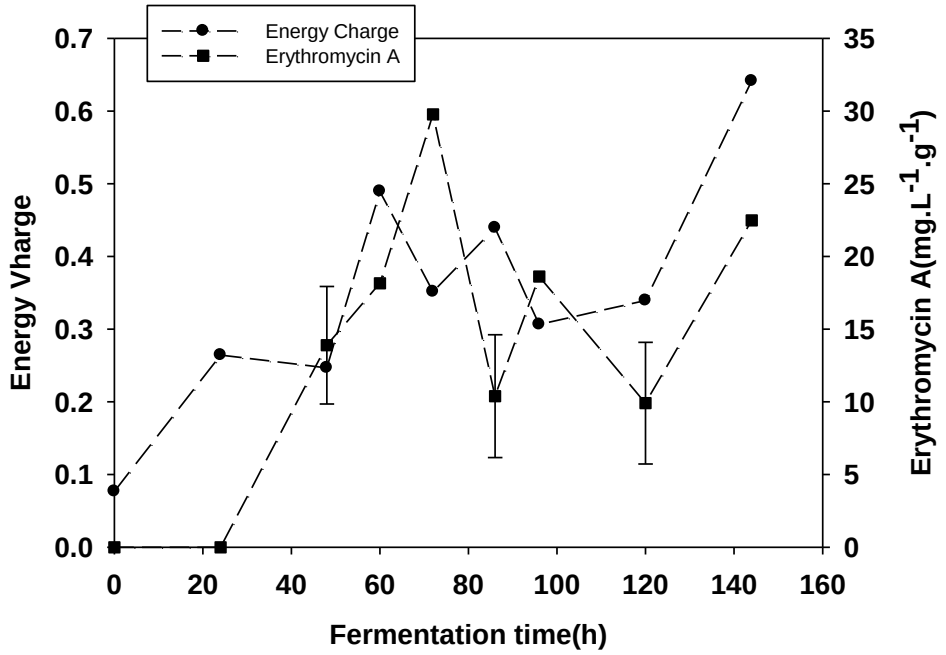

Fig. 51 Comparison of cell energetics with erythromycin production during the bolus feed additions fermentation. Arrows indicate time of methyl oleate addition. Data represent 3 biological replicates.

7.3.7 Comparison of the methyl oleate fed and oxaloacetate bolus feed addition cultures

Comparison of the data reveals that the two cultures grew at relatively the same growth rate (Table 19, Table 22). However, *S. erythraea* yielded a specific erythromycin concentration of 36 $mg.L^{-1}.g$ $Biomass^{-1}$ on oxakoacetate compared to 30 $mg.L^{-1}.g^{-1}$ for methyl oleate (Table 22). Though oxaloacetate supported the production of a higher level of erythromycin, biomass synthesis was enhanced on methyl oleate. Despite the producing a higher biomass, the yield of erythromycin for the methyl oleate culture was 17% lower. The reason for this discrepancy may lie in the rates of erythromycin production. Erythromycin was produced at a higher rate (0.31 $mg.L^{-1}.g^{-1}.h^{-1}$) on oxaloacetate compared 0.17 $mg.L^{-1}.g^{-1}.h^{-1}$ for methyl oleate (Table 18, Table 23). Though it formed a lower biomass, its higher rate of erythromycin production probably translated into higher yield. The supplemented precursor metabolites seem to be diverted to either erythromycin production or biomass formation.

However, it was noted that the culture fed with oxaloacetate produced 50% higher levels of the red pigment compared to the methyl oleate-fed culture (Fig. 42, Fig. 49). The rates of production of the red pigment were also higher for the same culture (Table 19, Table 23). In addition, the same culture excreted a maximum of 0.24 $mM.g^{-1}$ pyruvate while none of this metabolite was detected for the culture fed on methyl oleate. It is not known if these levels of the red pigment and pyruvate can account for the lower carbon amounts channelled to biomass production. On the other hand, the methyl oleate culture produced significantly higher amounts of succinate (87%) than the oxaloacetate one. The glyoxylate pathway flux increased significantly after methyl oleate supplementation (Fig. 47). The activity of isocitrate lyase, the enzyme that controls flux through the glyoxylate pathway, increased significantly after addition of methyl oleate at 60 h (Fig. 47). Given that flux from this pathway feeds directly into the succinate pool, it is possible that this metabolite levels were enhanced by methyl oleate addition. However, though the pyruvate node appeared to be flexible for the oxaloacetate-fed culture, the isocitrate node may be rigid when glucose is used as main carbon source. No isocitrate lyase activity was detected for this culture. In the case of the culture fed with methyl oleate, the level of isocitrate lyase activity was lower by a factor of 1000 compared to that of isocitrate dehydrogenase (Fig. 47). The rates of production of ATP and the pyridine cofactors, NADH and NADPH, were higher for the culture fed with oxaloacetate (Table 19, Table 22), possibly reflecting a higher demand.

In shake flask culture, methyl oleate produced a much higher level of erythromycin compared to oxaloacetate. The reason for improved erythromycin production for oxaloacetate in bioreactor culture in unclear.

The findings from the supplemented fermentations suggest that on glucose biomass formation and erythromycin production cannot be produced simultaneously. Feeding erythromycin enhanced the production of erythromycin while biomass formation was significantly decreased relative to the methyl oleate fermentation. On the other hand, methyl oleate enhanced biomass synthesis while erythromycin levels were lower relative to the oxaloacetate culture. Thus, while oxaloacetate enhanced the production of erythromycin, methyl oleate increased biomass synthesis. This negative correlation

between biomass synthesis and erythromycin production is in agreement with the findings of Rostamza *et al* (2008). In this study, biomass concentrations of 4.6 gL^{-1} and 22.8 gL^{-1} were associated with erythromycin yield of 0.6 $g.g^{-1}$ and 0.07 $g.g^{-1}$ respectively. This indirectly could mean that protein synthesis, which aids biomass formation, is negatively correlated with the production of erythromycin. The reasons for this could range from high energy demands to competition for precursor metabolite supply. The findings in batch shake flask studies and bolus feed additions suggest that competition for precursor metabolites prevents simultaneous production of biomass and erythromycin.

Table 23. Specific rates of substrate consumption, biomass production and product formation for bolus-feed additions fermentation of *S. erythraea* culture on glucose as main carbon source.

Parameter	Phase I (0-24h)	Phase II (24-48h)	Phase III (48-96h)
qO_2 [a]	- 0.60	- 0.13	- 0.02
qCO_2 [b]	0.06	0.13	0.02
qGlucose [c]	-0.02	-4.6×10^{-5}	- 0.04
qBIOMASS [d]	0.09	0.04	- 0.03
qEry [e]	-	0.17	-0.14
qα-KG [f]	1.8×10^{-3}	3×10^{-4}	- 0.01
qPYR [g]	-	-	3×10^{-4}
qSUC [h]	-	-	2×10^{-5}
qRED [i]	1.2×10^{-4}	6.1×10^{-4}	1.1×10^{-3}

[a]Specific O_2 uptake rate (mmole.$L^{-1}h^{-1}$g DCW^{-1})
[b]Specific CO_2 evolution rate (mmole.$L^{-1}h^{-1}$g DCW^{-1})
[c]Specific glucose consumption rate ($g.g^{-1}$ $DCWh^{-1}$)
[d]Biomass production rate ($g.L^{-1}h^{-1}$)
[e]Specific erythromycin production rate ($mg.L^{-1}$g $DCW^{-1}h^{-1}$)
[f]Specific α-ketoglutarate production rate ($mg.L^{-1}$g $DCW^{-1}h^{-1}$)
[g]Specific pyruvate production rate ($mg.L^{-1}$g $DCW^{-1}h^{-1}$)
[h]Specific succinate production rate ($mg.L^{-1}$g $DCW^{-1}h^{-1}$)
[i]Specific red pigment production rate ($mg.L^{-1}$g $DCW^{-1}h^{-1}$)

Table 24. Specific rate of adenylate and pyridine cofactor production during fed batch culture of *S. erythraea*.

Parameter	Phase I (0-24h)	Phase II (24-48h)	Phase III (48-96h)
qATP [a]	9 .8x10^{-4}	2.3 x10^{-4}	2.5 x10^{-3}
qADP [b]	6.5 x10^{-4}	2.4 x10^{-4}	8.2 x 10^{-4}
qAMP [c]	1.3 x10^{-4}	- 1.6 x10^{-6}	5 x10^{-4}
qNADH [d]	1.5 x 10^{-4}	-9 x10^{-6}	8.9 x 10^{-4}
qNADPH [e]	4.7 x 10^{-4}	2.5 x 10^{-4}	-3.9 x 10^{-5}

[a]Specific ATP production rate (µM.g DCW^{-1}h^{-1})
[b]Specific ADP production rate (µM.g DCW^{-1}h^{-1})
[c]Specific AMP production rate (µM.g DCW^{-1}h^{-1})
[d]Specific NADH production rate (µM.g DCW^{-1}h^{-1})
[e]Specific NADPH production rate (µM.g DCW^{-1}h^{-1})

7.4 Discussion

The dissolution of oxygen is dependent on the viscosity and rheology of the growth medium. Methyl oleate increases the viscosity of the growth medium and reduces its capacity to take up oxygen. Impaired oxygen uptake can reduce biomass synthesis. It is common for cultures fed with methyl oleate or other oil types to produce lower biomass. A more elaborate discussion of this has been provided in Chapter 1. High viscosity is often given as a reason for the reduced biomass formation in oil-based media. The current work does not have such data to support this claim.

Acetyl-CoA is one of the major precursor metabolites for polyketide antibiotics (Rokem *et al*., 2007). High levels of acetyl-CoA slow down the TCA cycle through its activation of pyruvate carboxylase or PEPC. Part of the rationale for selecting methyl oleate for feeding is its point of entry into the metabolic network. All odd-chain triacyl glycerides are degraded to valine through acetyl-Coenzyme A and ultimately propionyl-coenzyme A. ICD activity decreased after feeding which suggests that carbon fluxes were diverted to a different pathway. Since methyl oleate feeds directly into the acetyl-CoA pool, this could have reduced flux to the TCA cycle. One way of reducing TCA flux is through the activation of pyruvate synthetase. However, pyruvate levels remained below detectable levels after methyl oleate addition, suggesting that there was no accumulation. Pyruvate could have been rapidly diverted to the red pigment formation

which showed an increase after supplementation. Alternatively, there may be other unknown pathways to which flux was diverted. PEPC was not activated between 60 and 72 hours as its activity dropped after supplementation. Nevertheless, erythromycin production increased for 12 hours following supplementation at 60 hours. Following the second feeding at 86h, PEPC activity increased significantly while ICD decreased. This signalled a switch from the TCA cycle to the anaplerotic pathway (AP). It appears acetyl-CoA activated PEPC resulting in increased erythromycin production. Despite the decreases in the TCA cycle activity, α-ketoglutarate was excreted in almost the same amounts as for the batch fermentation and suggests that oil supplementation had little effect on its excretion. In chapter 4, increases in the production of erythromycin were associated with diversion of flux from the TCA cycle to the anaplerotic pathway. However, the improvement in the production of erythromycin appeared not to have been due to anaplerotic activity. Improvement in erythromycin levels between 60 and 72 hours coincided with decreased anaplerotic activity. Flux could have proceeded from pyruvate via malic enzyme to malate. Nevertheless, the findings confirm that with glucose as a carbon source, slowing down the TCA cycle improves the production of erythromycin. This is also consistent with the degradation of odd-chain fatty acids through valine (Voet & Voet, 2004). Valine is degraded by a succession of reactions to propionyl-Coenzyme A. Decarboxylation of propionyl-Co A yields propionate which is the priming unit required for assembly of erythromycin A by the modular polyketide synthase system (PKS).

The energy charge as well as ATP decreased with increasing production of erythromycin. The drop in the available energy probably reflects the high energetic demands of polyketide synthesis. This could also have been due to the switch of flux to an ATP consuming pathway such as AP. On the other hand, if methyl oleate increases the viscosity of the growth medium, oxygen transfer rate is likely to be reduced. Such a situation could interfere with ATP synthesis by the oxidative phosphorylation. Support for the argument comes from the effect of feeding on NADH levels. NADH generation increased each time the culture was fed with methyl oleate. ATP synthesis by the respiratory electron transport system is coupled to reduction in NADH generation. As such, the negative correlation between the levels of ATP and NADH supports the

conclusion that the effect of methyl oleate feeding on erythromycin production is exerted at the level of energy generation by the oxidative phosphorylation. However, it is worth pointing out that the degradation of odd-chain fatty acids through valine to propionyl-Co A generates NADH as well. Given this, the increase in NADH levels may not be surprising. The observed drop in NADPH level was possibly due to its role in reductive biosynthesis of polyketides.

The rate of respiration appears to be a critical parameter in controlling the partitioning of carbon fluxes in *S. erythraea* through its effect on the generation of NADH and ATP.

7.5 Conclusions

The findings from the bolus feed additions fermentations suggest that the production of erythromycin is constrained by limitations in the supply of precursor metabolites.

Oxaloacetate enhances precursor pools during the growth phase. Such precursors only enhance erythromycin production during the decelerated growth phase. However, fatty acid degradation generates both growth-related and non-growth-related precursors. Erythromycin levels could be enhanced during both the growth and the stationary phase. The effect of propionate depended on the time of feeding. When propionate was supplemented during the growth phase, increases in erythromycin production were observed 42 hours later. However, when feeding was done after the growth phase, the effect was observed after only 12 hours. It was concluded that certain precursor metabolites produced during the growth phase are necessary for the production of the antibiotic.

The pyruvate node was found to be flexible and amenable to manipulation to improve erythromycin production. The TCA cycle appears to drain the pyruvate pool, thereby constraining erythromycin production. The PEP metabolite node appears rigid and increasing its pool did not significantly enhance the level of erythromycin.

It was found that both biomass synthesis and erythromycin production draw heavily on precursor metabolites thereby draining the supply. Therefore, depleted precursor pools would be unable to support the production of erythromycin. The energy charge

correlated negatively with the production of erythromycin. Therefore, this parameter could be implicated in the regulation of erythromycin synthesis.

In summary, it can be stated that precursor metabolites generated during gluconeogenesis are essential for the biosynthesis of erythromycin. Limitations in their supply appear to constrain erythromycin production. PEP and α-ketoglutarate nodes appear rigid. However, the pyruvate node is flexible and can be manipulated to enhance erythromycin biosynthesis.

7.6 General observations and discussion

7.6.1 General discussion and conclusions

This work revealed, possibly for the first time, two phases, namely the erythromycin synthesis phase and the precursor accumulation phase during *S. erythraea* culture on either glucose or gluconate as sole or main carbon sources. A carbon flux distribution model was created for each of the phases based on the activities of key branch point enzymes. During the erythromycin synthesis phase, carbon fluxes appeared to be routed mainly through the pentose phosphate and the anaplerotic pathway. However, depletion of precursor metabolites switches fluxes to glycolysis and the TCA cycle during which precursor accumulation takes place.

In Chapter 4, it was found that the rate of carbon source uptake has a major influence on the split in branch point enzyme activities and the biosynthesis of erythromycin. Erythromycin was found to be enhanced by a low rate of carbon source consumption. The switch in pathway activity at key branch points was found to be dependent on the growth rate and the nature and the consumption rate of the carbon source. *S. erythraea* was found to regulate its consumption rate of carbon sources both during the growth and the stationary phase based on demand. Also, a decreased rate of respiration was found to coincide with increased erythromycin production.

It was proposed that NADH plays a major role in flux distribution. High levels of NADH were found to coincide with switch in pathway activity from the TCA cycle to the anaplerotic pathway possibly due to its inhibitory effect on pyruvate dehydrogenase. Flux to the TCA cycle could also be inhibited by the effect of a high ratio of [NADH/NAD^+] on citrate synthase.

In Chapter 4 and 5, it was noted that the production of erythromycin is constrained by limitations in the supply of precursor metabolites. Thus, externally feeding various precursors enhanced erythromycin levels. When precursors were fed during the accumulation phase, erythromycin synthesis increased. Feeding precursors towards the end of the synthesis phase resulted in the resumption of erythromycin synthesis.

In Chapter 4, the pyruvate node was found to be flexible and thus amenable to manipulation. When the pyruvate pool was increased by feeding oxaloacetate, erythromycin levels increased. It was concluded that the TCA possibly drains the

pyruvate pool. Methyl oleate was found to increase the succinate pool and enhance the production of erythromycin. It appears that enhancing the glyoxylate flux could improve erythromycin production.

Work presented in Chapter 4 and 5 suggest that *S. erythraea* may have limited respiratory capacity. As such, when its respiratory capacity is exceeded such as at high growth and carbon consumption rate, the excess precursors are excreted as overflow metabolites.

This work provides baseline information that can form a basis for genetic intervention efforts. It could also be useful for subsequent metabolic flux analysis (MFA) efforts which require detailed knowledge of the physiology.

7.6.2 Process scale implications for industrial biopharmaceutical production

The ratio of carbon source uptake to the respiration rate appears to be a critical parameter for the industrial production of biopharmaceuticals. Productivity of any fermentation is a function of the degree of substrate degradation and its conversion to product. This is dependent on the balance between the carbon source uptake rate and the respiration rate. Since this relationship is dynamic, the ratio is probably controllable giving the operator ability to optimise productivity. To increase titres and improve $Y_{p/s}$, the ability to improve the oxidation of the substrate and its conversion into the product is critical. Low titres demand the construction of larger manufacturing plants to take advantage of scale economics effect of cost reduction. However, though larger volumes reduce product cost, the excess production capacity has higher plant overhead costs unless the drug substance titres are improved. Therefore, optimising GUR/respiration rate ratio has the potential to improve product titres and reduce production cost. With improved titres, production capacity can be improved without necessarily increasing plant size. However, plant capacity has a larger impact on cost reduction than product manufacturing operations (Kelly, 2009). High titres only confer advantage when the manufacturing plant is operated at maximum capacity illustrating the interdependence of process technology and plant capacity. Biomanufacturing is mainly driven by the need for increased production capacity and pressures to reduce the cost of goods (COGS). COGS is known to be sensitive to changes in the key process parameters

(Kelly, 2009). Thus optimising GUR/respiration rate ratio has the potential to improve production titres and reduce the COGS.

An alternative to reducing overhead costs with improved production capacity is to spread the cost across multiple products. With improved titres and multiple products from the same plant, cost reduction is possible.

The parameter GUR or GLUR /respiration rate ratio will have a distinct advantage in disposable manufacturing given its potential to improve product titres. Disposable technology suffers from capacity limitations which often limits its usage in the biopharmaceutical industry. Improving product titres is likely to lower cost and make adopting the technology more attractive.

8.0 Future Work

There are various points noted during the current research that are worth pursuing. These are explored and discussed below.

In Chapter 4 and 5, the rate of carbon source uptake and growth rate were found to be potential regulators of the split ratio of pathway activities at the PPP/Glycolysis and AP/TCA cycle. In particular, erythromycin levels were increased by the combination of increased RQ and reduced rate of carbon source consumption. Growth rate was found to have a major influence on erythromycin synthesis. Using chemostat culture, the influence of growth rate on the rate of consumption can be investigated. Chemostat culture allows for more accurate control on the growth rate through controlling the rate of feeding. The role of energetics can be better studied when growth rate can be controlled.

Erythromycin was produced when fluxes were routed mainly through the pentose phosphate and the anaplerotic pathway simultaneously. Perhaps overexpressing the gene for phosphoenol pyruvate carboxylase could enhance AP flux. But this probably requires that flux through the pentose phosphate pathway be increased. In Chapter 6, feeding propionate produced high levels of erythromycin. Future focus could investigate the physiological basis for such high increases in the levels of erythromycin. In this regard, investigations into the pathway enzymes, ATP generation, organic acids excretion and the respiratory cofactors could yield important information.

Both the rate of carbon source consumption and that of respiration correlated negatively with increases in erythromycin levels. Though the two are not comparable as they were expressed in different units, both had individually the same effect on the levels of erythromycin. There may be a ratio of these two parameters at which the production of erythromycin is optimum. Consumed carbon source is dependent on the amount of oxygen available for degradation to generate energy and carbon backbones. Given this relationship, the ratio of glucose uptake rate to the rate of oxygen uptake is likely to have an effect on precursor generation, energy production and the biosynthesis of erythromycin. This relationship has been inferred from general trends. The relationship between the ratio of carbon source and OUR and the production of erythromycin can be

investigated directly in future experiments. This ratio could have critical importance in industrial production of biopharmaceuticals.

The findings presented in this work will add to the body of knowledge on the physiology of carbon source metabolism in *S. erythraea*. Together with existing information, this work could form the basis for subsequent efforts to elucidate the regulation of erythromycin biosynthesis in *S. erythraea*.

9.0 References

Agathos S N and Demain A L (1986). Appl. *Microbiol. Biotechnol*. 24: 319.
Alvarado A, Flores M E (2003). Characterization and regulation of NADP+-isoctrate dehydrogenase from *Saccharoplyspora erythraea*. *Biotechnology Letters* 25: 1175 - 1178.

Andersen K B, and von Meyenburg K (1980). Are growth rates of *Escherichia coli* in batch cultures limited by respiration? *J. Bacteriol*. 144 (1): 114 - 123.

Arnold S and Kadenbach B (1999). The intramitochondrial ATP/ADP ratio controls cytochrome *c* oxidase activity allosterically. *FEBS Letters* 443: 105 - 108.

Atkinson B and Mavituna F (1983). Biochemical Engineering and Biotechnology Handbook. Palgrave MacMillan Ltd, Surrey, England.

Avignone-Rossa C, White J, Kuiper A, Postma P W, Bib M and Teixeira de Mattos (2002). Carbon flux distribution in antibiotic-producing chemostat cultures of *Streptomyces lividans*. *Metabolic Engineering* 4: 138 - 150.

Ayar-Kayali H (2011). Pentose phosphate pathway flux analysis for glycopeptide antibiotic vancomycin production during glucose-limited cultivation of *Amycolaptosis orientalis. Prep. Biochem. Biotech.* 41: 94 - 105.

Ayar-Kayali H, Tarhan L, Sazak A and Sahin N (2011). Carbohydrate metabolite pathways and antibiotic production variations of a novel *Streptomyces* sp. M3004 depending on the concentration of carbon sources. *Appl. Biochem. Biotechnol.*41: 94 – 105.

Ball Jnr W J and Atkinson D E (1975). Adenylate energy charge in *Saccharomyces cerevisiae* during starvation. *Journal of Bacteriology* 121 (3): 975 - 982.

Banchio C and Gramajo H C, (1997). Medium- and long-chain fatty acid uptake and utilisation by *Streptomyces coelicolor* A3(2):first characterisation of a gram-positive bacterial system. *Microbiology* 143: 2439 - 2447.

Banin E, Vasil M L and Greenberg E P (2005). Iron and *Pseudomonas aeruginosa* biofilm formation. *Proc. Natl. Acad. Sci*. USA 102:11076 - 11081.

Bascaran V, Sanchez L, Hardisson C and Brana A F (1991). Stringent response and initiation of secondary metabolism in *Streptomyces clavuligerus*. *J. Gen. Microbiol*. 137: 1625 - 1634.

Becker J, Klopprogge C, Zelder O and Heinze E (2005). Amplified expression of fructose-1,6-bisphosphatase in *Corynebaterium glutamicum* increases in vivo flux through the pentose phosphate pathway and lysine production on different carbon sources. *Appl. Env. Microbiol*. 71(12): 8587 - 8596.

Beltrametti F, Jovetic S, Feroggio M, Selva C and Marinelli F (2003). Valine influences production and complex composition of glycopeptide antibiotic A40926 in fermentations of *Nonomuraea* sp. ATCC 39727. *J. Antibiotics* 57 (1): 37 - 44.

Boeck L D and Wetzel R W (1990). A54145, a new lipopeptide antibiotic complex: factor control through precursor directed biosynthesis. *J. Antibiotics 43: 607 - 615.*

Borodina I, Siebring J, Zhang J, Smith C P, van Keulen G and Dijkhuizen L (2008). Antibiotic overproduction in *Streptomyces coelicolor* A3(2) mediated by phosphofructokinase deletion. *Journal of Biological Chemistry* 283 (37): 25186 -25199.

Brekasis D and Paget M S B (2003). A novel sensor of NADH/NAD+ redox poise in *Streptomyces coelicolor* A3(2). *The EMBO Journal* 22 (18): 4856 - 4865.

Broer S, Eggeling L and Kramer R (1993). Strains of *Corynebacterium glutamicum* with different lysine productivities may have different lysine excretion systems. *Appl. Environ. Microbiol*. 59: 316 - 321.

Bruheim P, Butler M and Ellingsen T E (2002). A theoretical analysis of the biosynthesis of actinorhodin in a hyper-producing Streptomyces lividans strain cultivated on various carbon sources. *Applied Microbiol. Biotechnol*. 58: 735 - 742.

Brunker P, Minas W, Kallio P T and Bailey P E (1998). Genetic engineering of an industrial strain of *Saccharopolyspora erythraea* for stable expression of the *Vitreoscilla* haemoglobin gene (*vhb*). *Microbiology* 144: 2441 - 2448.

Bushell M E (1988). Growth, metabolism and fermentation technology. In *Biotechnology of the Actinomycetes*. Eds. Goodfellow M, Williams S T, Mordarski M, London Academic Press

Bushell M E, Bell S L, Scott M F, Wardell J N and Sanders P G (1994). Enhancement of monoclonal antibody yield by hybridoma fed batch culture, resulting in extended maintenance of viable cell population. *Biotechnol. Bioeng*. 44: 1099 - 1116.

Bushell M.E. and A. Fryday (1983) The application of materials balancing to the characterization of sequential secondary metabolite formation in *Streptomyces cattleya* NRRL 8057. *J Gen Microbiol*. 129(6),1733.

Bushell M E, Smith J and Lynch H C (1997). A physiological model for the control of erythromycin production in batch and cyclic fed batch culture. *Microbiology* 143: 475 - 480.

Butler M.J, Bruheim P, Jovetic S, Marinelli F, Postma P.W and Bibb M (2002). Engineering of primary metabolism for improved antibiotic production in *Streptomyces lividans*. *App.Env. Microbiol*. 68 (10): 4731- 4739.

Cavanagh M E, Ison A P, Lilly M D, Carley-Smith S W and Edwards J (1994). The utilisation of lipids during *Streptomyces fernemtations*. *Trans. Inst. Chem. Eng*. 72: 14 - 16.

Chen H C and Wilde F (1991). The effect of dissolved oxygen and aeration rate on antibiotic production of *Streptomyces fradiae*. *Biotechnol. Bioeng* 37: 591 - 595.

Chng C, Lum A M, Vroom J A and Kao C M (2008). A key developmental regulator controls the synthesis of the antibiotic erythromycin in *Saccharopolyspora erythraea*. *PNAS* 105 (32): 11346 - 11351.

Clark G J, Langley D and Bushell M E (1995). Oxygen limitation can induce microbial secondary metabolite formation: investigations with miniature electrodes in shaker and bioreactor culture. *Microbiology* 141: 663 - 669.

Cortes J, Velasco J, Foster G, Blackaby A P, Rudd B A M and Wilkinson B (2002). Identification and cloning of a type III polyketide synthase required for diffusible pigment biosynthesis in *Saccharopolyspora erythraea*. *Molecular Microbiology* 44 (5): 1213 - 1224.

Cotter P A, Melville S B, Albrecht J A and Gunsalus R P (1997). Aerobic regulation of cytochrome d oxidase (*cydAB*) operon expression in *Escherichia coli*: role of Fnr and Arca in repression and activation. *Mol. Microbiol* 25 (3): 605 - 615.

Daae E B and Ison A P (1999). Classification and sensitivity analysis of a proposed primary metabolic reaction network for *Streptomyces lividans*. *Metabolic Engineering* 1: 153 - 165.

David L, Loutheiller H, Bauchart D, Auboirou S, and Asselinou J (1992). *Biosci. Biotech. Biochem*. 56: 330.

Davies J L, Baganz F, Ison A P and Lye G J (2000). Studies on the interaction of fermentation and microfiltration operations: erythromycin recovery from *Saccharopolyspora erythraea* fermentation broths. *Biotechnol. Bioeng*. 69: 429 - 439.

Dawes E A (1986). *Microbial energetics*. Blackie & Son Ltd.

De Koning W and van Damm K (1992). A method for the determination of changes of glycolytic metabolites in yeast on a subsecond time scale using extraction at neutral pH. Anal. Biochem. 204: 118 - 123.

De Nisi P and Zocchi G (2000). Phosphoenolpyruvate carboxylase in cucumber (*Cucumis sativus* L.) roots under iron deficiency: activity and kinetic characterisation. *Journal of Experimental Botany* 51 (352): 1903 - 1909.

Djavadi F H S, Moradi M and Djavadi-Ohaniance L (1980). Direction of oxidation of NADPH by submitochondrial particles from *Saccharomyces cerevisiae*. *Eur. J. Biochem*. 107: 501 - 504.

Doran P M (1995). Bioprocess Engineering principles. Academic Press, London

Efthimiou G, Thumser A E and Avignone-Rossa C A (2008). A novel finding that *Streptomyces clavurigerus* can produce the antibiotic clavulanic acid using olive oil as a sole carbon source. *J. Appl. Microbiol*. 105: 2058 - 2064.

El-Enshasy H A, Mohamed N A, Farid M A and El-Diwany (2007). Improvement of erythromycin production by *Saccharopolyspora erythraea* in molasses based medium through cultivation medium optimization. *Bioresource Technology* 99: 4263 - 4268.

El-Mansi EMT and Holms H (1989). Control of carbon flux to acetate excretion during growth of *E. coli* in batch and continuous culture. *J. Gen. Microbiol*. 135: 2875 - 2883.

Faijes M, Mars A E and Smid E (2007). Comparison of quenching and extraction methodologies for metabolome analysis of *Lactobacillus plantarum*. *Microbial Cell Factories* 6:27.

Feng X, Page L, Rubens J, Chircus L, Colleti P Pakrasi H B and Tang Y J (2010). Bridging the gap between Fluxomics and Industrial Biotechnology. *Journal of Biomedicine and Biotechnology*. Vol 2010: 1 - 13.

Firn R D and Jones C D (2003). Natural products a simple model to explain chemical diversity. *Nat. Prod. Rep* 20: 382 - 391.

Fischer E and Sauer U (2005). *Nat. Genet*. 37 636 - 640.

Fraenkel, D.G and Levison, S.R (1967). Glucose and gluconate metabolism in an *Escherichia coli* mutant lacking phosphoglucose isomerase. *J. Bacteriol.* 93: 1571-1578.

Gojgic-Cvijovic G, Karadzic I and Vucetic J (2000). Effect of methyl oleate and Tween 80 on the antibiotic productivity and fatty acid composition of the total lipids of *Streptomyces hygroscopicus* CH-7. *J. Serb. Chem Soc.* 65 (8): 603 - 607.

Gonzalez B, Francois J and Renaud M (1997). A rapid and reliable method for metabolite extraction in yeast using boiling buffered ethanol. *Yeast* 13: 1347 - 1356.

Gonzalez-Lergier J, Broadbelt L J and Hatzimanikatis V (2006). Analysis of the maximum theoretical yield for the synthesis of erythromycin precursors in *Escherichia coli. Biotech. Bioeng*. 95 (4): 638 - 644.

Gray P P and Vu-Trong K (1987). Production of the macrolide antibiotic tylosin in cyclic fed batch culture. *Biotechnol. Bioeng*. 29: 33 - 40.

Hamedi J, Malekzadeh F and Saghafi-nia A E (2004). Enhancing of erythromycin production by *Saccharopolyspora erythraea* with common and uncommon oils. *J Ind Microbiol Biotechnol* 31: 447 - 456.

Henriksen C M, Christensen L H, Nielsen J and Villadsen J (1996). Growth energetics and metabolic fluxes in continuous ciltures of *Penicillium chrysogenum*. *Journal of Biotechnology* 45: 149 - 164.

Hernandez M E, Kappler A and Newman D K (2004). Phenazine and other redox-active antibiotics promote microbioal mineral reduction. *Appl. Environ. Microbiol*. 70: 921 - 928.

Hesketh A, Chen W J, Ryding J, Chang S and Bibb M (2007). The global role of ppGpp synthesis in morphological differentiation and antibiotic production in *Streptomyces coelicolor* A3 (2). *Genome Biology* 8 (8): R161.

Heydarian S M, Ison A P and Mirjalili N (1998). A rapid and simplified extraction method of erythromycin from fermentation broth with bond elut C18 cartridge for analysis by HPLC. *Biotechnology Techniques*: 12 (2): 155 - 158.

Hodgson D (2000). Primary metabolism and its control in streptomyces: A most unusual group of bacteria. *Advances in Microbial Physiology* 42: 49 - 238.

Hodgson D A (2000). Primary metabolism and its control in Streptomycetes: A most unusual group. *Adv. Microb.Phys*. 42: 47 - 238.

Holms H (1996). Flux analysis and control of the central metabolic pathway in *Escherichia coli. FEMS Microbiol. Rev*. 19: 85 - 116.

Horne R N, Anderson W B and Nordlie R C (1970).Glucose Dehydrogenase Activity of Yeast Glucose 6-Phosphate Dehydrogenase. Inhibition by Adenosine 5'-Triphosphate and other Nucleoside 5'-Triphosphates and Diphosphates. *Biochemistry* 9 (3): 610 - 616.

Hua Q, Yang C, Baba T, Mori H and Shimizu K (2003). Responses of the central metabolism in *Escherichia coli* to phosphoglucose isomerase and glucose-6-phosphate dehydrogenase knockouts. *J.Bacteriol*.185(24):7053-7067.

Huh J-H, Kim D, Zhao X-Q, Li M, Jo Y-Y, Yoon T-M, Shin S-K, Yong J-H, Ryu Y-W, Yang Y-Y and Suh J-W (2004). Widespread activation of antibiotic biosynthesis by *S*-Adenosylmethionine in streptomycetes. *FEMS Microbiol. Lett*. 238: 439 - 447.

Hult K, Veide A and Gatenbeck S (1980). The disruption of the NADPH regenerating mannitol cycle among fungal species. *Arch. Microbiol*. 128: 253 - 255.

Hutchinson C R, Decker H, Madduri K, Otten S L and Tang L (1993). Genetic control of polyketide biosynthesis in the genus *Streptomyces*. *Antonie van Leeuenhoek* 64: 165 - 176.

Ikeda H, Kotaki H, Tanaka H and Omura S (1988). Involvement of glucose catabolism in avermectin production by *Streptomyces*. *Antimicrob Agents Chemother*, 32: 282-284.

Jaques C.M (2004). *PhD Thesis*. Modelling of metabolite pathways of *Saccharopolyspora erythraea* using flux balance analysis.

Jonsbu E, Christensen B and Nielsen J (2001). Changes of in vivo fluxes through central metabolic pathways during the production of nystatin by *Streptomyces noursei* culture. *Appl. Microbiol. Biotechnol*. 56 93 - 100.

Jung H-M, Kim S-Y, Moon H-J, Oh D-K and Lee J-K (2007). Optimization of culture conditions and scale-up to pilot and plant scales for vancomycin production by *Amycolaptosis orientalis*. *Appl Micrbiol Biotechnol* 77: 789 - 795.

Kelly B (2009). Industrialisation of mAb production technology: The bioprocessing industry at a crossroads. *Landes Bioscience* 1 (5): 443 - 452.

Kim D-J, Huh J-H, Yang Y-Y, Kang C-M, Lee I-H, Hyun C-G, Hong S-K and Suh J-W (2003). Accumulation of *S*-Adenosyl-L-Methionine enhances production of

actinorhodin but inhibits sporulation in *Streptomyces lividans* TK23. *J. Bacteriol*. 185 (2): 592 - 600.

Kim H B, Smith C P, Micklefield J and Mavituna F (2004). Metabolic analysis for calcium-dependent antibiotic (CDA) production in *Streptomyces coelicolor*. *Metabolic Engineering* 6: 313 - 325.

Kim H K, Kim Y T and Lee S Y (2008). Metabolic flux analysis and metabolic engineering of microorganisms. *Mol. BioSyst*. 4: 113 - 120.

Kirk S, Avignone-Rossa C A and Bushell M E (2000). Growth limiting substrate affects antibiotic production and associated metabolic fluxes in *Streptomyces clavuligerus*. *Biotechnol. Lett*. 22: 1803 - 1809.

Kleijn R J, Liu F, van Winden W A, van Gulik W M, Ras C and Heijnen J J (2007). Cytosolic NADPH metabolism in penicillin-G producing and non-producing chemostat cultures of *Penicillium chrysogenum*. *Metabolic Engineering* 9: 112 - 123.

Koch A L (1980). The inefficiency of ribosomes functioningin *Escherichia coli* growing at moderate rates. *J. Gen. Microbiol*. 116: 165 - 171.

Krispin O and Allmansberger R (1998). The *Bacillus subtilis* AraE protein displays a broad substrate specificity for several different sugars. *J. Bacteriol*. 180 (12): 3250 – 3252.

Lamond A I, Travers A A (1985). Stringent control of bacterial transcription. *Cell* 41: 313 - 334.

Large K OP, Ison A P and Williams D J (1998). The effect of agitation rate on lipid utilisation and clavulanic acid utilisation in *Streptomyces clavuligerus. J. Biotechnol*. 63:111 - 119.

Li L, Zheng H and Yuan Y (2007). Effects of streptolydigin and carbon flux distribution in *Streptomyces lydicus* AS 4.2501. *Chin. J Chem Eng.* 15 (12): 143 - 149.

Li R and Townsend C A (2006). Rational strain improvement for enhanced clavulanic acid production by genetic engineering of the glycolytic pathway in *Streptomyces clavuligerus*. *Metab. Eng*. 8: 240 - 252.

Loftus T M, Hall L V, Anderson S L and McAlister-Henn I (1994). Isolation, characterisation and disruption of the yeast gene encoding cytosolic NADP-specific isocitrate dehydrogenase. *Biochemistry* 33: 9661 - 9667.

Lynch C H and Bushell M E (1995). The physiology of erythromycin biosynthesis in cyclic fed batch culture. *Microbiology* 141: 3105 - 3111.

Marsden A F A, Wilkinson B, Cortes J, Dunster N, Staunton J and Leadlay P F (1998). Engineering broader specificity into an antibiotic-producing polyketide synthase. *Science* 279: 199 - 202.

Marti J F (2004). Phosphate control of the biosynthesis of antibiotics and other secondary metabolites is mediated by the PhoR-PhoP system: an unfinished story. *J Bacteriol* 186: 5197 - 5201.

Martin J F and Demain A L (1980). Control of antibiotic biosynthesis. *Microbiological Reviews* 44 (2): 230 - 251.

Mashego M R, Jansen M L A, Vinke J L, van Gulik W M and Heijnen J J (2005). Changes in the metabolone of Saccharomyces cerevisiaea associated evolution in aerobic glucose-limited chemostat. *Yeast Res*. 5: 419 - 430.

Matsumura, H and Miyachi, S (1980). Cycling assay for nicotinamide adenine dinucleotides. *Methods in enzymology*. 69: 465-470.

Medema M H, Alam M T, Heijne H M, van den Berg M A, Muller U, Trefzer A, Bovenberg R A L, Beitling R and Takano E (2011). Genome-wide gene expression changes in an industrial clavulanic acid overproduction strain of *Streptomyces clavuligerus*. *Microbial Technology* 4 (2): 300 - 305.

McIntyre J J, Bunch A W and Bunch A T (1999). Vancomycin production is enhanced in chemostat culture with biomass recycle. *Biotechno Bioeng* 62: 576 - 582.

Minas W, Brunker P, Kallio P T and Bailey J E (1998). Improved erythromycin production in a genetically engineered industrial strain of *Saccharopolyspora erythraea*. *Biotechnol. Prog*. 14: 561 - 566.

Mirjalili N, Zormpaidis V V, Leadlay P F and Ison A P (1999). The effect of rapeseed oil uptake on the production of erythromycin and triketidelactone by *Saccharopolyspora erythraea. Biotechnol Bioprog* 15: 911 - 918.

Moragues M D, Estevez J J, Rementeria A and Sevilla M J (1994). Effect of n-alcohols on acidification curves of *Aureobasidium pullulans* suspensions. *Exp. Mycol* 18: 1 - 6.

Moritz B, Striegel K, de Graaf A A and Sahm H (2000). Kinetic properties of the glucose-6-phosphate and 6-phosphogluconate dehydrogenases from *Corynebacterium glutamicum* and their application for predicting pentose phosphate pathway flux in vivo. *Eur. J. Biochem*. 267: 3442 - 3452.

Mouslin J, El-Haloui N-E and David L (1997). Influence of fatty acids and detergents on polyether antibiotic production by *Streptomyces hygroscopicus* NRR B-1865. *Canadian J. Microbiology* 43: 879 - 883.

Nielsen J (2003). Title? *J. Bacteriol*. 185: 7031 - 7038.

Obanye A I C, Hobbs G, Gardner D C J and Oliver S G (1996). Correlation between carbon flux through the pentose phosphate pathway and production of the antibiotic methylenomycin in *Streptomyces noursei*. *Microbiology* 142: 133 - 137.

Okamoto S, Lezhave A, Hosaka T, Okamoto-Hosoya Y and Ochi K (2003). Enhanced expressionof *S*-Adenosylmethionine synthetase causes overproduction of actinorhodin in *Streptomyces coelicolor* A3 (2). *J. Bacteriol*. 185 (2): 601 - 609.

Palsson B O, Price N D and Papin J A (2003). Title? *Trends Biotechnol*. 21: 195 - 198.

Peacock L, Ward J, Ratledge C, Dickinson F M and Ison A (2003). How *Streptomyces lividans* uses oil and sugars as mixed substrates. *Enzyme and Microbial Technology* 32: 157 - 166.

Penzikova G.A and Levitov M.M (1966). Patterns of carbohydrate metabolism of *Actinomyces fradiae* grown on media containing starch or glucose. *Biokhimiya,* 31: 1073-1077.

Penzikova G.A and Levitov M.M (1966). Patterns of carbohydrate metabolism of *Actinomyces fradiae* grown on media containing starch or glucose. *Biokhimiya,* 31: 1073-1077.

Pfeifer B A, Admiraal S J, Gramajo H, Cane D E and Khosla C (2001). Biosynthesis of complex polyketides in a metabolically engineered strain of *E. coli. Science* 291: 1790 - 1792.

Picon A, Teixeira de Mattos M.J and Postma P.W (2005). Reducing the glucose uptake rate in *Escherichia coli* affects growth rate but not protein production. *Biotech. Bioeng*. 90 (2): 191 - 200.

Postma E, Verduyn C, Scheffers W A and van Dijken J P (1989). Enzymatic analysis of the crab-tree effect in glucose-limited chemistat cultures of *Saccharomyces cerevisiae*. *Appl. Environ. Microbiol*. 53: 468 - 477.

Price-Whelan A, Dietrich L E P and Newman D K (2006). Rethinking 'secondary' metabolism: physiological roles of phenazine antibiotics. *Nature Chemical Biology* 2 (2): 71 - 78).

Rawlings B J (2001). Type I polyketide biosynthesis in bacteria (Part A – erythromycin biosynthesis). *Nat. Prod. Rep*. 18: 190 - 227.

Reed G and Peppler H J (1973). Title? *Yeast Technology*, pp. 664 - 668. Westport: AVI.

Reeve L M and Baumberg S (1998). Physiological controls of erythromycin production by *Saccharopolyspora erythraea* are exerted at least in part at the level of transcription. *Biotechnol. Lett*. 20 (6): 585 - 589.

Reeves A R, Brikun I A, Cernota W H, Leach B I, Gonzalez M C and Weber J M (2007). Engineering of the methylmalonyl-CoA metabolite node of *Saccharopolyspora erythraea* for increased erythromycin production. *Metabolic Engineering* 9: 293 - 303.

Reeves A R, Cernota W H, Brikum I A, Wesley R K and Weber J M (2004). Engineering precursor flow in *Aeromicrobium erythreum. Metab. Eng*. 6: 300 - 312.

Rice C W and Hempfling W P (1978). Oxygen-limited continuous culture and respiratory energy conservation in *Escherichia coli. J Bacteriol* 134: 115 - 124.

Rokem J S, Lantz A E and Nielsen J (2007). Systems biology of antibiotic production by microorganisms. *Nat. Prod. Rep*. 24: 1262 -1287.

Ryu Y, Butler M, Chater K.F, Lee K J (2006). Engineering carbohydrate metabolism for increased production of actinorhodin in *Streptomyces coelicolor*. *Appl. Env. Microbiol*. 72 (11): 7132-7139.

Rollins M J, Jensen S E and Westlake D W S (1988). *L Ind. Microbiol*. 3: 357.

Roszkowski J, Ruczaj Z, Sawnor-Korszynska D, Kotiuszko D, Morawska H, Siejko D and Raczsynska-Bojanowska K (1971). NADPH-generating systems in microorganisms producing macrolide antibiotics. *Acta Microbiologia Polonica Series* B 3: 97 - 106.

Rowe C J, Cortes J, Gaisser S, Stauntin J and Leadlay P F (1998). Construction of new vectors for high level expression in Actinomycetes. *Gene* 216: 215 - 223.

Rostamza M, Noohi A and Hamedi J (2008). Enhancement in production of erythromycin by *Saccharopolyspora erythraea* by the use of suitable seeding-media. *Daru* 16: 13 - 17.

Ryu Y, Butler M, Chater K.F and Lee K J (2006). Engineering carbohydrate metabolism for increased production of actinorhodin in *Streptomyces coelicolor*. *Appl.Env. Microbiol*. 72 (11): 7132-7139.

San K Y, Bennett G N, Berrios-Rivera S J and Vadali R, Horton E, Rudolph F B, Sariyar B, Blackwood K (2002). Metabolic engineering through cofactor manipulation and its effects on metabolic flux redistribution in *Escherichia coli*. *Met. Eng*. 4:182-192.

Sauer U (2006). Metabolic networks in motion: 13C-based flux analysis. *Molecular Systems Biology* 62: 1 - 10.

Shen L and Atkinson D (1970). Regulation of pyruvate dehydrogenase from *Escherichia coli*: interaction of adenylate energy charge and other regulatory mechanisms. *The Journal of Biological Chemistry* 245: 5974 - 5978.

Shin S-K, Xu D, Kwon H-J and Suh J-W (2006). *S*-adenosylmethionine activates adpA transcription and promotes streptomycin biosynthesis in *Streptomyces griseus*. *FEMS Microbiol. Lett*. 259:53 - 59.

Shryock J C, Rubio R and Berne R M (1986). Extraction of adenine nucleotides from cultured endothelial cells. Anal. Biochem. 159: 73 - 81.

Slonczewski, J L, Foster J W (2009) Microbiology: An Evolving Science: New York: W. W. Norton & Company, Inc. p. 257-300.

Smart A G, Amaral L A N and Ottino J M (2008). Cascading failure and robustness in metabolic networks. *PNAS* 105 (36): 13223 - 13228.

Smolke C D (2010). The metabolic pathway engineering handbook: fundamentals. CRC Press.

Staunton J and Wilkinson B (1997). Biosynthesis of erythromycin and rapamycin. *Chem. Rev*. 97: 2611 - 2629.

Stowell J D (1987). The application of iol and fats in antibiotic processes. In *Carbon substances in biotechnology*, Stowell J D., Ed.: IRL Press, Oxford, UK.

Taanman J-W, Turina P and Capaldi R A (1994). Regulation of Cytochrome c Oxidase by Interaction of ATP at Two Binding Sites. *Biochemistry* 33: 11833-11841.

Takano E (2006). γ-Butyrolactones: *Streptomyces* signalling molecules regulating antibiotic production and differentiation. *Curr. Op. Microbiol*. 9: 287 - 294.

Theobald U, Mailinger W, Baltes M and Reuss M (1997). In vivo analysis of metabolic dynamics in Saccharomyces cerevisiaea: Experimental observations. Bioetchnol. Bioeng. 55: 305 - 316.

Tian J, Bryk R, Itoh M, Suematsu M and Nathan C (2005). Variant tricarboxylic acid cycle in *Mycobacterium tuberculosis*: identification of α-ketoglutarate decarboxylase. *PNAS*, 102(30): 10670-10675.

Ushio, M (2003). PhD Thesis. A metabolic engineering approach to examine polyketide production by *Saccharoployspora erythraea.*

Vadali R, Bennett G and San K-Y (2004). Cofactor engineering of intracellular CoA/acetyl-CoA and its effect on metabolic flux redistribution in *Escherichia coli. Mtab. Eng*. 6: 13 - 139.

Vallino J J and Stephanopoulos G (1994). Carbon flux distributions at the glucose-6-phosphate branch point in *Corynebacterium glutamicum* during lysine production. *Biotechnology Progress* 10: 327 - 334.

Van Gulik W M, de Laat W T A M, Vinke J L and Heijnen J J (2000). Application of metabolic flux analysis for the identification of metabolic bottlenecks in the biosynthesis of penicillin-G. *Biotech. Bioeng*. 68 (6): 602 - 618.

VanDamme E J, Leyman D, DeVischer P, DeBuyserD and Vansteenkiste G (1981). *Chem. Tech. Biotechnol*. 31: 247.

Vardar F and Lilly M D (1982). Title? *Appl. Microbiol. Biotechnol* 14: 203.

Vaseghi S, Baumeister A, Rizzi M and Reuss M (1999). *In vivo* dynamics of the Pentose Phosphate pathway in *Saccharomyces cerevisiae*. *Metabolic Engineering* 1: 128 - 140.

Vermuri G N, Eiteman M A, McEwen J E, Olsson L and Nielsen J (2007). Increasing NADH oxidationreduces overflow metabolism in *Saccharomyces cerevisiae. PNAS* 104 (7): 2402 - 2407.

Voet D and Voet J G (2004). Biochemistry 3rd Edition, Wiley & Sons, New York.

Wang Y, Boghigian B A and Pfeifer B A (2007). Improving heterologous polyketide production in *Escherichia coli* by overexpression of an *S*-adenosylmethionine synthetase gene. *Appl. Microbiol. Biotechnol*.: 77: 367 - 373.

Wang Y, Wang Y and Zhang S (2007). High frequency transformation of the industrial erythromycin-producing bacterium *Saccharopolyspora erythraea. Biotechnol. Lett*. 30: 357-361.

Wang Y, Wang Y G, Chu J, Zhuang Y, Zhang L and Zhang S (2007). Improved production of erythromycin A by expression of a heterologous gene encoding *S*-adenosylmethionine synthetase. *Appl. Microbiol. Biotechnol*. 75: 837 - 842.

Weitzman P D J (1972). Regulation of α-ketoglutarate dehydrogenase activity in *Acinetobacter. FEBS Letters* 22 (3): 323 - 326.

White D (2007). The physiology and biochemistry of prokaryotes, Third Edition. Oxford: Oxford University Press Inc.

Wilson G C and Bushell M E (1995). The induction of antibiotic synthesis in *Saccharopolyspora erythraea* and *Streptomyces hygroscopicus* by growth rate decrease is accompanied by a down-regulation of protein synthesis rate. *FEMS Microbiology Letters* 129: 89 - 96.

Wilson G C and Bushell M E (1995). The induction of antibiotic synthesis in *Saccharopolyspora erythraea* and *Streptomyces hygroscopicus* by growth rate decrease is accompanied by a down-regulation of protein synthesis rate. *FEMS Microbiol. Lett*.129: 89 - 96.

Zhuang K, Vemuri G N and Mahadevan R (2011). Economics of membrane occupancy and respiro-fermentation. *Molecular Systems Biology* 7 (500): 1 - 9.

Zmijewski M J Jr, Briggs B and Ocolowitz J (1986). Role of branched chain fatty acid precursors in regulating factor profile in the biosynthesis of A21978 C complex. *J. Antibiotics* 39: 1483 - 1485.

.